# Mechanisms of brain dysfunction in myotonic dystrophy type 1 : impact of the CTG expansion on neuronal and astroglial physiology

Diana Mihaela Dincã

# Université Paris Descartes

**Ecole doctorale Bio Sorbonne Paris Cité**

*Spécialité : Développement, Génétique, Neurobiologie, Reproduction et Vieillissement*

# Mechanisms of brain dysfunction in myotonic dystrophy type 1:

# Impact of the CTG expansion on neuronal and astroglial physiology


Présenté par

**Diana Mihaela DINCĂ**


**Thèse de doctorat de Neurobiologie et Génétique Humaine**

**Présentée et soutenue publiquement le 31 Octobre 2017**

**Devant un jury composé de :**

| | |
|---|---|
| **Mr. le Dr. Mário GOMES-PEREIRA** | **Directeur de thèse** |
| **Mme. le Dr. Laurence COLLEAUX** | **Présidente du jury** |
| **Mr. le Dr. Berend WIERINGA** | **Rapporteur** |
| **Mr. le Dr. John DAY** | **Rapporteur** |
| **Mme. le Dr. Geneviève GOURDON** | **Examinateur** |
| **Mr. le Dr. Nicolas SERGEANT** | **Examinateur** |
| **Mme. le Dr. Céline DOGAN** | **Examinateur** |

*"Above all, don't fear difficult moments. The best comes from them"*

Rita Levi-Montalcini

# *ACKNOWLEDGMENTS*

*At the end of this research journey I would like to kindly thank, from all my heart, my advisor Dr. Mário Gomes-Pereira, for all his patience and extremely useful advices, both in research and in every-day life. It was a great journey, somewhat difficult, but I guess that's what makes it beautiful. And a big thanks to Dr Geneviève Gourdon, for all her insightful remarks throughout this journey, that have continuously helped improving my results. Thanks to your combined work I learned to be more patient and tenacious and to communicate precisely on my work and, through time, I have become a more mature scientist.*

*I would also like to thank the members of my jury, Prof. Wieringa, Prof. Day, Dr. Colleaux, Dr. Sergeant and Dr. Dogan for having accepted to examine my manuscript.*

*This journey wouldn't have been possible without a volunteer internship I carried out in Dr. Rubén Artero's laboratory at the University of Valencia, Spain, where under the close supervision of now Dr. Amparo Garcia López and Dr. Juan Manuel Fernandez Costa, I learned about CTG repeats and MBNL proteins and how to use drosophila genetics to understand DM1 mechanisms. After my Erasmus year in Paris, where I met Mário in a Human Genetics course at Paris-Sud University, and knowing my newly developed interest for understanding the cellular mechanisms that control the brain function, Amparo and Juanma pointed me to contact Mário, who was starting to tackle DM1 mechanisms in the central nervous system. And like that, the stars aligned and I started my PhD project in the CTGDM lab, trying to understand the mechanisms of brain dysfunction in DM1, and I am grateful to all of them for that.*

*An enormous thanks goes to all my lab colleagues, with whom the everyday life of performing experiments went smoother, under a Ricky Martin song. Thank you Louison for being my adventure buddy, Sandra for being a fountain of knowledge, Elodie for all those amazing drawings, Aline for sharing positivity all around the lab (besides endlessly juggling with the mice), and Steph for keeping our feet on the ground. And of course all former colleagues, like Noëmy, and Snanon, Clémence, Aicha and Alexis who shared nice moments with us.*

*This journey was mostly carried out at the Imagine Institute, with a common objective of better understanding rare genetic disorders, such as DM1, with the hope of developing new*

*therapies. And this common objective brought great scientists together and I was lucky enough that some of them crossed my path and helped me at the right moment. I must thank Meriem and Nicolas for their help with the microscopes and Chiara for her help with proteomics, and Fernando and Julien C. and Rémy for their attempts to make me love the FACS machines, and Flora for her kind help in using and understanding the xCELLigence. And all the other neighbors for useful advice and precious antibodies. And, even if outside of Imagine, a huge thank you to Jean Baptiste and Matthias, who brought the IncuCyte into my life (and 3 into the institute) and sped up my research as well as my negotiation skills.*

*And although the journey had a scientific path to follow, non-scientific acquaintances have popped-up all the way, and I stayed fit thanks to Sonny's ambition to create and delegate to me and Julien F. the Imagine Sports Association, and thanks to the Young Reasearcher's of Imagine Institute association and Clarise's motivation I started organizing social events pushing young scientists to think about their future career. And on the way I got involved in the BIOTechno Forum organization, and met Sarah, and Guigui, and David and Perrine, and I enjoyed their efficiency and positive attitude, and it was a pleasure to work with them. I am also grateful to Dr. Victor Mamou, Dr. Pierre Girard and Dr. Denis Lafeuille for giving me a hint of strategy consulting and entrepreneurship, opening new doors for my future.*

*And of course last but not least I am most grateful to my family for always believing in me and motivating me to go one step further. Thank you Olivier for all your love and your patience throughout stressful moments. I am extremely lucky to have you by my side.*

*Dragã Mami, Tati, Rãzvan, Mamaie, Tataie, dragã familie, vã mulţumesc enorm cã sunteţi alãturi de mine, cã mã motivaţi sã fiu ambiţioasã, sã am încredere în mine şi sã-mi continui visurile, chiar dacã asta înseamnã sã locuim în ţãri diferite. Sunt mândrã cã suntem o familie unitã iar toatã munca aceasta vi-o dedic vouã, cãci nimic nu ar fi fost posibil fãrã încrederea şi sprijinul vostru. Vã iubesc!*

# *RÉSUMÉ*

La dystrophie myotonique de type 1 (DM1), ou maladie de Steinert, est une maladie qui touche plusieurs tissus, dont le système nerveux central (SNC). L'atteinte neurologique est variable et inclut des troubles de la fonction exécutive, des changements de comportement et une hypersomnolence dans la forme adulte, ainsi qu'une déficience intellectuelle marquée dans la forme congénitale. Dans leur ensemble, les symptômes neurologiques ont un fort impact sur le parcours académique, professionnel et les interactions sociales. Aujourd'hui aucune thérapie n'existe pour cette maladie.

La DM1 est due à une expansion anormale d'un triplet CTG non-codant dans le gène DMPK. Les ARN messagers DMPK, porteurs de l'expansion, s'accumulent dans le noyau des cellules (sous forme de foci) et perturbent la localisation et la fonction de protéines de liaison à l'ARN, notamment des familles MBNL et CELF, ce qui entraine des défauts d'épissage alternatif, d'expression, de polyadenylation et de localisation d'autres ARN cibles. Malgré le progrès récent dans la compréhension des mécanismes de la maladie, les aspects cellulaires et moléculaires de l'atteinte neurologique restent méconnus: nous ne connaissons ni la contribution de chaque type cellulaire du cerveau, ni les voies moléculaires spécifiquement dérégulées dans chaque type cellulaire. L'objectif de ma thèse a été de répondre à ces deux questions importantes en utilisant un modèle de souris transgéniques et des cellules primaires dérivées de celui-ci.

Pour mon projet, j'ai utilisé les souris DMSXL générées par mon laboratoire. Ces souris reproduisent des caractéristiques importantes de la DM1, notamment l'accumulation des ARN toxiques et la dérégulation de l'épissage alternatif dans plusieurs tissus. L'impacte fonctionnel des transcrits *DMPK* toxiques dans le SNC des souris DMSXL se traduit par des problèmes comportementaux et cognitifs et par des défauts de la plasticité synaptique. Afin d'identifier les mécanismes moléculaires associés à ces anomalies, une étude protéomique globale a montré une dérégulation de protéines neuronales et astrocytaires dans le cerveau des souris DMSXL. De plus, l'étude de la distribution des foci d'ARN dans les cerveaux des souris et des patients a montré un contenu plus élevé dans les astrocytes par rapport aux neurones. Ensemble, ces résultats suggèrent une contribution à la fois neuronale et gliale dans la neuropathogenèse de la DM1.

L'étude protéomique globale des cerveaux des souris DMSXL, a aussi montré des défauts de protéines synaptiques spécifiques des neurones, que nous avons par la suite validés dans le cerveau des patients. SYN1 est hyperphosphorylée d'une façon CELF-dépendante et RAB3A est surexprimé en réponse à l'inactivation de MBNL1. Les protéines MBNL et CELF régulent l'épissage alternatif d'un groupe de transcrits au cours du développement, et leur dérégulation dans la DM1 entraine l'expression anormale d'isoformes d'épissage embryonnaires dans le tissu adulte. Dans ce contexte, j'ai étudié si les défauts des protéines RAB3A et SYN1 sont associés à une dérégulation d'épissage, et si les anomalies des protéines synaptiques identifiées dans la DM1 reproduisent des évènements embryonnaires de la régulation de RAB3A et SYN1. Mes résultats indiquent que les défauts de ces protéines dans les cerveaux adultes ne sont pas dus à une altération de l'épissage alternatif des transcrits et ne recréent pas des évènements embryonnaires. La neuropathogenèse de la DM1 va, donc, au delà de la dérégulation de l'épissage et d'autres voies moléculaires restent à explorer dans les cerveaux DM1.

Afin d'identifier des sous-populations cellulaires susceptibles à l'accumulation des ARN

toxiques, nous avons étudié la distribution des foci dans plusieurs régions cérébrales. Nous avons trouvé une accumulation très prononcée des ARN toxiques dans les astrocytes de Bergmann du cervelet des souris DMSXL et des malades DM1, en association avec une hyperactivité neuronale des cellules de Purkinje. Une analyse protéomique quantitative a montré une diminution significative de la protéine GLT1 – un transporteur du glutamate exprimé par les astrocytes, notamment par les cellules de Bergmann du cervelet. J'ai confirmé le défaut de GLT1 dans d'autres régions du cerveau murin et humain. La recapture du glutamate par les astrocytes est essentielle pour la physiologie cérébrale, donc je me suis intéressée aux causes et aux conséquences de la diminution de GLT1 dans la DM1. J'ai montré que les niveaux d'ARN GLT1 sont diminués suite à l'inactivation de MBNL1, ce qui pourrait expliquer le défaut de ce transporteur dans la DM1. Mes résultats indiquent que le déficit en GLT1 réduit la recapture du glutamate par les astrocytes DMSXL et entraine une neurotoxicité par le glutamate en co-cultures. De façon importante, l'excitotoxicité neuronale est corrigée par la surexpression de GLT1 dans les astrocytes.

Pour mieux comprendre la spécificité cellulaire de la DM1 dans le SNC, j'ai établi et caractérisé des cultures primaires des neurones et astrocytes dérivées des souris DMSXL. J'ai confirmé une toxicité des ARNs plus sévère dans les astrocytes DMSXL par rapport aux neurones. De plus, les astrocytes DMSXL montrent des défauts de la dynamique de croissance, particulièrement au niveau de l'adhésion, en association avec une diminution des adhésions focales, des défauts de polarisation du cytosquelette et des anomalies de migration. En revanche, les neurones DMSXL montrent des défauts tardifs de neuritogenèse, qui deviennent plus prononcés en co-culture avec des astrocytes DMSXL. Au niveau moléculaire, l'étude protéomique globale des cultures primaires homogènes a indiqué une dérégulation de protéines d'adhésion, essentielles dans le fonctionnement de la synapse tripartite. Ces résultats montrent une forte implication des astrocytes et de la communication neurogliale dans la neuropathogenèse de la DM1.

Enfin, suite à l'hyperphosphorylation de protéines dans la DM1 (comme CELF, MAPT ou SYN1) je me suis intéressée à l'activité des kinases dans le SNC. J'ai étudié les niveaux d'expression et activation des kinases candidates GSK3 et CDK5, connues pour phosphoryler MAPT et SYN1 respectivement, dans les cerveaux des souris DMSXL et des patients DM1. J'ai ensuite élargit l'étude aux neurones et astrocytes DMSXL par une analyse du phosphoproteome, afin de mieux comprendre quelles kinases et voies de phosphorylation sont dérégulées dans la DM1.

Les résultats obtenus pendant ma thèse contribuent à mieux comprendre les mécanismes neuropathologiques de la DM1 et permettront d'identifier d'autres pistes pour de nouveaux

# *ABSTRACT*

Myotonic dystrophy type 1 (DM1) is a severe disorder that affects many tissues, including the central nervous system (CNS). The degree of brain impairment ranges from executive dysfunction, attention deficits, low processing speed, behavioural changes and hypersomnia in the adult form, to pronounced intellectual disability in the congenital cases. The neurological manifestations have a tremendous impact on the academic, professional, social and emotional aspects of daily life. Today there is no cure for this devastating condition.

DM1 is caused by the abnormal expansion of a CTG trinucleotide repeat in the 3'UTR of the *DMPK* gene. Expanded *DMPK* transcripts accumulate in RNA aggregates (or foci) in the nucleus of DM1 cells, disrupting the activity of important RNA-binding proteins, like the MBNL and CELF families, and leading to abnormalities in alternative splicing, gene expression, RNA polyadenylation, localisation and translation. In spite of recent progress, fundamental gaps in our understanding of the molecular and cellular mechanisms behind the neurological manifestations still exist: we do not know the contribution of each cell type of the CNS to brain dysfunction, or the molecular pathways specifically deregulated in response to the CTG expansion. The aim of my PhD project has been to gain insight into these two important questions using a relevant transgenic mouse model of DM1 and cell cultures derived thereof.

In my studies I used the DMSXL mice, previously generated in my host laboratory. The DMSXL mice express expanded *DMPK* mRNA with more than 1,000 CTG repeats. They recreate relevant DM1 features, such as RNA foci and missplicing in multiple tissues. The functional impact of expanded *DMPK* transcripts in the CNS of DMSXL mice translates into behavioural and cognitive abnormalities and defective synaptic plasticity. To identify the molecular mechanisms behind these abnormalities, a global proteomics analysis revealed changes in both **neuron-specific** and **glial-specific** proteins in DMSXL brain. We also investigated RNA foci in DMSXL and human DM1 brains and found non-homogenous distribution between cell types, with a higher foci content in astrocytes relative to neurons. Together these results suggest that both neuronal and glial defects contribute to DM1 neuropathogenesis.

The global proteomics analysis of DMSXL brains also identified abnormalities in neuronal synaptic proteins that we have validated in human brain samples. SYN1 is hyperphosphorilated in a CELF-dependent manner while RAB3A is upregulated in association with MBNL1 depletion. CELF and MBNL proteins regulate the alternative splicing of a subset of transcripts throughout development, and their deregulation in DM1 leads to abnormal expression of fetal splicing isoforms in adult DM1 brains. In this context, I have studied if RAB3A and SYN1 deregulations observed in adult brains are associated with splicing abnormalities or if they recreated embryonic expression and phosphorylation events. My results indicate that the synaptic proteins abnormalities observed in adult DMSXL brains are not caused by defective alternative splicing and do not recreate embryonic events. Thus, DM1 neuropathogenesis goes beyond missplicing and other molecular pathways must be explored in DM1 brains.

To better understand the cellular sub-populations susceptible of accumulating toxic RNA foci we have studied foci distribution in different brain regions. We identified pronounced accumulation of toxic RNAs in Bergman astrocytes of DMSXL mice cerebellum and DM1

patients, associated with neuronal hyperactivity of Purkinje cells. A quantitative proteomics analysis revealed a significant downregulation of GLT1 – a glial glutamate transporter expressed by the Bergmann cell in the cerebellum. I have confirmed the GLT1 downregulation in other brain regions of mouse and human brain. As glutamate uptake by the astrocytes is essential for brain physiology I have studied the cause and consequences of the GLT1 downregulation in DM1. I show that *GLT1* mRNA is downregulated as a consequence of MBNL1 inactivation, which could explain the abnormalities of this glutamate transporter in DM1. My results also indicate that the GLT1 deficit is associated with decreased uptake of glutamate by DMSXL astrocytes and leads to glutamate-induced neurotoxicity in co-cultures. Interestingly, neuronal excitotoxicity is corrected by GLT1 overexpression in the astrocytes.

To gain insight into the brain-cell type specificity of DM1, I have established and studied neuronal and astroglial primary cultures derived from DMSXL brains. I confirmed higher RNA toxicity in DMSXL astrocytes relative to neurons. Moreover, primary DMSXL astrocytes show deficits in growth dynamics, particularly in adhesion, associated with a decrease in focal adhesions, abnormal cytoskeleton polarization and erratic migration. In contrast DMSXL neurons show late neuritogenesis defects, which become more pronounced in co-culture with DMSXL astrocytes. At a molecular level, a global proteomics analysis of homogeneous cultures revealed abnormalities in proteins regulating cell adhesion, important for the proper functioning of the tripartite synapse. These results indicate an important role for the astrocytes and neuroglial interplay in DM1 neuropathogenesis.

Finally, as different proteins have been reported hyperphosphorilated in DM1, like CELF, SYN1 and MAPT, I got interested in the kinases activity in the CNS. I have studied the expression and activity levels of two of the candidate kinases, GSK3 and CDK5, known to phosphorylate MAPT and SYN1 respectively, in DMSXL and DM1 brains. I next extended this study to DMSXL neurons and astrocytes with a phosphoproteomics analysis to better understand the kinases and phosphorylation pathways deregulated in the DM1 brain.

In conclusion, my PhD project contributes to better understand **DM1 brain disease** by providing a better insight into the cell-specific mechanisms operating in the DM1 brain, guiding us closer to efficient CNS therapies.

# *TABLE OF CONTENTS*

# *LIST OF FIGURES*

# *LIST OF TABLES*

# Chapter I. Myotonic dystrophy type 1 – from clinics to therapeutic trials

*"Right now I don't think that the public knows very much about myotonic dystrophy but I feel like it's getting there. I know that it affects his muscles mostly… and the heart, lungs and brain… and that he's not able to focus for very long. Sam has taught me a ton about courage, he teaches me how I'm always ready to help people and how I can help people and how I should help people."*

Extract of "Hope & Inspiration: MDF Community Voices"

Will Florence talks about his brother Sam's journey with congenital myotonic dystrophy. A journey of hope and inspiration, about which both public and scientists did not know much, 25 years ago. A journey that turned out to follow a very difficult path; a path that affects on its way several organs and tissue systems of the people who take up this challenging trail. A complex journey that taught scientists new ways of understanding molecular genetics, of studying the numerous biological consequences of one sole mutation in different types of cells, and pushed them towards new and innovative ways to treat and help the people who have set forth on the myotonic dystrophy journey.

# I.A. Unstable microsatellite repeats and human neurological diseases

About 3% of the human genome is composed of simple sequence repeats of 2-10 nucleotides, known as microsatellites, distributed in both coding and non-coding regions (Lander et al. 2001). Among them, tri- and hexanucleotides are more abundant in exons and, even if the overall abundance of microsatellites is relatively uniform across the genome, the chromosome 19 shows the highest microsatellite density (Subramanian et al. 2003).

Abnormal expansion of a certain group of microsatellites can lead to neurological/neuromuscular disorders, and among them, trinucleotide expansions are the most common group of disease-associated microsatellites. The expanded microsatellite can be located in different regions of a gene and thus have different pathological mechanisms (**Fig. I.1**). A loss of function of the gene, due to disrupted transcription, is observed in the fragile X syndrome (FXS) and Friedreich's ataxia (FRDA); a toxic protein gain of function, due to translation of expanded polyglutamine sequences, is observed in the HD (HD) and several types of spinocerebellar ataxias (SCAs); and a toxic gain of function of the RNA, linked to aggregation and sequestration of disease modulators, is the main cause of myotonic dystrophy type 1 (DM1) and type 2 (DM2), as well as familial amyotrophic lateral sclerosis with frontotemporal dementia (ALS/FTD). Additionally a combined toxicity of protein and RNA is observed in Huntington's disease-like 2 (HDL2) and spinocerebellar ataxia 8 (SCA8). While most of these neurological diseases are caused by expansion of trinucleotides, some are associated with different types of expanded repeats. For instance, DM2 is caused by the abnormal expansion of a tetranucleotide, SCA10 and SCA31 are caused by a pentanucleotide expansion, and ALS/FTD is caused by the abnormal expansion of a hexanucleotide. A summary of these expanded microsatellite diseases, including the causing microsatellite, its location and pathological threshold and main clinical features is presented in **Table I.1**.

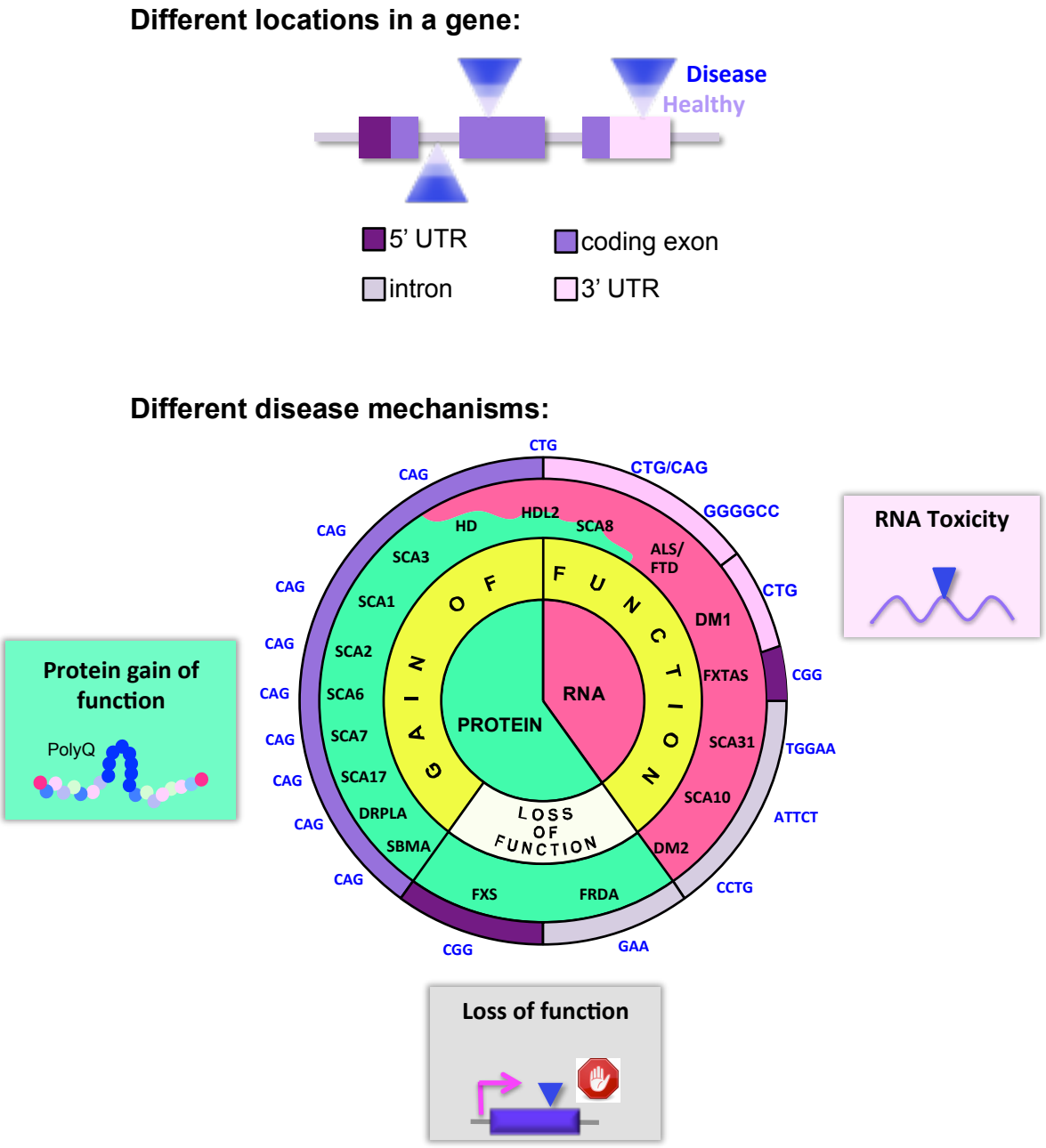


**Figure I.1. Schematic representation of inherited human neurological disorders associated with microsatellite expansions**

Some human neurological disorders are associated with microsatellite expansions in different regions of many different genes, and are mediated by different pathological mechanisms, including gene loss of function, or toxic gain of function of the mutant protein or RNA (adapted from Wojciechowska & Krzyzosiak 2011).

**Table I.1. Summary of some relevant neurological diseases caused by unstable microsatellite expansions.**

| Category | Disease | Microsat. exp | Repeat location | Normal size | Disease size | Main clinical features |
|---|---|---|---|---|---|---|
| Loss of function | Friedreich's Ataxia (FRDA) | GAA | *FXN* Intron 1 | 5-30 | 70-1000 | Progressive ataxia, muscle weakness, sensory loss, cardiomyopathy, diabetes |
| | Fragile X syndrome (FXS) | CGG | *FMR1* 5'UTR | 6-50 | 200-4000 | Severe intellectual disability, ASD, macroorchidism |
| Protein gain of function | Huntington's disease (HD) | CAG | *HTT* Exon 1 | 6-29 | 38-180 | Chorea, dystonia, cognitive decline, psychiatric disease |
| | Spinal and bulbar muscular atrophy (SBMA) | CAG | *AR* Exon1 | 10-36 | 38-62 | Proximal muscle weakness, muscle atrophy, gynecomastia |
| | Dentatorubral-pallidolusyan atrophy (DRPLA) | CAG | *ATN1* Exon 5 | 6-35 | 49-88 | Seizures, cognitive decline, ataxia, choreoathetosis |
| | Spinocerebellar Ataxia 1 (SCA1) | CAG | *ATXN1* Exon 8 | 6-39 | 41-83 | Ataxia, dysarthria, spasticity, ophthalmoplegia |
| | Spinocerebellar Ataxia 2 (SCA2) | CAG | *ATXN2* Exon 1 | <31 | 32-200 | Ataxia, slow eye movement, hyporeflexia, motor disease, occasional parkinsonism |
| | Spinocerebellar Ataxia 3 (SCA3) | CAG | *ATXN3* Exon 8 | 12-40 | 52-86 | Ataxia, dystonia, lower motor neuron disease |
| | Spinocerebellar Ataxia 6 (SCA6) | CAG | *CACNA1A* Exon 47 | <18 | 20-33 | Ataxia, dysarthria, sensory loss |
| | Spinocerebellar Ataxia 7 (SCA7) | CAG | *ATXN7* Exon 3 | 4-17 | >36 to >460 | Ataxia, dysarthria, cone-rod dystrophy retinal disease |
| | Spinocerebellar Ataxia 17 (SCA17) | CAG | *TBP* Exon 3 | 25-42 | 45-66 | Ataxia, dementia, chorea, seizures, dystonia |
| RNA gain of function | Myotonic dystrophy type 1 (DM1) | CTG | *DMPK* 3'UTR | 5-37 | >50 to >4000 | Myotonia and muscle weakness, cardiac-endocrine-endocrine-GI-defects, cognitive and behavioral abnormalities… |
| | Myotonic dystrophy type 2 (DM2) | CCTG | *CNBP* Intron 1 | <30 | 55-1100 | Proximal myotonia and muscle weakness, multisystemic abnormalities, cognitive and behavioral dysfunction |
| | Fragile X tremor/ataxia syndrome (FXTAS) | CGG | *FMR1* 5'UTR | 6-50 | 55-200 | Intellectual disability |
| | Spinocerebellar Ataxia 10 (SCA10) | ATTCT | *ATXN10* Intron 9 | 15-34 | 89-250 | Ataxia, dysarthria, seizures, dysphagia |
| | Amyotrophic lateral sclerosis & frontotemporal dementia (ALS/FTD) | GGGGCC | *C9ORF72* Intron1 | 2-30 | 300-3800 | Motoneuron degeneration, muscle wasting, weakness, pre-senile dementia |
| Combined mechanism | Huntington's disease -like 2 (HDL2) | CTG | *JPH3* Exon 2A / 3'UTR | 6-27 | 36-57 | Chorea, dystonia, cognitive decline |
| | Spinocerebellar Ataxia 8 (SCA8) | CTG/CAG | *ATXN8/OS* 3'UTR | 15-50 | 71-21.300 | Ataxic dysarthria, nustagmus, limb and gait ataxia, cerebellar atrophy |

# I.B. Clinical and genetic aspects of DM1

Described for the first time in 1909 by Steinert and, independently, by Batten and Gibb, myotonic dystrophy type 1 (DM1) is today the most common form of adult muscular dystrophy. Although many reports cite a worldwide prevalence of 1 in 8,000 individuals (Harper 2001), recent literature review studies point out the great variability between geographical regions, ranging from 1/200,000 to 1/5,500 (Theadom et al. 2014), without taking into account the high prevalence of 1/632 people in Saguenay-Lac-St-Jean, a geographically isolated region northeast of Quebec, Canada (Mathieu and Prevost 2012).

## I.B.I Genetic mechanisms behind DM1

The autosomal dominant mode of inheritance of DM1 was known since 1918, as well as the appearance of symptoms at an earlier age in subsequent generations within a DM1 pedigree, a phenomenon that we call today *anticipation* (Harper et al. 1992). Additionally, the symptoms become more severe from one generation to the next: while the grandparents usually show mild cataracts with minimal muscular involvement, the parents show more severe neuromuscular symptoms and the affected children (usually in the third generation of a typical DM1 family) show severe neurological as well as muscular symptoms. Interestingly, the severe congenital form of the disease is mostly, but not exclusively, inherited from affected mothers. For a long time, this increase in severity of one genetic disease, in addition to the influence of the gender of the transmitting parent, was difficult to understand in the context of Mendelian inheritance.

The discovery of the dynamic mutation leading to DM1 shed light on this puzzling genetic condition. Positional cloning strategies allowed the identification of an abnormally expanded CTG trinucleotide in the 3' untranslated region (UTR) of what we know today as the *DM protein kinase* (*DMPK*) gene (Aslanidis et al. 1992; Brook et al. 1992; Fu et al. 1992; Mahadevan et al. 1992), located on the chromosome 19q13.32, between the upstream *Dystrophia Myotonica WD Repeat Containing* (*DMWD*) gene and the downstream *Sine Oculis Homeobox Homolog*

*5* (*SIX5*) gene (**Fig. I.2**). The size of the CTG expansion is highly polymorphic, varying between 5 and 37 repeats in the non-affected population, while DM1 patients carry more than 50 CTG repeats. Subsequent studies indicated a positive correlation between the number of the CTG repeats and the severity of the symptoms, and a negative correlation with the age of onset (Harley et al. 1993). Disease-associated CTG repeats are highly unstable, increasing in size during intergenerational transmission. Intergenerational instability also plays an important role in DM1, resulting in the transmission of a larger repeat number from one generation to the next, which will generally give rise to more severe symptoms, appearing at a younger age, accounting thus for the anticipation phenomenon. Moreover, the gender and CTG repeat size of the parent can influence the expansion size of the child. When the parent shows <±100 CTG repeats, the larger expansions are inherited by paternal transmission; whereas when the parents have >±500 CTG repeats, paternal transmission usually results in CTG contraction while maternal transmission leads to dramatically high CTG lengths, that are usually associated to the congenital form in the newborn (Barceló et al. 1993; Brunner et al. 1993). Interestingly, the same transmission dynamics is also observed for the 38 to 50 CTG repeats premutation. These premutations are not directly pathogenic but can result in pathogenic expansion in the following generation, acting thus as a reservoir of DM1 mutations in the healthy population (Imbert et al. 1993; Martorell et al. 2001).

The expanded repeats are also unstable in somatic tissues, throughout the life on an individual, resulting in the accumulation of larger repeats over time. The somatic instability generates a range of different sizes of CTG repeats within a tissue known as somatic mosaicism. Different degrees of repeat size variability among different tissues could contribute to the phenotypical variability of DM1 (Martorell et al. 1995; Martorell et al. 1998). Indeed, larger expansions occur in the most affected tissues, like muscle, brain or liver, which can reach 2- to 13-fold greater sizes compared to blood leucocytes (Zatz et al. 1995; Thornton et al. 1994). It has been proposed that expansion-biased, age-dependent somatic instability, may contribute to the

aggravation of disease symptoms with age (Ashizawa T, Dubel JR 1993; Monckton et al. 1995; Gomes-Pereira & Monckton 2006).

A second type of DM, called DM2 or proximal myotonic myopathy (PROMM), clinically related to DM1, is caused by the expansion of a CCTG tetranucleotide in the first intron of the *CCHC-type zinc finger nucleic acid binding protein* (*CNBP*) gene, previously known as *zinc finger 9* (ZNF9) (Liquori 2001). DM2 patients show similar muscular, cardiac and CNS-related symptoms, as well as molecular and histological abnormalities, pointing to a common pathological mechanism between DM1 and DM2 (Cho & Tapscott 2007).

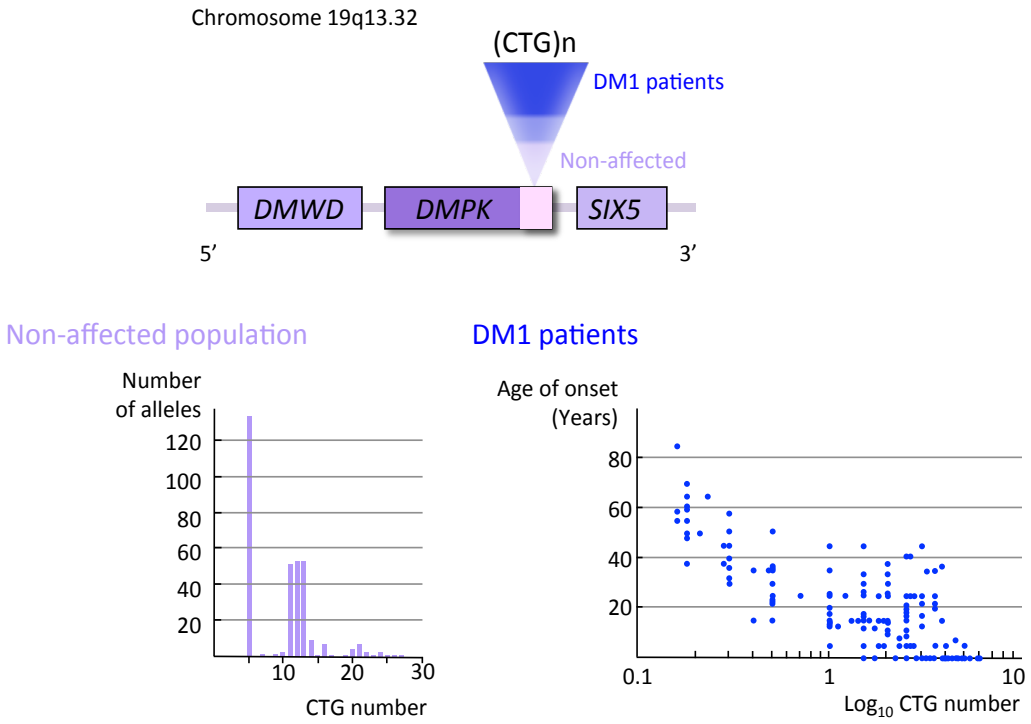


**Figure I.2. Representation of the *DM1* locus and CTG repeat number in non-affected and DM1 population**
**(A)** DM1 locus on chromosome 19q13.32 including DMWD, DMPK and SIX5 genes and the CTG repeat in the 3'UTR of DMPK. **(B)** Distribution of CTG alleles in the non-affected population (adapted from Brook et al. 1992). **(C)** Distribution of CTG repeats at age of onset in DM1 patients (adapted from Harley et al. 1993).

# I.B.II DM1 clinical spectrum

Myotonic dystrophy type 1 (DM1, OMIM #160900) is a very complex neuromuscular disorder with multisystemic clinical manifestations. From a clinical point of view the disease manifests through myotonia (delayed muscle relaxation), progressive muscle weakness, cardiac conduction defects, insulin resistance, gastrointestinal (GI) dysfunction, posterior iridescent cataracts, cognitive and behavioral abnormalities, as well as excessive daytime sleepiness (Harper 2001; Schara & Schoser 2006). The clinical spectrum of DM1 is thus highly variable, making the clinical diagnosis very difficult, as well as the application of standardized medical aid and the establishment of homogeneous groups for clinical studies. Recently the French DM-Scope Registry integrated data from 2167 French patients to support the establishment of five main clinical categories: congenital, infantile, juvenile, adult and late-onset, based on the occurrence and onset of the main symptoms of DM1 and the distribution of the CTG size (De Antonio et al. 2016; Dogan et al. 2016). The CTG repeat size was broadly distributed within each clinical form and it increased significantly with the severity of the symptoms.

## I.B.II.1 Late-onset form.

It represents the mildest form of the disease, often asymptomatic and thus frequently undetected. The age of onset of the symptoms is around 50 years and the search for posterior subcapsular iridescent cataracts is often helpful for clinical diagnosis. Mild myotonia can also be present in some late-onset patients.

## I.B.II.2 Adult form.

The adult form of DM1, sometimes referred as *classical* form, is highly multisystemic, with an onset of symptoms around 35 years of age. It is generally characterized by myotonia (delayed relaxation after voluntary muscle contraction) and distal muscle weakness and wasting, as well as cardiac conduction defects that can lead to arrhythmia and, sometimes, sudden death. Muscular

biopsies reveal histopathological changes in skeletal and cardiac muscles, which include increased variation in muscle fibers, splitting and atrophic fibers, centrally-located nuclei and fibrosis. Other DM1 features include insulin insensitivity, endocrine disorders that can lead to reduced fertility and testicular atrophy, early-onset cataracts, dysphagia and GI tract dysfunction. The CNS is also affected to a variable degree: patients frequently show behavioral dysfunction (including hypersomnolence, avoidant personality and apathy), attention deficits, low IQ scores, frontal dysexecutive syndrome and impaired ability to infer other people's mental states, thought and feelings (known as *Theory of Mind*) (Winblad et al. 2006; Sistiaga et al. 2010; Jean et al. 2014).

### I.B.II.3 Juvenile form.

With an onset of symptoms between 10 and 20 years of age, juvenile patients show more severe cognitive impairment than adult form patients. The prevalent cognitive impairment of juvenile patients is mainly characterized by visuo-spatial deficits, executive dysfunction and learning abnormalities (Douniol et al. 2009). Together they translate into learning problems at school and employment difficulties, and they often require medical attention. The muscular symptoms, typically associated with the adult form, can be absent at young age, appearing later on during adulthood, but with greater severity when compared to patients suffering from the adult form (De Antonio et al. 2016).

### I.B.II.4 Infantile form.

CNS manifestations are more severe in infantile patients than in the juvenile form. In this group, they usually manifest between the age of 1 month and 10 years. The CNS-related symptoms include more pronounced cognitive impairment and reduced IQ values, attention deficits, communication problems, visuo-spatial impairment and they are sometimes associated with autism spectrum disorder (Ekström et al. 2008; Douniol et al. 2012). Myotonia is present at a very early age, followed by muscle weakness, GI troubles and cardiac and respiratory defects (De Antonio et al. 2016).

### I.B.II.5 Congenital form.

It represents the most severe form of the disease and manifests during pregnancy, with reduced fetal movement and polyhydramnios. Newborns present severe hypotonia and muscle weakness, sucking or swallowing difficulties and facial dysmorphism. Respiratory complications are frequent in neonates, leading to the need of mechanical ventilation and high perinatal mortality. Patients who survive the neonatal period show a pronounced delay in psychomotor development as well as severe cognitive impairment (Douniol et al. 2009; Echenne & Bassez 2013).

## I.B.III CNS involvement in DM1

Although classically described as a muscular disease, personality and cognitive disturbances have been widely reported in DM1 patients since the first clinical descriptions. Today the implication of the CNS is well recognized thanks to the increased number of clinical, neuropsychological and neuroimaging studies, recently reviewed in Gourdon & Meola 2017 and Okkersen et al. 2017.

### I.B.III.1 Clinical CNS data

Both behavioral and cognitive impairment are observed in DM1 patients and the severity of the CNS symptoms is often correlated with the size of CTG repeats (Gourdon & Meola 2017). Moreover, the anticipation phenomenon is noticeable in the CNS-related symptoms alone in DM1 pedigrees.

Cognitive impairment, for instance, can range from mild in adult patients to marked intellectual disability in the most severe congenital cases. In adult patients, cognitive impairment manifests through low IQ, affecting both verbal and non-verbal abilities of more than 60% of adult DM1 patients, and it is not a consequence of motor impairment (Jean et al. 2014; Perini et al. 1999). Studies of the childhood form of DM1 indicate low efficiency in coding the visuo-

spatial information of complex special representations, suggesting abnormalities in the fronto-parietal network, which connects two brain regions responsible for the processing and integration of visual spatial relationships and for the subsequent transmission to the action systems (Angeard et al. 2007; Angeard et al. 2011). In addition to intellectual disability, congenital patients present language and speech delays that often require special educational support (Campbell 2012). Verbal and non-verbal episodic memory problems, strategic planning difficulties, impairment of visuospatial, visuoconstructive and executive abilities, as well as visual memory deficits, are often reported in all forms of DM1. Overall cognitive abilities decline progressively with the age of the patient, suggestive of an early and accelerated aging process (Gallais et al. 2017).

Behavioral abnormalities are also often reported in DM1 patients. Besides low initiative, apathy and decreased emotional participation, dysfunction of the cognitive abilities is associated with anxiety and depressiveness in adult patients, as well as some paranoid and aggressive traits, which impact their quality of life (Sistiaga et al. 2010). Juvenile patients, however, report a lower impact of the CNS-related symptoms on their quality of life, even in those cases when the cognitive and psychiatric symptoms are the only clinical manifestations of the disease. This observation could either indicate that they accustom to living with the symptoms, or that the cognitive impairment affects their self-perception more dramatically than in adult patients (Rakocevic-Stojanovic et al. 2014). Infants and congenital patients present avoidant personality, apathy, lack of initiative and difficulties in social interaction, associated with attention deficits, hyperactivity, anxiety and ASD (Meola & Sansone 2007; Ekström et al. 2008). Social cognition is also affected to certain extent in DM1 patients, with recent studies reporting impairments in their "Theory of Mind" or ability to understand the mental state, thought and feelings of others (Kobayakawa et al. 2012; Serra, Cercignani, et al. 2016).

Excessive daytime sleepiness, or hypersomnia, is one of the earliest and most frequent non-muscular symptoms to appear, and it is present in all forms of the disease, severely impacting the day-to-day life. DM1 patients show increased daytime and nighttime REM sleep

propensity, sleep-disordered breathing problems and increased periodic limb movement during sleep, suggestive of motor disinhibition and brainstem deregulation (Yu et al. 2011). However, levels of hypocretin, the main neuropeptide regulating sleep and arousal, and the splicing of hypocretin receptor do not seem to be affected (Ciafaloni et al. 2008; Romigi et al. 2013). The molecular and cellular bases of hypersomnia remain unknown

Lack of initiative, sleep disturbances, lack of physical activity and pain lead to an increased experienced fatigue (not to be confused with muscular fatigue) in around 70% of patients with DM1 (van Engelen 2015). Additionally, emotional and cognitive deficits also affect daily life, family interactions, school and work performance, further increasing their social withdrawal and isolation (Smith & Gutmann 2016).

All together these data demonstrate the impact of the neurological manifestations on the daily like of DM1 patients, and anticipate the benefits of therapies targeting the underlying mechanisms. Thus, continuous research aimed at deciphering the molecular, cellular and pathophysiological mechanisms of CNS dysfunction is an essential step towards promising therapeutical approaches.

### I.B.III.2 Neuroimaging data

An increasing number of neuroimaging studies of DM1 brains have been reported in recent years. There is a clear advantage of such studies compared to post-mortem brain autopsies, as the cognitive and behavioral state of the patients can be assessed in parallel, in the search for correlation with structural and brain connectivity defects. Moreover, they provide an opportunity for longitudinal studies. Recent neuroimaging findings have been reviewed by Okkersen et al and a brief summary is presented below.

Most of the studies published report generalized brain atrophy with reduction of gray matter volume and cortical thickness in frontal, temporal, and parietal cortex, as well as in cerebellum. White matter hyperintensities, small vessels abnormalities, usually associated with

progressive cognitive impairment, dementia and stroke, are observed in MRI studies of DM1 patients in frontal, temporal and parietal lobes (Wardlaw et al. 2015). Decreased fractional anisotropy in diffusion MRI in association, projection and commissural white matter tracts, reveals reduced connectivity in regions correlated with visuospatial reasoning, while abnormally increased connectivity is observed between the cerebellum and sensorimotor areas, similar to patients with autism spectrum disorder (Serra, Mancini, et al. 2016). Decreased brain perfusion, indicating reduced cerebral blood flow, is also reported in frontal, temporal and parietal lobes of DM1 patients, similar to patients suffering from attention deficit hyperactivity disorder (ADHD), schizophrenia, anxiety and depression (Santra & Kumar 2014).

Interestingly, the structural abnormalities reported in these studies occur within brain areas relevant for the CNS symptoms of DM1 patients. The frontal lobe controls the cognitive skills, including emotional expression, problem solving, memory and language; the temporal lobe processes memories related to taste, sound, vision and touch, while the parietal lobe integrates sensory information to form a single perception, including the input from the visual system. It is conceivable, thus, that structural abnormalities in these areas contribute to the executive and visuo-spatial dysfunction of DM1 patients.

Other DM1 brain abnormalities revealed by functional imaging studies include low uptake of glucose (main source of energy in the brain); low levels of N-acetylaspartate (a marker for neuronal integrity that can act as a reservoir for the synthesis of glutamate neurotransmitter); and abnormalities in glutamate-related metabolites (suggestive of deregulated glutamate neurotransmission) (Okkersen et al. 2017).

The recent progress in imaging techniques has provided detailed characterization of brain abnormalities in, and the identification of most affected brain regions and networks in DM1. Future longitudinal studies in homogenous populations of patients, and increasing technical resolution will allow further research progress.

## I.B.IV Histopathological data

Not many histological studies have been reported in DM1 brains, possibly given the difficulty to obtain good quality tissue samples for further processing and analysis. Early of post-mortem DM1 brains have reported cellular and structural abnormalities in DM1 brains. Cell loss in specific nuclei of the brain, including brainstem and cerebellum (Ono et al. 1995; Mizukami et al. 1999), could contribute to the cognitive and behavioral changes. Neurofibrillary tangles, hyperphosphorylated MAPT/Tau protein intracellular aggregates, similar to those seen in Alzheimer's disease have been reported (Yoshimura et al. 1990; Vermersch et al. 1996), in association with abnormal expression of Tau proteins isoforms (Sergeant et al. 2001), thereby placing DM1 in the group of tauopathies.

The combination of imaging and histopathological findings further support the involvement of brain in DM1, and highlight the need to understand the molecular and cellular mechanisms of brain dysfunction in DM1.

# I.C. Molecular pathogenesis of DM1

## I.C.I Mechanisms of repeat dynamics

Although many molecular mechanisms have been proposed to explain the CTG repeat expansion, like DNA polymerase slippage during replication or abnormal DNA repair, one of the best-documented hypotheses, particularly in mammalian systems, suggests the involvement of the mechanisms of mismatch repair (MMR). Indeed a functional MMR system is essential for the formation and accumulation of intergenerational and somatic expansions, while loss of its functional subunits, decreases the formation of expansions (van den Broek et al. 2002; Foiry et al. 2006; Tomé et al. 2009; Gomes-Pereira & Monckton 2004; Savouret et al. 2004). The current view suggests that the expanded sequence forms alternative DNA structures that are recognized by the components of the MMR system. In an attempt to repair the mismatch within the

repeated sequence, the MMR system may erroneously incorporate a higher number of CTG repeat units into the sequence, thus resulting in repeat expansion (Gomes-Pereira & Monckton 2006). Although this hypothesis is consistent with most of the experimental data obtained, particularly through the use of mouse models, we know that the dynamics of triplet repeats is governed by multiple factors, which are not fully understood. Other mechanisms, such as replication restart, other DNA repair systems or the epigenetic context and the chromatin structure of the repeat locus can influence the expansion (McMurray 2010). This field of study is continuously progressing, towards a better understand the mechanisms of microsatellite repeat expansions, hoping to develop therapeutic tools to modulate and/or stop repeat size gains in intergenerational transmissions and in somatic tissues.

## I.C.II *Cis* effects on *DMPK* and *SIX5*

The CTG repeat expansion is located in the 3'UTR region of *DMPK* and within the promoter region of *SIX5*. One the first hypotheses to explain DM1 molecular mechanisms suggested that the CTG expansion would have an effect in *cis*, by altering chromatin structure, promoting nucleosome assembly and inducing haploinsufficiency of *DMPK* and *SIX5* (Wang et al. 1994; Otten & Tapscott 1995). The development of transgenic mouse models allowed to test this hypothesis and contributed greatly to the understanding of DM1 molecular mechanisms. Homozygous *Dmpk* knock-out (KO) or *DMPK*-overexpressing mice did not develop all typical symptoms observed in DM1 patients, while showing only 50% decrease in muscular force, mild myopathy and cardiac conduction defects at later ages (Jansen et al. 1996; Reddy et al. 1996; Berul et al. 1999). On the other hand *Six5* KO mice developed progressive nuclear cataracts (although not of the same type as those described in DM1), reduced male fertility and cardiac dysfunction (Klesert et al. 2000; Sarkar et al. 2000). Thus, many of the major DM1 symptoms, including myotonia, were absent from these KO mouse models, indicating that a dosage effect of *DMPK* and *SIX5* cannot fully explain the etiology of DM1.

# I.C.III *Trans* effects, through mediator proteins

## I.C.III.1 MBNL and CELF deregulation

Nowadays we know that the DNA expansion of a non-coding repeat (transcribed, but not translated) leads to a toxic RNA gain of function. Different multisystemic or conditional murine models, expressing either the human *DMPK* locus, the 3'UTR of *DMPK* containing large expansions, or an unrelated gene containing the CTG expansion, have helped decipher the molecular consequences of the toxic RNA expansions. Progress in the understanding of disease mechanisms was also accelerated by the mapping of the DM2 mutation, a non-coding CCTG tetranucleotide expansion in the *CNBP* gene. The similarity between the clinical manifestations of DM1 and DM2 strongly suggested that the DM1 CTG expansion and the DM2 CCTG expansion should cause disease through similar mechanisms that share critical events and disease intermediates.

*DMPK* transcripts containing expanded CUG repeats form a hairpin secondary structure, and accumulate in the nucleus of DM1 cells, as RNA aggregates or *foci* (Taneja et al. 1995; Davis et al. 1997). These RNA *foci* are dynamic riboprotein structures that sequester and inactivate important RNA binding proteins, contributing to cell dysfunction and disease phenotype (Sicot & Gomes-Pereira 2013). The members of the MBNL (muscleblind-like) family of splicing factors are found among the most enriched proteins sequestered by the RNA foci (Fardaei et al. 2002). On the other hand, overexpression of CELF proteins has been observed in the skeletal muscle (Savkur et al. 2001), heart (Timchenko et al. 2001; Kuyumcu-Martinez et al. 2007) and brain (Dhaenens et al. 2011; Hernandez-Hernandez et al. 2013).

Similarly, CCUG-containing *CNBP* transcripts also accumulate in DM2 cells (Liquori 2001), triggering a similar sequence of pathogenic events. MBNL proteins in particular co-localize with CCUG RNA foci (Fardaei et al. 2002; Yuan et al. 2007), and CELF upregulation has been reported in some studies (Cho & Tapscott 2007).

I will particularly focus on the downstream mechanisms perturbed by the MBNL sequestration and CELF upregulation in DM1 cells in the following pages (a summary is represented in **Fig. I.3**). The disease mechanisms of DM2 are, however, very similar.

## I.C.III.2 Splicing defects

*Mbnl* KO and CELF-overexpressing mouse models have helped dissect the molecular and phenotypical consequences dependent on each one of these DM1 mediators.

MBNL and CELF proteins have an antagonist function in the regulation of alternative splicing throughout development (Kalsotra et al. 2008), Their deregulation in DM1 affects the alternative splicing of numerous downstream target transcripts, resulting in the abnormal expression of fetal splicing isoforms in adult DM1 tissues (Sicot et al. 2011).

Some splicing abnormalities have been directly correlated to some of the muscular symptoms. The abnormal inclusion of exon 2 and exon 7a of the chloride channel (*CLCN1*) has a critical role in the onset of DM1 myotonia, clearly demonstrated in DM1 mouse models (Wheeler et al. 2007). The skipping of exon 11 of bridging integrator 1 (*BIN1*) and of exon 29 of calcium voltage-gated channel subunit alpha1 S (*CACNA1S*) have both been linked to muscle weakness (Fugier et al. 2011; Tang et al. 2012). The increased skipping of the insulin receptor (*IR*) exon 11 is most likely the molecular cause of insulin resistance in DM1 patients (Savkur et al. 2001). Finally the missplicing of the cardiac voltage-gated Na+ channel (*SCN5A*) was suggested as the cause of cardiac conduction delays and arrhythmia (Freyermuth et al. 2016). Some of the splicing abnormalities reported in human muscle were also detected in the muscle of different DM1 mouse models expressing large CUG-containing RNA transcripts (Mankodi et al. 2000; Wang et al. 2007; Guiraud-Dogan et al. 2007). Although many splicing defects have been found in DM1 brains by gene candidate approaches and RNA sequencing, the relevance of these events for the etiology of specific neurological manifestations has not been established.

Splicing abnormalities in DM1 patient brain were first reported in 2001 by the group of André Delacourte (Lille, France), showing an abnormal exclusion of *MAPT* exon 2 in three DM1 cases (Sergeant et al. 2001). Subsequent studies confirmed aberrant splicing events in *MAPT* transcript (Dhaenens et al. 2011; Caillet-Boudin et al. 2014). In 2004 the group of Charles Thornton screened 45 exons of 31 genes known to undergo alternative splicing in the brain, and reported abnormal exclusion of *APP* exon 7, exclusion of *MAPT* exon 2 and exon 10 and abnormal inclusion of *NMDAR1* exon 5 in all seven DM1 brain samples included in their study (Jiang et al. 2004). Different laboratories have shown that these splicing abnormalities represent an increased expression of fetal isoforms in DM1 adult brain and some of them have been observed in other neurological diseases, including Alzheimer's disease, other tauopathies, such as frontotemporal dementia with parkinsonism (FTDP-17), further supporting the deleterious role of missplicing for brain function.

In 2007 our laboratory reported missplicing events for the first time in the CNS of a DM1 mouse model. CTG-expressing DMSXL mice (described in **section I.D.I**) displayed abnormal exclusion of *NMDAR1* exon 21, *MAPT* exon 2 and exon 10 and abnormal inclusion of *MBNL1* and *MBNL2* exon 7 in the frontal cortex (Gomes-Pereira et al. 2007). In the following years different laboratories working on other complementary DM1 mouse models reported additional splicing abnormalities in the brain (Charizanis et al. 2012; Suenaga et al. 2012; Goodwin et al. 2015; Wang et al. 2017), providing new mechanistic insight into brain splicing deregulation and the mechanisms behind the neurological manifestations of the disease, as discussed later in the context of DM1 mouse models of brain disease.

### I.C.III.3 Alternative polyadenylation

Recent polyA-RNA sequencing studies reported abnormal alternative polyadenylation (APA) of a large number of transcripts in DM1 skeletal muscle, $HSA^{LR}$ mouse muscle and *Mbnl* triple KO mouse embryonic fibroblasts (Batra et al. 2014), as well as in the brain of DM1 patients

and *Mbnl1/Mbnl2* double KO mice (Goodwin et al. 2015). MBNL proteins and the APA machinery compete to bind to APA sites of a subset of transcripts, in a mechanism that results in the fine regulation of the 3'UTR, with subsequent implications for mRNA stability and translation. As a result, the sequestration of MBNL proteins by the expanded RNAs leads to aberrant 3' end processing of the target transcripts. Similar to the DM1 splicing abnormalities, many of the deregulated APA events identified in mouse and human DM1 tissues represent a return to a fetal profile. However the degree of contribution of the abnormal APA to DM1 symptoms remains still to be elucidated.

### I.C.III.4 Abnormal localization of mRNAs

MBNL proteins participate to the regulation of mRNA localization within the cell. Transcriptomics analysis of subcellular fractions of mouse myoblasts, following knocking down MBNL1 and MBNL2, indicated a reduction in membrane-associated mRNAs and an increase in transcripts in the cytoplasm fraction. These results support a direct contribution of MBNL1 and MBNL2 in regulating mRNA trafficking and localization within the cells, through the binding to 3'UTRs and in facilitating transport across the cytoskeleton (Wang et al. 2012). The implications of these findings are particularly interesting for the DM1 molecular pathogenesis in highly polarized cells, such as brain cells, notably the neurons. Correct transport of mRNAs and proper localization into specialized cell locations (such as axons, dendrites and synapses in neurons) is essential for the control of localized translation and the proper functioning of the cell. mRNA transport deregulation may result in abnormal cell function and disease

### I.C.III.5 Transcription abnormalities

Molecular abnormalities of DM1 go beyond missplicing and other mechanisms have been proposed to explain disease pathogenesis. Several transcription factors are found sequestered by the *DMPK* transcript, even if not necessarily bound to the foci (Sicot & Gomes-Pereira 2013). Such is the case for SP1, SP2, SP3, RARγ, STAT1 and STAT3 (Ebralidze et al. 2004), which are

leached from the chromatin, leading to significant decrease of target mRNA expression. NKX2-5 (NK homeobox 5) transcription factor (Yadava et al. 2008), and SPEN/SHARP (SPEN homolog) transcriptional regulator (Dansithong et al. 2011) are also deregulated by the DM1 mutation, leading to changes in gene expression in DM1 muscular and cardiac cells, likely contributing to muscular and cardiac symptoms of DM1 patients. Moreover, MBNL1 sequestration by toxic CUG RNA foci can also lead to abnormal transcription of certain targets. Transcriptional profiling of *Mbnl1* KO mice showed that the majority of transcriptome changes in mice expressing expanded CTG repeats can be attributed to MBNL1 loss of function, including alternative splicing changes and altered transcription of target transcripts (Osborne et al. 2009).

### I.C.III.6 Deregulated mRNA decay

CELF and MBNL family members not only regulate alternative splicing but also other post-transcriptional mechanisms, such as the control of mRNA decay. By binding to the 3'UTR of target transcripts, MBNL1 and CELF1 proteins destabilize their mRNA targets and facilitate their decay. Interestingly, MBNL1 binds and accelerates the decay of *Celf1* transcript, while CELF1 binds and promotes decay of *Mbnl1*. MBNL1 sequestration by the expanded RNA foci could lead to a decreased decay of Celf1, thus further contributing to overexpression of CELF1 in DM1 (Masuda et al. 2012). However, the possible contributing role of MBNL1 to CELF1 upregulation must be further explored, as *Mbnl* KO mice do not show increased CELF1 expression (Kanadia et al. 2003).

### I.C.III.7 Deregulation of microRNAs

Increasing numbers of studies are focusing on the deregulation of microRNAs in DM1. On one hand, microRNA deregulation could explain the origin of individual DM1 molecular events and associated symptoms. On the other hand, microRNAs may be useful in the future as non-invasive serum biomarkers of DM1 disease progression. To substantiate this hypothesis

different microRNAs are deregulated in DM1 skeletal muscle (Perbellini et al. 2011) and heart tissue (Rau et al. 2011), as well as in plasma of DM1 patients (Koutsoulidou et al. 2015; Perfetti et al. 2016) (**Table I.2**).

One of the best-documented microRNA deregulation in DM1 is the abnormal expression of miR-1. Rau et al have reported in 2011 the downregulation of miR-1 in the cardiac muscle of DM1 patients. MBNL1 is essential for the cleavage of pre-miR-1 into miR-1, and the sequestration of MBNL1 by the toxic CUG RNA foci leads to lower amounts of functional miR-1. To illustrate the consequences of miR-1 downregulation, two of its targets were found upregulated in DM1 heart: the cardiac L-type calcium channel gene (CACNA1C, the main calcium channel in the heart) and connexin43 (GJA1, which controls intra cardiomyocyte conductance) (Rau et al. 2011) CACNA1C and GJA1 deregulation might subsequently contribute to arrhythmias and cardiac conduction defects in DM1 patients. The same year Perbellini et al. reported an upregulation and aberrant localization of miR-1 in DM1 skeletal muscle, in association with the upregulation of its targets (Perbellini et al. 2011). The discrepancy in the reported miR-1 levels could be explained by differential regulation of miR-1 expression between studied tissues. In all cases, the outcome of miR-1 abnormal expression and localization in DM1 is an upregulation of its targets, likely mediated an impairment of the miR-1 function. Such molecular abnormalities could contribute to DM1 pathology.

However, the direct link between the CTG expansion and the functional contribution of microRNA deregulations to DM1 pathology still needs to be investigated. Moreover, microRNA status in DM1 brain should also be assessed, as microRNAs play an essential role in CNS development and function (Rao & Pak 2016).

**Table I.2. microRNA deregulation in DM1**

| MicroRNA | Physiological function | Deregulation in DM1 | Tissue studied | Reference |
|---|---|---|---|---|
| miR-1 (miR-1a, miR-1b) | Myogenesis, cardiogenesis, control of cardiac conduction, inhibition of proliferation | Downregulation | Heart | Rau 2011 Perbellini 2011 |
| | | Upregulation and abnormal localization | Skeletal muscle | Perbellini 2011 |
| | | Upregulation | Plasma | Perfetti 2016 |
| miR-27b | | Downregulation | Plasma | Perfetti 2016 |
| miR-29b, miR-29c | Cardiac adaption to stress | Downregulation | Skeletal muscle | Perbellini 2011 |
| miR-33 | Cholesterol metabolism Cell proliferation | Downregulation | Skeletal muscle | Perbellini 2011 |
| miR-133 (miR-133a, miR-133b) | Myogenesis Control of cardiac conduction Muscle hypertrophy Apoptosis | Abnormal localization | Skeletal muscle | Perbellini 2011 |
| | | Upregulation | Plasma | Perfetti 2016 & Koutsoulidou 2015 |
| miR-140-3p | Myofibroblast differentiation, chondrocyte proliferation | Upregulation | Plasma | Perfetti 2016 |
| miR-206 | Myogenesis | Abnormal localization | Skeletal muscle | Perbellini 2011 |
| | | Upregulation | Plasma | Perfetti 2016 & Koutsoulidou 2015 |
| miR-335 | Muscle regeneration | Upregulation | Skeletal muscle | Perbellini 2011 |
| miR-454 | Tumor suppressor | Upregulation | Plasma | Perfetti 2016 |
| miR-574 | Cell differentiation | Upregulation | Plasma | Perfetti 2016 |

## I.C.III.8 Antisense transcription at the *DMPK* locus

More than 70% of the mammalian genome presents anti-sense transcription, occurring from the opposite DNA strand to a sense transcript (Katayama et al. 2005). This phenomenon also occurs at the *DMPK* locus, where an anti-sense transcript starts at the *SIX5* regulatory region and extends towards *DMPK*. In the healthy population CTCF-binding sites are located on each side of the CTG repeat, promoting nucleosome assembly and transcriptional silencing of the *DMPK* 3'UTR. The anti-sense transcription results in small 21 nucleotide fragments in the healthy population. In DM1 the CTG expansion leads to loss of the CTCF binding, spread of heterochromatin and expression of a long anti-sense transcript that covers the expansion on the opposite DNA strand (Cho et al. 2005). The expression of this CAG anti-sense transcript is

detected in adult and congenital DM1 patient tissues, including heart, skeletal muscle, diaphragm and brain as well as in DMSXL transgenic mouse model, forming toxic RNA foci (Huguet et al. 2012; Michel et al. 2015). However its contribution to DM1 has not been fully resolved. In cell culture models, the CAG repeats form nuclear foci, sequester MBNL and result in missplicing suggesting a role in DM1 pathogenesis (Mykowska et al. 2011). This hypothesis is further supported by recent reports indicating that in DM1 the anti-sense transcript spans >6 kb, uses alternative transcription start sites and polyadenylation sites and undergoes alternative splicing that can remove the CUG repeat as part of an intron. Moreover, its expression level increases with disease severity (Gudde et al. 2017) suggesting that the anti-sense transcript can contribute to DM1 pathogenesis.

### I.C.III.9 Translational abnormalities

CELF has been implicated in the regulation translation of important proteins, such as p21 and MEF2A. These proteins are essential in regulating cell cycle arrest and skeletal muscle differentiation. In line with this view, the overexpression of CELF1 results in abnormally high levels of MEF2A and p21, and in the inhibition of myogenesis. Overexpression of p21 and MEF2A was reported in the skeletal muscle of DM1 patients and it could contribute to muscle phenotypes (Timchenko et al. 2004).

Since MBNL proteins regulate mRNA localization, they could subsequently impact localized translation of specific transcripts expressed in particular cell locations. Analysis of ribosome-associated mRNAs in MBNL-depleted myoblasts indicated a reduction in the overall abundance of these ribosome-bound mRNAs, suggesting that MBNL depletion results in reduced translation of this subset of mRNAs (Wang et al. 2012).

### I.C.III.10 RAN translation

Repeat-associated non-ATG translation (RAN translation) has been identified for the first time in spinocerebellar ataxia type 8 (SCA8). In this novel and non-orthodox translation,

trinucleotide RNA expansions can undergo translation without the need of an initiation ATG codon, producing homopolymeric proteins in all three reading frames (Cleary & Ranum 2013). Both SCA8 and DM1 are caused by the abnormal expansion of the same trinucleotide, CTG/CAG, which could be RAN translated to produce six different polypeptides: the CUG RNA transcript would result in polyLeu, polyCys and polyAla while the CAG RNA would be translated into polyGln, polyAla and polySer. DMSXL mice were shown to accumulate some polyGln aggregates in cardiac myocytes and in leukocytes, while DM1 patients display polyGln in myoblasts, skeletal muscle and blood (Zu et al. 2011). Moreover the polyGln aggregates colocalize with the early indicator of apoptosis, caspase-8, suggestive of a toxic pro-apoptotic effect of RAN proteins. However the pathological contribution of RAN-translated products in DM1 pathological required further investigation.

### I.C.III.11 Post-translational modifications

Several proteins show abnormal phosphorylation in different tissues of DM1 patients, hinting at a possible global deregulation of the cell kinome in DM1. Among them, hyperphosphorylation of CELF1 is observed in DM1 skeletal muscle, heart and brain (Savkur et al. 2001; Timchenko et al. 2001; Hernandez-Hernandez et al. 2013), associated with increased phosphorylation and activity of PKCα/βII in DM1 heart (Kuyumcu-Martinez et al. 2007). In DM1 brains, hyperphosphorylation of Tau has been reported in association to neurofibrillary tangles (NFTs) (Sergeant et al. 2001). Synapsin 1 is hyperphosphorylated in association with CELF upregulation (Hernandez-Hernandez et al. 2013). Several kinases of the mTORC1 pathway appear deregulated, including AKT, GSK3β and rpS6 in DM1 patient-derived neural stem cells (NSCs) (Denis et al. 2013) and $HSA^{LR}$ mice (Brockhoff et al. 2017). All together these results suggest significant phosphorylation changes in DM1 brains. However, global kinase activity and changes in the DM1 phosphoproteome have not been systematically assessed.

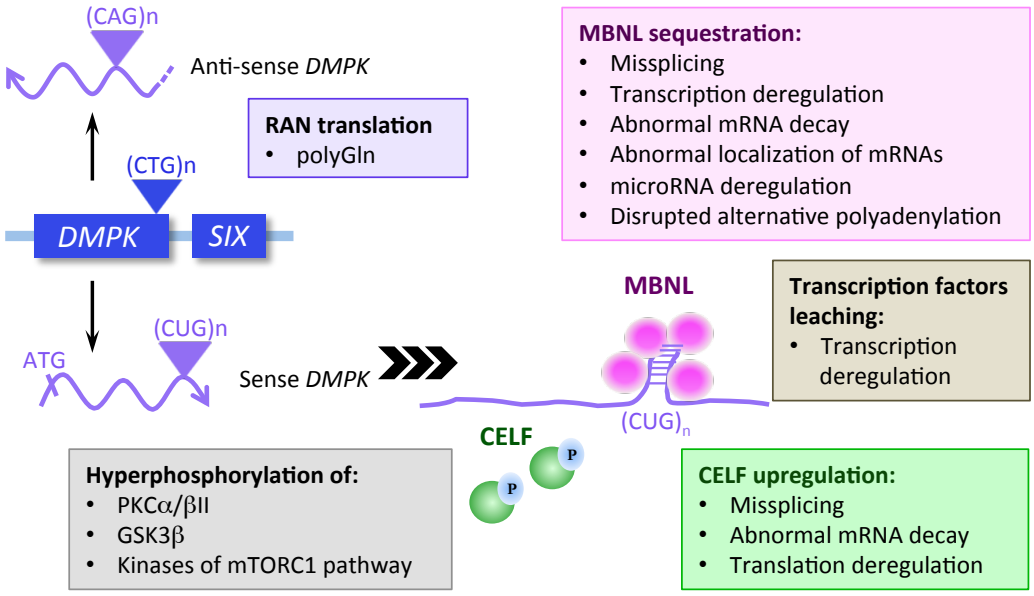


**Figure I.3. Representation of the molecular pathogenesis of DM1.**
The expanded DMPK gene is transcribed into sense and antisense transcripts that accumulate into toxic nuclear foci, deregulating downstream mediators. MBNL family members are sequestered by the expanded transcripts, resulting downstream abnormal RNA metabolism. Upregulation of CELF proteins though hyperphosphorylation leads to perturbed splicing, mRNA decay and abnormal translation. Abnormal RAN translation also occurs from the expanded transcripts. Other transcription factors and protein kinases are also directly or indirectly affected by the CTG expansion.

# I.D. Transgenic mouse models for DM1 pathology

## I.D.I DMSXL mouse model - a powerful tool to study the disease

In order to explore the molecular and cellular mechanisms of DM1, our laboratory created a transgenic mouse model containing a large number of CTG repeats within the human *DMPK* locus. The first transgenic mice contained a large fragment of 45 kb of genomic DNA from a mildly affected patient, with 55 CTG repeats (Gourdon et al. 1997). The 3' region of *DMPK* of the daughter of this patient was cloned into the same 45 kb of human genomic DNA to create the DM300 mice, which carried originally 360 CTG repeats. A fragment with 20 CTG repeats was also cloned within the large *DMPK* locus to create the DM20 control mice (Seznec et al. 2000). The marked expansion-biased intergenerational instability of the DM300 mice gave rise

to progeny carrying increasing CTG sizes over the years, reaching today more than 1,000 CTG repeats (and up to ~2000 CTG) in the DMSXL mice (Gomes-Pereira et al. 2007). The increase in CTG size in DMSXL mice was accompanied by an increase in the severity of the phenotype, with higher mortality, severe growth retardation, splicing abnormalities and more severe myotonia and muscle weakness (Gomes-Pereira et al. 2007, Huguet et al. 2012).

The DMSXL mice have been used to address different research questions in our laboratory. Since the CTG repeats are embedded in their human genomic context, surrounded by most of their regulatory elements, our DM1 transgenic mice have been used to understand the mechanisms driving the instability of CTG repeat expansions in DM1. By crossing the DM300 mice with different mouse lines deficient in DNA repair proteins, our laboratory has demonstrated the need for a functional MMR repair system for the generation of intergenerational and somatic repeat expansions ((Savouret et al. 2003; Savouret et al. 2004; Foiry et al. 2006; Tomé et al. 2009).

The expanded *DMPK* transgene is expressed under the control of its human promoter, which allows ubiquitous expression in many mouse tissues. Therefore, the DMSXL line has been used to investigate the downstream mechanisms of DM1 pathophysiology in multiple tissues. A description of DM300/DMSXL phenotypes and abnormalities is detailed in **Table I.3**, and a summary is presented below.

Homozygous DMSXL mice express enough toxic RNA to produce toxic CUG RNA foci in multiple tissues, MBNL1 and MBNL2 sequestration, CELF1 and CELF2 overexpression, splicing defects in multiple tissues and, as a result, they develop a multisystemic phenotype (Seznec et al. 2001; Huguet et al. 2012; Hernandez-Hernandez et al. 2013; Michel et al. 2015; Sicot et al. 2017) Interestingly, antisense *DMPK* transcripts are also expressed in DMSXL mice and accumulate in nuclear foci (Michel et al. 2015). The laboratory is continuously studying the mechanistic link between the repeat expansion and the different phenotypes recreated in DMSXL mice (particularly in the CNS and in the early post-natal period), to establish the

foundations of therapies in the future. In the meantime, and through international collaborations, the DMSXL mice are already being used to test the outcomes of different ongoing therapeutic assays, which will be detailed at the end of this chapter.

The DMSXL mice were until recent the only mouse model expressing large CTG repeats expansion in the CNS, representing thus a valuable tool to study the disease mechanisms in the brain. Indeed, they show cognitive and behavioral abnormalities including low exploratory activity, increased anxiety, working memory impairment and anhedonic-like behavior and cerebellum-dependent motor incoordination. These phenotypical defects have been associated with electrophysiological abnormalities in synaptic transmission and Purkinje cell firing and molecular deregulations of RAB3A and SYN1 synaptic proteins, as well as the glial GLT1 glutamate transporter (Hernandez 2013, Sicot 2017). Studies in DMSXL mice and cell cultures derived thereof indicate that both neuronal and astroglial brain cells are affected by the CTG expansion. The previous global proteomics approaches performed in our laboratory corroborate this view. When we analyzed expression and phosphorylation changes in the proteome of different DMSXL brain regions, we found abnormalities in proteins primarily expressed in neurons, astrocytes or oligodendrocytes, further suggesting that all these cell types are affected by the repeat expansion. Therefore, future research should be focused on understanding the molecular intermediates and pathways deregulated in different brain cells in response to the CTG expansion.

**Table I.3. Phenotypical and molecular abnormalities reported in DM300/DMSXL mice.**

| Type of defect | Observed abnormality | Affected tissue | Reference |
|---|---|---|---|
| Phenotypical | Mild myotonia<br>Muscle weakness | Skeletal muscle and heart | Seznec 2001<br>Huguet 2012 |
| | Novelty-induced inhibition, anxiety, spatial and working memory impairment, anhedonia, cerebellum-dependent motor incoordination | CNS | Hernandez 2013<br>Sicot 2017 |
| | Impaired respiratory function | Diaphragm | Panaite 2013 |
| Histological | Centronuclear fibers, interfascicular connective tissue, reduced fiber size | Skeletal muscle, diaphragm | Seznec 2001<br>Huguet 2012<br>Panaite 2012 |
| | Reduced myelination in motor axons, partial denervation and reduced complexity of neuromuscular junction | Sciatic nerves, Diaphragm | Panaite 2011, 2012 |
| Electrophysiological | Reduced paired-pulse facilitation (short term synaptic plasticity) | CNS (Hippocampus) | Hernandez 2013 |
| | Purkinje cell hyperactivity | CNS (Cerebellum) | Sicot 2017 |
| Metabolic | Low levels of Insulin and Insulin-like growth factor binding protein-3 | Serum | Huguet 2012 |
| | Dopamine reduction<br>Increased serotonin metabolites | CNS (Frontal cortex, brainstem) | Hernandez 2013 |
| Molecular | Toxic CUG RNA foci | Almost all tissues studied, including CNS | Seznec 2001<br>Huguet 2012<br>Michel 2015 |
| | Anti-sense RNA foci | Muscle, heart and CNS | Huguet 2012<br>Michel 2015 |
| | Expansion-biased CTG instability (intergenerational and somatic) | Almost all tissues | Seznec 2000<br>Gomes-Pereira 2007 |
| | Co-localization with MBNL1 and MBNL2 | CNS | Hernandez 2013 |
| | CELF upregulation | CNS | Hernandez 2013 |
| | Splicing defects | Skeletal muscle (TA, Diaphragm, Soleus, Gastrocnemius, Plantaris), heart, pancreas, liver and CNS (Frontal cortex, Brainstem, Spinal cord, cerebellum) | Gomes-pereira 2001<br>Guiraud-Dogan 2005<br>Huguet 2012<br>Hernandez 2013<br>Sicot 2017 |
| | Polyglutamine homopolymers of RAN translation products | Heart | Zu 2011 |
| | Altered expression of Tau isoforms | CNS | Seznec 2001 |
| | MAP2 downregulation | Hippocampus | Velazquez-Bernandino 2011 |
| | RAB3A upregulation<br>SYN1 hyperphosphorylation<br>GLT1 downregulation | CNS (Frontal cortex, brainstem, hippocampus) | Hernandez 2013<br>Sicot 2017 |

## I.D.II Other DM1 models and their contribution to CNS studies

Different murine models have contributed greatly to the knowledge of DM1 disease mechanisms, from RNA toxicity to the abnormal expression and function of mediators, ultimately leading to broad phenotypical consequences (Gomes-Pereira et al. 2011). Among them the $HSA^{LR}$ mouse model, was one of the first to provide evidence of the *trans*-dominant role of the CTG repeat in DM1 pathology. Indeed, the sole expression in the mouse genome of 250 CTG repeats in the final exon of the human skeletal actin (HSA) gene, unrelated to *DMPK*, was sufficient to produce nuclear RNA foci that sequester MBNL1 and missplicing in different transcripts, and subsequent myotonia, myopathy and centronucleated muscle fibers heterogeneous in size (Mankodi et al. 2000; Lin et al. 2006). CELF1 levels did not differ in the skeletal muscle of $HSA^{LR}$ mice compared to WT (Kanadia et al. 2003) but later studies reported increased CELF1 levels in the soleus of these mice (Lin et al. 2006). The restriction of the expression of the expanded transcripts to the muscular tissue impedes however the use of these mice to study other tissues affected by the CTG repeat expansion.

Another mouse model that contributed to the comprehension of the consequences of the CTG expansion is the EpA960 mouse model that expresses inducible 960 CTG repeats within *DMPK* exon 15. Expression of the EpA960 transgene in mouse heart induced severe cardiomyopathy, leading to death within 2 weeks, while expression in skeletal muscle resulted in myotonic discharges, muscle wasting and degeneration associated again with nuclear foci, MBNL1 sequestration, CELF1 and CELF2 upregulation and missplicing both in heart and muscle (Wang et al. 2007; Orengo et al. 2008). Increased phosphorylation of PKCα/βII was also reported in the heart of these mice (Kuyumcu-Martinez et al. 2007), and suggested to be the cause of CELF1 protein hyperphosphorylation, stabilization and upregulation.

Recently these mice have been crossed with CamKII-Cre mice to specifically induce the regional expression of the CTG repeats in the neurons of the forebrain. The EpA960/CaMKII-

Cre mice show nuclear foci that sequester MBNL1 and MBNL2 and misregulate alternative splicing. MBNL1 was reduced in the neuronal cytoplasm at 6 months, followed by dendrite degeneration, without signs of missplicing at this age. MBNL2 expression in both nucleus and cytoplasm was reduced at 12 months accompanied by missplicing. As a consequence, EpA960/CaMKII-Cre mice display CNS structural changes, including brain atrophy and degeneration of axons and dendrites, and impairment of hippocampus-dependent learning and synaptic potentiation (Wang et al. 2017). These results suggest that MBNL1 and MBNL2 have two functional roles in the CNS: while MBNL1 is involved in the maintenance of neural projections and dendrites, independently of missplicing; MBNL2 controls alternative splicing and its deregulation in DM1 leads to neurodegeneration.

The pivotal contributing role of MBNL protein sequestration to CNS dysfunction has been demonstrated by the generation of *Mbnl* KO lines. *Mbnl1* KO mice, lacking the CUG-RNA binding MBNL1, develop myotonia, dust-like cataracts, cardiac conduction defects, lack of motivation and apathy as well as splicing defects which are severe in in muscle and heart, but mild in the brain (Kanadia et al. 2003, Suenaga et al. 2012). In contrast, *Mbnl2* KO mice develop mild muscular phenotypes, but significant CNS defects including spliceopathy, sleep disturbance, cognitive deficits and impaired synaptic transmission (Charizanis et al. 2012). These results indicate that, while MBNL1 regulates different molecular mechanisms in multiple tissues, with an important role in muscle pathology, MBNL2 has an essential role in regulating CNS function. The subsequent generation of double *Mbnl1*/*Mbnl2* KO mice resulted in embryonic mortality, but conditional double knock-outs developed more severe muscular, cardiac and brain phenotypes, as well as and missplicing events than *Mbnl1* or *Mbnl2* single KO (Rahul N. Kanadia, Carl R. Urbinati, Valerie J. Crusselle, Defang Luo, Young-Jae Lee, Jeffrey K. Harrison, S. Paul Oh 2003; Goodwin et al. 2015), possibly because functional compensation between MBNL cannot occur in animals lacking both genes.

CELF proteins are upregulated in the skeletal muscle (Savkur et al. 2001) and patient's brain (Dhaenens et al. 2011; Hernandez-Hernandez et al. 2013), suggesting a pathogenic role. The manipulation of CELF expression in mouse models of has provided important insight into this question. CELF1-overexpressing mice develop marked growth retardation, delayed myogenesis, histological abnormalities, missplicing and high mortality, resembling the congenital form of DM1 (Timchenko et al. 2004). Conditional overexpression of CELF1 in adult skeletal muscle recreates abnormal histology and impairs muscle function (Ward et al. 2010), while overexpression in the adult heart leads to cardiac conduction defects and accelerated death (Koshelev et al. 2010). However, the involvement of CELF proteins in DM1 brain has only been demonstrated by missplicing analysis in DM1 cellular models (Zhang et al. 2002; Leroy et al. 2006; Dhaenens et al. 2011). The molecular and physiological consequences of CELF1 or CELF2 upregulation in the brain has not yet been investigated in overexpressing mouse lines (Timchenko et al. 2004; Koshelev et al. 2010).

The availability of complementary murine models is a great asset in the field, which will helped us to better understand the mechanistic behind DM1 pathology, in different tissues and at different molecular levels. The availability of these different models allows the cross-testing of novel identified mechanisms and replication of the results in different models by independent laboratories, contributing for the robustness of the results and working models proposed.

## I.D.III Molecular CNS data

DM1 shows a vast complexity of deregulated molecular mechanisms that add up to the multisystemic nature of the disease. Among all the molecular mechanisms deregulated in DM1, **Table I.4.** summarizes those that have been described in the CNS and that have been mentioned in this chapter.

**Table I.4. Summary of main electrophysiological and mollecular findings in DM1 brain**

| Mechanism affected | Identified defect | Affected tissue in DM1 model | Reference |
|---|---|---|---|
| Electrophysiological activity | Reduced paired-pulse facilitation | Hippocampus DMSXL | Hernandez 2013 |
| | Reduced field excitatory postsynaptic potentials | Hippocampus EpA960/CamKII-Cre | Wang 2017 |
| | Hyperactivity of Purkinje neurons | Cerebellum DMSXL | Sicot 2017 |
| | Reduced field excitatory postsynaptic potentials | Hippocampus *Mbnl2* KO | Charizanis 2012 |
| Molecular | Toxic RNA foci | Most of brain regions of DMSXL, EpA960/CamKII-Cre | Hernandez 2013, Sicot 2017, Michel 2015, Wang 2017 |
| | Anti-sense foci | Frontal cortex DMSXL | Michel 2015 |
| | MBNL1 and 2 sequestration | Frontal cortex DMSXL, EpA960/CamKII-Cre | Hernandez 2013, Michel 2015 |
| | CELF upregulation | Frontal cortex DMSXL | Hernandez |
| Missplicing | *Mapt/Tau* | DMSXL, *Mbnl2* KO & double KO | Gomes-prereira 2007, Hernandez 2013, Charizanis 2012 |
| | *APP, Mapt/Tau, NMDAR1* | DMSXL, CELF1 and 2 upregulation cell models, *Mbnl2* KO | Gomes-Pereira 2007, Hernandez 2013, Jiang 2004, Dhaenens 2011, Leroy 2006, Zhang 2002, Goowin 2015 |
| | *Tanc2, Kcnma1, Limch1, Spna2, St3gal3, Ndrg4, Csnk1d, Ppp1r12a, Cacna1d, Add1, Dlg2, Grin1* | Hipoccampus and forebrain *Mbnl2* KO | Charizanis 2012 |
| | *Sorbs1, Spag9, Dclk1, Mprio, Camk2d,* | Hippocampus and cerebellum of *Mbnl1* KO | Suenaga 2012 |
| Altered protein expression | Altered expression of Tau isoforms | DM300 brain | Seznec 2001, Vermesch 2006 |
| | RAB3A upregulation SYN1 hyperphosphorylation | DMSXL frontal cortex, brainstem, hippocampus | Hernandez 2013 |
| | GLT1 downregulation | DMSXL cerebellum, frontal cortex, brainstem | Sicot 2017 |
| APA | Rgs9, Sptb, Fzr1 | *Mbnl1*&*2* DKO brain | Goodwin 2015 |

# I.E. Therapeutic strategies

Although the research on DM1 molecular mechanisms has progressed remarkably since the initial description of the genetic cause, no curative therapy is available today. However the collaborative efforts of different research groups within the international DM community led to a better characterization and molecular dissection of DM1 disease mechanisms, establishing a rationale for therapy development through the identification of individual events that can be therapeutically targeted. Future therapeutic tools will certainly target different steps in the DM1 pathology mechanisms, from the transcription of the CTG expansion, the formation of toxic RNA foci, and MBNL and CELF deregulation to the deregulation of downstream targets. Of course, targeting DM1 mechanisms as early in the molecular cascade as possible would lead to broader positive effects. Targeting the mutation itself would be ideal, but the task is not easy. Alternatively, in recent years researchers have been developing compounds that target downstream steps in DM1 molecular pathogenesis, trying to ameliorate some symptoms or slow down disease progression. Some of the most promising results are presented below.

## I.E.I Neutralization of RNA toxicity

It is now established that the major pathological agent in DM1 is the expanded CUG RNA. Strategies to destroy or neutralize its effects should therefore be beneficial and reverse DM1 symptoms. The proof of concept that DM1 manifestations are reversible was provided in the conditional GFP-DMPK-$(CTG)_5$ mouse model (Mahadevan et al. 2006). These mice express high levels of a small 5-CTG repeat in the context of *DMPK* 3'UTR, and under the control of an inducible promoter. The expression levels of the short repeat in this mouse line is so high that it is sufficient to trigger myotonia, myopathy and cardiac conduction defects, and modest missplicing but without toxic foci or MBNL sequestration. Importantly, mouse phenotypes are reversed upon transgene silencing, demonstrating that silencing of the toxic expansion can be an efficient therapeutic strategy.

In this context, antisense oligonucleotides (ASOs) have shown very promising results in the neutralization of toxic RNA, either by disrupting MBNL-CUG RNA interaction, thereby avoiding MBNL sequestration and inactivation (Wheeler et al. 2009), or by knocking down the expanded CUG RNA through RNase-H cleavage (Mulders et al. 2009; Lee et al. 2012). Both local and systemic injection of ASOs with different chemistries in CUG-expressing DM1 mice dissolved the nuclear foci, corrected alternative splicing defects and/or improved physiological, histopathological and transcriptomic abnormalities of these mice ((Mulders et al. 2009; Lee et al. 2012; Wheeler et al. 2009; Wheeler et al. 2012).

The promising results obtained by the use of ASOs in mouse models of DM1, together with the low toxicity of these compounds tested in mice and in healthy individuals, led to the first phase 1/2a clinical trial held by Ionis Pharmaceuticals (USA). They have tested the IONIS-DMPK-2.5$_{RX}$, a gapmer-ASO aimed at destroying *DMPK* transcripts in muscle (clinical trial NCT02312011). Even if some reduction of misspliced transcripts was detected, the levels of therapeutic chemical in the biopsies of muscle patients were not high enough to achieve good efficiency, which led to the decision of interrupting further tests with this drug, and instead developing new improved chemistries for future more potent drugs for DM1.

Interestingly other chemistries have been already been tested in DM1 mouse models. Newly modified ASOs have also been successful in decreasing by 70% the expression of the toxic *DMPK* RNA in skeletal muscle and by 30% in the heart of the DMSXL mice, improving body weight, muscular strength and muscle histology, with no obvious toxic effects detected ((Jauvin et al. 2017). Thus different research groups continue to design and develop new ASO chemistries to improve bioavailability and biological efficiency of the therapeutic agents for future clinical trials.

Chemical modulation of the transcription of the CTG expansion could have beneficial effects for DM1 pathology, since it would result in the elimination of the pathogenic element causing disease, the toxic CUG RNA. Actinomycin D, a transcription inhibitor, has a positive

affinity for the CTG-rich sequences and has already been successfully tested in cell models and in $HSA^{LR}$ mice. Intraperitoneal injection of doses that are already approved for human use led to a decrease in transcription of the expanded transcript and improved several missplicing events in $HSA^{LR}$ mice (Siboni et al. 2015).

*New ligand 9* is a rationally-designed small chemical compound that binds CTG and CUG expansions inhibiting the transcription of toxic RNAs and the subsequent formation of MBNL-sequestering foci. Moreover it presents an RNase A-like activity, selectively cleaving the CUG expanded RNAs *in vitro*. The use of this small molecule in a *Drosophila* model of DM1 rescued neurodegeneration, rough-eye phenotype and larvae locomotor function (Nguyen et al. 2015). Although *New ligand 9* seems like a promising therapeutic tool, its efficiency and target specificity should also be tested in other DM1 models.

Derivatives of pentamidine, a small FDA-approved chemical compound, have proven successful in reverting DM1 molecular defects, such as the accumulation of toxic RNA foci and missplicing. These compounds can inhibit transcription of the CTG expansion in a dose-dependent manner, reduce the stability of the toxic transcript or bind to the expanded RNA, thereby liberating MBNL protein from sequestration into foci (Warf et al. 2009)Continuous improvement of the chemical structure led to a less toxic compound, known as furamidine, that efficiently reversed missplicing in cellular models, as well in the quadriceps of $HSA^{LR}$ mice (Siboni et al. 2015). The benefits of this chemical in other tissues remain unknown.

## I.E.II Modulation of disease interemediates

The beneficial effects of MBNL upregulation in DM1 mouse models have been tested, either through AAV-mediated MBNL1 delivery, or by genome manipulation. Both strategies resulted in a recovery of myopathy and improved muscle histopathology, muscle strength and muscular activity, while also showing that MBNL1 overexpressing is not overtly toxic (Lin et al. 2006; Chamberlain & Ranum 2012). These approaches opened the basis for therapeutic

interventions based on the overexpression of MBNL, or on the inhibition of its sequestration by the toxic expansions. Phenybutazone, an already-approved anti-inflammatory drug, has proven efficient in DM1 mouse models. Administration of the drug in the drinking water of the $HSA^{LR}$ mice, during twelve weeks, led to increased transcription of *Mbnl1* by suppressing DNA methylation, decreased sequestration of MBNL1 by the toxic foci, improved muscle histopathology, increased muscle strength and mouse activity performance, and partially corrected missplicing of *Clcn1* leading to increased protein expression (Chen et al. 2016).

Erythromycin has also shown beneficial effects in the $HSA^{LR}$ mouse model. Systemic and oral administration of this natural antibiotic inhibited MBNL1 sequestration by toxic foci, thereby increasing the levels of functional MBNL1. The compound rescued missplicing in a dose-dependent manner and improved myotonia (Nakamori et al. 2016). Thus, this antibiotic could result in a safe promising therapy for DM1 patients.

A PKC inhibitor was also proposed as an efficient DM1 treatment after being tested in EpA960 mice PCK inhibitor administration reduced the levels and hyperphosphorylation of CELF1, prevented CELF-dependent missplicing events, improved cardiac function and reduced the mortality rate of the EpA960 mice (Wang et al. 2009). However knockout of PCKα/β in the GFP-DMPK-$(CTG)_5$ mice did not affect the abnormal CELF1 expression, missplicing or abnormal muscular histology, raising questions on the implication of PKC in DM1 pathology, at least in skeletal muscle (Kim et al. 2016).

GSK3β has been found upregulated in $HSA^{LR}$ mice and DM1 neural stem cells, as well as in patient skeletal muscle. Inhibition of GSK3β in $HSA^{LR}$ mice reduced myotonia, muscle weakness and muscle histopathology (Jones et al. 2012), while the use of GSK3 inhibitors is known to reverse cognitive and behavioral changes in mouse models of FXS ((Mines & Jope 2011). Thus GSK3 inhibitors might be a promising therapy for DM1 patients. A phase 2 clinical trial is currently ongoing by AMO Pharma and it aims to evaluate the safety and efficacy of the

GSK3β inhibitor tideglusib in patients suffering from juvenile and congenital form of DM1 (trial NCT02858908). Results of this clinical trial have not yet been reported.

## I.E.III Empirical strategies and natural compounds

Empirical screening of disease modulators indicate new possible therapeutical targets. Recently the AMPK and mTORC1 pathway were reported deregulated, in association with autophagy, in the skeletal muscle of the $HSA^{LR}$ mice. Two inhibitors of these pathways, AICAR and rapamycin respectively, ameliorate the phenotype of the mice: while AICAR treatment reduces foci content, decreases myotonia, and improves *Clcn1* splicing and protein levels, rapamycin improves mouse muscle force, without affecting splicing (Brockhoff et al. 2017).

Many of these promising drugs and compounds have only been tested in the $HSA^{LR}$ mice, which show a strong phenotype but only in skeletal muscle. Given the multisystemic nature of DM1, the efficiency of these possible treatments must also be tested in other tissues such as heart and brain, in order to fully assess their therapeutic potential.

Natural compounds such as reservatrol (flavonoid found in grapes) and thiamine (vitamin B1) have proved beneficial in rescuing splicing defects or improving patients' symptoms. Although the mode of action is unknown, reservatrol improved splicing defects of *IR* in DM1 patients-derived fibroblasts (Takarada et al. 2015) and thiamine administration, twice a week for 11 months, improved muscular strength, and muscular symptomathology in two DM1 patients.

Among the drugs that alleviate patient symptoms, modafinil, which is efficiently used in the treatment of narcolepsy and excessive daytime sleepiness, is prescribed to DM1 patients that suffer of excessive daytime sleepiness. In a study of 145 patents and 146 relatives and caregivers, modafinil use has been reported beneficial by 90% of the treated patients and 95% of the relatives and caregivers (Hilton-Jones et al. 2012).

While waiting for molecular or pharmacological treatment of CNS-related symptoms, researchers and medical doctors from France, the Netherlands, Germany and United Kingdom

have set up the OPTIMISTIC trial: *Observational Prolonged Trial In Myotonic dystrophy type 1 to Improve Quality of Life- Standards, a Target Identification Collaboration*. This trial aims to improve the quality of life of DM1 patients by using exercise and cognitive behavioral therapy to stimulate active lifestyle, reduce fatigue and decrease the disease burden (van Engelen 2015). The results of the trial should be published in the near future.

## I.E.IV Future gene-editing tools

Recent development of gene editing tools such as the Zinc Finger Nucleases (ZFNs), TALEN (Transcription Activator-Like Effector Nucleases) and CRISPR (Clustered Regulatory Interspaced Short Palindromic Repeats)/Cas9 systems have proven to be effective and reliable tools for genome engineering. ZFNs recognize modules of 30 trinucleotides (or codons) to target the FokI endonuclease activity that will cleave DNA when dimerized. TALEN proteins recognize 33-35 nucleotides to guide the FOKI endonuclease. The CRISPR/Cas9 system uses a guide RNA (gRNA) of 20 nucleotides that will bind and address the Cas9 endonuclease to the target sequence to produce the double strand DNA brake (DSB). Although the three systems are currently used in genome editing, the CRISPR/Cas9 system has several advantages over the ZFNs and TALENs: the design and delivery of the 20 nucleotide targeting RNA is easier than the elaborated design of the protein domains of the ZFNs and TALENs; importantly the multiplexing of different gRNAs targeting different regions and one sole Cas9 endonuclease is possible. However this ease of development and delivery is counteracted by the lower specificity of the CRISPR/Cas9, compared to the ZFNs and TALENs, as the latter need the correct recognition of + and – strands of the DNA for the dimerization and activation of FokI (Kim 2016).

In the field of DM1, many laboratories have been testing the efficiency of the ZFNs, TALENs and CRISPR/Cas9 system to cleave the CTG repeat expansion in somatic cells, thus removing permanently the DM1 mutation, or to eliminate the toxic RNA foci.

An innovative approach has been reported by Gao et al. in 2016. Using TALEN-induced homologous recombination they inserted premature polyadenylation signals (PASs) in the *DMPK* gene, upstream of the CTG repeats. PASs insertion in patients-derived iPS cells led to elimination of the toxic RNAs and reversal of aberrant splicing in the differentiated neurons, astrocytes and cardiomyocytes, opening the possibility for future autologous stem-cells transplantation approaches for DM1. However, the integration of the PAS at the desired locus must be further improved, since less than 10% of the cells showed correct insertion of the PAS and complete loss of the nuclear RNA foci (Gao et al. 2016).

Among the most recent reports that efficiently remove the CTG repeats in DM1 models, van Agtmaal et al. have shown complete and precise excision of the CTG/CAG repeat (+ and - DNA strands) in DM300 and DM1 patients myoblasts, leading to loss of toxic foci formation, normal myoblasts differentiation into myotubes and rescue of splicing defects. Moreover in DM300 myoblasts one single CRISPR cleavage on only one side of the CTG repeat led to large gaps across the CTG sequence (van Agtmaal et al. 2017). Interestingly, induction of DSB within the CTG repeats causes both expansions and contractions, while single-strand breaks induced by CRISPR-Cas9 D10A nickase induced only contractions (Cinesi et al. 2016), suggesting that single strand editing could induce shrinkage of the CTG expansion.

Another recent publication highlights the efficiency of nuclease-null "deactivated" Cas9 (dCas9), which can be packed and delivered by an AAV, in eliminating CUG, CCUG, CAG and GGGCC expanded RNA foci just by binding to the expanded sequence, opening promising routes for the use of the CRISPR/Cas9 system for DM1, DM2, HD, SBMA, various SCAs and ALS. Fusion of the dCas9 to a PIN RNA endonuclease (RCas9) has been tested to act directly at the RNA level to promote the elimination of the expanded repeats in DM1 and DM2 patient primary cells, liberating MBNL proteins and reversing missplicing (Batra et al. 2017).

However careful analysis is essential in this type of DNA-editing approaches, since frequent inversions occur upon double cleavage (van Agtmaal et al. 2017). Another challenge of

the use of gene-editing tools it the high risk of *off target* effects, and special attention should be given to their occurrence before using these systems as gene therapy in patients. Batra et al. propose the use of an RNA-targeted Cas9 system that would avoid the permanent genetic lesion of patient's DNA, while efficiently eliminating the expanded RNA transcripts.

Many types of possible therapeutic approaches for DM1 pathology are being developed and tested in different DM1 models. However not many have tested the biodistribution and efficiency in the CNS. Indeed the design of the chosen therapeutic strategy should take into account the low permeability of the blood-brain barrier, while providing a feasible mode of administration for clinical trials. Although some strategies have managed to eliminate toxic RNAs in iPS-derived neural stem cells (Xia et al. 2015; Gao et al. 2016), gene therapeutic approaches for DM1 brain abnormalities still need to be tested and developed. In the meantime, a better understanding of the molecular and cellular mechanisms operating in DM1 brains is essential, in order to identify critical events of the pathological cascade that can be targeted and corrected by therapeutic strategies based on the use of small, non-toxic molecules with high bio-availability.

# Chapter II. Objectives and thesis structure

The general objective of my PhD project has been to gain insight into the molecular and cellular mechanisms deregulated in DM1 brain. More specifically, I aimed to better understand the contribution of each brain cell type to DM1 CNS dysfunction, and to characterize the molecular pathways specifically deregulated in response to the CTG expansion. To do so, I used the DMSXL mouse model, primary neurons and astrocytes cultures derived thereof and human post-mortem DM1 brain tissues.

Before my arrival to the laboratory our research group had identified abnormal expression and phosphorylation of RAB3A and SYN1 synaptic vesicle proteins, respectively, and a downregulation of GLT1 glial glutamate transporter. My first project focused on the investigation of the mechanisms behind RAB3A and SYN1 proteins abnormalities. I studied the possible contribution of abnormal alternative splicing and disrupted developmental deregulation to the upregulation of RAB3A and hyperphosphorylation of SYN1. The results of this project were reported in the following article:

Oscar Hernández-Hernández, Géraldine Sicot, Diana M. Dincã, Aline Huguet, Annie Nicole, Luc Buée, Arnold Munnich, Nicolas Sergeant, Geneviève Gourdon and Mário Gomes-Pereira. **Synaptic protein dysregulation in myotonic dystrophy type 1 – Rare diseases** (2013) 1: e25553

My second project focused on the deregulation of GLT1 that we found in DMSXL and DM1 brains. Given the essential role of GLT1 in the fine regulation of glutamate levels in the CNS, my aim was to determine which molecular mechanisms are responsible for GLT1 downregulation in DM1, and what are the functional consequences of this downregulation. The

experimental results obtained in this study are presented in the following article, in which I am co-first author (*):

Géraldine Sicot *, Laurent Servais *, Diana M. Dincã *, Axelle Leroy, Cynthia Prigogine, Fadia Medja, Sandra O. Braz, Aline Huguet-Lachon, Cerina Chhuon, Annie Nicole, Noëmy Gueriba, Ruan Oliveira, Bernard Dan, Denis Furling, Maurice S. Swanson, Ida Chiara Guerrera, Guy Cheron, Geneviève Gourdon and Mário Gomes-Pereira **Downregulation of the Glial GLT1 Glutamate Transporter and Purkinje Cell Dysfunction in a Mouse Model of Myotonic Dystrophy** – Cell Reports (2017) 19, 2718-2729

The study of synaptic and glial proteins deregulation was integrated in a wider research line in the laboratory, aimed at understanding the molecular mechanisms deregulated in the CNS in response to the CTG expansion. In this project our group has reported the accumulation of toxic RNA foci in both neurons and astrocytes in different brain regions of DMSXL mice and DM1 patients. These results indicate that the CTG repeat expansion affects both neurons and astroglial cells and that DM1 neuropathogenesis involves both brain cell types. However we did not know how the CTG expansion affected each major brain cell type and what cellular and molecular pathways were specifically affected in each brain cell. In my third project I used DMSXL mice as a source of primary brain cells to investigate the functional consequences of the CTG repeat expansion on the cellular phenotypes and on the global proteome of two individual brain cell types: neurons and astrocytes. The experimental results of this study will be submitted soon for publication to the *Journal of Neuroscience*:

Diana Dincã, Géraldine Sicot, Aline Huguet-Lachon, Cerina Chuuon, Chiara Ida Guerrera, Geneviève Gourdon, Mário Gomes-Pereira. **GUG RNA toxicity is associated with adhesion and migration deficits in astrocytes and abnormal neuritogenesis in myotonic dystrophy .**

I have presented the results of this project in different scientific meetings and I was awarded the prize for the **best poster presentation** at the *10th International Myotonic Dystrophy Consortium* meeting and the *Colloque des Jeunes Chercheurs AFMTéléthon* meeting, and with the prize for the **best oral presentation** at the *Young Researchers in Life Sciences* meeting.

Finally, I performed a preliminary study of the changes in the phosphoproteome in DM1 CNS. Given the phosphorylation defects observed in different DM1 tissues and cells I hypothesized that DM1 brain disease mechanisms may involve global deregulation of key kinases and significant changes in the phosphoproteome. I have started to test this hypothesis by analyzing two main candidate kinases of interest: GSK3β and CDK5. Then, I went one step further and performed a global and unbiased phosphoproteomics analysis on DMSXL neurons and DMSXL astrocytes. The results of this fourth project are detailed in Chapter VI.

The results that I have obtained in the different projects are structured in four results chapters.

**Chapter III** – Synaptic proteins deregulation in DM1 brain – role of alternative splicing

**Chapter IV** – Mechanisms and consequences of the downregulation of GLT1 glial glutamate transporter in DM1 cerebellum

**Chapter V** – Patophysiological consequences of the DM1 CTG repeat expansion on neurons and astrocytes

**Chapter VI** – Changes in the phosphoproteome and the mechanisms of brain disease in DM1 – a preliminary study.

The first three of these chapters are based on research articles to which I have contributed significantly. The materials and methods used are detailed in each publication of the first three results chapters, and as supplementary materials and methods at the end of chapter VI.

# Chapter III. Synaptic proteins deregulation in DM1 brain – role of alternative splicing.

# III.A. Introduction

## III.A.I Developmental regulation of gene expression in the CNS

The molecular mechanisms of DM1 include abnormalities in developmentally regulated events, such as alternative splicing and polyadenylation, not only in muscle, but also in brain. Brain development in particular, is highly complex and multifaceted. The disruption of any of the underlying events can lead to CNS pathology. Today, the contribution of neurodevelopmental delays to DM1 neurological manifestations is not fully resolved.

Brain development is multilayered and involves many molecular dimensions. Global genetic and epigenetic mechanisms regulate brain development and synaptic connectivity within and between brain regions. The fine regulation of gene expression is essential since the first stages of development, when the main body axes of the embryo are determined and the expression and/or inhibition of developmental master genes determine the future body plan. Different signaling molecules are expressed in different locations at different moments during embryogenesis, controlling the antero-posterior and dorso-ventral patterning of the neural tube. This spatial regionalization is essential for further activation of specific transcription factors that will regulate neuronal differentiation. As an example, the generation of cortical glutamatergic neurons takes place in the ventricular zone of the dorsal telencephalon, expressing a particular set of transcription factors, while the cortical GABAergic interneurons originate in the ventral telencephalon, induced by a different set of transcription factors (Puelles et al. 2000; Bellion & Métin 2005).

The regulation of brain development and function goes beyond genetic control of protein expression. Chromatin accessibility, levels of histone acetylation and DNA post-translational modifications, non-coding RNA-mediated processes, transcription and post-transcriptional modifications, translation and post-translational modifications also regulate the neuronal connectivity, dendritic spines and axonal branching, as well as the synaptic strength (Rajarajan et

al. 2016). As an example, over 10,000 enhancers regulate gene expression in response to neuronal activity in mouse cortical neurons (Kim et al. 2010). Finally, three-dimensional (3D) conformation of the nuclear genome and the chromosomal loopings allow the contact between far apart promoters and enhancers, thereby contributing to the long-range control of gene expression and protein content in the brain (Rajarajan et al. 2016).

In summary, different molecular mechanisms control protein levels and activity and this fine regulation is essential throughout brain development. This complex, multifactorial process is crucial for proper brain connectivity and neurological function. Molecular defects before, during or after translation will affect the correct expression and activity of CNS proteins resulting in neurological abnormalities.

## III.A.II Splicing control of isoforms expression in the CNS

Another major mechanism controlling the protein expression and activity is alternative splicing. This process is particularly important in the CNS, where different splicing isoforms can regulate the properties and fate of many different types of neurons (Lee & Irizarry 2003). Alternative splicing involvement is detected at different levels, from the first steps of neuronal development, until the regulation of synapse strength in adult neurons (Li et al. 2007).

An example of a critical effect of alternative splicing on brain development is the regional expression of fibroblast growth factor 8 (FGF8) isoforms to control the midbrain-hindbrain boundary. The use of an alternative 3' splice site in the exon 1d of *FGF8* gives 2 isoforms, *FGF8a* and *FGF8b*, which differ in only 11 amino acids in the N-terminus of the protein but which play two different functions in brain development. FGF8a determines the commitment of the neural tube towards the development of the midbrain, while FGF8b induces the differentiation of the cerebellar tissue (**Fig. III.1A**) (Sato et al. 2004; Alam et al. 2009).

The establishment of cortical layers is also sensitive to alternative splicing. Cortical lamination involves the migration of neurons from the ventricular zone to the upper layers, using

the radial glia as a scaffold, and their detachment to integrate one particular layer. The Reelin pathway, and particularly Disabled-1 (DAB1), is essential for this detachment from the radial glia and positioning in a cortical layer. Full length DAB1 regulates neuronal detachment and cortical lamination in response to Reelin during the late stages of brain development. However, in the early stages of development, neuronal migration requires *DAB1* exon 7b and 7c skipping, which is dependent of NOVA2 splicing factor. Loss of NOVA2, or overexpression of full length *DAB1* in early stages of development, leads to migration defects and abnormal laminar distribution of neurons in the mouse cortex (**Fig. III.1B**) (Yano et al. 2010; Grabowski 2011; Gao & Godbout 2013).

Another example of the involvement of alternative splicing in synaptic regulation is the reversible skipping of *NMDAR1* exon 5 and exon 21, in response to cell excitation and membrane depolarization regulated by Ca2+/calmodulin dependent protein kinase (CaMK) IV (Xie et al. 2005). One sole gene codes for the NMDAR1 subunit of the NMDA receptor, but alternative splicing generates different variants. *NMDAR1* exon 5 encodes the extracellular N1 cassette that regulates the NMDA activity by interacting with several pharmacological modulators (Dingledine et al. 1999), while the exon 21 encodes the C1 cassette, a domain required for the trafficking from the ER to the plasma membrane, phosphorylation by protein kinase C (PKC) and A (PKA) and interaction with calmodulin and neurofilament L (**Fig. III.1C**) (Lee et al. 2007). Thus alternative splicing plays an important role in the regulation of the main glutamate receptor in the brain, directly impacting the synaptic plasticity, learning and memory.

Many neurological diseases are linked to missplicing of important transcripts in the brain. Such is the case of tauopathies, including Alzheimer's disease, in which mutations within or around exon 10 of the microtubule-associated protein tau (*MAPT*) gene affect the 1:1 inclusion/exclusion ratio of this exon and result in aggregation of the Tau protein into neurofibrillary tangles (Liu & Gong 2008). In the adult brain *MAPT/Tau* presents six different isoforms, generated by the alternative inclusion or exclusion of exons 2, 3 and 10, with the exon

3 being present only in isoforms that include exon 2 (**Fig. III.1D**). All these exons are excluded from the fetal *MAPT* isoform (Caillet-Boudin et al. 2014). Even though exon 2 and 3 do not seem to promote aggregation of Tau protein, all six brain isoforms are found in neurofibrillary tangles in different classes of tauopathies (Sergeant et al. 2005).

These examples, demonstrate the critical role of alternative splicing regulation for proper brain development, connectivity and function, and illustrate how alterations in the splicing pattern can give rise to pathological situations.

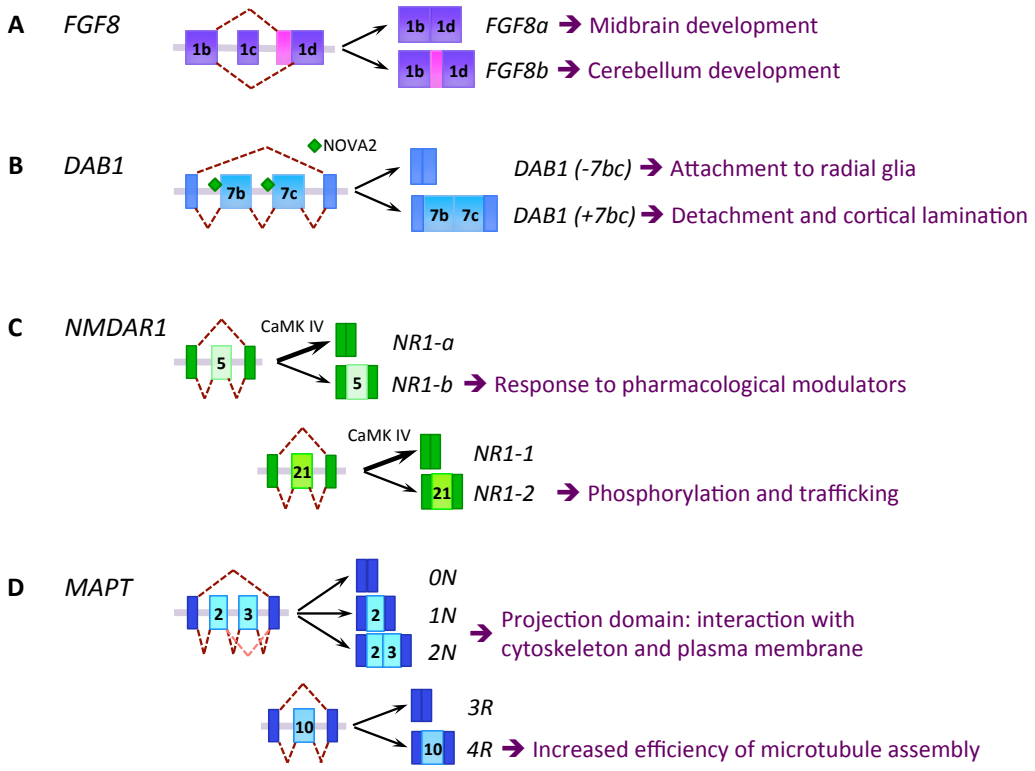


**Figure III.1. Alternative splicing controlling brain development and function.**
Schematic representation of alternative splicing events regulating brain development and function. **(A)** FGF8 splicing determines the midbrain-hindbrain boundary, **(B)** DAB1 splicing, controlled by NOVA2, regulates cortical lamination, **(C)** NMDAR1 splicing, modulated by CaMK IV activity, coordinates glutamatergic signaling and **(D)** MAPT splicing regulates microtubule polymerzation and cytoskeleton interaction.

# III.B. Context of the study

## III.B.I Splicing abnormalities in DM1 brain

In DM1 molecular pathogenesis, the toxic accumulation of expanded CUG RNAs perturbs the localization and/or function of MBNL and CELF splicing regulators, leading to global abnormalities in developmentally-regulated alternative splicing and abnormal expression of fetal isoforms in the adult brain, among other cellular mechanisms (Sicot et al. 2011; Gourdon & Meola 2017).

Splicing abnormalities have been reported in the brain of DM1 patients, in numerous transcripts, including *APP*, *MAPT, NMDAR1, SORBS1, MPRIP, CAMK2D, TANC2, KCNMA1, CSNK1D* and *CACNA1D* (Sergeant et al. 2001; Jiang et al. 2004; Dhaenens et al. 2011; Caillet-Boudin et al. 2014; Suenaga et al. 2012; Charizanis et al. 2012; Goodwin et al. 2015). *In vitro* and *in vivo* models have allowed the identification of the mediators linking the CTG expansion to these splicing abnormalities. Such is the case for CELF2 controlling *MAPT* and *NMDAR1* splicing, MBNL1 controlling *SORBS1, MPRIP* and *CAMK2D* splicing, and MBNL2 controlling *TANC2, KCNMA1, CSNK1D* and *CACNA1D*. All these missplicing events lead to increased expression of fetal splicing patterns in the adult brain, disturbing the fine regulation of gene expression and likely affecting CNS physiology. Moreover, global RNA sequencing approaches revealed show splicing abnormalities in many transcripts, as a consequence of MBNL1 and/or MBNL2 loss of function in mouse brain (Suenaga et al. 2001; Charizanis et al. 2012 ; Goodwin et al. 2015). However, the consequences of these events on CNS function and their direct involvement in DM1 neuropathology have not yet been dissected.

## III.B.II Molecular abnormalities in DMSXL mice brain

Before my arrival to the laboratory, our group had started the characterization of the molecular mechanisms deregulated in DMSXL mice brain and their consequences on behavior

(Hernandez-Hernandez et al. 2013). We reported toxic RNA foci accumulation in neurons and astrocytes, in multiple regions of the brain including frontal and temporal cortex, hippocampus, brainstem and cerebellum, co-localizing with MBNL1 and MBNL2. Furthermore, both CELF1 and CELF2 are upregulated in the frontal cortex of the mice.

As a consequence, the developmentally regulated splicing pattern of candidate transcripts was mis-regulated, with an increased expression of fetal isoforms in the frontal cortex and brainstem of DMSXL mice, two regions with high content of toxic RNA foci. The analysis of DMSXL brains showed an increase in the embryonic isoforms of *Nmdar1*, *Mapt*, *App*, *Mbnl1* and *Mbnl2,* as previously reported in human DM1 brains. Interestingly, we found dysregulation of both MBNL1-dependent splicing of *Ldb3* and CELF1-dependent splicing of *Fxr1*, previously described in the heart of MBNL1 KO and CELF1 upregulation mouse models. These missplicing events, which recreated abnormal embryonic profiles in adult mouse brain, confirmed the important role of MBNL and CELF proteins in regulating splicing transitions during brain development.

DMSXL mice show behavioral and electrophysiological abnormalities (Hernandez-Hernandez et al. 2013). In an attempt to find the underlying molecular pathways contributing to CNS dysfunction, our laboratory performed a global proteomics analysis, and found, MBNL1-dependent upregulation of RAB3A and CELF1- and CELF2-dependent hyperphosporylation of Synapsin1 (SYN 1) in DMSXL mice and DM1 post-mortem brains. RAB3A and SYN1 are two abundant proteins involved in the regulation of presynaptic vesicles release.

# III.C. Research objectives

Following this study two questions remained unanswered:

1) Do RAB3A upregulation and SYN1 hyperphosphorylation also recreate **embryonic events** in the adult DMSXL and DM1 brain, like the missplicing events previously studied?

2) Do *RAB3A* and *SYN1* transcripts present **splicing abnormalities** that could explain the protein expression and phosphorylation abnormalities observed in DMSXL and DM1 brains?

I answered these questions by analyzing the expression and phosphorylation of RAB3A and SYN1 throughout WT mouse brain development and aging, as well as the splicing of alternative exons previously described in the literature for *RAB3A* and *SYN1* transcripts, in DMSXL mouse and human DM1 brain samples.

# III.D. Results

The results of RAB3A expression and SYN1 phosphorylation throughout mouse brain development, and the analysis of alternative splicing of their transcripts are reported in the following article and in the supplementary **Figures III.S1-S3**. The main findings are summarized below:

Oscar Hernández-Hernández, Géraldine Sicot, **Diana M. Dincă**, Aline Huguet, Annie Nicole, Luc Buée, Arnold Munnich, Nicolas Sergeant, Geneviève Gourdon and Mário Gomes-Pereira. **Synaptic protein dysregulation in myotonic dystrophy type 1** – *Rare diseases* (2013) 1: e25553

My contribution to this work was the analysis of RAB3A expression and SYN1 phosphorylation during the WT mouse brain development and aging, in order to determine if the protein abnormalities observed in the DMSXL adult brain recreate WT fetal levels of expression. Both RAB3A expression and SYN1 phosphorylation increased in WT mouse brain from postnatal day 8 onward and were maintained at high levels during adulthood. These results indicate that the RAB3A overexpression and SYN1 hyperphosphorylation observed in adult DMSXL brains do not recreate embryonic expression patterns.

RAB3A upregulation is correlated with MBNL1 loss of function and SYN1 hyperphosphorylation is induced by upregulation of CELF1 and CELF2 (Hernandez-Hernandez et al. 2013). Given the major role of MBNL and CELF in the regulation of alternative splicing I have studied the described alternative exons of *RAB3A* and *SYN1* in the frontal cortex of WT

and DMSXL mice, by RT-PCR. I performed the analysis at 4 months, when protein abnormalities were previously detected, and at 1 month, when splicing defects are usually more pronounced in DMSXL brains. As RAB3A and SYN1 protein abnormalities are more pronounced in human DM1 brains (Hernandez-Hernandez et al. 2013), I have also extended the splicing analysis to human DM1 brain samples. I detected no splicing defects in *RAB3A* and *SYN1* transcripts, neither in human nor in murine frontal cortex (additional transcripts not reported in the article are shown in supplementary **Figure III.S1-S3**).

These results demonstrate that, even if mediated by MBNL loss of function and CELF upregulation, RAB3A and SYN1 protein abnormalities in DM1 brain do not recreate embryonic events, and are not caused by missplicing.

# III.E. Discussion

Synaptic proteins are deregulated in the brain of DM1 murine model. Together, these molecular deregulations are associated with cognitive and behavioral phenotypes, abnormal presynaptic neurotransmitter release and defective levels of dopamine and serotonin (Hernandez-Hernandez et al. 2013). Although induced by MBNL1 depletion and CELF upregulation, the DM1 synaptic proteins abnormalities do not recreate an embryonic expression profile and are not associated with abnormal splicing. These results indicate that DM1 brain pathology is not only mediated by neurodevelopmental splicing defects, but functional deregulations can also contribute to DM1 CNS involvement, pointing out the need of better understanding the consequences of the CTG repeat expansion in DM1 brain at the molecular, cellular and physiological level. Further investigation of the molecular mechanisms connecting the CTG expansion to the synaptic proteins abnormalities are essential in order to better understand DM1 neuropathogenesis.

The contribution of RAB3A upregulation and SYN1 hyperphosphorylation to DM1 CNS manifestations is still elusive. It is conceivable that abnormalities in RAB3A expression and

SYN1 phosphorylation lead to abnormal vesicle release at the presynaptic terminals contributing to the electrophysiological defects observed in DMSXL brains. Indeed RAB3A regulates the vesicle dynamics at the presynaptic terminal by controlling the docking, fusion and recycling of the synaptic vesicles, while SYN1 attaches the synaptic vesicles to the actin cytoskeleton and liberates them in a phosphorylation-dependent manner regulating the availability of synaptic vesicles for exocytosis. The upregulation of RAB3A and hyperphosphorylation of SYN1 in DM1 brain possibly deregulate the neuronal exocytosis and synaptic vesicles release.

The detailed analysis of the contributing role of RAB3A and SYN1 abnormalities to vesicle dynamics and release in DMSXL and DM1 neurons will give a better insight on DM1 brain dysfunction. Moreover it will shed light into the possibility of using RAB3A and SYN1 as therapeutic targets.

ARTICLE ADDENDUM

Rare Diseases 1, e25553; 2013; © 2013 Landes Bioscience

# Synaptic protein dysregulation in myotonic dystrophy type 1

## Disease neuropathogenesis beyond missplicing

Oscar Hernández-Hernández,[1,2,†] Géraldine Sicot,[1,3,†] Diana M. Dinca,[1,3] Aline Huguet,[1,3] Annie Nicole,[1,3] Luc Buée,[4] Arnold Munnich,[1,3] Nicolas Sergeant,[4] Geneviève Gourdon[1,3] and Mário Gomes-Pereira[1,3,*]

[1]Inserm U781; Hôpital Necker Enfants Malades; Paris, France; [2]Laboratorio de Medicina Genómica; Departamento de Genética; Instituto Nacional de Rehabilitación; Calzada México Xochimilco, México; [3]Université Paris Descartes—Sorbonne Paris Cité; Institut *Imagine*; Paris, France; [4]Inserm U837-1; Alzheimer and Tauopathies; Université Lille Nord de France; Centre Jean Pierre Aubert; Lille, France

[†]These authors contributed equally to this work.



**Keywords:** myotonic dystrophy type 1, trinucleotide repeat expansion, RNA toxicity, RNA splicing, central nervous system, transgenic mice, synaptic function, synaptic protein, RAB3A, synapsin I

**Abbreviations:** CELF, CUGBP/Elav-like factor; CUGBP, CUG RNA binding protein; DM, myotonic dystrophy; DM1, myotonic dystrophy type 1; DMPK, DM protein kinase; MBNL, muscleblind-like; RAB, RAS oncogene family; UTR, untranslated region

Submitted: 05/17/13

Revised: 06/24/13

Accepted: 06/25/13

Published Online: 07/23/13

Citation: Hernández-Hernández O, Sicot G, Dinca DM, Huguet A, Nicole A, Buée L, et al. Synaptic protein dysregulation in myotonic dystrophy type 1: Disease neuropathogenesis beyond missplicing. Rare Diseases 2013; 1:e25553; http://dx.doi.org/10.4161/rdis.25553

*Correspondence to: Mário Gomes-Pereira; Email: mario.pereira@inserm.fr

Addendum to: Hernández-Hernández O, Guiraud-Dogan C, Sicot G, Huguet A, Luilier S, Steidl E, et al. Myotonic dystrophy CTG expansion affects synaptic vesicle proteins, neurotransmission and mouse behaviour. Brain 2013; 136:957-70; PMID:23404338; http://dx.doi.org/10.1093/brain/aws367

**The toxicity of expanded transcripts in myotonic dystrophy type 1 (DM1) is mainly mediated by the disruption of alternative splicing. However, the detailed disease mechanisms in the central nervous system (CNS) have not been fully elucidated. In our recent study, we demonstrated that the accumulation of mutant transcripts in the CNS of a mouse model of DM1 disturbs splicing in a region-specific manner. We now discuss that the spatial- and temporal-regulated expression of splicing factors may contribute to the region-specific spliceopathy in DM1 brains. In the search for disease mechanisms operating in the CNS, we found that the expression of expanded CUG-containing RNA affects the expression and phosphorylation of synaptic vesicle proteins, possibly contributing to DM1 neurological phenotypes. Although mediated by splicing regulators with a described role in DM1, the misregulation of synaptic proteins was not associated with missplicing of their coding transcripts, supporting the view that DM1 mechanisms in the CNS have also far-reaching implications beyond the disruption of a splicing program.**

### Myotonic Dystrophy and the Central Nervous System

Myotonic dystrophy type 1 (DM1) is the most common form of inherited muscular dystrophy in adults, with a worldwide incidence of 1 in 8,000 individuals. DM1 is a typical multisystemic disease, affecting a large number of tissues and organs in the human body.[1] The central nervous system (CNS) is compromised to different extents in adult, juvenile and congenital forms of the disease. Several neuropsychological symptoms have been reported in adult-onset DM1 patients, such as excessive daytime sleepiness and fatigue, visuoconstructive impairment, attention deficits, reduced initiative and apathy, increased anxiety and anhedonia, as well as reduced intelligence quotients. Marked mental retardation and delayed psychomotor development are found in the congenital cases.[2] In addition to the clinical evidence, imaging and histopathological techniques have also illustrated brain dysfunction in DM1. MRI scans have revealed that white and gray matter are affected in DM1 brains, while PET-SPECT imaging techniques revealed deficits in brain glucose metabolism and hypoperfusion.[3,4] The histopathological distribution of tau protein in the brain revealed the accumulation of pathogenic protein isoforms in DM1 individuals,[5] in association with changes in the alternative splicing of tau transcripts,[6] resulting in the classification of DM1 as a tauopathy.

The neurological manifestations of the disease are highly debilitating and have a tremendous impact on the quality of life of DM1 patients and their families. As a result of their intellectual impairment and

behavioral deficits, DM1 patients experience low education achievements, low employment, poor familial environment, as well as social, economic and material deprivation.[7]

## Unraveling the Molecular Mechanisms of DM1 in the CNS

DM1 is caused by the abnormal expansion of a non-coding CTG trinucleotide repeat in the 3'UTR of the *DMPK* gene.[8] Experimental evidence supports a prevailing model of disease pathogenesis, in which the DM1 phenotype is mainly mediated by a deleterious gain-of-function of expanded *DMPK* transcripts.[9,10] CUG repeat-containing expanded transcripts form secondary RNA structures that bind to and sequester muscleblind-like proteins (MBNL) into ribonuclear inclusions or nuclear RNA foci,[11] and upregulate the CUG/Elav-like family (CELF) proteins.[12] Given the antagonistic role of MBNL and CELF proteins in the control of a developmentally regulated splicing program, CUG-associated RNA toxicity results in the aberrant expression of embryonic isoforms in adult skeletal muscle and heart.[12,13] Typical DM1 symptoms, such as myotonia, muscle weakness and insulin resistance, are explained by abnormal splicing of the *CLCN1* chloride channel,[14,15] *BIN1* bridging integrator protein[16] and the insulin receptor,[17] respectively. Although splicing defects have been described in human DM1 brains,[18] we do not understand the functional impact of *MAPT/TAU*, *GRIN/NMDAR1 and APP* RNA missplicing in DM1 neuropathophysiology. Nor do we know the cell populations, neuronal circuits, molecular pathways and neurological functions that are primarily disturbed in DM1 brains.

In addition to spliceopathy, evidence has shown that additional elements may contribute to (or at least modify) disease pathogenesis, such as chromatin rearrangements within the DM1 locus, leaching of transcription factors away from active chromatin, dysregulated miRNA metabolism, altered protein translation, and accumulation of toxic peptides resulting from non-conventional repeat-associated RNA translation.[9,10]

## Recreating RNA Toxicity in the CNS of DM1 Transgenic Mice

Given the compromised function of the CNS in DM1 patients and the impact of the neurological symptoms on their daily life, a growing effort has been made to unravel the mechanisms of DM1 neuropathogenesis over the last few years. We have been tackling this question by using DMSXL transgenic mice, previously generated in our laboratory.[19,20] These animals carry a large fragment of the human DM1 locus containing more than 1000 CTG repeats in the 3'UTR of the *DMPK* gene. Homozygous DMSXL mice produce sufficient toxic RNA transcripts to reproduce some critical and highly relevant molecular features of DM1, such as RNA foci accumulation and missplicing, as well as muscle phenotypes.[21] In order to investigate whether RNA toxicity extended to the CNS, we have studied nuclear RNA foci accumulation and found CUG-containing ribonuclear inclusions in DMSXL mice, not only in the brain, but also in the spinal cord.[22] RNA foci were particularly abundant in the frontal cortex and in some neuronal nuclei of the brainstem—two brain regions that are considered to play critical roles in the development of some of the most characteristic neurological symptoms of DM1. The nuclear accumulation of toxic RNA foci was associated with sequestration of MBNL proteins, upregulation of CELF proteins and resulted in the disruption of alternative splicing in DMSXL frontal cortex and brainstem.[22]

While most of the exons misspliced in DMSXL brains were previously reported as misregulated in post-mortem DM1 brains,[6,18] the missplicing of *GRIN1/NMDAR1* exon 21, *MBNL1* and *MBNL2* exon 7 in human patients was poorly documented. To confirm that the splicing changes of these exons in DMSXL mice recreate relevant molecular events characteristic of DM1, we have now validated these abnormalities in human DM1 frontal cortex and brainstem. The RT-PCR analysis confirmed increased inclusion of *GRIN1/NMDAR1* exon 21, *MBNL1* exon 7 and *MBNL2* exon 7 in human DM1 frontal cortex and brainstem, relative to non-DM1 control individuals (**Fig. 1A**), suggesting that the DMSXL splicing changes detected mimic true DM1 molecular features. Our RT-PCR analysis also revealed that missplicing was more pronounced in human frontal cortex than in brainstem, particularly for *MBNL1* and *MBNL2* transcripts. Coincidentally, the missplicing of *Mbnl1* and *Mbnl2* are among the most noticeable and reproducible defects detected in the brain of DMSXL mice, and may provide useful molecular biomarkers for the pre-clinical assessment of therapies aiming to correct DM1-spliceopathy in the CNS.

The extent and nature of the spliceopathy in DMSXL brains is region-specific, as illustrated by *Grin1/Nmdar1* transcripts. *Grin1/Nmdar1* exon 5 is abnormally excluded in DMSXL brainstem (but not in frontal cortex), while exon 21 is abnormally excluded in DMSXL frontal cortex (while it remains unaffected in brainstem).[22] The regional splicing defects of this gene (and others) might be the consequence of a spatially regulated splicing program. In support of physiological region-specific mechanisms of splicing regulation, we have found that the distribution of *Grin1/Nmdar1* isoforms varied between frontal cortex and brainstem in wild-type animals: while exon 5 is preferentially included in brainstem, exon 21 shows a much higher inclusion ratio in frontal cortex.[22] These differences suggest that the levels and/or activity of the key splicing regulators that control these events vary between different brain territories. We have addressed this hypothesis and found higher levels of CELF1 and CELF2 proteins in adult frontal cortex than in brainstem of wild-type mice. In contrast, the levels of MBNL proteins were higher in brainstem than in frontal cortex.[22] Additionally, the distribution of MBNL2 protein isoforms differed significantly between frontal cortex and brainstem: western blot immunodetection following long electrophoresis migration revealed high molecular weight isoforms that were specifically present in frontal cortex, as well as a higher expression of low molecular weight isoforms in brainstem (**Fig. 1B**). Given the role of CELF and MBNL proteins in the control of alternative splicing in the CNS,[23-25] these

differences may contribute to the regional splicing profiles in wild-type brains, and to the region-specific susceptibility of alternative exons to the accumulation of toxic RNA transcripts in DMSXL mice. Consistent with this view, a role of CELF2 in the regional regulation of alternative splicing in the mouse brain has been previously reported.[26] Our data suggest that the regional distribution of different splicing isoforms in the brain is regulated by the interplay between multiple RNA-binding proteins, which include not only CELF family members, but also MBNL proteins.

Missplicing in DMSXL CNS was not confined to frontal cortex and brainstem areas of the brain, and it was found throughout the CNS to a variable extent, including the hippocampus[22] and spinal cord (**Fig. 1C**), among other regions. These results demonstrate that CUG toxicity operates throughout the entire CNS. In agreement with this view, signs of neuronopathy, the expression of pathological forms of MAPT/tau protein and a reduced number of lumbar motor neurons were reported in the spinal cord of DMSXL mice.[27] However, the correlation between histopathology and splicing dysregulation in spinal cord remains to be further explored.

## Expression of Splicing Regulators is Regulated during Mouse CNS Development

The missplicing events detected in DMSXL brains increased the expression of embryonic splicing profiles in adult animals, to a limited extent,[22] as previously reported in skeletal muscle and heart.[12,13] To gain insight into the mechanisms underlying the developmental splicing program in the CNS, we have studied the steady-state levels of MBNL and CELF proteins throughout brain development and aging in wild-type mice. We found that CELF1 and CELF2 protein levels experienced a pronounced decrease in brainstem. In the frontal cortex, however, only CELF1 displayed a very mild decrease from embryonic day 12.5 (E12.5) onwards. In contrast, MBNL1 and MBNL2 levels increased significantly in adult frontal cortex and brainstem, particularly between post-natal day eight (P8) and the first month of age (M1). MBNL1 and MBNL2 were hardly detected in embryonic stages and at post-natal day 1 (P1) even following long exposures (**Fig. 1D**). The dramatic change in MBNL1 levels at one month of age coincided with a striking switch in the splicing patterns of *Mbnl1* and *Ldb3/Cypher* transcripts previously detected.[22] This is not surprising, since the alternative splicing of the alternative exons in these genes is specifically regulated by MBNL1.[28] In contrast, the splicing profile of *Fxr1* (a gene specifically regulated by CELF1) showed a less pronounced developmental splicing transition,[22] possibly due to the mild changes in the levels of CELF1 throughout brain development.

More importantly, the analysis of CELF and MBNL protein levels throughout wild-type brain development and aging revealed that DM1-associated CELF upregulation (particularly in the brainstem), and the functional inactivation of MBNL proteins by sequestration into ribonuclear foci recreated an embryonic scenario, thereby contributing to the abnormal expression of embryonic isoforms in adult DMSXL brain tissues.

We have extended our analysis to the hnRNP H ribonucleoprotein, an alternative splicing regulator with a described role in DM1 spliceopathy.[29] hnRNP H steady-state levels exhibited a marked decrease from wild-type embryonic stages to adult ages, in both frontal cortex and brainstem to similar extent (**Fig. 1D**). In contrast to the upregulation of hnRNP H reported in DM1 myoblasts,[29] the steady-state levels of hnRNP H did not differ significantly between DMSXL and wild-type brain regions at one month of age (**Fig. 1E**).

## Changes in Synaptic Vesicle Proteins are not Associated with Missplicing

To identify dysfunctional disease intermediates and pathways behind CUG-associated brain dysfunction, we investigated the proteomic profile of DM1 transgenic mice and found abnormal RAB3A upregulation and synapsin I (SYN1) hyperphosphorylation relative to control animals. We extended our findings from mouse to human brains, and confirmed a statistically significant RAB3A upregulation and SYN1 hyperphosphorylation in post-mortem DM1 frontal cortex.[22] Furthermore, higher RAB3A levels and SYN1 phosphorylation were also detected in neuronal-like PC12 cells expressing expanded CUG-containing transcripts. In these cells, the abnormal metabolism of synaptic vesicle proteins was associated with aberrant exocytosis, indicating a physiologically relevant consequence of the expression of toxic *DMPK* transcripts in neuronal cell lineages. Overall, we gathered electrophysiological, neurochemical, cellular and molecular data suggesting that the DM1 neuropsychological manifestations are mediated by the dysregulation of synaptic vesicle proteins, which likely affects neuronal vesicle release and exocytosis, and disrupts synaptic function in the CNS.

Since it has been suggested that DM1 molecular features, particularly splicing dysregulation, recreate embryonic events,[13] we asked whether synaptic protein expression and/or phosphorylation were also developmentally regulated. More importantly, we were interested in investigating whether RAB3A upregulation and SYN1 hyperphosphorylation in adult DMSXL mice recreated embryonic events, and supported a contribution of neurodevelopmental deficits behind DM1 neuropathology. To answer these questions, we studied protein expression and/or phosphorylation levels throughout wild-type brain development and aging (**Fig. 2A**). The analysis revealed that RAB3A levels increased at one month of age (M1), and indicated that RAB3A upregulation detected at four months of age did not mimic an embryonic expression profile, and it was unlikely to be a direct consequence of defective developmental regulation of this protein. Similarly, the total levels of SYN1 also showed a marked post-natal increase, particularly after one month of age. However, SYN1 phosphorylation at residues serine-9 and serine-553 preceded the pronounced increase in the steady-state levels of this protein. As a result, the phosphorylation of SYN1 appears to peak at post-natal day eight (P8), but mainly as a result of the low steady-state of SYN1 at this stage (**Fig. 2A**). This situation differs from the SYN1

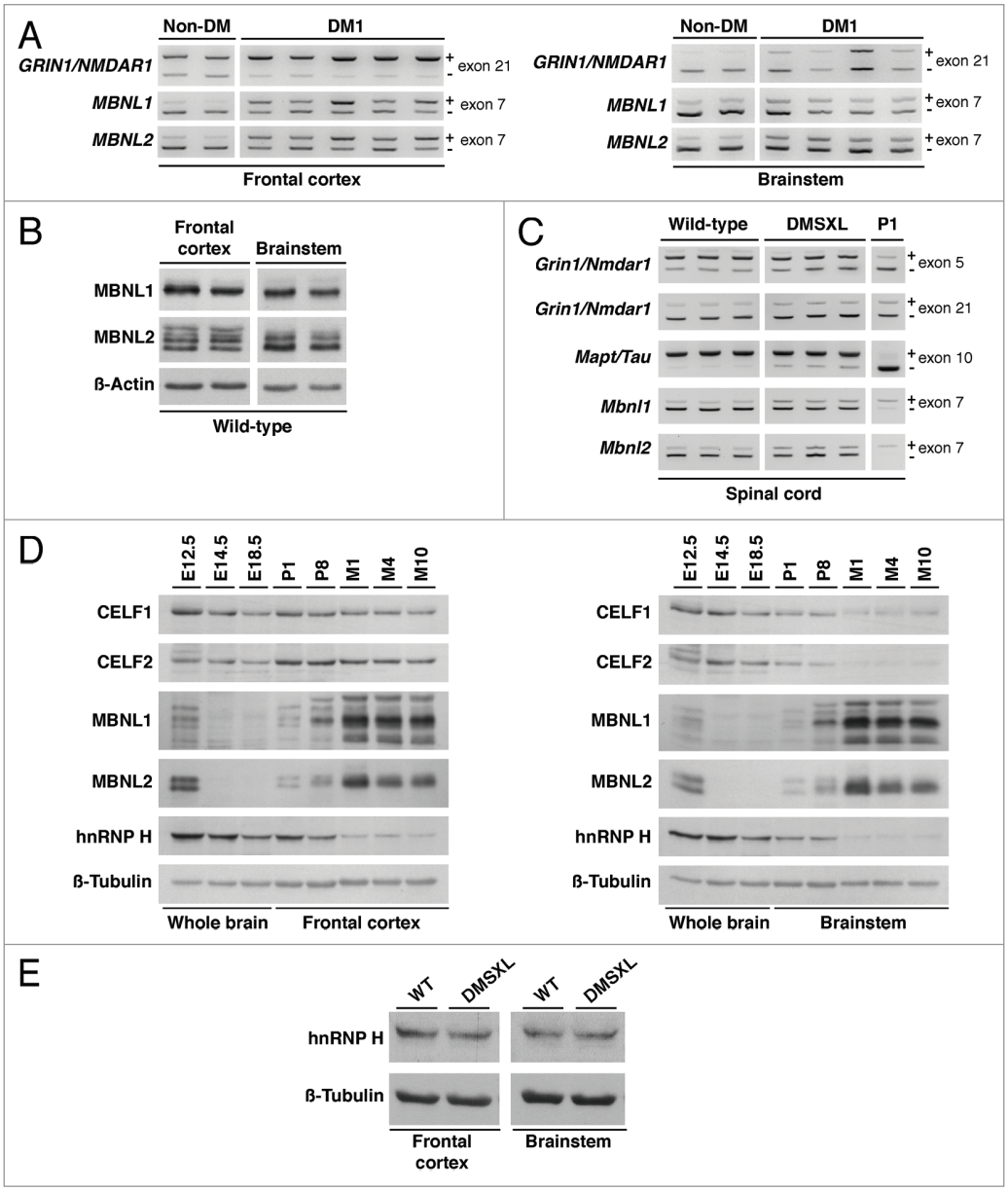


**Figure 1.** DM1-associated RNA spliceopathy and the expression of splicing regulators in the CNS. (**A**) Representative splicing analysis of candidate genes in the frontal cortex and brainstem of DM1 patients (n = 4–5) and non-DM controls (n = 2) by RT-PCR (**Table S1**). The alternative exons are indicated on the right of each panel. The higher molecular product results from the amplification of the transcript that includes the alternative exon (+); the lower band does not include the alternative exon (–). (**B**) Western blot analysis of MBNL1 and MBNL2 in the frontal cortex and brainstem of wild-type animals (**Table S1**), following long migration times to increase resolution and separation of protein isoforms. β-Actin was used as loading control. (**C**) Representative splicing analysis of alternative exons of *Grin1/Nmdar1*, *Mapt/Tau*, *Mbnl1* and *Mbnl2* by RT-PCR (**Table S1**) in the spinal cord of one-month-old DMSXL homozygous mice and wild-type controls (n = 3, per genotype). Newborn splicing profiles (P1) were determined in a cDNA pool prepared from three wild-type animals. Notably, DMSXL spinal cord exhibited increased exclusion of both *Grin1/Nmdar1* exon 5 and *Mapt/Tau* exon 10, as well as a mild increase in the inclusion of both *Mbnl1* exon 7 and *Mbnl2* exon 7. (**D**) Western blot analysis of splicing regulators throughout wild-type embryonic development (E12.5, E14.5, E18.5), in newborn (P1), postnatal day 8 (P8), and adult mice aged one (M1), four (M4) and 10 (M10) months (**Table S2**). Protein extracts from three individual animals were pooled for each developmental stage, electrophoresed and analyzed in three independent assays. Representative western blots are shown for frontal cortex and brainstem. Over-exposed of MBNL1 and MBNL2 western blots are shown to confirm low protein expression during embryonic stages and at P1. (**E**) Western blot analysis of hnRNP H in the frontal cortex and brainstem of DMSXL and wild-type animals at one month of age (**Table S2**), when missplicing dysregulation is more pronounced. Protein extracts from three individual animals of each genotype were pooled. β-Tubulin was used as loading control.

profiles in adult DMSXL mice, which show increased SYN1 phosphorylation but unchanged steady-state levels relative to wild-type control mice.[22] Therefore, we conclude that the hyperphosphorylation of SYN1 in adult DMSXL brains does not

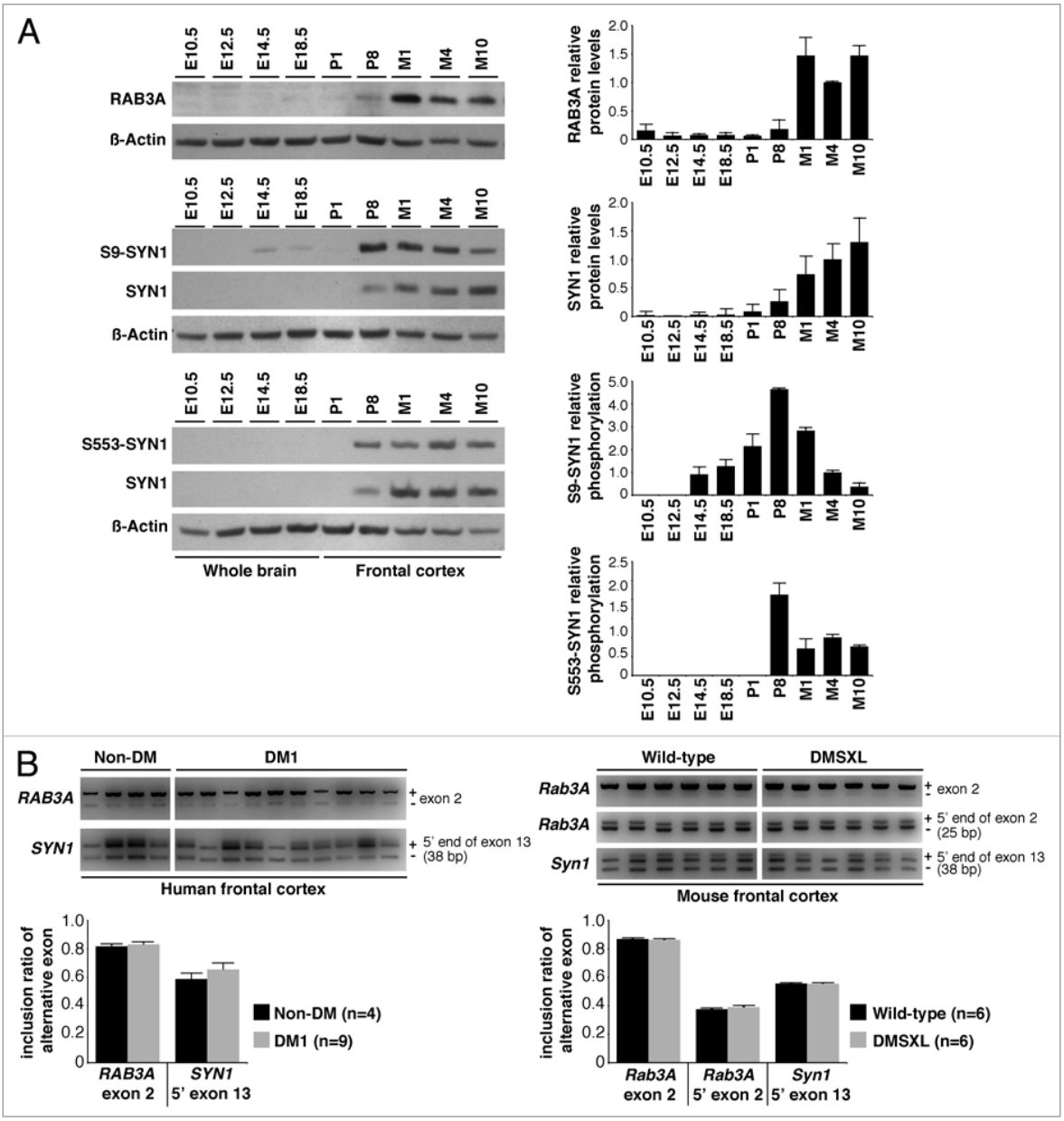


**Figure 2.** Expression, phosphorylation, and alternative splicing of RAB3A and SYN1. (**A**) Quantification of RAB3A steady-state levels and SYN1 phosphorylation throughout wild-type brain embryonic development (E10.4, E12.5, E14.5, E18.5), in newborn (P1), postnatal day 8 (P8), and adult mice aged one (M1), four (M4) and 10 (M10) months (**Table S2**). Frontal cortex protein extracts from three individual animals were pooled for each developmental stage and analyzed in two independent western blot assays (only one is shown). The graphs on the right represent the mean RAB3A and SYN1 steady-state levels (± SD) throughout the development and aging of mouse frontal cortex, as well as mean SYN1 phosphorylation on amino acid residues serine-9 (S9) and serine-553 (S553). (**B**) Representative RT-PCR splicing analysis of *RAB3A* exon 2 and the 5' end of *SYN1* exon 13 in the frontal cortex of DM1 (n = 9) and non-DM individuals (n = 4), as well as in DMSXL and wild-type mice at four months of age (n = 6, each genotype) (**Table S1**). The 5' end of exon 2 of *Rab3A* is alternatively spliced only in mouse, and included in the analysis. The graphs show the mean inclusion ratio (± SEM) of each alternative exon or alternative 5' end.

truly mimic the early post-natal metabolism of this protein. In summary, our data are consistent with the view that DM1-associated RAB3A upregulation and SYN1 phosphorylation is more likely mediated by neurofunctional abnormalities, rather than CUG-associated neurodevelopmental deficits.

To gain insight into the mechanisms of synaptic protein dysregulation, we studied additional mouse and cell models of DM1. We found that RAB3A was upregulated in mouse brain in response to the inactivation of MBNL1, while SYN1 was hyperphosphorylated in PC12 cells overexpressing CELF1 or CELF2.[22] Given the role of MBNL and CELF protein families in the regulation of alternative splicing,

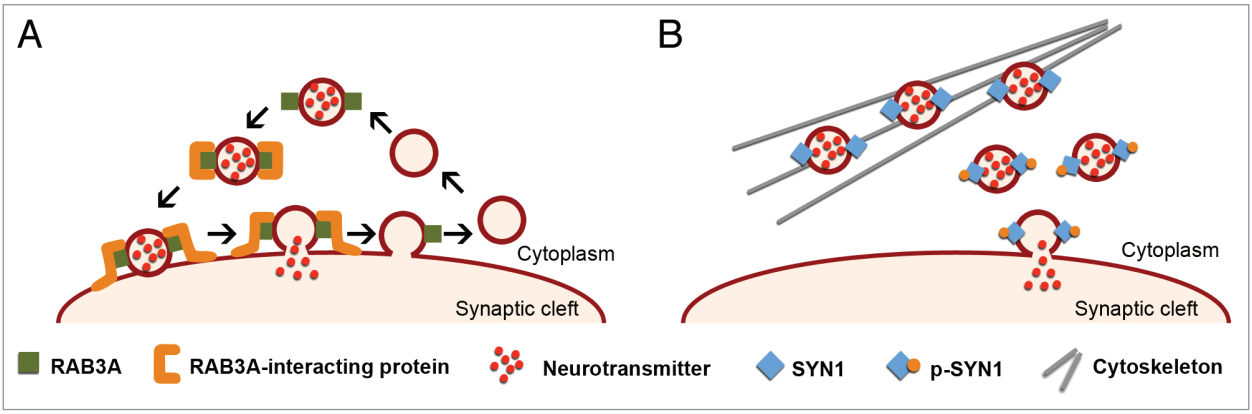


**Figure 3.** Schematic representation of the role of RAB3A and SYN1 in the dynamics of synaptic vesicles. (**A**) RAB3A is an abundant vesicle-associated protein that regulates synaptic efficiency. The reported functions of RAB3A in exocytosis range from docking and fusion of the synaptic vesicle to its subsequent recycling. RAB3A functions through a variety of interactions with multiple effector proteins. The upregulation of RAB3A likely perturbs the highly regulated vesicle dynamics and release, affecting neurotransmission and synaptic function in DM1. (**B**) SYN1 is expressed in mature neurons, where it associates with the cytoplasmic surface of synaptic vesicles. SYN1 regulates the supply of synaptic vesicles available for exocytosis by binding to both vesicles and actin cytoskeleton in a phosphorylation-dependent manner. Under resting conditions, non-phosphorylated SYN1 attaches synaptic vesicles to the actin cytoskeleton. Synaptic stimulation induces SYN1 phosphorylation that facilitates vesicle dissociation from cytoskeleton and potentiates exocytosis. Abnormal SYN1 hyperphosphorylation in DM1 likely dysregulates neuronal exocytosis and vesicle release.



and the prevalent role of RNA spliceopathy in the etiology of DM1, we sought to investigate whether RAB3A and SYN1 protein abnormalities were associated with missplicing of the corresponding transcripts. We initially studied the splicing profiles of the main alternative exons previously described in the literature and found no differences between DMSXL and wild-type mice at four months, an age when protein abnormalities were noticeable.[22] We have now extended this analysis to the remaining internal exons of the mouse and human genes. Our RT-PCR analysis confirmed additional splicing events in the *RAB3A* and *SYN1* genes previously described in the literature, such as the alternative inclusion of exon 2 in both human and mouse *RAB3A* transcripts; the inclusion of an additional 25-bp sequence through the use of an alternative 5' splice site in mouse *Rab3A* exon 2; and the inclusion of a short 38-bp sequence due to the use of an alternative 5' splice site of exon 13 in both human and mouse *SYN1* transcripts (**Fig. 2B**). Nevertheless, we did not detect significant splicing changes induced by the expression of toxic CUG-containing transcripts in mouse or human brains (**Fig. 2B**). Our data demonstrate that, although mediated by the inactivation of MBNL1 splicing regulator, RAB3A upregulation appears to be independent of missplicing events. Similarly, even if SYN1 is hyperphosphorylated as a result of the upregulation of CELF1 and/or CELF2 splicing regulators, the splicing of *SYN1* transcripts remains unaltered. In summary, although involving the dysfunction of known splicing factors (such as MBNL and CELF family members), DM1 neuropathogenesis goes beyond the abnormal expression of embryonic splicing isoforms, and implicates other molecular mechanisms.

## Conclusion

DMSXL mice recreate relevant signs of RNA toxicity in the CNS, associated with behavioral, electrophysiological and neurochemical changes. In the search for the mechanisms and dysfunctional pathways behind these phenotypes, we found altered expression and phosphorylation of synaptic proteins, which are independent of splicing dysregulation. RAB3A is an abundant synaptic vesicle protein that regulates neurotransmission, through the interaction with other synaptic proteins that control vesicle fusion to the cell membrane.[30] SYN1 regulates neuronal vesicle release in a phosphorylation-dependent manner[31] (**Fig. 3**). As a result, RAB3A upregulation and SYN1 hyperphosphorylation disrupts synaptic function and neurotransmitter release, likely contributing to the cognitive and behavioral deficits of DMSXL mice and the neuropsychological manifestations of DM1 patients.

### Disclosure of Potential Conflicts of Interest

No potential conflict of interest was disclosed.

### Acknowledgments

We are grateful to Amine Bouallague, the personnel of CERFE (Centre d'Exploration et de Recherche Fonctionelle Expérimentale, Genopole, Evry, France) and LEAT (Laboratoire d'Expérimentation Animale et de Transgénèse, Faculté de Médecine Paris Descartes) for attentively caring for the mice. We thank our colleagues at Inserm U781 and the DM1 French Splicing Network for helpful discussions. This work was supported by ANR (Agence Nationale de Recherche, France; project grant "DM1MICE"), AFM (Association Française contre les Myopathies, France; project grant number 14687), INSERM (Institute National de la Santé et Recherche Médicale, France) and Université Paris Descartes (Paris, France). O.H.H. was partially funded by a postdoctoral fellowship and research grant from CONACyT (Consejo Nacional de Ciencia y Tecnología, Mexico; grant number 183697). G.S. was awarded a PhD student fellowship from Ministère Français de la Recherche et Technologie and AFM.

## Supplemental Material

Supplemental materials may be found here:
www.landesbioscience.com/journals/rarediseases/article/25553

## References


1. Harper PS. Myotonic Dystrophy. WB Saunders, 2001.
2. Meola G, Sansone V. Cerebral involvement in myotonic dystrophies. Muscle Nerve 2007; 36:294-306; PMID:17486579; http://dx.doi.org/10.1002/mus.20800
3. Minnerop M, Weber B, Schoene-Bake JC, Roeske S, Mirbach S, Anspach C, et al. The brain in myotonic dystrophy 1 and 2: evidence for a predominant white matter disease. Brain 2011; 134:3530-46; PMID:22131273; http://dx.doi.org/10.1093/brain/awr299
4. Romeo V, Pegoraro E, Squarzanti F, Sorarù G, Ferrati C, Ermani M, et al. Retrospective study on PET-SPECT imaging in a large cohort of myotonic dystrophy type 1 patients. Neurol Sci 2010; 31:757-63; PMID:20842397; http://dx.doi.org/10.1007/s10072-010-0406-2
5. Vermersch P, Sergeant N, Ruchoux MM, Hofmann-Radvanyi H, Wattez A, Petit H, et al. Specific tau variants in the brains of patients with myotonic dystrophy. Neurology 1996; 47:711-7; PMID:8797469; http://dx.doi.org/10.1212/WNL.47.3.711
6. Sergeant N, Sablonnière B, Schraen-Maschke S, Ghestem A, Maurage CA, Wattez A, et al. Dysregulation of human brain microtubule-associated tau mRNA maturation in myotonic dystrophy type 1. Hum Mol Genet 2001; 10:2143-55; PMID:11590131; http://dx.doi.org/10.1093/hmg/10.19.2143
7. Laberge L, Veillette S, Mathieu J, Auclair J, Perron M. The correlation of CTG repeat length with material and social deprivation in myotonic dystrophy. Clin Genet 2007; 71:59-66; PMID:17204048; http://dx.doi.org/10.1111/j.1399-0004.2007.00732.x
8. Brook JD, McCurrach ME, Harley HG, Buckler AJ, Church D, Aburatani H, et al. Molecular basis of myotonic dystrophy: expansion of a trinucleotide (CTG) repeat at the 3' end of a transcript encoding a protein kinase family member. Cell 1992; 68:799-808; PMID:1310900; http://dx.doi.org/10.1016/0092-8674(92)90154-5
9. Sicot G, Gomes-Pereira M. RNA toxicity in human disease and animal models: From the uncovering of a new mechanism to the development of promising therapies. Biochim Biophys Acta 2013; 1832:1390-409; PMID:23500957; http://dx.doi.org/10.1016/j.bbadis.2013.03.002
10. Sicot G, Gourdon G, Gomes-Pereira M. Myotonic dystrophy, when simple repeats reveal complex pathogenic entities: new findings and future challenges. Hum Mol Genet 2011; 20(R2):R116-23; PMID:21821673; http://dx.doi.org/10.1093/hmg/ddr343
11. Miller JW, Urbinati CR, Teng-Umnuay P, Stenberg MG, Byrne BJ, Thornton CA, et al. Recruitment of human muscleblind proteins to (CUG)(n) expansions associated with myotonic dystrophy. EMBO J 2000; 19:4439-48; PMID:10970838; http://dx.doi.org/10.1093/emboj/19.17.4439
12. Wang GS, Kearney DL, De Biasi M, Taffet G, Cooper TA. Elevation of RNA-binding protein CUGBP1 is an early event in an inducible heart-specific mouse model of myotonic dystrophy. J Clin Invest 2007; 117:2802-11; PMID:17823658; http://dx.doi.org/10.1172/JCI32308
13. Lin X, Miller JW, Mankodi A, Kanadia RN, Yuan Y, Moxley RT, et al. Failure of MBNL1-dependent post-natal splicing transitions in myotonic dystrophy. Hum Mol Genet 2006; 15:2087-97; PMID:16717059; http://dx.doi.org/10.1093/hmg/ddl132
14. Charlet-B N, Savkur RS, Singh G, Philips AV, Grice EA, Cooper TA. Loss of the muscle-specific chloride channel in type 1 myotonic dystrophy due to misregulated alternative splicing. Mol Cell 2002; 10:45-53; PMID:12150906; http://dx.doi.org/10.1016/S1097-2765(02)00572-5
15. Mankodi A, Takahashi MP, Jiang H, Beck CL, Bowers WJ, Moxley RT, et al. Expanded CUG repeats trigger aberrant splicing of ClC-1 chloride channel pre-mRNA and hyperexcitability of skeletal muscle in myotonic dystrophy. Mol Cell 2002; 10:35-44; PMID:12150905; http://dx.doi.org/10.1016/S1097-2765(02)00563-4
16. Fugier C, Klein AF, Hammer C, Vassilopoulos S, Ivarsson Y, Toussaint A, et al. Misregulated alternative splicing of BIN1 is associated with T tubule alterations and muscle weakness in myotonic dystrophy. Nat Med 2011; 17:720-5; PMID:21623381; http://dx.doi.org/10.1038/nm.2374
17. Savkur RS, Philips AV, Cooper TA. Aberrant regulation of insulin receptor alternative splicing is associated with insulin resistance in myotonic dystrophy. Nat Genet 2001; 29:40-7; PMID:11528389; http://dx.doi.org/10.1038/ng704
18. Jiang H, Mankodi A, Swanson MS, Moxley RT, Thornton CA. Myotonic dystrophy type 1 is associated with nuclear foci of mutant RNA, sequestration of muscleblind proteins and deregulated alternative splicing in neurons. Hum Mol Genet 2004; 13:3079-88; PMID:15496431; http://dx.doi.org/10.1093/hmg/ddh327
19. Seznec H, Lia-Baldini AS, Duros C, Fouquet C, Lacroix C, Hofmann-Radvanyi H, et al. Transgenic mice carrying large human genomic sequences with expanded CTG repeat mimic closely the DM CTG repeat intergenerational and somatic instability. Hum Mol Genet 2000; 9:1185-94; PMID:10767343; http://dx.doi.org/10.1093/hmg/9.8.1185
20. Gomes-Pereira M, Foiry L, Nicole A, Huguet A, Junien C, Munnich A, et al. CTG trinucleotide repeat "big jumps": large expansions, small mice. PLoS Genet 2007; 3:e52; PMID:17411343; http://dx.doi.org/10.1371/journal.pgen.0030052
21. Huguet A, Medja F, Nicole A, Vignaud A, Guiraud-Dogan C, Ferry A, et al. Molecular, physiological, and motor performance defects in DMSXL mice carrying > 1,000 CTG repeats from the human DM1 locus. PLoS Genet 2012; 8:e1003043; PMID:23209425; http://dx.doi.org/10.1371/journal.pgen.1003043
22. Hernández-Hernández O, Guiraud-Dogan C, Sicot G, Huguet A, Luilier S, Steidl E, et al. Myotonic dystrophy CTG expansion affects synaptic vesicle proteins, neurotransmission and mouse behaviour. Brain 2013; 136:957-70; PMID:23404338; http://dx.doi.org/10.1093/brain/aws367
23. Ladd AN. CUG-BP, Elav-like family (CELF)-mediated alternative splicing regulation in the brain during health and disease. Mol Cell Neurosci 2012; In press; PMID:23247071; http://dx.doi.org/10.1016/j.mcn.2012.12.003.
24. Charizanis K, Lee KY, Batra R, Goodwin M, Zhang C, Yuan Y, et al. Muscleblind-like 2-mediated alternative splicing in the developing brain and dysregulation in myotonic dystrophy. Neuron 2012; 75:437-50; PMID:22884328; http://dx.doi.org/10.1016/j.neuron.2012.05.029
25. Suenaga K, Lee KY, Nakamori M, Tatsumi Y, Takahashi MP, Fujimura H, et al. Muscleblind-like 1 knockout mice reveal novel splicing defects in the myotonic dystrophy brain. PLoS One 2012; 7:e33218; PMID:22427994; http://dx.doi.org/10.1371/journal.pone.0033218
26. Zhang W, Liu H, Han K, Grabowski PJ. Region-specific alternative splicing in the nervous system: implications for regulation by the RNA-binding protein NAPOR. RNA 2002; 8:671-85; PMID:12022233; http://dx.doi.org/10.1017/S1355838202027036
27. Panaite PA, Kielar M, Kraftsik R, Gourdon G, Kuntzer T, Barakat-Walter I. Peripheral neuropathy is linked to a severe form of myotonic dystrophy in transgenic mice. J Neuropathol Exp Neurol 2011; 70:678-85; PMID:21760538; http://dx.doi.org/10.1097/NEN.0b013e3182260939
28. Kalsotra A, Xiao X, Ward AJ, Castle JC, Johnson JM, Burge CB, et al. A postnatal switch of CELF and MBNL proteins reprograms alternative splicing in the developing heart. Proc Natl Acad Sci U S A 2008; 105:20333-8; PMID:19075228; http://dx.doi.org/10.1073/pnas.0809045105
29. Paul S, Dansithong W, Kim D, Rossi J, Webster NJ, Comai L, et al. Interaction of muscleblind, CUG-BP1 and hnRNP H proteins in DM1-associated aberrant IR splicing. EMBO J 2006; 25:4271-83; PMID:16946708; http://dx.doi.org/10.1038/sj.emboj.7601296
30. Sudhof TC. The synaptic vesicle cycle. Annu Rev Neurosci 2004; 27:509-47; PMID:15217342; http://dx.doi.org/10.1146/annurev.neuro.26.041002.131412
31. Rosahl TW, Geppert M, Spillane D, Herz J, Hammer RE, Malenka RC, et al. Short-term synaptic plasticity is altered in mice lacking synapsin I. Cell 1993; 75:661-70; PMID:7902212; http://dx.doi.org/10.1016/0092-8674(93)90487-B

Landes Bioscience www.landesbioscience.com

# Supplemental Material to:

Oscar Hernández-Hernández, Géraldine Sicot, Diana M. Dinca, Aline Huguet, Annie Nicole, Luc Buée, Arnold Munnich, Nicolas Sergeant, Geneviève Gourdon, and Mário Gomes-Pereira

## Synaptic protein dysregulation in myotonic dystrophy type 1: Disease neuropathogenesis beyond missplicing

Rare Diseases 2013; 1(3)
http://dx.doi.org/10.4161/rdis.25553

http://www.landesbioscience.com/journals/rarediseases/article/25553/

# Synaptic protein dysregulation in myotonic dystrophy type 1: disease neuropathogenesis beyond missplicing

Oscar Hernández-Hernández[1,2], Géraldine Sicot[1,3], Diana M. Dinca[1,3], Aline Huguet[1,3], Annie Nicole[1,3], Luc Buée[4], Arnold Munnich[1,3], Nicolas Sergeant[4], Geneviève Gourdon[1,3] and Mário Gomes-Pereira[1,3,*]

[1] Inserm U781, Hôpital Necker Enfants Malades, 75015 Paris, France.

[2] Laboratorio de Medicina Genómica, Departamento de Genética, Instituto Nacional de Rehabilitación, Calzada México Xochimilco 289, C.P. 14389, México D.F., México.

[3] Université Paris Descartes – Sorbonne Paris Cité, Institut *Imagine*, Paris, France.

[4] Inserm U837-1, Alzheimer and Tauopathies, Université Lille Nord de France, Centre Jean Pierre Aubert, 59045 Lille, France

## SUPPLEMENTARY INFORMATION

**Supplementary Table 1.** Oligonucleotide primer sequences.

**Supplementary Table 2.** Primary antibodies used for protein immunodetection in western blot analysis (WB)

**Supplementary Table 1.** Oligonucleotide primer sequences.

| Gene | Exon | Forward primer | Reverse primer | PCR product size (bp) |
|---|---|---|---|---|
| **Mouse transcripts** | | | | |
| *Grin1/ Nmdar1* | 5 | AGCGTCGTCCTCGCTTGCAGAA | GACAAGAGCATCCACCTGAGCT | 360 (+5)<br>297 (-5) |
| *Grin1/ Nmdar1* | 21 | GCAGCTGGCCCTCCTCCCTCTC | ATGCCCCTGCCACCCTCACTTTT | 381 (+21)<br>270 (-21) |
| *Mapt/ Tau* | 10 | CTGAAGCACCAGCCAGGAGG | TGGTCTGTCTTGGCTTTGGC | 367 (+10)<br>274 (-10) |
| *Mbnl1* | 7 | TGGTGGGAGAAATGCTGTATGC | GCTGCCCAATACCAGGTCAAC | 270 (+7)<br>216 (-7) |
| *Mbnl2* | 7 | CTTTGGTAAGGGATGAAGAGCAC | ACCGTAACCGTTTGTATGGATTAC | 255 (+7)<br>201 (-7) |
| *Rab3A* | 2 | CCAGCGTTGTCTCAGCTTAGAGAG | CGGTAATAGGCTGTGGTGATGG | 303 (+2)<br>75 (-2) |
| *Rab3A* | 2 (5') | ATCCCCCGCATCCTCTTCTG | GGTGCTGACAAAGGCTGGAGTG | 270<br>245 |
| *Syn1* | 13 (5') | AAACCCAGCCAGGATGTGC | GGATGTCAGTCGGAGAAGAGG | 209<br>171 |
| **Human transcripts** | | | | |
| *GRIN1/ NMDAR1* | 21 | CGTGTGGCGGAAGAACCTG | CTGTCTGCGGGGGAGGGG | 292 (+21)<br>181 (-21) |
| *MBNL1* | 7 | GCTGCCCAATACCAGGTCAAC | TGGTGGGAGAAATGCTGTATGC | 216 (+7)<br>162 (-7) |
| *MBNL2* | 7 | ACAAGTGACAACACCGTAACCG | TTTGGTAAAGGATGAAGAGCACC | 212 (+7)<br>158 (-7) |
| *RAB3A* | 2 | CCACCGCCAAAAAAGTCAC | ATGAGGATGAAGCCCATAGC | 358 (+2)<br>130 (-2) |
| *SYN1* | 13 (5') | CCACCCACCACGCAGCAG | GCTTTCACCTCGTCCTGGCTAAG | 224<br>186 |

**Supplementary Table 2.** Primary antibodies used for protein immunodetection in western blot analysis (WB)

| Antigen | Supplier Reference # | PAGE (%) | Species origin | Incubation conditions | Ab dilution |
|---|---|---|---|---|---|
| Actin | BD laboratories 612656 | 10-12 | Mouse | 5% blotto, 1h, RT | 1:5000 |
| CELF1 | Upstate, 05-621 | 10 | Mouse | 5% blotto, 1h, RT | 1:1000 |
| CELF2 | Sigma, C9367 | 10 | Mouse | 2h, RT | 1:1000 |
| hnRNP H | Santa Cruz sc10042 | 10 | Goat | 5% blotto, O/N, 4°C | 1:500 |
| MBNL1 | G. Morris, MB1a (gift) | 10 | Mouse | 5% blotto, 1 h, RT | 1:1000 |
| MBNL2 | G. Morris, MB2a (gift) | 10 | Mouse | 5% blotto, 1 h, RT | 1:1000 |
| RAB3A | Abcam, ab3335 | 12 | Rabbit | 10% blotto, 1h, RT | 1:1000 |
| ß-Tubulin | Sigma, T4026 | 10-12 | Mouse | 5% blotto, 1 h, RT | 1:2000 |
| Synapsin I | Abcam, ab8 | 10 | Rabbit | 5% blotto, O/N, 4°C | 1:10000 |
| Synapsin I Ser553 | Epitomics, 1532-1 | 10 | Rabbit | 5% blotto, O/N, 4°C | 1:5000 |
| Synapsin I Ser9 | Epitomics, 2228-1 | 10 | Rabbit | 5% blotto, O/N, 4°C | 1:5000 |

## SUPPLEMENTARY FIGURES:

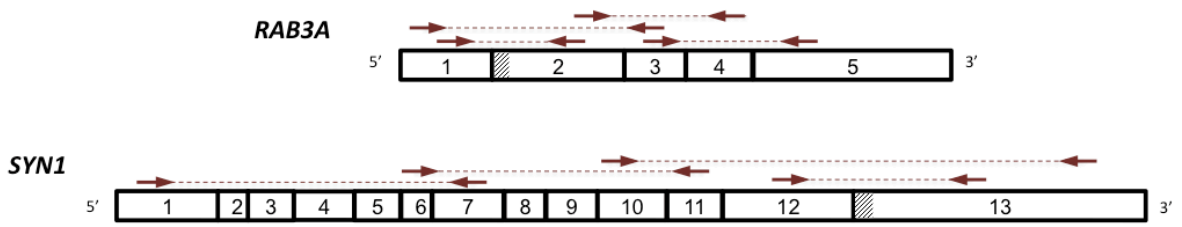


**Figure III.S1. Schematic representation of *RAB3A* and *SYN1* transcripts**
The figure shows the position of oligonucleotide primers and PCR products amplified for the analysis of RAB3A and SYN1 alternative splicing. Stripped pattern indicates alternative spliced sequences previously described.

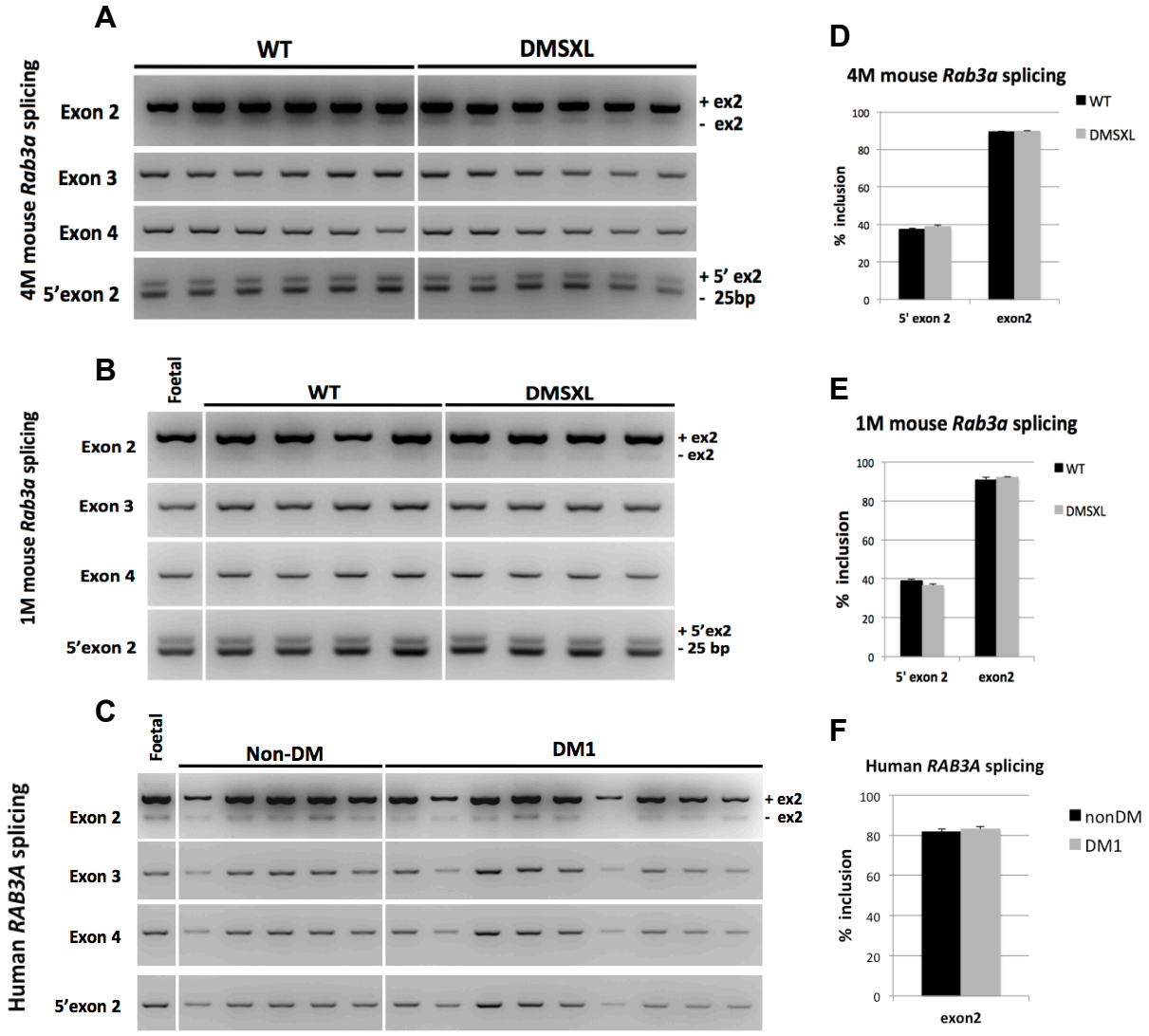


**Figure III.S2. *RAB3A* splicing analysis in DMSXL mice and human DM1 frontal cortex.**
RT-PCR analysis of Rab3a splicing in DMSXL mice and wild-type (WT) controls frontal cortex, at **(A)** 4 months of age (4M; n=6 for each genotype) and **(B)** 1 month (1M; n=4 for each genotype). **(C)** Representative analysis of RAB3A splicing in DM1 patients frontal cortex (n=9) and non-DM control

individuals (n=5). Fetal mouse and human samples were included in the study. **(D, E)** Percentage of inclusion of the alternatively spliced exon 2 and the 5' region of exon 2, in mouse frontal cortex (± SEM) and **(F)** in human frontal cortex (± SEM).

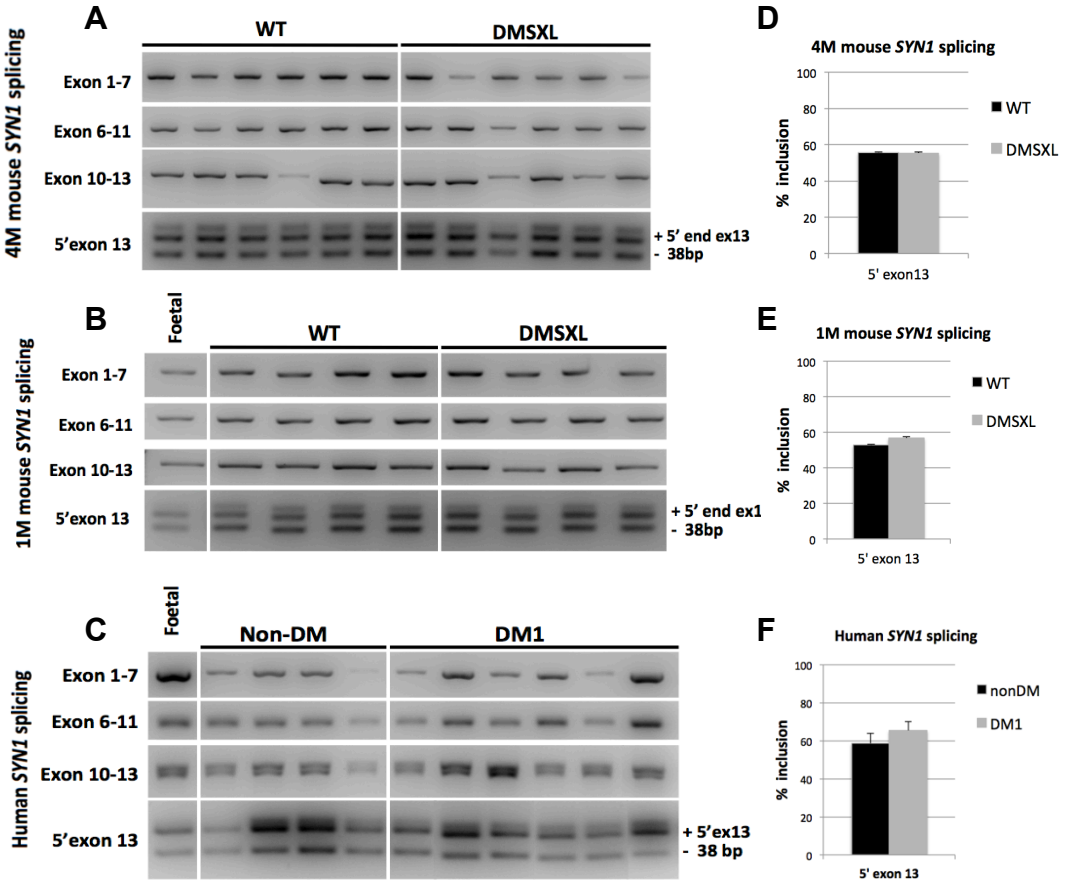


**Figure III.S3. *SYN1* alternative splicing analysis in DMSXL mice and human DM1 frontal cortex.** RT-PCR analysis of SYN1 splicing in DMSXL mice and wild-type controls, at **(A)** 4 months of age (4M, n=6 for each genotype) and **(B)** 1 month (1M, n=4 for each genotype). **(C)** RT-PCR analysis of SYN1 splicing in DM1 patients frontal cortex (n=6) and non-DM control individuals (n=4). Fetal mouse and human samples were included in the study. **(D, E)** Percentage of inclusion of the alternatively spliced 5'region of exon 13 in in mouse frontal cortex (± SEM) and in **(F)** human frontal cortex (± SEM).

# Chapter IV. Mechanisms and consequences of the downregulation of GLT1 glial glutamate transporter in DM1 cerebellum.

# IV.A. Introduction

## IV.A.I Glutamate transport in the brain

Brain activity is controlled by neurotransmitters. These are endogenous chemicals produced by the presynaptic neurons, loaded into synaptic vesicles and released into the synaptic cleft to induce an effect on the postsynaptic neuron. Depending on the effect on the postsynaptic cell, the neurotransmitters are divided in excitatory, when the postsynaptic neuron is depolarized and produces an action potential; or inhibitory, when the postsynaptic neuron is hyperpolarized. The major mediator of excitatory synapses in the mammalian CNS is the amino acid glutamate. It plays an essential role in normal brain function, including cognition, memory and learning through active participation in synapse formation and elimination, cell migration, differentiation and death (Danbolt 2001).

Glutamate is present at high concentrations of 5-15 mmol/kg in the brain, mostly in the cytoplasm of glutamatergic neurons, where it reaches concentrations of 5-10 mM. The concentration of glutamate is further increased in synaptic vesicles reaching 100 mM or more, thanks to proton/glutamate antiport proteins called vesicular glutamate transporters (VGluts) (Takamori 2006). At the synaptic cleft the basal concentrations of glutamate are of 0.5-5 μM, but during excitatory synaptic transmission the synaptic vesicles fuse to the plasma membrane of the presynaptic neuron releasing up to several hundred μM of glutamate into the synaptic cleft, to activate the receptors of the postsynaptic neuron. The excitatory signal is terminated when the glial and neuronal glutamate transporters actively uptake the excess glutamate from the synaptic cleft. A failure to uptake the excess glutamate from the synaptic cleft leads to overactivation of glutamate receptors, excitotoxicity and death of the postsynaptic neurons as well as spillover of glutamate between synapses and loss of the specificity of synaptic input (Danbolt 2001; Mattson 2008; Murphy-Royal et al. 2017). Astroglial cells convert glutamate to glutamine and transport it back to the neurons, where glutamine is converted back to glutamate for a new cycle to begin.

## IV.A.II Glutamate receptors

Two major types of neuronal glutamate receptors have been described based on their functional properties: metabotropic and ionotropic glutamate receptors (Kew & Kemp 2005; Niswender & Conn 2010; Zhuo 2017):

**Metabotropic receptors (mGluRs)** are seven-pass transmembrane proteins, which activate intracellular signalling cascades via G-proteins coupling, upon glutamate binding. There are eight genes encoding mGluRs, clasified in three major groups based on sequence homology, G-protein coupling and ligand selectivity. Group I mGluRs activate downstream phospholipase C pathways, increasing $Ca^{2+}$ intracellular levels, activity of PKC and neuronal excitability. Group II and group III mGluRs inhibit adenylate cyclase activity, decreasing the intracellular levels of cAMP and ihibiting neurotransmitter release.

**Ionotropic receptors (iGluRs)** are multimeric glutamate-gated ion channels that change conformation upon glutamate binding, allowing cation flow though plasma membrane and leading to depolarisation of the postsynaptic neuron. There are also three types of iGluRs named after the agonists that activate them : NMDA (N-methyl-D-aspartate), AMPA (α-amino-3-hydroxyl-5-methyl-4-isoxazole-propionate) and kainate receptors. NMDA receptors play a critical role in long-term synaptic plasticity, as their activation initiates $Ca^{2+}$-dependent signalling cascades that lead to changes in gene expression. AMPA receptors mediate fast excitatory transmission, while kainate receptors play a minor contribution in single synaptic responses.

## IV.A.III Glutamate transporters

The role of the glutamate transporters is essential in maintaining very low extracellular glutamate levels, while intracellular glutamate concentrations are several thousand-fold higher. Five glutamate transporters (excitatory amino acid transporters or EAATs), sharing 50-60% amino acid sequence identity, have been cloned and characherized. They are summarized in **Table IV.1** and reviewed in Grewer et al. 2014. All of them uptake glutamate from the

extracellular space, using the electrochemical gradient across the plasma membrane, by cotransporting 3 $Na^+$ and 1 $H^+$ and countertransporting 1 $K^+$.

**Table IV.1. Nomenclature and expression pattern of EAATs**

| Gene name | Alias | Cell-specific expression | Anatomic localization |
|---|---|---|---|
| *SLC1A3* | EAAT1, GLAST | Astrocytes | Cerebellum, cortex, spinal cord |
| *SLC1A2* | EAAT2, GLT1 | Astrocytes mainly, in some neurons at low levels | All CNS |
| *SLC1A1* | EAAT3, EAAC1 | Neurons | Hippocampus, cerebellum, striatum |
| *SLC1A6* | EAAT4 | Purkinje neurons | Cerebellum |
| *SLC1A7* | EAAT5 | Photoreceptors and bipolar cells | Retina |

GLT1/EAAT2 is considered the most important glutamate transporter in the CNS, as it accounts for about 95% of the total glutamate uptake in the brain (Danbolt et al. 1992; Haugeto et al. 1996). Loss of GLT1 in mouse brain leads to lethal spontaneous seizures and increased susceptibility to acute cortical injury (Tanaka et al. 1997). GLT1 protein is mainly expressed in astrocytes and located at the glial membrane in the normal adult brain and spinal cord (Danbolt 2001; Furness et al. 2008). However, recent results indicate that GLT1 is also detected in axon terminals in hippocampal, somatosensorial and striatal neurons, contributing to uptake of glutamate from the synaptic cleft (Petr et al. 2015).

Expression of GLT1 is regulated in a very complex manner, at different levels:

- **Epigenetically**, by DNA methylation-mediated inhibition at the CpG island, close to the translationsl start site (Zschocke et al. 2005).

- **Transcriptionally**, by the nuclear transcription factor-kappa B (NFκB), activated by cAMP, TGFα and EGF. β-lactam antibiotics such as ceftriaxone also induce NFκB-mediated transcription of GLT1 (Lee et al. 2008).

- Post-transcriptionally, upon **alternative splicing** and **alternative polyadenylation.** At least 3 different C-terminal, 4 distinct N-terminal regions and 4 events of exon skipping have been reported so far in rat, mouse and human *GLT1* (Grewer et al. 2014), as well as alternative

polyadenylation after the STOP codon (Münch et al. 2000) or in intronic regions (Flomen & Makoff 2011).

**- Micro-RNAs mediation,** such as the upregulation of GLT1 protein by exosome-mediated intracellular transfer of miR-124a from neurons to astrocytes (Morel et al. 2013).

**- Posttranslationally** by PKC-induced and NEDD4-2 mediated ubiquitination (Garcia-Tandon et al. 2012), sumoylation (Foran et al. 2014) and clustering and redistribution close to synapse (Benediktsson et al. 2012).

The fine regulation of GLT1 levels underlines the importance of a rigorous control of the availability of functional GLT1 in the brain. Defective regulation of GLT1 expression will lead to aberrant glutamate uptake, abnormal synaptic activity and neurological deficits.

## IV.A.IV GLT1 in neurological diseases

Alterations in some of the mechanisms controlling the levels of functional GLT1/EAAT2 have been reported in different CNS pathologies.

In **ischemia** oxygen and glucose supply is reduced, impairing the ATP synthesis and thus the $Na^+$ and $K^+$ gradients, leading to reverse transport of glutamate and increased synaptic glutamate concentrations and excitotoxicity (Takahashi et al. 2015). Therapeutic strategies to reduce extracellular glutamate or enhance the expression of glutamate transporters, such as ceftriaxone treatment, have proven beneficial in ischemia animal models (Hu et al. 2015).

The central role of GLT1/EAAT2 in **epilepsy** has been well established through the generation of the first *Glt1* KO murine model (Tanaka et al. 1997) and the demonstration that pharmacological upregulation of GLT1/EAAT2 expression reduces spontaneous seizures and mortality in epilepsy mouse models (Goodrich et al. 2013; Kong et al. 2014).

GLT1/EAAT2 has also been reported as downregulated in the CNS of **amyotrophic lateral sclerosis (ALS)** patients as well as in transgenic rodent models (Rothstein et al. 1995; Bendotti et al. 2001; Howland et al. 2002).

In animal models of **HD (HD)** GLT1/EAAT2 levels are decreased at mRNA and protein level, and ceftriaxone-induced upregulation of this glutamate transporter attenuates the disease phenotype in the severely-affected R6/2 HD transgenic mouse model (Miller et al. 2008).

Other neurological disorders have been linked to GLT1/EAAT2 downregulation such as **Alzheimer's disease (AD)**, **major depresive disorder (MDD), FXS (FXS), taumatic brain injury (TBI)** and **Parkinson's disease (PD).** Pharmachological upregulation by means of ceftriaxone or LDN/OSU-0212320, a novel translational activator, result in a rescue of the phenotye of the respective disease models (Takahashi et al. 2015), pointing to the potential modulation of GLT1 in the treatment of major neurological disorders.

## IV.A.V Cerebellum as a model for neuroglial interaction

The cerebellum represents a very elegant model to study the synaptic circuitry and neuroglial interaction, as the neuronal circuits and the release of excitatory and inhibitory neurotransmitters are well defined and characterized (**Fig. IV.1**) (Watson et al. 2012).

The cerebellar cortex can be divided in three morphologically distinct layers: the granular layer, which contains numerous granule neurons and scattered Golgi neurons and less studied Lugaro cells and unipolar brush cells; the Purkinje cell layer, a monolayer formed by the soma of the Purkinje neurons and Bergman glia; and the molecular layer, in which stellate and basket interneurons are located as well as the Purkinje cells dendritic arborization, Bergmann glia processes and the axons of the granule cells forming the parallel fibers.

Two major synaptic inputs, both excitatory, arrive to the cerebellar cortex: the mossy fibers from the neurons in the thalamus, brainstem and spinal cord; and the climbing fibers from the neurons in the inferior olivary nucleus of the medulla oblongata in the brainstem. Both mossy and climbing fibers project glutamatergic synapses to the deep cerebellar nuclei, as well as to the cerebellar cortex. In the cerebellar cortex, the mossy fibers form excitatory synapses on the granule cells. The axons of the granule cells will form glutamatergic synapses on the distal

dendrites of the Purkinje neurons, in the molecular layer. On the other hand, the climbing fibers form excitatory synapses directly on the cell body and proximal dendrites of the Purkinje cells. The Bergmann glia tightly wraps the Purkinje cells synapses, preventing prolonged excitation and spillover of the glutamate to adjacent synapses through the re-uptake of excessive glutamate.

Inhibitory interneurons, such as Golgi cells in the granule cell layer and stellate and basket cells in the molecular layer, assure the fine-tuning of the cerebellar synaptic transmission.

Finally, axons of the Purkinje cells form inhibitory synapses on the neurons of the deep cerebellar nuclei, which will send the cerebellar outputs towards the cortex and the brainstem, to modulate the motor control.

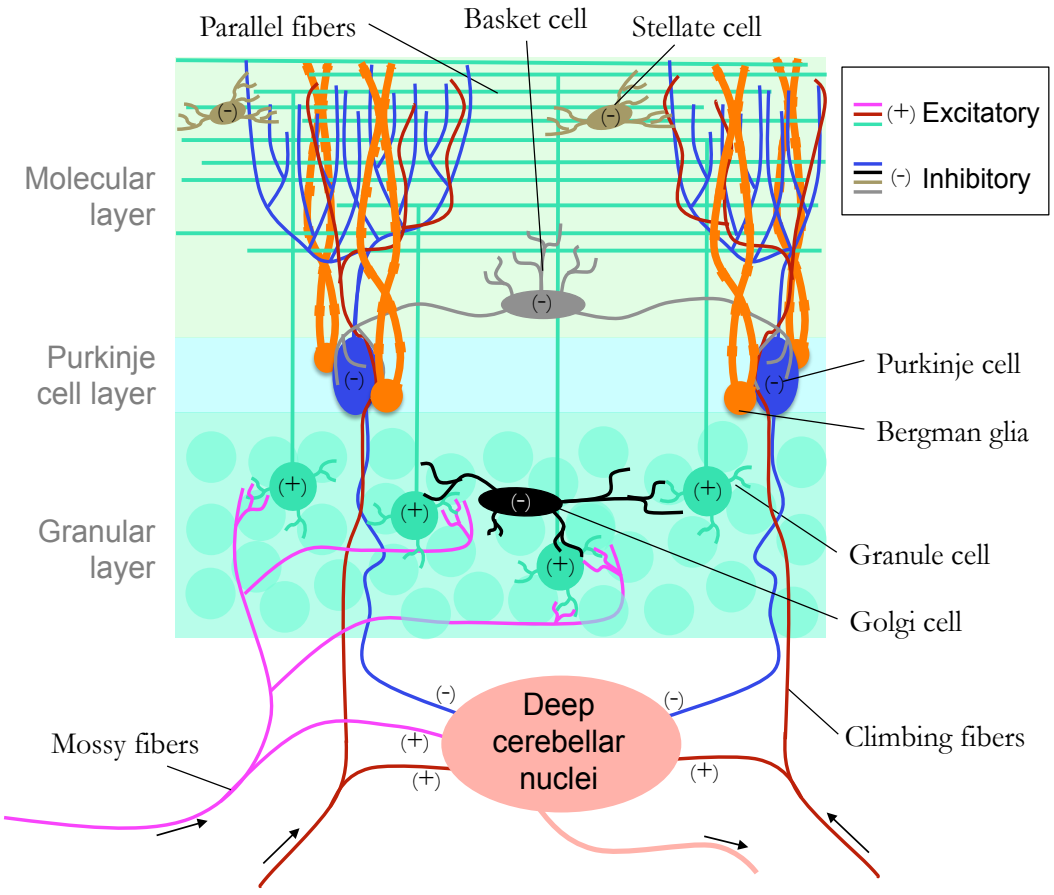


**Figure IV.1. Schematic representation of the main neuronal circuits in the cerebellar cortex.**
Major cell types of the cerebellar cortex are represented inside the cerebellar layers. Inputs and outputs of the cerebellum are indicated by black arrows. Excitatory and inhibitory neurons and synapses are indicated by (+) and (-) respectively.

Besides motor control, the cerebellum regulates movement of distal and proximal muscles, maintenance of posture and equilibrium and also highly skilled movements, including eye movement and speech. In recent years, the cerebellum has also been linked to language, spatial and cognitive functions, including visuo-motor learning (Glickstein et al. 2011). Thus, abnormalities in cerebellar excitatory and inhibitory neurons, synaptic transmission or Bergmann glia function will disrupt the fine control of coordinated movement and visuospatial learning, resulting in different types of ataxia, dysarthria and cerebellar cognitive affective syndrome (Schmahmann 2004).

# IV.B. Context of the study

## IV.B.I Glutamatergic neurotransmission in DM1 brain

While structural imaging studies provide increasing data on brain connectivity and gray and white matter changes in the brain of DM1 patients, the metabolic status of DM1 brain is today still largely unknown. Some studies have reported abnormal levels of neurotransmitters and brain metabolites, such as a reduction in N-acetylaspartate, creatine and choline in different brain regions (Chang et al. 1998; Vielhaber et al. 2006), and one recent study reported abnormalities in the glutamatergic system in DM1 brain (Takado et al. 2015). However, a wider and detailed study of neurotransmitters and metabolites must be performed in different regions of DM1 brain, on a large cohort of patients, to better understand the neurochemical mechanisms of CNS impairment. The use of proton magnetic resonance spectroscopy (H-MRS) to detect early changes in brain metabolites, together with the use of already available pharmacological approaches to correct those changes, could provide palliative treatment for DM1 neuropathology, while waiting for efficient molecular therapies targeting the CTG/CUG expansion.

## IV.B.II Cerebellar dysfunction in DMSXL mice

With a general aim of better understanding the molecular and pathophysiological consequences of the CTG expansion, our laboratory has been increasingly focusing on deciphering the CNS abnormalities and neurophysiological impairment observed in DM1 patients, with the help of DMSXL transgenic mice. The DMSXL mouse model is today the only research model expressing human *DMPK* transcripts, with more than 1500 CTG repeats, in many tissues, including the brain. Thus, DMSXL mice represent a powerful tool to study the molecular and cellular mechanisms linking the CTG expansion to DM1 neurological symptoms, including the regional distribution of toxic RNA foci throughout brain regions, the abnormalities in transcriptome and proteome and the behavioral abnormalities in response to the CTG expansion.

Before my arrival to the laboratory, the research group had found abundant CUG foci in the Bergman glia in the cerebellum of DMSXL mice, which co-localized with MBNL1 and MBNL2 and were associated with more pronounced spliceopathy in these cells relative to the neighboring Purkinje cells. The high RNA toxicity in the Bergman glia was correlated with abnormal electrophysiological activity of the Purkinje neurons, as well as motor incoordination in the runway test, which assesses cerebellum-dependent motor behavior. Interestingly, proteomics analysis revealed downregulation of the glial glutamate transporter GLT1 in DMSXL mice cerebellum, frontal cortex and brainstem, which could explain the DMSXL Purkinje cells hyperexcitability through defective neuroglial communication. These molecular abnormalities were validated in human DM1 post-mortem cerebellum, pointing to the cerebellum as a possible contributor to DM1 neuropathology.

# IV.C. Research objectives

Given the essential role of GLT1 in fine regulation of glutamate levels in the CNS, my aim was to determine which **molecular mechanisms** are responsible for GLT1 downregulation in DM1, and what are the **functional consequences** of this downregulation.

I have first studied the possible contribution of missplicing to GLT1 downregulation as well as the impact of MBNL knock down and CELF upregulation on the levels of GLT1 protein and mRNA. Next I analyzed the functional consequences of GLT1 downregulation on glutamate uptake and excitotoxicity in neuroglial co-cultures and the possibility of rescuing the observed phenotypes by upregulation of GLT1 levels.

# IV.D. Results

The experimental results obtained in this study are presented in the following article, in which I am co-first author (*):

Géraldine Sicot *, Laurent Servais *, **Diana M. Dincã** *, Axelle Leroy, Cynthia Prigogine, Fadia Medja, Sandra O. Braz, Aline Huguet-Lachon, Cerina Chhuon, Annie Nicole, Noëmy Gueriba, Ruan Oliveira, Bernard Dan, Denis Furling, Maurice S. Swanson, Ida Chiara Guerrera, Guy Cheron, Geneviève Gourdon and Mário Gomes-Pereira **Downregulation of the Glial GLT1 Glutamate Transporter and Purkinje Cell Dysfunction in a Mouse Model of Myotonic Dystrophy** – *Cell Reports* (2017) *19*, 2718-2729

A brief summary of my contribution to this work is presented below:

First of all, to determine if the electrophysiological abnormalities observed in the DMSXL cerebellum were not mediated by other mechanisms besides GLT1 downregulation I measured the expression levels of key calcium-binding proteins (calbindin, calretinin and parvalbumin) and of the other major glial glutamate transporter in the cerebellum (GLAST). None of these proteins showed deregulated expression in DMSXL cerebellum, further supporting the specific mediating role of GLT1 in DMSXL cerebellum dysfunction.

Second, I studied the **molecular mechanisms of GLT1 downregulation** in DM1. I confirmed the downregulation of GLT1 at the mRNA level in human astroglioma cells in response to the CTG expansion, and analyzed the possible contribution of abnormal splicing events in both mouse and human brains. None of the missplicing events previously described in

other neurodegenerative conditions were detected in DMSXL mice or DM1 patients' post-mortem brains.

Next I assessed the contribution of CELF upregulation and MBNL depletion to GLT1 downregulation: CELF 1 and CELF 2 do not play a major role, as their overexpression in human astroglioma cells did not affect GLT1 expression. On the other hand, MBNL1 inactivation in human cells was sufficient to reduce *GLT1* mRNA levels, and the loss of MBNL1 in *Mbnl1* KO and *Mbnl1*/*Mbnl2* DKO mice significantly reduced GLT1 protein levels *in vivo,* confirming the mediating role of MBNL1 in GLT1 expression regulation, independent of CELF proteins. Loss of MBNL2 in *Mbnl2* KO mice did not affect GLT1 levels, probably due to the compensation by MBNL1. The critical role of MBNL1 in the regulation of glial GLT1 was associated with a 2-fold increase of MBNL1/MBNL2 ratio in homogenous DMSXL astrocytes compared to neurons, which may suggest a more important role of MBNL1 in the astroglial population.

Finally I studied the pathophysiological **consequences of GLT1 downregulation** in DMSXL brains. Lower levels of GLT1, confirmed both in the cytoplasm as well as membrane-bound fraction in DMSXL cerebellum, are expected to decreased uptake of glutamate from the extracellular space. My results indicated a decrease in glutamate uptake by DMSXL cultured astrocytes, which was rescued by the overexpression of GLT1. The reduced glutamate uptake was not mediated by defects in GLAST expression, since the levels of this glutamate transporter were unchanged in DMSXL primary astrocytes. I next tested the consequences of lower glutamate uptake on the neuroglial interactions in mixed co-cultures. An excess of glutamate at the synapse has excitotoxic effects on the postsynaptic neurons, leading to neurites collapse and neuronal death. Interestingly, neurons cultured in presence of DMSXL astrocytes displayed increased susceptibility to glutamate-induced excitotoxicity, showing a faster collapse of their neurites than in the presence of WT astrocytes. This enhanced neurotoxicity was rescued by the overexpression of GLT1 via plasmid transfection or ceftriaxone treatment. The positive effect of ceftriaxone in DMSXL mice was further confirmed by our collaborators, who demonstrated that

5 days of treatment with this antibiotic resulted in a significant improvement of DMSXL motor coordination, and a significant decrease in Purkinje cells hyperexcitability. Together these results open a promising route to pharmacological modulation of GLT1 expression and glutamate activity in DM1 brains.

# IV.E. Discussion

The defective expression of GLT1 in DMSXL cerebellum is associated with Purkinje cell hyperexcitability and mouse motor incoordination. Toxic CUG RNAs sequester and deplete MBNL1 from the cells, leading to downregulation of GLT1. As a consequence, glutamate uptake by DMSXL astrocytes is decreased and glutamate-mediated neuronal excitotoxicity is increased in neuroglial co-cultures. Pharmacological upregulation of GLT1 rescues the cellular and behavioral abnormalities of DMSXL mice, demonstrating the important role that glial abnormalities play in the control of CNS functions and opening the way for preclinical assessment of novel therapies in DM1.

The promising results obtained in this project have paved the route to a new ongoing study aimed to characterize the glutamate homeostasis and evaluate the therapeutic modulation of glutamate neurotransmission in DM1 CNS. It is important to determine if GLT1 downregulation in DMSXL brains leads to impaired glutamate uptake and exitotocicity *in vivo,* by measuring the extracellular glutamate concentrations by microdialysis and evaluating synaptic and neuronal ultrastructure by electron microscopy.

The cerebellum represents a good model for studying synaptic abnormalities and neuroglial interaction defects, as different cell types are juxtaposed and easy to identify, the synaptic projections are well characterized and the output of the Purkinje cells activity is easy to measure from a technical point of view. In this study we have centered our attention on the cerebellum, given its high content in toxic RNA foci, splicing abnormalities and behavioral defects associated with this brain area in DMSXL mice. Even if clinical reports have not centered

their attention on the cerebellum of DM1 patients, the high frequency of stumbles and falls (Wiles et al. 2006) and abnormal connectivity observed in DM1 cerebellum (Serra, Mancini, et al. 2016) strongly suggest that this brain region should no longer be overlooked in DM1 patients.

GLT1 downregulation is not confined to DM1 cerebellum but it also extends to frontal cortex, brainstem and possibly to other brain regions. Electrophysiological measurements of neuronal activity in these regions could give an indication of the functional impact of GLT1 downregulation, and its possible link to the abnormal behaviors previously described in DMSXL mice (Hernandez-Hernandez et al. 2013) and DM1 patients (Gourdon & Meola 2017). Moreover, DMSXL behavior can be re-assessed after ceftriaxone treatment or other means pharmacological intervention to upregulate GLT1 expression. These experiments will clarify the relationship between abnormal glutamate neurotransmission and the behavior abnormalities described and allow the identification of the most promising molecule to modulate DM1 brain glutamatergic transmission for possible future clinical trials.

Since the identification of increased GLT1 expression induced by β-lactam antibiotics (Rothstein et al. 2005), many studies have focused on the beneficial effects of this class of compounds on neurological diseases. Ceftriaxone has proved to have positive effects in several animal models of neurological diseases (Takahashi et al. 2015), including delay loss of neurons and muscle strength and increase survival in a mouse model of ALS (Rothstein et al. 2005), improve glutamate uptake and behavioral phenotype in the R6/2 mouse model of HD (Miller et al. 2008) and reduce regional gliosis and post-traumatic seizures in in a rat model of epileptogenic traumatic brain injury (Goodrich et al. 2013). Given its positive effects and low toxicity, ceftriaxone has been included in clinical trials for the treatment of bipolar disorders and ALS. No results have been reported yet for the use of ceftriaxone as a treatment for bipolar disorders (Clinical trial identifier: NCT00512616). The three-stage clinical trial of ceftriaxone in ALS indicated that ceftriaxone presents promising pharmacokinetics (stage 1) and safety (stage 2), with a slower functional decline in ceftriaxone-treated patients compared to placebo (stage 2).

However during the efficacy (stage 3) trial, which included more than 500 ALS patients, the functional decline did not differ between treatment and placebo, and neither did the survival rate between groups (Cudkowicz et al. 2014). Ceftriaxone did not demonstrate high efficacy on ALS patients, who suffer from a very rapid motoneuron decline, which demands and highly efficient therapeutic strategies in a short time window. Despite these negative results in ALS, it still remains possible that ceftriaxone will improve the neurological manifestations of DM1, which are slow progressing over long periods of time, and include defects in high order executive function, visuospatial memory and learning. As no curative treatment is currently available for DM1 patients, the repositioning of a drug (already in the market) that could slow down the progression of CNS-related symptoms would represent a major breakthrough and could significantly improve the quality of life of DM1 patients.

Article

Cell Reports

# Downregulation of the Glial GLT1 Glutamate Transporter and Purkinje Cell Dysfunction in a Mouse Model of Myotonic Dystrophy

## Graphical Abstract

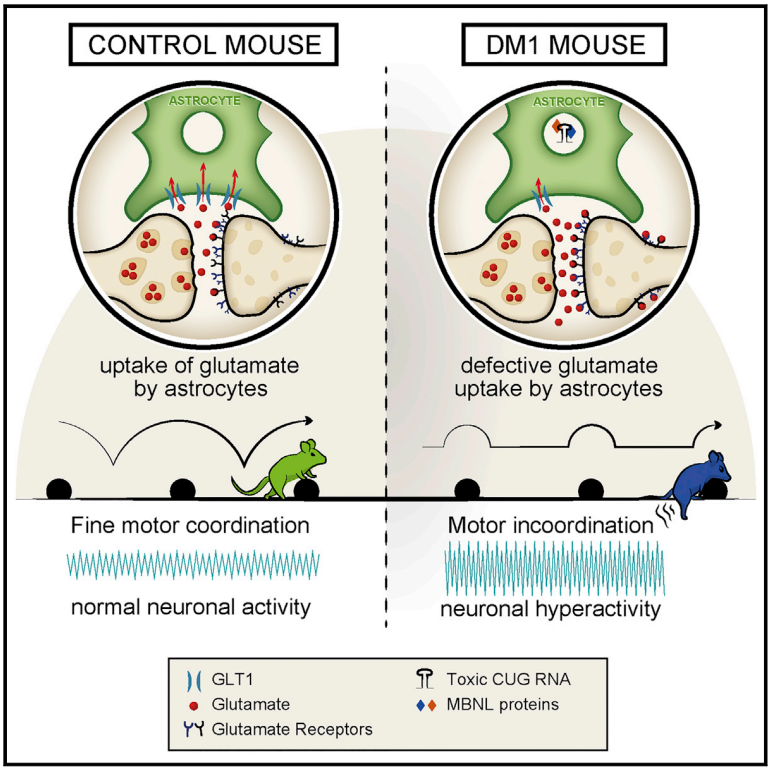


## Highlights

- Bergmann glia show marked RNA toxicity in the cerebellum of DM1 mice and patients
- DM1 mice show reduced motor coordination associated with Purkinje cell hyperexcitability
- GLT1 is downregulated in astrocytes, causing glutamate neurotoxicity
- GLT1 upregulation rescues excitotoxicity, Purkinje firing, and motor coordination

## Authors

Géraldine Sicot, Laurent Servais, Diana M. Dinca, ..., Guy Cheron, Geneviève Gourdon, Mário Gomes-Pereira

## Correspondence

genevieve.gourdon@inserm.fr (G.G.), mario.pereira@inserm.fr (M.G.-P.)

## In Brief

Neural dysfunction in myotonic dystrophy is not fully understood. Using a transgenic mouse model of the disease, Sicot et al. find electrophysiological and motor evidence for cerebellar dysfunction in association with pronounced signs of RNA toxicity in Bergmann glia. Upregulation of a defective glial-specific glutamate transporter corrects cerebellum phenotypes.

Sicot et al., 2017, Cell Reports *19*, 2718–2729
June 27, 2017 
http://dx.doi.org/10.1016/j.celrep.2017.06.006

CellPress

OPEN ACCESS
CellPress

Cell Reports
Article

# Downregulation of the Glial GLT1 Glutamate Transporter and Purkinje Cell Dysfunction in a Mouse Model of Myotonic Dystrophy

Géraldine Sicot,[1,2,10] Laurent Servais,[3,10] Diana M. Dinca,[1,2,10] Axelle Leroy,[4,5] Cynthia Prigogine,[4,5] Fadia Medja,[1,2] Sandra O. Braz,[1,2] Aline Huguet-Lachon,[1,2] Cerina Chhuon,[6] Annie Nicole,[1,2] Noëmy Gueriba,[1,2] Ruan Oliveira,[7] Bernard Dan,[4,8] Denis Furling,[9] Maurice S. Swanson,[7] Ida Chiara Guerrera,[6] Guy Cheron,[4,5] Geneviève Gourdon,[1,2,*] and Mário Gomes-Pereira[1,2,11,*]

[1]Laboratory *CTGDM*, Inserm UMR1163, 75015 Paris, France
[2]Institut Imagine, Université Paris Descartes-Sorbonne Paris Cité, 75015 Paris, France
[3]Institut I-Motion, Hôpital Armand Trousseau, 75012 Paris, France
[4]Laboratory of Neurophysiology and Movement Biomechanics, Université Libre de Bruxelles, 1050 Brussels, Belgium
[5]Laboratory of Electrophysiology, University of Mons, 7000 Mons, Belgium
[6]Proteomics Platform 3P5-Necker, Université Paris Descartes-Structure Fédérative de Recherche Necker, Inserm US24/CNRS UMS3633, 75014 Paris, France
[7]Department of Molecular Genetics and Microbiology, Center for NeuroGenetics and the Genetics Institute, University of Florida College of Medicine, Gainesville, FL 32610, USA
[8]Inkendaal Rehabilitation Hospital, Vlezenbeek B-1602, Belgium
[9]Sorbonne Universités UPMC Université Paris 06, Inserm, Centre de Recherche en Myologie UMRS974, Institut de Myologie, Groupe Hospitalier Pitié-Salpêtrière, 75013 Paris, France
[10]These authors contributed equally
[11]Lead Contact
*Correspondence: genevieve.gourdon@inserm.fr (G.G.), mario.pereira@inserm.fr (M.G.-P.)
http://dx.doi.org/10.1016/j.celrep.2017.06.006

## SUMMARY

**Brain function is compromised in myotonic dystrophy type 1 (DM1), but the underlying mechanisms are not fully understood. To gain insight into the cellular and molecular pathways primarily affected, we studied a mouse model of DM1 and brains of adult patients. We found pronounced RNA toxicity in the Bergmann glia of the cerebellum, in association with abnormal Purkinje cell firing and fine motor incoordination in DM1 mice. A global proteomics approach revealed downregulation of the GLT1 glutamate transporter in DM1 mice and human patients, which we found to be the result of MBNL1 inactivation. GLT1 downregulation in DM1 astrocytes increases glutamate neurotoxicity and is detrimental to neurons. Finally, we demonstrated that the upregulation of GLT1 corrected Purkinje cell firing and motor incoordination in DM1 mice. Our findings show that glial defects are critical in DM1 brain pathophysiology and open promising therapeutic perspectives through the modulation of glutamate levels.**

## INTRODUCTION

Repeat-containing RNA can cause neurological diseases through a *trans*-dominant gain of function (Mohan et al., 2014; Sicot and Gomes-Pereira, 2013). RNA toxicity is best described in myotonic dystrophy type 1 (DM1), but it operates in an increasing number of conditions (Sicot et al., 2011). DM1 is the most common muscular dystrophy in adults, with a variable prevalence ranging from 0.5 to 18 cases in 100,000 individuals (Theadom et al., 2014). DM1 is a multisystemic disorder that affects the skeletal muscle, heart, and the CNS, among other tissues (Udd and Krahe, 2012). Five main clinical forms of DM1 can be distinguished based on age at onset: congenital, childhood, juvenile, adult, and mild or late onset (Dogan et al., 2016). CNS impairment is more pronounced in the early-onset cases. Among these, the congenital patients exhibit moderate to severe intellectual disability. The childhood- and juvenile-onset cases can also show reduced IQ, low cognitive processing speed, and visuospatial impairment, as well as attention and executive deficits (Angeard et al., 2007, 2011). The main CNS manifestations in the adult form include dysexecutive behavior (such as apathy, lack of motivation, and inflexibility), reduced attention and visuospatial construction ability, daytime sleepiness, and impaired social cognition (Meola and Sansone, 2007; Serra et al., 2016; Sistiaga et al., 2010). Overall, the quality of life of DM1 patients is significantly impaired by their cognitive deficits (Antonini et al., 2006; Dogan et al., 2016). Brain disease is further supported by histopathological changes, such as the aggregation of hyperphosphorylated Tau protein isoforms, particularly in the amygdala, hippocampus, and entorhinal and temporal cortex (Caillet-Boudin et al., 2014). White matter lesions, gray matter changes, metabolic deficits, and changes in functional connectivity were reported in multiple brain areas (Caliandro et al., 2013; Minnerop et al., 2011; Serra et al.,

2014, 2015; Weber et al., 2010; Wozniak et al., 2014), implicating the dysregulation of complex brain networks and various cell types (Schneider-Gold et al., 2015; Serra et al., 2016). However, the link between the distribution of DM1 pathology across brain territories and cell types and the neurological symptoms of the disease must be further elucidated.

DM1 is caused by the expansion of an unstable CTG repeat in the 3′ untranslated region (3′ UTR) of the DM protein kinase (*DMPK*) gene (Brook et al., 1992). Repeat number correlates with disease severity and inversely with age of onset. Expanded *DMPK* transcripts accumulate in nuclear RNA foci and perturb the activity of multiple RNA-binding proteins. Among these, the sequestration of muscleblind-like (MBNL) proteins and the upregulation of the CUGBP/Elav-like family (CELF) affect primarily alternative splicing but also RNA transcription, localization and polyadenylation, miRNA processing, protein translation, and phosphorylation of downstream targets (Batra et al., 2014; Goodwin et al., 2015; Hernández-Hernández et al., 2013a, 2013b; Sicot et al., 2011; Wang et al., 2012). Today we do not know the extent or distribution of these events in the CNS, their cellular specificity, or how they contribute to neuropathogenesis.

To investigate DM1 brain disease, we have been using DMSXL mice, which carry a human *DMPK* transgene containing >1,000 CTG repeats (Gomes-Pereira et al., 2007; Seznec et al., 2000). DMSXL homozygotes express enough toxic transcripts to perturb muscular, cardiac, and respiratory function (Algalarrondo et al., 2015; Huguet et al., 2012; Panaite et al., 2013), in association with RNA foci and missplicing (Hernández-Hernández et al., 2013a; Huguet et al., 2012). The expression of expanded CUG RNA in the CNS affects behavior and synaptic function of DMSXL mice (Hernández-Hernández et al., 2013a). In contrast, DM20 mice, overexpressing short *DMPK* transcripts, do not show RNA foci accumulation, obvious phenotypes, or synaptic protein dysfunction (Hernández-Hernández et al., 2013a; Seznec et al., 2001). The differences between mouse lines corroborate the toxicity of expanded CUG RNA repeats in the CNS of DMSXL mice. However, the underlying molecular and cellular mechanisms leading to brain impairment are not entirely known, which delays the development of efficient therapeutic strategies in the CNS.

To overcome this limitation, we have combined molecular, electrophysiological, and behavioral approaches to gain insight into the susceptible cell populations, dysfunctional connections, and affected molecular pathways in the CNS of DM1. It was our aim to better understand brain disease pathogenesis and find promising therapeutic targets. We found evidence of cerebellar glial dysfunction, which is caused by the downregulation of a glutamate transporter that affects neuronal physiology.

## RESULTS

### Bergmann Glia Show Abundant RNA Accumulation in DMSXL Cerebellum

To investigate the impact of the DM1 expansion on different cell populations and networks in the CNS, we investigated the distribution of the canonical molecular signs of the disease (the toxic CUG RNA foci) in different areas of the DMSXL mouse brain. We were particularly intrigued by the distinctive and peculiar distribution of RNA foci in the cerebellum. The cerebellum is a well-organized brain region with a highly specific and uniform laminar arrangement of cells into distinct, easily identified anatomical layers (Voogd and Glickstein, 1998). Fluorescence in situ hybridization (FISH) revealed that CUG RNA foci were rarely found in Purkinje cells, but in contrast, they were abundant in a population of neighboring cells, extending toward the molecular layer. MBNL1 and MBNL2 co-localized with RNA in these foci-rich cells in DMSXL mice (Figure 1A), in contrast to wild-type animals (Figure S1A). MBNL proteins remained distributed throughout the nucleus and cytoplasm of DMSXL Purkinje cells, even in those rare neurons showing RNA foci accumulation, without pronounced sequestration (Figure 1A).

Given the intriguing distribution of RNA foci in DMSXL cerebellum, we sought to identify the nature of foci-rich cells through immunodetection of cell-specific markers. NeuN stains almost exclusively mature granular neurons, whereas Fox1 and Fox2 stain Purkinje and Golgi cells; Fox2 stains also the granular neurons (Kim et al., 2011). We found that foci accumulated preferentially in non-neuronal cells of the molecular layer, which did not express NeuN, Fox1, or Fox2. The non-neuronal nature of these cells was confirmed by GFAP staining (Figure 1B). The distinctive localization around the Purkinje cells into the molecular layer of the cerebellum, the expression of GFAP, and the lack of neuronal markers strongly suggested that the foci-rich cells were Bergmann astrocytes. We have confirmed their nature by the immunodetection of GLAST/SLC1A3, a glial glutamate transporter, which in adult mouse cerebellum is primarily expressed in Bergmann glia (Regan et al., 2007): immunofluorescence combined with FISH revealed greater GLAST expression near Purkinje cells, usually in foci-rich cells (Figure 1B).

To elucidate the reasons behind the preferential accumulation of CUG RNA foci in Bergmann glia, we quantified the levels of expanded *DMPK* transcripts in Bergmann astrocytes and Purkinje cells collected from DMSXL cerebellum by laser capture microdissection. The purity of the collected cells was controlled by RT-PCR amplification of cell-specific transcripts (Figure S1B). qRT-PCR revealed levels of toxic CUG RNA nearly three times higher in Bergmann glia than in adjacent Purkinje cells (Figure 1C). We conclude that higher transgene expression in cerebellar Bergmann glia contributes to the higher foci abundance in this cell type.

### RNA Spliceopathy Is More Pronounced in the Bergmann Glia of the Cerebellum

Higher levels of CUG RNA and foci in Bergmann astrocytes predict pronounced spliceopathy in this cell type. Thus, we studied splicing defects in microdissected DMSXL Bergmann and Purkinje cells. We have previously shown that *Mbnl1* and *Mbnl2* transcripts show consistent missplicing in DMSXL mouse brains (Hernández-Hernández et al., 2013a) and serve as robust markers of spliceopathy in our mouse model. In line with our hypothesis, *Mbnl1* and *Mbnl2* splicing was significantly dysregulated in DMSXL Bergmann glia while remaining unaltered in Purkinje cells (Figure 1D). Overall, the missplicing of these transcripts was mild in the analysis of whole DMSXL cerebellum (Figure S1C), suggesting that splicing abnormalities are pronounced in Bergmann astrocytes but diluted in whole-tissue samples.

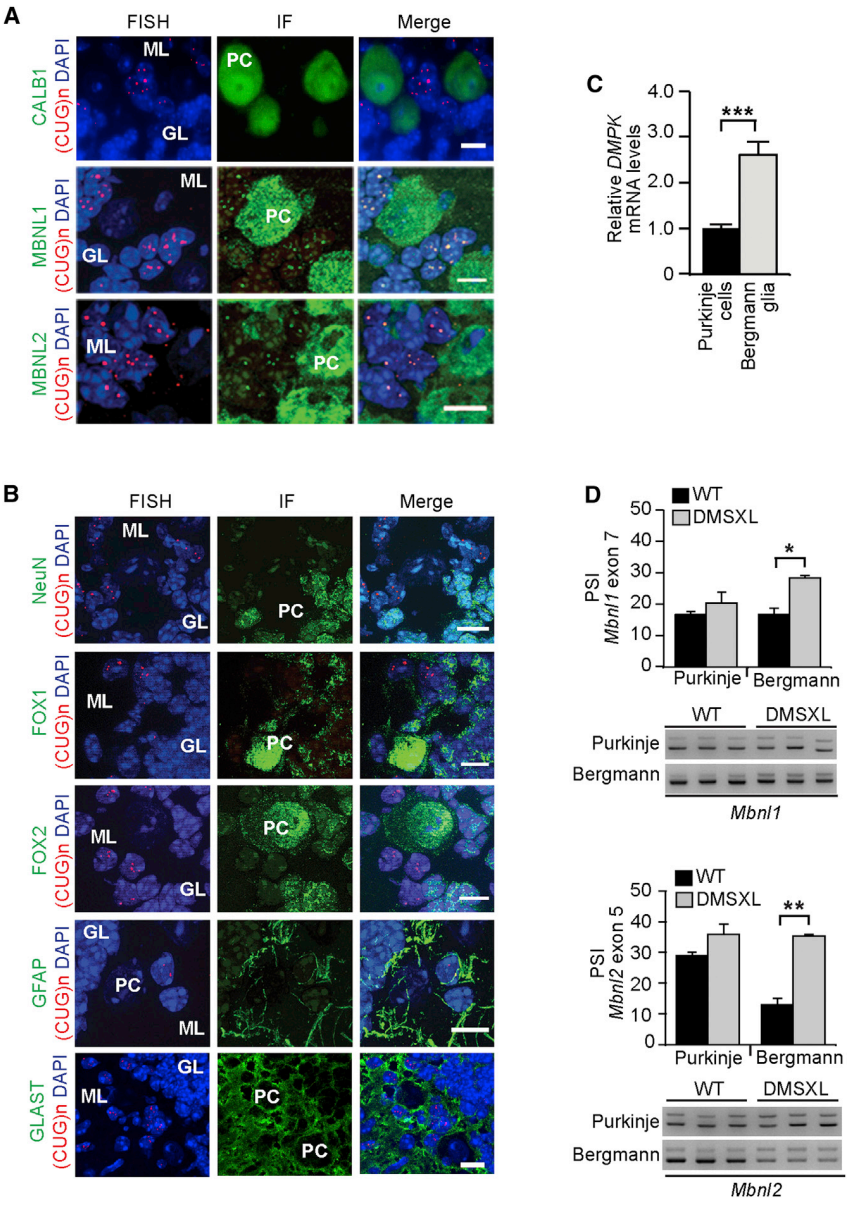


**Figure 1. RNA Foci Accumulate in Cerebellar Bergmann Astrocytes and Deregulate Alternative Splicing**

(A) FISH detection of RNA foci (red) and immunofluorescence of calbindin 1 (CALB1) and MBNL proteins (green) in mouse cerebellum. An example of a rare foci-positive Purkinje cell is shown in the bottom panel.

(B) Identification of cell types showing abundant nuclear RNA foci (red) in DMSXL cerebellum through immunodetection of NeuN, Fox1, Fox2, GFAP, or GLAST (green). DAPI was used for nuclear staining.

(C) Nested qRT-PCR of *DMPK* transgene expression (±SEM) in Purkinje cells and Bergmann astrocytes microdissected from DMSXL cerebellum (n = 3).

(D) Percent of spliced in (PSI) of alternative exon 7 of *Mbnl1* and exon 5 of *Mbnl2* transcripts (±SEM). Purkinje cells and neighboring Bergmann glia were collected by laser microdissection from DMSXL and wild-type (WT) mice (n = 3, each genotype). Three independent technical replicates were studied for each mouse. Representative analyses of alternative splicing by nested RT-PCR are shown.

PC, Purkinje cells; GL, granular layer; ML, molecular layer. The scale bar represents 10 μm. *p < 0.05, **p < 0.01, ***p < 0.001; Mann-Whitney U test. See also Figure S1.

Finally, we assessed the contributing role of CELF proteins to cerebellum pathology. Western blot analysis in whole DMSXL cerebellum revealed mild upregulation of CELF2 but no significant changes in CELF1 levels (Figure S1D).

## Electrophysiological Abnormalities of Purkinje Cells in DMSXL Cerebellum

We next investigated whether Bergmann RNA toxicity in DMSXL mice was sufficient to affect cerebellar function. The functional output of the cerebellar cortex is determined by the Purkinje cell firing, which can be electrophysiologically identified by two types of firing patterns: complex spikes and simple spikes (Cheron et al., 2013). We performed electrophysiological recordings in the Purkinje cell layer of alert DMSXL mice and found significantly higher simple spike firing rates (86.8 ± 7.6 versus 50.5 ± 4.2 Hz) and rhythmicity index (0.13 ± 0.02 versus 0.07 ± 0.01) in DMSXL mice relative to the wild-type controls, indicative of neuronal hyperactivity of Purkinje cells (Figure 2A). In addition, spontaneous fast local field potential (LFP) oscillations were found throughout the cerebellum in all DMSXL mice but were absent in wild-type controls. DMSXL fast LFP oscillations appeared as spindle-shaped episodes of oscillation with a frequency of 200 ± 27 Hz and maximal amplitude of 0.48 ± 0.26 mV (Figure 2B). We quantified calcium buffering proteins and studied DMSXL cerebellum histology, but we did not find obvious changes in steady-state protein levels or overt histopathology that could contribute to the defective Purkinje neuronal activity and cerebellum dysfunction (Figures S2A and S2B).

## Cerebellum-Dependent Motor Incoordination in DMSXL Mice

To confirm cerebellar dysfunction in DMSXL mice, we assessed a cerebellum-dependent behavior phenotype. In the runway test, mice run along an elevated platform and must surmount low obstacles intended to impede their progress. The test assesses cerebellum-dependent motor coordination, and in contrast with rotarod, it is minimally influenced by muscle

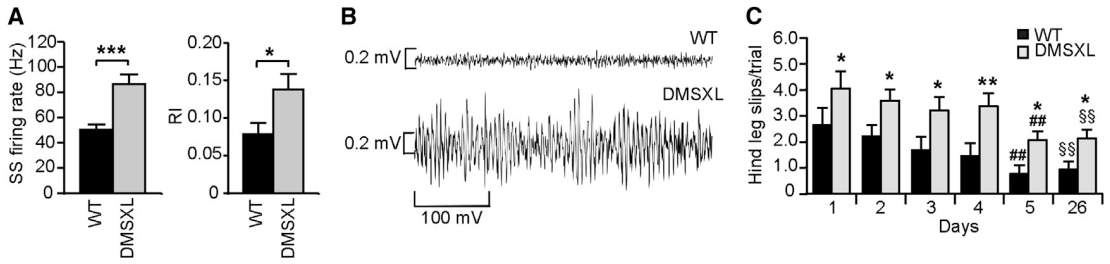


**Figure 2. Cerebellum Dysfunction in DMSXL Mice Revealed by Behavioral and Electrophysiological Phenotyping**

(A) In vivo electrophysiological recordings of single spike (SS) frequency and rhythmicity index (RI) in 2-month-old alert DMSXL (n = 4) and WT mice (n = 3). Error bars represent the SEM. *p < 0.05, ***p < 0.001; Mann-Whitney U test.

(B) Representative fast LFP oscillation in the cerebellum of one DMSXL compared to WT control.

(C) Assessment of cerebellum-dependent motor-coordination of DMSXL (n = 20) and WT controls (n = 21), at 3–4 months in the runway test over 5 consecutive days (days 1–5). The graph represents the average number of hind leg slips per trial (±SEM) (*p < 0.05, **p < 0.01; two-way ANOVA). Learning was assessed by the number of slips at day 5 relative to day 1 (##p < 0.01; two-way ANOVA). Retention of the task was assessed at day 26, following a period of 3 weeks without testing, relative to day 1 (§§p < 0.01; two-way ANOVA).

See also Figure S2.

performance (Bearzatto et al., 2005). The number of slips of the right hind leg is a direct indication of motor incoordination.

Both wild-type and DMSXL showed a progressive and significant decrease in number of hind leg slips from day 1 to day 5 (Figure 2C), indicating the capacity to learn new cerebellum-dependent tasks. However, DMSXL mice showed significantly higher numbers of slips from day 1, pointing to deficits in the fine-tuning of movements and cerebellar dysfunction. After 3 weeks, the test still revealed significantly lower number of slips relative to day 1 in both wild-type and DMSXL mice, demonstrating efficient task retention by both genotypes (Figure 2C). In summary, although capable of acquiring and retaining new cerebellum-dependent motor tasks, DMSXL mice showed signs of motor incoordination.

In conclusion, both electrophysiological and behavioral assessment demonstrated that the expression and accumulation of toxic RNA foci in DMSXL cerebellum (particularly in Bergmann glia) are associated with cerebellum pathology, which is characterized by abnormal Purkinje cell firing and fine motor incoordination.

## The GLT1 Glutamate Transporter Is Downregulated in DMSXL Cerebellum

To decipher the mechanisms of abnormal Purkinje cell activity and cerebellar dysfunction, we used global proteomics to identify expression changes and dysregulated pathways in DMSXL cerebellum. We first studied whole-cell lysates and found that the expression of 241 proteins was altered in DMSXL cerebellum. A Gene Ontology analysis on this 241-protein set revealed that many altered proteins were membrane-bound, but we did not find a biological process predominantly dysregulated in DMSXL cerebellum (Figure 3A). To refine our search, we specifically investigated the membrane-bound proteome of mouse cerebellum and found 60 proteins with altered expression in DMSXL cerebellum. This protein set showed enrichment for ion transport, synaptic transmission, and glutamate signaling (Figure 3B) and included the glial high-affinity glutamate transporter (GLT1) (excitatory amino acid transporter 2 [EAAT2] or solute carrier family 1 member 2 [SLC1A2]). GLT1 is a membrane transporter that in the cerebellum is mainly expressed by the Bergmann glia to clear glutamate released during synaptic transmission from the extracellular space, avoiding excessive stimulation of postsynaptic neurons (Kanai and Hediger, 2004). Therefore, we tested the hypothesis that abnormal GLT1 expression in DMSXL cerebellum results in defective neuroglial communication and abnormal DMSXL Purkinje cell firing.

We first confirmed GLT1 downregulation by western blot in DMSXL cerebellum (Figure 3C), as well as in other mouse brain regions (Figure S3A), but not in control DM20 mice (Figure S3B). Semiquantitative analysis of GLT1 immunofluorescence intensity by confocal microscopy showed a significant reduction in the DMSXL molecular layer, close to the Purkinje cells (Figure S3C). In contrast to GLT1, the levels of GLAST remained unchanged in DMSXL brains (Figure S3D), demonstrating that the impact of expanded *DMPK* transcripts is specific to the GLT1 glutamate transporter. Fractioning of DMSXL cerebellar tissue revealed downregulation of GLT1 in the membrane-bound protein faction (Figure 3D), in line with defective glutamate transport across the membrane. To investigate the functional impact of reduced GLT1 levels, we measured the uptake of radioactive glutamate by DMSXL astrocytes in the presence of WAY213623 (GLT1-specific inhibitor), UCPH (GLAST-specific inhibitor), or TBOA (pan-glutamate transporter inhibitor). We found a significant reduction in total and in GLT1-mediated glutamate uptake when compared to wild-type controls (Figure 3E), consistent with GLT1 downregulation in DMSXL astrocytes (Figure S3E). In contrast, GLAST-mediated transport was unaltered, while TBOA nearly abolished glutamate uptake in both cultures. Transfection of DMSXL astrocytes with GLT1-expressing plasmids corrected defective glutamate transport (Figure 3E). Altogether, these results demonstrate the causative role of GLT1 downregulation in defective glutamate transport by DMSXL astrocytes. GLT1 downregulation is not explained by Bergmann cell loss, as revealed by the quantification of Bergmann-specific transcripts in DMSXL cerebellum, which showed no reduced expression relative to wild-type controls (Figure S3F). Overall, the reduction of GLT1 within the molecular layer is consistent with Bergmann dysfunction.

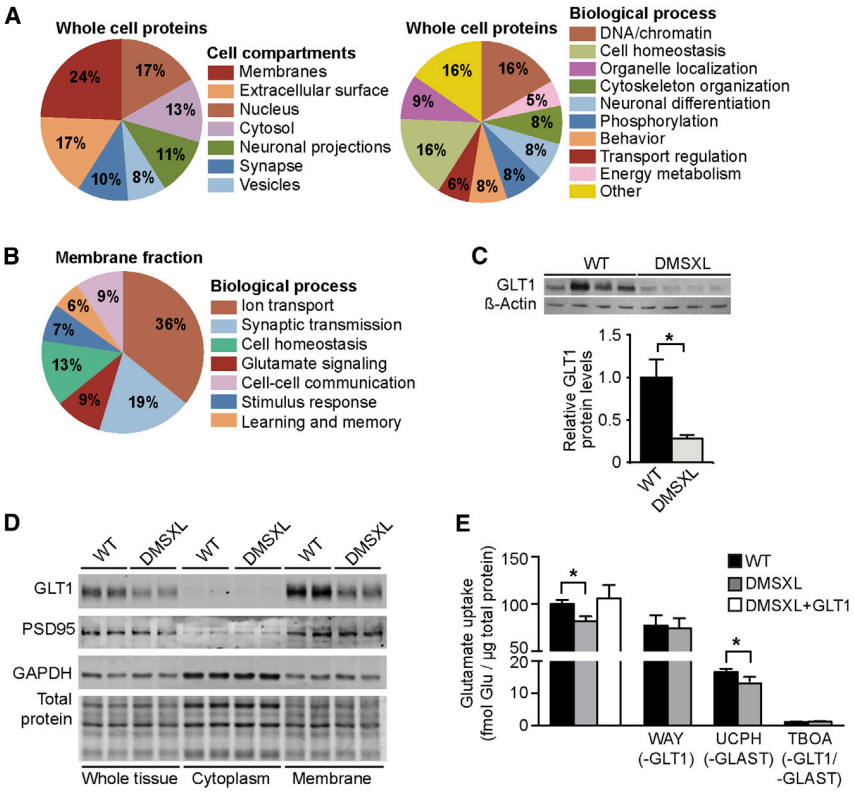


**Figure 3. GLT1 Downregulation in DMSXL Cerebellum**

(A) Isobaric tag for relative and absolute quantification (iTRAQ) analysis of whole cell protein fractions collected from the cerebellum of 2-month-old DMSXL mice and WT littermates (n = 4, each genotype). Pie charts indicate the percentage of altered proteins in the cellular components and biological processes showing the highest significant enrichment in the proteomics expression data.

(B) Quantitative proteomics analysis of the membrane-bound proteins from the cerebellum of 2-month-old DMSXL mice and WT littermates (n = 2, each genotype). Pie charts indicate the percentage of altered membrane proteins in the biological processes showing the highest significant enrichment.

(C) Western blot quantification of GLT1 protein levels in the cerebellum of DMSXL and WT mice (n = 4, each genotype) at 2 months of age. β-actin was used as loading control.

(D) Western blot detection of GLT1 in cytosolic and membrane protein fractions of DMSXL and WT cerebellum at 2 months of age (n = 2, each genotype). GAPDH and PSD95 confirmed cytosolic and membrane protein enrichment, respectively. Total protein was visualized by stain-free protocols and used as loading control.

(E) Uptake of radioactive glutamate by WT and DMSXL astrocytes: under control conditions, following DMSXL transfection with GLT1-expressing plasmids, or upon selective inhibition of GLT1 (WAY213623), GLAST (UCPH 101), or both (TBOA) (n = 3, each group).

Errors bars represent the SEM. *p < 0.05; Mann-Whitney U test. See also Figure S3.

## Human DM1 Cerebellum Shows Bergmann-Specific RNA Foci Accumulation and GLT1 Downregulation

We then assessed the implications of the mouse findings to the human condition through the analysis of post-mortem DM1 brains. In human DM1 cerebellum, although small foci were rarely detected in Purkinje cells, large and more abundant foci accumulated predominantly in calbindin 1 (CALB1)-negative cells, co-localizing with MBNL1 and MBNL2 (Figure 4A). Like in DMSXL mice, the preferential accumulation of RNA foci was concentrated in the Bergmann glia, which expressed GFAP and GLAST in the absence of NeuN, Fox1, or Fox2 neuronal markers (Figure 4B). The analysis of selected MBNL1 and MBNL2 candidate splicing events revealed that human DM1 cerebellar tissue showed mild spliceopathy (Figure S4A), in association with CELF2 upregulation (Figure S4B).

Finally, we studied GLT1 protein expression in human DM1 cerebellum and found a dramatic reduction in five of seven adult DM1 patients: overall, GLT1 was reduced by ~50% relative to non-DM controls (Figure 4C). GLT1 was also decreased in DM1 frontal cortex and brainstem (Figure S4C), indicating wider dysregulation of this glutamate transporter throughout the CNS.

## GLT1 Downregulation Is Mediated by MBNL1 Inactivation

To gain insight into the mechanisms of GLT1 downregulation, we quantified transcript levels and found significantly lower levels of *GLT1* mRNA in the cerebellum and frontal cortex of the DM1 patients with pronounced protein downregulation (Figure 5A). In amyotrophic lateral sclerosis (ALS), missplicing of *GLT1* results in RNA degradation and loss of protein (Lin et al., 1998). To test whether similar mechanisms operate in DM1, we studied ALS-associated exon missplicing and abnormal intron retention. We did not find obvious splicing abnormalities in DM1 patients or in DMSXL mice (Figures 5SA and 5SB).

We then tested whether GLT1 downregulation was the direct result of the expression of CUG-containing RNA or a secondary consequence associated with DM1 brain disease progression. To this end, we transfected human T98G glioblastoma cells with expanded *DMPK* constructs and found that CUG RNA expansions reduced *GLT1* transcript levels relative to no-repeat control constructs (Figure 5B).

MBNL proteins regulate various aspects of RNA metabolism. Hence, we tested whether MBNL1 or MBNL2 inactivation was sufficient to lower GLT1 levels. We used short hairpin RNA (shRNA) to knockdown MBNL1 and/or MBNL2 in T98G cells (Figure S5C). qRT-PCR revealed that MBNL1 downregulation alone was sufficient to decrease *GLT1* mRNA levels, while MBNL2 inactivation left *GLT1* transcripts unchanged (Figure 5C). The simultaneous treatment with MBNL1 and MBNL2 shRNA resulted in a modest downregulation of both MBNL proteins (Figure S5C), which was insufficient to affect *GLT1* mRNA levels. We confirmed the determinant role of MBNL1 in vivo through

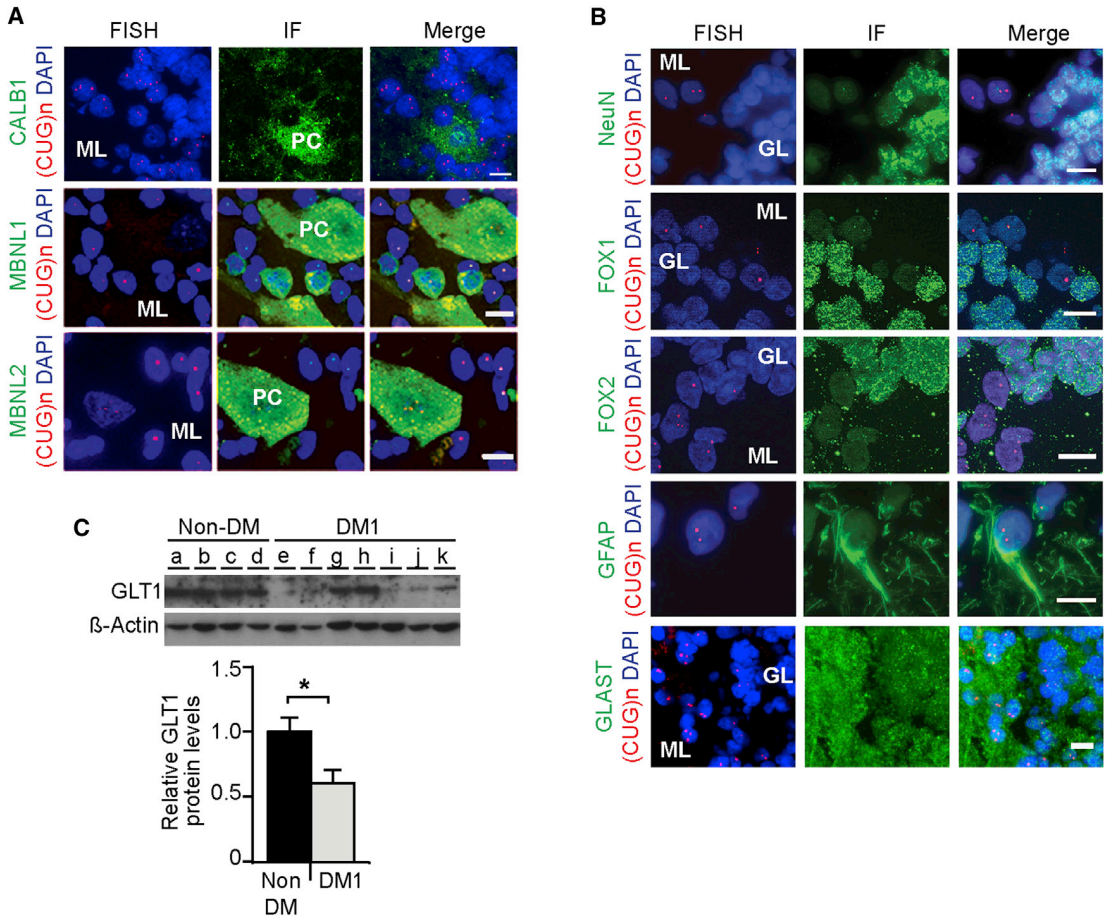


**Figure 4. Analysis of RNA Foci Accumulation and GLT1 Downregulation in Human DM1 Cerebellum**

(A) FISH of RNA foci (red) combined with immunofluorescence detection of CALB1 and MBNL proteins (green) in post-mortem brains from adult DM1 patients. Some rare and small RNA foci were detected in human Purkinje cells but were not associated with pronounced sequestration of MBNL proteins.

(B) FISH of RNA foci (red) and protein markers (green) of different cerebellar cell populations near Purkinje cells.

(C) Western blot quantification of GLT1 in DM1 cerebellum (n = 7) relative to non-DM controls (n = 4). β-actin was used as loading control.

The scale bar represents 10 μm. Error bars represent the SEM. *$p < 0.05$; Mann-Whitney U test. See also Figure S4.

the analysis of *Mbnl1* and *Mbnl2* knockout (KO) mice (Charizanis et al., 2012; Kanadia et al., 2003): only the cerebellum of *Mbnl1*$^{-/-}$ mice showed significant downregulation of GLT1. In contrast to double-shRNA-transfected T98G cells, the inactivation of MBNL1 and MBNL2 proteins in *Mbnl1*/*Mbnl2* double-KO mice (Goodwin et al., 2015) significantly reduced GLT1 levels (Figures 5D and S5D).

In an attempt to provide insight into the prevalent role of MBNL1 over MBNL2 in the regulation of the glial-specific GLT1 glutamate transporter, we quantified the expression of MBNL proteins in mouse primary neurons and astrocytes. The analysis revealed that the relative expression of MBNL1 is 2-fold higher in mouse primary astrocytes relative to neurons (Figure S5E), suggesting a more important role of MBNL1 in glial cells.

Because CELF2 is upregulated in DM1 brains, we also studied whether CELF proteins could regulate GLT1 expression and contribute to abnormal GLT1 levels. Transient transfection of CELF1 and CELF2 in T98G cells (Figure S5F) did not result in lower *GLT1* mRNA levels (Figure 5E).

In summary, our results demonstrate that GLT1 protein downregulation in DM1 is associated with lower transcript levels without evidence of missplicing and is mediated by partial inactivation of MBNL1 in glial cells, independently of CELF proteins.

## GLT1 Downregulation in DMSXL Astrocytes Is Associated with Increased Glutamate Neurotoxicity

Glutamate transporters guard against prolonged elevation of extracellular glutamate concentration and protect neurons from excitotoxicity (Kanai and Hediger, 2004). To investigate the impact of GLT1 downregulation on neuronal physiology in DM1, we tested whether primary DMSXL astrocytes expressing significantly lower levels of GLT1 (Figure S3E) failed to protect neurons against glutamate neurotoxicity in culture. To this end, we co-cultured neurons and astrocytes of mixed genotypes and allowed neurites to extend for 8 days. Then, we added 50 μM of glutamate to the medium and monitored neuronal damage by measuring neurite collapse by fluorescence live-cell videomicroscopy (Figure 6A). Neurite collapse was significantly

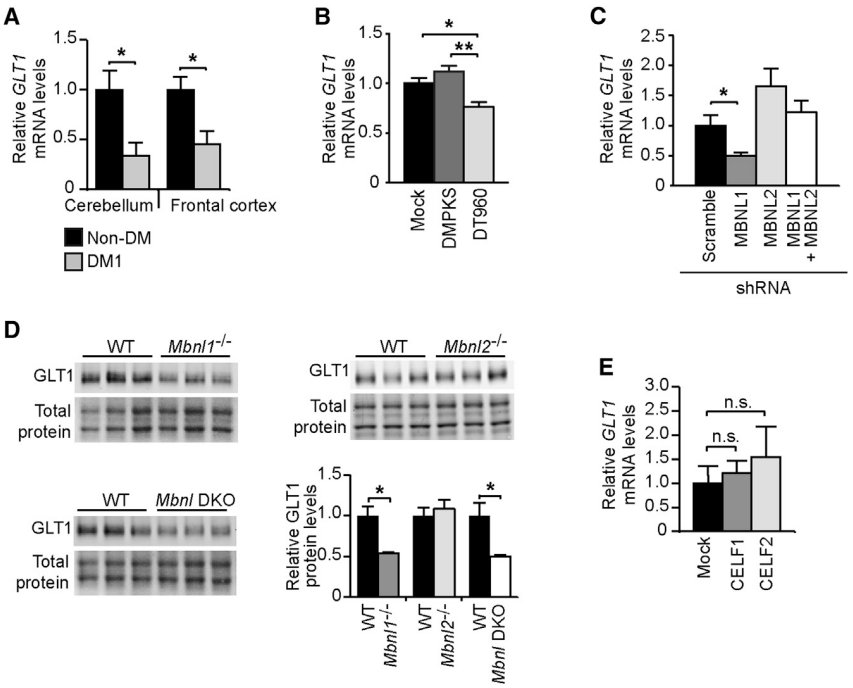


**Figure 5. Transcriptional *GLT1* Downregulation Is Mediated by MBNL1 Inactivation**

(A) Quantification of *GLT1* transcripts (±SEM) in the cerebellum and frontal cortex of DM1 patients showing the most pronounced protein decrease (n = 5) relative to non-DM controls (n = 4).

(B) Quantification of *GLT1* transcripts in human T98G glial cells transfected with expanded *DMPK* constructs containing 960 interrupted CTG repeats (DT960) relative to no-repeat (DMPKS) and mock transfected controls.

(C) Quantification of *GLT1* mRNA following MBNL1 and/or MBNL2 knockdown in T98G cells.

(D) Western blot quantification of GLT1 protein levels in 2- to 4-month-old *Mbnl1* KO, *Mbnl2* KO, in *Mbnl1*/*Mbnl2* double-KO mice (DKO) relative to WT littermates (n = 3, each genotype). Representative western blot membranes of at least three technical replicates. Total protein was visualized by stain-free protocols and used as loading control.

(E) Quantification of *GLT1* mRNA in T98G cells overexpressing CELF1 or CELF2.

Data are represented as the mean (±SEM) of three independent experiments in (B), (C), and (E). *$p < 0.05$, **$p < 0.01$; Mann-Whitney U test in (A) and (D), one-way ANOVA in (B) and (C); n.s., not statistically significant. See also Figure S5.

more pronounced in wild-type and DMSXL neurons co-cultured with DMSXL astrocytes than in neurons grown with wild-type astrocytes (Figure 6B). Antagonists of NMDA and AMPA receptors reduced glutamate-induced neurite collapse and eliminated differences between genotypes (Figure 6B), demonstrating the mediating role of glutamate receptors in the neurotoxicity detected in neuroglial cultures. The increased glutamate neurotoxicity in the presence of DMSXL astrocytes was not accounted for by significant changes in the expression of NMDA and AMPA receptors: western blot quantification GRIN1 (NMDA receptor subunit type 1) and GRIA2 (AMPA receptor subunit type 2) did not show significant changes in DMSXL cell cultures (Figure 6C) or in brain tissue (Figures S6A and S6B). To determine whether the deleterious effect of astrocytes on neurons was directly mediated by GLT1 downregulation, we transfected DMSXL astrocytes with GLT1 before glutamate neurotoxicity assessment. GLT1 transfection of DMSXL astrocytes rescued the neurite collapse (of both wild-type and DMSXL neurons) to levels that were indistinguishable from those measured in the presence of wild-type astrocytes (Figure 6D).

Altogether, these results demonstrate that the downregulation of GLT1 in DMSXL astrocytes perturbs the neuroglial interplay and has a negative impact on neuronal physiology, failing to protect against glutamate excitotoxicity.

## GLT1 Upregulation by Ceftriaxone Corrects the Cerebellum Phenotype of DMSXL Mice

To explore the role of GLT1 downregulation in DMSXL cerebellar dysfunction, we first used LFP oscillations in the Purkinje cell layer of the cerebellar vermis to compare the extracellular electrical activity of DMSXL and *Glt1*-deficient mice, which show a ~60% reduction in GLT1 (Tanaka et al., 1997). Both DMSXL and heterozygous $Glt1^{+/-}$ mice exhibited a frequency peak of oscillations around 200 Hz, similar to wild-type controls (Figures 7A and 7B), but the amplitude of the power peak of LFP oscillations was significantly higher in $Glt1^{+/-}$ and in DMSXL mice (Figures 7C and 7D). In other words, the abnormal neuronal activity of DMSXL Purkinje cells is recreated by the partial inactivation of *Glt1*, in agreement with a mediating role of GLT1 downregulation in the onset of DMSXL cerebellar phenotypes.

To further demonstrate the implications of GLT1 in DMSXL cerebellar dysfunction, we injected DMSXL animals with ceftriaxone for 5 consecutive days. Ceftriaxone is a β-lactam antibiotic that activates GLT1 expression (Rothstein et al., 2005). Ceftriaxone corrected GLT1 protein levels in DMSXL cerebellum (Figure S7A) and glutamate neurotoxicity in DMSXL neuroglial co-cultures (Figure 6D). LFP oscillations were recorded in the same animal before and following ceftriaxone treatment. Ceftriaxone did not change the frequency peak of LFP oscillations in DMSXL mice (Figure 7B) but resulted in a remarkable reduction in the amplitude of the power peak of $Glt1^{+/-}$ and DMSXL Purkinje LFP oscillations down to wild-type values (Figures 7C and 7D). In contrast, Purkinje LFP oscillations did not change significantly in sham-treated DMSXL mice.

Finally, we assessed whether ceftriaxone-induced GLT1 upregulation (Figure S7A) ameliorated DMSXL motor coordination. A 5-day regimen of ceftriaxone significantly reduced the average number of hind leg slips from day 1 relative to PBS-injected DMSXL controls (Figure 7E). From day 2, the number of slips of ceftriaxone-treated DMSXL mice was indistinguishable from wild-type controls. To investigate whether improved Purkinje cell firing and mouse motor performance could be mediated by an effect of ceftriaxone on transgene expression, we measured *DMPK* transcripts following treatment, but we did not find

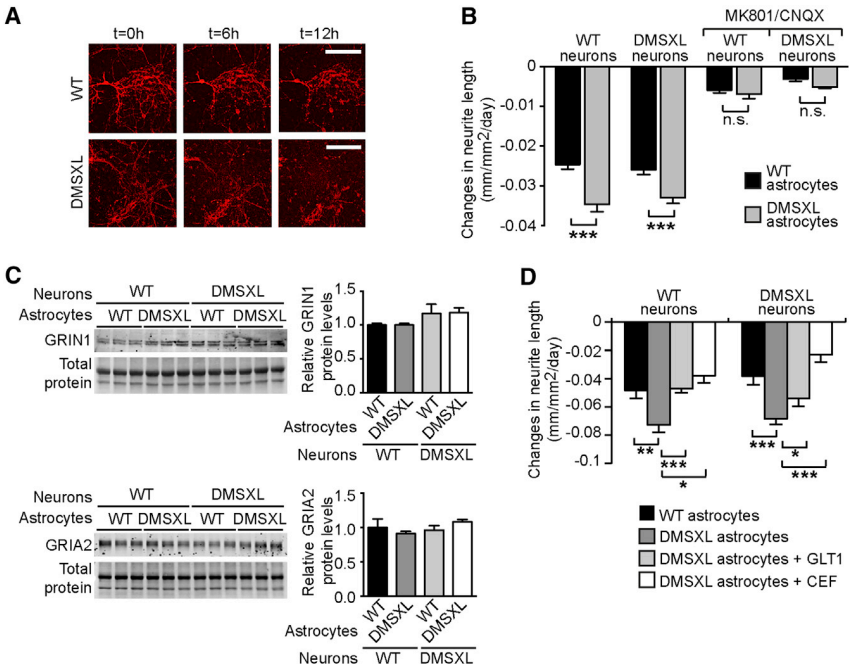


**Figure 6. Neuronal Glutamate Toxicity in Mixed Cultures of Neurons and Astrocytes**

(A) Representative images of WT neurite collapse co-cultured with WT and DMSXL astrocytes. Glutamate (50 μM) was added to the medium at t = 0 hr, and neurite length was monitored by the expression of fluorescent red mKate2 protein under the control of the neuron-specific synapsin-1 promoter. The scale bar represents 200 μm.

(B) Rate of glutamate-induced neurite collapse of WT and DMSXL primary neurons, cultured with WT or DMSXL astrocytes. (+)-MK 801 (NMDA receptor antagonist) and CNQX (AMPA receptor antagonist) were added to block glutamate receptors (n = 4 independent co-cultures, each mixed genotype combination). The graph shows the quantification of three independent experiments (±SEM).

(C) Representative western blot of GRIN1 (NMDA receptor subunit) and GRIA2 (AMPA receptor subunit) in mixed neuroglial cultures (n = 3 independent mixed cultures). Data are represented as the mean (±SEM). Total protein was visualized by stain-free protocols and used as loading control.

(D) Rate of glutamate-induced neurite collapse of WT and DMSXL neurons. Mouse primary neurons were cultured with WT astrocytes, control DMSXL astrocytes, DMSXL astrocytes transfected with GLT1, or DMSXL astrocytes treated with 10 μM ceftriaxone (CEF) (n = 4 independent co-cultures, each combination).

Error bars represent the SEM. *p < 0.05, **p < 0.01, ***p < 0.001; one way-ANOVA; n.s., not statistically significant. See also Figure S6.

differences relative to PBS-injected DMSXL controls (Figure S7B). Overall, these results demonstrate that reduced GLT1 is a critical contributing factor to DMSXL cerebellar pathophysiology, which can be rescued by ceftriaxone-induced upregulation of this glutamate transporter.

## DISCUSSION

We found prevalent signs of RNA toxicity in the Bergmann glia of a mouse model of DM1, in association with cerebellar abnormalities, such as network-mediated Purkinje cell excitability and motor incoordination. We demonstrated that defective expression of GLT1 glutamate transporter in astrocytes plays a determinant role in mediating these phenotypes.

Bergmann glia consist of a population of astrocytes whose cell bodies are embedded in the Purkinje layer. Their cellular processes create a microenvironment essential for the good functioning of the Purkinje synapses (Bellamy, 2006). Purkinje cells are the sole output of the cerebellar cortex. Their firing is an integrated response to their intrinsic excitability and to the excitatory and inhibitory inputs from the cerebellar network (Cheron et al., 2013). Thus, the electrophysiological recordings of spontaneous firing rate and rhythmicity in vivo provide an efficient way of assessing the functional states of the cerebellar neuronal network, independently of confounding factors, such as the muscle pathology and the reduced body weight of DMSXL mice (Gomes-Pereira et al., 2007; Huguet et al., 2012). Hence, the fast LFP oscillations registered in DMSXL mice revealed pathological changes in integrated Purkinje cell activity (Cheron et al., 2008), which may result from the synchronization of high-frequency rhythmic firing caused by intrinsic Purkinje cell excitability (Cheron et al., 2004), granular cell hyperexcitability (Bearzatto et al., 2006; Cheron et al., 2004), or altered synaptic plasticity (Servais et al., 2007). Abnormal spontaneous fast LFP oscillations were previously reported in ataxic mice showing cerebellum-dependent motor incoordination (Bearzatto et al., 2006; Cheron et al., 2004, 2005; Servais et al., 2007), supporting their contribution to the motor phenotype of DMSXL mice in the runway test. In contrast, other patterns of abnormal firing, such as slow firing (Servais and Cheron, 2005) or bursting (Cheron et al., 2009), were associated with milder or more severe incoordination, respectively.

Despite their functional abnormalities, Purkinje cells did not display abundant RNA foci or pronounced missplicing in DMSXL mice, hinting that neuronal hyperactivity is not mediated by an autonomous *trans*-dominant effect of CUG repeats operating in Purkinje cells alone. Our data suggest that *DMPK* transcript levels in Purkinje cells are insufficient to trigger RNA foci accumulation and toxicity. We propose that Purkinje cell hyperexcitation is mediated by abnormalities in the neighboring Bergmann glia, which show high *DMPK* expression and abundant RNA foci, in association with GLT1 downregulation.

GLT1 is a glial-specific glutamate transporter that recaptures excitatory glutamate from the synaptic cleft and protects from neurotoxicity due to excessive glutamate stimulation (Bellamy, 2006). The most important role of the glial glutamate transporters in the cerebellum is to avoid neurotransmitter spillover and activation of extra-synaptic receptors, thereby maintaining synapse independence. In the cerebellum, Bergmann astrocytes closely appose Purkinje cells, dictating a robust effect of GLT1 on

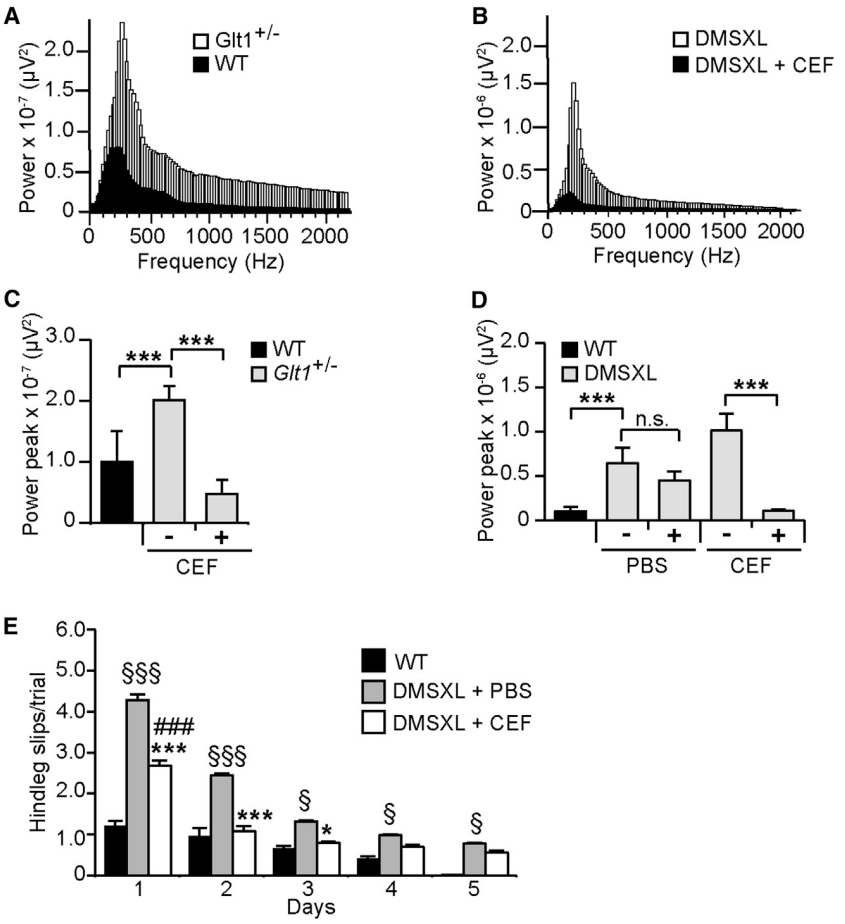


**Figure 7. Rescuing of DMSXL Cerebellum Phenotype following GLT1 Upregulation by Ceftriaxone**

(A) Representative profiles of LFP oscillations recorded over 690 min in the Purkinje cell layer of a *Glt1*$^{+/-}$ mouse and a WT control.

(B) Representative profiles of LFP oscillations recorded over 690 min in DMSXL mice before and following ceftriaxone injection.

(C) The power peak of the LFP oscillation (±SEM) was calculated by fast Fourier transform (FFT) analysis in *Glt1*$^{+/-}$ mice (n = 4) and WT controls (n = 3). *Glt1*$^{+/-}$ LFP oscillations were assessed before and following ceftriaxone injection. ***p < 0.001; one-way ANOVA.

(D) Effect of ceftriaxone on the power peak of the LFP oscillation (±SEM) in DMSXL mice (n = 5). Control DMSXL mice were injected with PBS (n = 4). Non-injected WT mice are shown as controls (n = 3). ***p < 0.001; one-way ANOVA; n.s., not statistically significant.

(E) Runway assessment of motor coordination of DMSXL mice injected with ceftriaxone relative to control DMSXL animals injected with PBS (n = 9, each group; *p < 0.001, ***p < 0.001; two-way ANOVA). The graphs represent the mean number of hind leg slips per trial (±SEM). Ceftriaxone-treated animals were compared with non-treated WT controls (n = 9; ###p < 0.001 at day 1; two-way ANOVA). DMSXL mice injected with PBS performed consistently worse than WT controls throughout the entire test (§p < 0.05, §§§p < 0.001; two-way ANOVA). Mice were studied at 2 months of age.

See also Figure S7.

synaptic transmission through proximity: even small changes in the density of Bergmann GLT1 transporters have a significant impact on Purkinje cell function (Tzingounis and Wadiche, 2007). Therefore, GLT1 downregulation can lead to increased synaptic glutamate, chronic Purkinje cell hyperexcitation, and emergence of fast oscillations. The critical role of GLT1 downregulation in the cerebellar dysfunction of DMSXL mice is corroborated by two observations. First, heterozygous *Glt1*$^{+/-}$ mice show similar electrophysiological LFP abnormalities. Second, ceftriaxone-mediated GLT1 upregulation corrects the spontaneous hyperactivity of DMSXL Purkinje cells and motor incoordination. The similar benefits of ceftriaxone treatment and GLT1 transfection on neuronal physiology in co-cultures strongly point to a rescuing mechanism of ceftriaxone mediated by GLT1 upregulation. Moreover, ceftriaxone was capable of correcting the Purkinje cell activity in *Glt1*$^{+/-}$ mice, in further support of a specific effect on this target. In conclusion, the benefits of GLT1 upregulation in DMSXL neuroglial co-cultures and in mice demonstrate the role of defective neuroglial interactions in DM1 brain disease.

Inactivation of *Glt1* causes lethal spontaneous seizures in KO mice, in association with selective hippocampal neurodegeneration, but no morphological changes in the cerebellum or signs of ataxia (Tanaka et al., 1997). Heterozygous *Glt1*$^{+/-}$ mice show a ~60% reduction in GLT1 protein levels, and like DMSXL mice, they exhibit abnormally high cerebellar fast oscillations, together with mild behavioral phenotypes in the absence of neurodegeneration (Kiryk et al., 2008). Altogether, our results suggest that partial inactivation of GLT1 in DM1 is more likely associated with neuronal dysfunction than cell death. Broader neuronal hyperexcitability and dysfunction in DM1 beyond cerebellum is supported by the observation of GLT1 downregulation in multiple brain areas and by the increased susceptibility of DMSXL mice to pentylenetetrazol (PTZ)-induced seizures (Charizanis et al., 2012).

GLT1 is a highly regulated transporter, modulated by changes in RNA transcription, splicing and stability, post-translational modifications, and protein activity (Kim et al., 2011). MBNL1 inactivation alone decreased *GLT1* transcripts and protein. In contrast, MBNL2 inactivation alone did not affect GLT1 levels, maybe because of the compensating increase of MBNL1 protein levels (Batra et al., 2014; Goodwin et al., 2015; Mohan et al., 2014). It is conceivable that MBNL1, but not MBNL2, specifically regulates GLT1 expression in glial cells. In line with this view, the higher expression of MBNL1 in mouse primary astrocytes, when compared to mouse primary neurons, hints at a predominant role of MBNL1 in the regulation of glia-specific transcripts. Poly(A)-RNA sequencing revealed changes in the alternative

polyadenylation of the *GLT1* transcripts in the brain of DM1 and myotonic dystrophy type 2 (DM2) patients and in *Mbnl* double-KO mice (Goodwin et al., 2015). These data suggest that MBNL loss of function perturbs GLT1 polyadenylation, leading to altered levels of this glutamate transporter.

Deficits in GLT1 were reported in several neurological diseases, including Alzheimer's disease, Huntington's disease, ALS, and fragile X syndrome (Kim et al., 2011), but the underlying mechanisms and contribution to disease manifestations have not been fully resolved. As in our DM1 mouse model, GLT1 downregulation in mouse models of fragile X syndrome is associated with enhanced neuronal excitability (Higashimori et al., 2013). In DM1, the downregulation of GLT1 and altered glutamate levels in adult patients (Takado et al., 2015) suggest an impairment of the glutamatergic system. Regulation of GLT1 activity and extracellular glutamate may improve the homeostasis and neurotransmission in DM1 brains. Ceftriaxone, in particular, is well tolerated, permeable to the blood-brain barrier, and augments GLT1 promoter activity and glutamate uptake, but other small-molecule GLT1 activators have been described (Kong et al., 2014).

The cerebellum controls motor coordination, skilled voluntary movements, posture, and gait. The implication of the cerebellum in DM1 neuropathology has not been sufficiently studied. However, imaging studies suggest cerebellar abnormalities: brain voxel-based morphometry revealed white matter decrease (Minnerop et al., 2011), while fMRI showed altered connectivity in cerebellar regions implicated in planning of movements and motor coordination (Serra et al., 2016). The frequency of stumbles and falls in DM1 is 10-fold higher than in healthy controls (Wiles et al., 2006). Several aspects of DM1 disease biology could lead to gait difficulties, among these the weakness of the leg muscles (Hammarén et al., 2014). However, because in these studies muscular impairment was often an inclusion criterion, the results are only generalizable to muscularly impaired DM1 individuals, excluding those that show gait affection without muscle weakness. A study demonstrated limited contribution of muscle weakness to gait abnormalities in DM1 and suggested a role for sensory deficits (Bachasson et al., 2016). In line with this view, altered brain connectivity has been associated with patients' motor deficits (Toth et al., 2015). Adaptive cognitive strategies usually mitigate the risk of falls caused by muscle impairment, but they might be compromised in DM1 due to brain dysfunction. There is a need for clinical assessment of cerebellum deficits and their contribution to impaired balance and frequent stumbles and falls in DM1. The cerebellum may also participate in DM1 through non-motor functions. Cerebellar lesions can result in executive dysfunction, blunting or flattening of affect, constrictions in social interaction, and impaired spatial cognition (Schmahmann and Sherman, 1998). Defective Bergmann or Purkinje cell communication could mediate, at least partly, similar cognitive and behavioral deficits previously reported in DM1, but further studies are required.

In summary, our data provide insight into DM1 brain mechanisms and demonstrate how glial molecular abnormalities affect neuronal activity through neuroglial miscommunication. They open the route to the clinic, providing exciting therapeutic perspectives through the modulation of GLT1 levels and glutamate signaling. Therapies aiming to restore GLT1 protein and glutamate neurotransmission could have applicability in DM1.

## EXPERIMENTAL PROCEDURES

### Transgenic Mice

All animal experiments were conducted according to the ARRIVE guidelines (Animal Research: Reporting In Vivo Experiments). This project has been conducted with the authorization for animal experimentation No. 75 003 in the animal facility with the approval No. B 91 228 107, both delivered by Prefecture de Police and the French Veterinary Department.

### Human Tissue Samples

Mouse cerebellum tissues were microdissected at different ages and stored at −80°C. Human cerebellum samples were collected from different laboratories: Dr. Yasuhiro Suzuki (Asahikawa Medical Center) and Dr. Tohru Matsuura (Okayama University). All experiments using human samples were approved by the ethics committees of the host institutions. Written informed-consent specimen use for research was obtained from all patients. Information relative to patients was previously described (Hernández-Hernández et al., 2013a) and is summarized in Tables S1 and S2.

### Statistical Analysis

Statistical analyses were performed with Prism (GraphPad), SPSS (v.14.0, SPSS), Statistica (v.6.0, StatSoft), and/or Excel software. When two groups were compared, we first performed a normality test. Parametric data were compared using a two-tailed Student's t test (with equal or unequal variance, as appropriate). Non-parametric data were compared using a two-tailed Mann-Whitney U test. For one-way ANOVA, if statistical significance was achieved, we performed post-test analysis to account for multiple comparisons. Statistical significance was set at $p < 0.05$. The data are presented as mean ± SEM.

## SUPPLEMENTAL INFORMATION

Supplemental Information includes Supplemental Experimental Procedures, seven figures, and seven tables and can be found with this article online at http://dx.doi.org/10.1016/j.celrep.2017.06.006.

## AUTHOR CONTRIBUTIONS

Conceptualization, L.S., G.C., G.G., and M.G.-P.; Methodology, G.S., L.S., D.M.D., I.C.G., G.C., G.G., M.G.-P.; Investigation, G.S., L.S., D.M.D., A.L., C.P., S.O.B., B.D., F.M., C.C., A.H.-L., A.N., N.G., R.O., I.C.G., G.C., and M.G.-P.; Formal Analysis, G.S., L.S., D.M.D., A.L., S.O.B., B.D., F.M., I.C.G., D.F., G.C., G.G., and M.G.P.; Resources, L.S., D.F., M.S.S., I.C.G., G.C., G.G., and M.G.-P.; Writing – Original Draft, G.S., L.S., D.M.D., I.C.G., C.G., and M.G.-P.; Writing – Review and Editing, G.S., L.S., D.M.D., C.G., G.G., and M.G.-P.; Funding Acquisition, L.S., G.C., G.G., and M.G.-P.

## ACKNOWLEDGMENTS

We thank Dr. Thomas Cooper for providing the DMPKS, DT960, CELF1, and CELF2 plasmids; Dr. Nicolas Reyes for the GLT1-EGFP-expressing plasmid; Dr. Rob Willemsen for FXTAS mouse brain slices; and Dr. Jeffrey Rothstein for anti-GLT1 antibody. We are grateful to the personnel of CERFE (Centre d'Exploration et de Recherche Fonctionelle Expérimentale, Genopole, Evry, France) and LEAT (Laboratoire d'Experimentation Animale, Imagine Institute, Paris, France) for attentively caring for the mice. We thank Léonard Bertrand and Elodie Dandelot for help with the graphical abstract. This study was supported by grants from AFM-Téléthon (France, project grant 16161 to M.G.-P.), INSERM (France), Université Paris Descartes (France), and Fondation ARC (France); as well as PhD fellowships from Ministère Français de la Recherche et Technologie (France, to G.S. and D.M.D.), AFM-Téléthon (France, to G.S.) and Imagine Foundation (France, to S.O.B.). This program received a state subsidy managed by the National Research Agency under the "Investments

for the Future" program bearing the reference ANR-10-IAHU-01 and under the program ANR-10BLAN-1121-01. L.S., G.C., G.G., and M.G.-P. have a patent on GLT1 upregulation in DM1.

Received: January 15, 2017
Revised: April 27, 2017
Accepted: May 26, 2017
Published: June 27, 2017

## REFERENCES

Algalarrondo, V., Wahbi, K., Sebag, F., Gourdon, G., Beldjord, C., Azibi, K., Balse, E., Coulombe, A., Fischmeister, R., Eymard, B., et al. (2015). Abnormal sodium current properties contribute to cardiac electrical and contractile dysfunction in a mouse model of myotonic dystrophy type 1. Neuromuscul. Disord. *25*, 308–320.

Angeard, N., Gargiulo, M., Jacquette, A., Radvanyi, H., Eymard, B., and Héron, D. (2007). Cognitive profile in childhood myotonic dystrophy type 1: is there a global impairment? Neuromuscul. Disord. *17*, 451–458.

Angeard, N., Jacquette, A., Gargiulo, M., Radvanyi, H., Moutier, S., Eymard, B., and Héron, D. (2011). A new window on neurocognitive dysfunction in the childhood form of myotonic dystrophy type 1 (DM1). Neuromuscul. Disord. *21*, 468–476.

Antonini, G., Soscia, F., Giubilei, F., De Carolis, A., Gragnani, F., Morino, S., Ruberto, A., and Tatarelli, R. (2006). Health-related quality of life in myotonic dystrophy type 1 and its relationship with cognitive and emotional functioning. J. Rehabil. Med. *38*, 181–185.

Bachasson, D., Moraux, A., Ollivier, G., Decostre, V., Ledoux, I., Gidaro, T., Servais, L., Behin, A., Stojkovic, T., Hébert, L.J., et al. (2016). Relationship between muscle impairments, postural stability, and gait parameters assessed with lower-trunk accelerometry in myotonic dystrophy type 1. Neuromuscul. Disord. *26*, 428–435.

Batra, R., Charizanis, K., Manchanda, M., Mohan, A., Li, M., Finn, D.J., Goodwin, M., Zhang, C., Sobczak, K., Thornton, C.A., and Swanson, M.S. (2014). Loss of MBNL leads to disruption of developmentally regulated alternative polyadenylation in RNA-mediated disease. Mol. Cell *56*, 311–322.

Bearzatto, B., Servais, L., Cheron, G., and Schiffmann, S.N. (2005). Age dependence of strain determinant on mice motor coordination. Brain Res. *1039*, 37–42.

Bearzatto, B., Servais, L., Roussel, C., Gall, D., Baba-Aïssa, F., Schurmans, S., de Kerchove d'Exaerde, A., Cheron, G., and Schiffmann, S.N. (2006). Targeted calretinin expression in granule cells of calretinin-null mice restores normal cerebellar functions. FASEB J. *20*, 380–382.

Bellamy, T.C. (2006). Interactions between Purkinje neurones and Bergmann glia. Cerebellum *5*, 116–126.

Brook, J.D., McCurrach, M.E., Harley, H.G., Buckler, A.J., Church, D., Aburatani, H., Hunter, K., Stanton, V.P., Thirion, J.P., Hudson, T., et al. (1992). Molecular basis of myotonic dystrophy: expansion of a trinucleotide (CTG) repeat at the 3′ end of a transcript encoding a protein kinase family member. Cell *68*, 799–808.

Caillet-Boudin, M.L., Fernandez-Gomez, F.J., Tran, H., Dhaenens, C.M., Buee, L., and Sergeant, N. (2014). Brain pathology in myotonic dystrophy: when tauopathy meets spliceopathy and RNAopathy. Front. Mol. Neurosci. *6*, 57.

Caliandro, P., Silvestri, G., Padua, L., Bianchi, M.L., Simbolotti, C., Russo, G., Masciullo, M., and Rossini, P.M. (2013). fNIRS evaluation during a phonemic verbal task reveals prefrontal hypometabolism in patients affected by myotonic dystrophy type 1. Clin. Neurophysiol. *124*, 2269–2276.

Charizanis, K., Lee, K.Y., Batra, R., Goodwin, M., Zhang, C., Yuan, Y., Shiue, L., Cline, M., Scotti, M.M., Xia, G., et al. (2012). Muscleblind-like 2-mediated alternative splicing in the developing brain and dysregulation in myotonic dystrophy. Neuron *75*, 437–450.

Cheron, G., Gall, D., Servais, L., Dan, B., Maex, R., and Schiffmann, S.N. (2004). Inactivation of calcium-binding protein genes induces 160 Hz oscillations in the cerebellar cortex of alert mice. J. Neurosci. *24*, 434–441.

Cheron, G., Servais, L., Wagstaff, J., and Dan, B. (2005). Fast cerebellar oscillation associated with ataxia in a mouse model of Angelman syndrome. Neuroscience *130*, 631–637.

Cheron, G., Servais, L., and Dan, B. (2008). Cerebellar network plasticity: from genes to fast oscillation. Neuroscience *153*, 1–19.

Cheron, G., Sausbier, M., Sausbier, U., Neuhuber, W., Ruth, P., Dan, B., and Servais, L. (2009). BK channels control cerebellar Purkinje and Golgi cell rhythmicity in vivo. PLoS ONE *4*, e7991.

Cheron, G., Dan, B., and Márquez-Ruiz, J. (2013). Translational approach to behavioral learning: lessons from cerebellar plasticity. Neural Plast. *2013*, 853654.

Dogan, C., De Antonio, M., Hamroun, D., Varet, H., Fabbro, M., Rougier, F., Amarof, K., Arne Bes, M.C., Bedat-Millet, A.L., Behin, A., et al. (2016). Gender as a modifying factor influencing myotonic dystrophy type 1 phenotype severity and mortality: a nationwide multiple databases cross-sectional observational study. PLoS ONE *11*, e0148264.

Gomes-Pereira, M., Foiry, L., Nicole, A., Huguet, A., Junien, C., Munnich, A., and Gourdon, G. (2007). CTG trinucleotide repeat "big jumps": large expansions, small mice. PLoS Genet. *3*, e52.

Goodwin, M., Mohan, A., Batra, R., Lee, K.Y., Charizanis, K., Fernández Gómez, F.J., Eddarkaoui, S., Sergeant, N., Buée, L., Kimura, T., et al. (2015). MBNL sequestration by toxic RNAs and RNA misprocessing in the myotonic dystrophy brain. Cell Rep. *12*, 1159–1168.

Hammarén, E., Kjellby-Wendt, G., Kowalski, J., and Lindberg, C. (2014). Factors of importance for dynamic balance impairment and frequency of falls in individuals with myotonic dystrophy type 1—a cross-sectional study—including reference values of Timed Up & Go, 10m walk and step test. Neuromuscul. Disord. *24*, 207–215.

Hernández-Hernández, O., Guiraud-Dogan, C., Sicot, G., Huguet, A., Luilier, S., Steidl, E., Saenger, S., Marciniak, E., Obriot, H., Chevarin, C., et al. (2013a). Myotonic dystrophy CTG expansion affects synaptic vesicle proteins, neurotransmission and mouse behaviour. Brain *136*, 957–970.

Hernández-Hernández, O., Sicot, G., Dinca, D.M., Huguet, A., Nicole, A., Buée, L., Munnich, A., Sergeant, N., Gourdon, G., and Gomes-Pereira, M. (2013b). Synaptic protein dysregulation in myotonic dystrophy type 1: disease neuropathogenesis beyond missplicing. Rare Dis. *1*, e25553.

Higashimori, H., Morel, L., Huth, J., Lindemann, L., Dulla, C., Taylor, A., Freeman, M., and Yang, Y. (2013). Astroglial FMRP-dependent translational down-regulation of mGluR5 underlies glutamate transporter GLT1 dysregulation in the fragile X mouse. Hum. Mol. Genet. *22*, 2041–2054.

Huguet, A., Medja, F., Nicole, A., Vignaud, A., Guiraud-Dogan, C., Ferry, A., Decostre, V., Hogrel, J.Y., Metzger, F., Hoeflich, A., et al. (2012). Molecular, physiological, and motor performance defects in DMSXL mice carrying >1,000 CTG repeats from the human DM1 locus. PLoS Genet. *8*, e1003043.

Kanadia, R.N., Johnstone, K.A., Mankodi, A., Lungu, C., Thornton, C.A., Esson, D., Timmers, A.M., Hauswirth, W.W., and Swanson, M.S. (2003). A muscleblind knockout model for myotonic dystrophy. Science *302*, 1978–1980.

Kanai, Y., and Hediger, M.A. (2004). The glutamate/neutral amino acid transporter family SLC1: molecular, physiological and pharmacological aspects. Pflugers Arch. *447*, 469–479.

Kim, K., Lee, S.G., Kegelman, T.P., Su, Z.Z., Das, S.K., Dash, R., Dasgupta, S., Barral, P.M., Hedvat, M., Diaz, P., et al. (2011). Role of excitatory amino acid transporter-2 (EAAT2) and glutamate in neurodegeneration: opportunities for developing novel therapeutics. J. Cell. Physiol. *226*, 2484–2493.

Kiryk, A., Aida, T., Tanaka, K., Banerjee, P., Wilczynski, G.M., Meyza, K., Knapska, E., Filipkowski, R.K., Kaczmarek, L., and Danysz, W. (2008). Behavioral characterization of GLT1 (+/−) mice as a model of mild glutamatergic hyperfunction. Neurotox. Res. *13*, 19–30.

Kong, Q., Chang, L.C., Takahashi, K., Liu, Q., Schulte, D.A., Lai, L., Ibabao, B., Lin, Y., Stouffer, N., Das Mukhopadhyay, C., et al. (2014). Small-molecule activator of glutamate transporter EAAT2 translation provides neuroprotection. J. Clin. Invest. *124*, 1255–1267.

Lin, C.L., Bristol, L.A., Jin, L., Dykes-Hoberg, M., Crawford, T., Clawson, L., and Rothstein, J.D. (1998). Aberrant RNA processing in a neurodegenerative disease: the cause for absent EAAT2, a glutamate transporter, in amyotrophic lateral sclerosis. Neuron *20*, 589–602.

Meola, G., and Sansone, V. (2007). Cerebral involvement in myotonic dystrophies. Muscle Nerve *36*, 294–306.

Minnerop, M., Weber, B., Schoene-Bake, J.C., Roeske, S., Mirbach, S., Anspach, C., Schneider-Gold, C., Betz, R.C., Helmstaedter, C., Tittgemeyer, M., et al. (2011). The brain in myotonic dystrophy 1 and 2: evidence for a predominant white matter disease. Brain *134*, 3530–3546.

Mohan, A., Goodwin, M., and Swanson, M.S. (2014). RNA-protein interactions in unstable microsatellite diseases. Brain Res. *1584*, 3–14.

Panaite, P.A., Kuntzer, T., Gourdon, G., Lobrinus, J.A., and Barakat-Walter, I. (2013). Functional and histopathological identification of the respiratory failure in a DMSXL transgenic mouse model of myotonic dystrophy. Dis. Model. Mech. *6*, 622–631.

Regan, M.R., Huang, Y.H., Kim, Y.S., Dykes-Hoberg, M.I., Jin, L., Watkins, A.M., Bergles, D.E., and Rothstein, J.D. (2007). Variations in promoter activity reveal a differential expression and physiology of glutamate transporters by glia in the developing and mature CNS. J. Neurosci. *27*, 6607–6619.

Rothstein, J.D., Patel, S., Regan, M.R., Haenggeli, C., Huang, Y.H., Bergles, D.E., Jin, L., Dykes Hoberg, M., Vidensky, S., Chung, D.S., et al. (2005). Beta-lactam antibiotics offer neuroprotection by increasing glutamate transporter expression. Nature *433*, 73–77.

Schmahmann, J.D., and Sherman, J.C. (1998). The cerebellar cognitive affective syndrome. Brain *121*, 561–579.

Schneider-Gold, C., Bellenberg, B., Prehn, C., Krogias, C., Schneider, R., Klein, J., Gold, R., and Lukas, C. (2015). Cortical and subcortical grey and white matter atrophy in myotonic dystrophies type 1 and 2 is associated with cognitive impairment, depression and daytime sleepiness. PLoS ONE *10*, e0130352.

Serra, L., Silvestri, G., Petrucci, A., Basile, B., Masciullo, M., Makovac, E., Torso, M., Spanò, B., Mastropasqua, C., Harrison, N.A., et al. (2014). Abnormal functional brain connectivity and personality traits in myotonic dystrophy type 1. JAMA Neurol. *71*, 603–611.

Serra, L., Petrucci, A., Spanò, B., Torso, M., Olivito, G., Lispi, L., Costanzi-Porrini, S., Giulietti, G., Koch, G., Giacanelli, M., et al. (2015). How genetics affects the brain to produce higher-level dysfunctions in myotonic dystrophy type 1. Funct. Neurol. *30*, 21–31.

Serra, L., Cercignani, M., Bruschini, M., Cipolotti, L., Mancini, M., Silvestri, G., Petrucci, A., Bucci, E., Antonini, G., Licchelli, L., et al. (2016). "I know that you know that I know": neural substrates associated with social cognition deficits in DM1 patients. PLoS ONE *11*, e0156901.

Servais, L., and Cheron, G. (2005). Purkinje cell rhythmicity and synchronicity during modulation of fast cerebellar oscillation. Neuroscience *134*, 1247–1259.

Servais, L., Hourez, R., Bearzatto, B., Gall, D., Schiffmann, S.N., and Cheron, G. (2007). Purkinje cell dysfunction and alteration of long-term synaptic plasticity in fetal alcohol syndrome. Proc. Natl. Acad. Sci. USA *104*, 9858–9863.

Seznec, H., Lia-Baldini, A.S., Duros, C., Fouquet, C., Lacroix, C., Hofmann-Radvanyi, H., Junien, C., and Gourdon, G. (2000). Transgenic mice carrying large human genomic sequences with expanded CTG repeat mimic closely the DM CTG repeat intergenerational and somatic instability. Hum. Mol. Genet. *9*, 1185–1194.

Seznec, H., Agbulut, O., Sergeant, N., Savouret, C., Ghestem, A., Tabti, N., Willer, J.C., Ourth, L., Duros, C., Brisson, E., et al. (2001). Mice transgenic for the human myotonic dystrophy region with expanded CTG repeats display muscular and brain abnormalities. Hum. Mol. Genet. *10*, 2717–2726.

Sicot, G., and Gomes-Pereira, M. (2013). RNA toxicity in human disease and animal models: from the uncovering of a new mechanism to the development of promising therapies. Biochim. Biophys. Acta *1832*, 1390–1409.

Sicot, G., Gourdon, G., and Gomes-Pereira, M. (2011). Myotonic dystrophy, when simple repeats reveal complex pathogenic entities: new findings and future challenges. Hum. Mol. Genet. *20* (*R2*), R116–R123.

Sistiaga, A., Urreta, I., Jodar, M., Cobo, A.M., Emparanza, J., Otaegui, D., Poza, J.J., Merino, J.J., Imaz, H., Martí-Massó, J.F., and López de Munain, A. (2010). Cognitive/personality pattern and triplet expansion size in adult myotonic dystrophy type 1 (DM1): CTG repeats, cognition and personality in DM1. Psychol. Med. *40*, 487–495.

Takado, Y., Terajima, K., Ohkubo, M., Okamoto, K., Shimohata, T., Nishizawa, M., Igarashi, H., and Nakada, T. (2015). Diffuse brain abnormalities in myotonic dystrophy type 1 detected by 3.0 T proton magnetic resonance spectroscopy. Eur. Neurol. *73*, 247–256.

Tanaka, K., Watase, K., Manabe, T., Yamada, K., Watanabe, M., Takahashi, K., Iwama, H., Nishikawa, T., Ichihara, N., Kikuchi, T., et al. (1997). Epilepsy and exacerbation of brain injury in mice lacking the glutamate transporter GLT-1. Science *276*, 1699–1702.

Theadom, A., Rodrigues, M., Roxburgh, R., Balalla, S., Higgins, C., Bhattacharjee, R., Jones, K., Krishnamurthi, R., and Feigin, V. (2014). Prevalence of muscular dystrophies: a systematic literature review. Neuroepidemiology *43*, 259–268.

Toth, A., Lovadi, E., Komoly, S., Schwarcz, A., Orsi, G., Perlaki, G., Bogner, P., Sebok, A., Kovacs, N., Pal, E., and Janszky, J. (2015). Cortical involvement during myotonia in myotonic dystrophy: an fMRI study. Acta Neurol. Scand. *132*, 65–72.

Tzingounis, A.V., and Wadiche, J.I. (2007). Glutamate transporters: confining runaway excitation by shaping synaptic transmission. Nat. Rev. Neurosci. *8*, 935–947.

Udd, B., and Krahe, R. (2012). The myotonic dystrophies: molecular, clinical, and therapeutic challenges. Lancet Neurol. *11*, 891–905.

Voogd, J., and Glickstein, M. (1998). The anatomy of the cerebellum. Trends Cogn. Sci. *2*, 307–313.

Wang, E.T., Cody, N.A., Jog, S., Biancolella, M., Wang, T.T., Treacy, D.J., Luo, S., Schroth, G.P., Housman, D.E., Reddy, S., et al. (2012). Transcriptome-wide regulation of pre-mRNA splicing and mRNA localization by muscleblind proteins. Cell *150*, 710–724.

Weber, Y.G., Roebling, R., Kassubek, J., Hoffmann, S., Rosenbohm, A., Wolf, M., Steinbach, P., Jurkat-Rott, K., Walter, H., Reske, S.N., et al. (2010). Comparative analysis of brain structure, metabolism, and cognition in myotonic dystrophy 1 and 2. Neurology *74*, 1108–1117.

Wiles, C.M., Busse, M.E., Sampson, C.M., Rogers, M.T., Fenton-May, J., and van Deursen, R. (2006). Falls and stumbles in myotonic dystrophy. J. Neurol. Neurosurg. Psychiatry *77*, 393–396.

Wozniak, J.R., Mueller, B.A., Lim, K.O., Hemmy, L.S., and Day, J.W. (2014). Tractography reveals diffuse white matter abnormalities in myotonic dystrophy type 1. J. Neurol. Sci. *341*, 73–78.

**Cell Reports, Volume *19***

## Supplemental Information

# Downregulation of the Glial GLT1 Glutamate Transporter and Purkinje Cell Dysfunction in a Mouse Model of Myotonic Dystrophy

**Géraldine Sicot, Laurent Servais, Diana M. Dinca, Axelle Leroy, Cynthia Prigogine, Fadia Medja, Sandra O. Braz, Aline Huguet-Lachon, Cerina Chhuon, Annie Nicole, Noëmy Gueriba, Ruan Oliveira, Bernard Dan, Denis Furling, Maurice S. Swanson, Ida Chiara Guerrera, Guy Cheron, Geneviève Gourdon, and Mário Gomes-Pereira**

## SUPPLEMENTAL TABLES

**Table S1. Clinical data of control individuals (related to Figure 4).**

| | Non-DM controls | | | |
|---|---|---|---|---|
| | **a** | **b** | **c** | **d** |
| **Sex** | M | M | M | M |
| **Diagnosis** | N/A, | Charcot-Marie-Tooth Disease; | Rheumathoide arthritis | Limb-girdle muscular dystrophy |
| **Neuropsychological profile** | N/D | N/D | N/D | N/D |
| **Neuroimaging** | N/D | N/D | N/D | N/D |
| **Age; cause of death** | 79; *Pneumocystis* pneumonia | 71; pneumonia | 76; interstitial pneumonia | 66; cardiac failure |

**Table S2. Clinical data of DM1 individuals (related to Figure 4).**

| | DM1 samples | | | | | | |
|---|---|---|---|---|---|---|---|
| | **e** | **f** | **g** | **h** | **i** | **j** | **k** |
| **Sex** | **F** | **F** | **F** | **M** | **F** | **M** | **M** |
| **CTGs in blood (age of analysis)** | 1300-1400 (40) | >2500 (N/D) | N/D | N/D | 1730 (73) | 700-1100 (30) | 1600-1800 (40) |
| **CTGs in cerebellum (age of analysis)** | 400 (69) | 450 (64) | 200 (62) | 500 (58) | 350 (73) | 350 (67) | 400 (62) |
| **Age of onset** | 40 | Unknown | 54 | 46 | 40 | 30 | 40 |
| **Clinical form of DM** | Adult DM1 | N/D | Late onset DM1 | Adult DM1 | Adult DM1 | Adult DM1 | Adult DM1 |
| **DM main symptoms** | Gait problems | Gait problems | Cardiac arrhythmia; gait problems | Limb muscle weakness | Muscle weakness and atrophy in all extremities | Gait problems | Gait problems |
| **Neuropsychological profile** | WAIS-R (VIQ74, PIQ73, IQ73) | N/D | N/D | N/D | Memory loss | N/D | N/D |
| **Neuroimaging** | Diffuse atrophy | General brain atrophy | N/D | N/D | Bilateral fronto-temporal atrophy | N/D | Normal |
| **Age; cause of death** | 69; pneumonia | 64; ARDS | 62; pneumonia | 58; pneumonia | 73; pneumonia | 67; pneumonia | 62; heart failure |

ARDS, acute respiratory distress syndrome; N/A not applicable; N/D, not determined.

**Table S3. Primary antibodies for immunofluorescence and immunohistochemistry (related to Figures 1 and 4).**

| Antigene | Supplier; vendor reference; RRID | Species origin | Blocking and incubation conditions | Ab dilution |
|---|---|---|---|---|
| CALB1 | Swant; CB38; AB_10000340 | mouse | 10% NGS, 1h, RT | 1/400 |
| FOX1 | Abcam; ab83574; AB_1859807 | mouse | 10% NGS, 1h, RT | 1/400 |
| FOX2 | Abcam; ab57154; AB_2285090 | mouse | 10% NGS, 1h, RT | 1/400 |
| GFAP | DakoCytomation; Z0334; AB_10013382 | rabbit | 10% NGS, 1h, RT | 1/400 |
| GLAST | Abcam; ab416; AB_304334 | rabbit | 10% NGS, 1h, RT | 1/200 |
| GLT1 | Alomone; AGC-022; AB_2039891 | rabbit | 10% NGS, 1h, RT | 1/200 |
| MBNL1 | MB1A from Glen Morris (gift) | mouse | 0.1% BSA, 10% NGS, 1H, RT | 1/10 |
| MBNL2 | MB2A from Glen Morris (gift) | mouse | 0.1% BSA, 10% NGS, 1h, RT | 1/10 |
| NeuN | Chemicon; MAB377; AB_2298772 | mouse | 10% NGS, 1h, RT | 1/400 |
| Ubiquitin | Dako Cytomation; Z0458; AB_2315524 | rabbit | 10% NSS, 1h, RT | 1/500 |

BSA, bovine serum albumin; NGS, normal-goat serum; NSS, normal swine serum; RT, room temperature.

**Table S4. Oligonucleotide primers sequences for RT-PCR analysis of laser micro-dissected mouse cells (related to Figure 1).**

| Gene | Exon | Primer 1 | Primer 2 | Primer 3 | PCR product size (bp) |
|---|---|---|---|---|---|
| ***Calb1*** | N/A | GTGCTTTGGGTGACAGTCCT | TGAGCTGGATGCTTTGCTGA | TGGATTTCCCCGAAAATCTACCA | 139 |
| ***Glast*** | N/A | GGGGAGCACAAATCTGGTGA | CCGTGCCTGGATCTGTGAAT | GTAACCCGGAAGAACCCCTG | 159 |
| ***Mbnl1*** | 7 | CAATGTTGGTCACGGGGAATC | GCTGCCCAATACCAGGTCAAC | TGGTGGGAGAAATGCTGTATGC | 270/216 |
| ***Mbnl2*** | 5 | CCATAGGGACAAATGCGG | ACCGTAACCGTTTGTATGGATTAC | TTGGTAAGGGATGAAGAGC | 255/201 |

N/A, not applicable.

**Table S5. Oligonucleotide primer sequences for mouse and human RT-PCR analysis (related to Figure 1).**

| Gene | Species | Exon | Forward primer | Reverse primer | PCR product size (bp) |
|---|---|---|---|---|---|
| ***18S*** | Mouse | qRT-PCR | CAGTGAAACTGCGAATGG | CGGGTTGGTTTTGATCTG | 165 |
| ***18S*** | Human | qRT-PCR | CAGTGAAACTGCGAATGG | CGGGTTGGTTTTGATCTG | 165 |
| ***Fabp7*** | Mouse | qRT-PCR | TACATGAAAGCTCTGGGCGTG | TGTCCGGATCACCACTTTGC | 105 |
| ***Glt1*** | Mouse | Whole transcript | CCGTTAAATACCGCTCTCCGC | GCTGGGGAGTTTATTCAAGAATTG | 1854 |
| ***Glt1*** | Mouse | 13 | TGCTGGAACTTTGCCTGTTACC | GTGTTGGGAGTCAATGGTGTCC | 433/298 |
| ***Glt1*** | Mouse | Intron 11 | TCATCGCCATCAAGGACTTAGAAG | GCTGGGAATACTGGCTGC<br>GAGAGAAACAGGAAGCAGCAAATG | -In11: 434<br>+In 11: 266 |
| ***Glt1*** | Mouse | qRT-PCR | TGGACTGGCTGCTGGATAGA | CGGTGTTGGGAGTCAATGGT | 118 |
| ***GLT1*** | Human | Whole transcript | ACCGTCCTCTGCCACCACTCT | ACGCTGGGGAGTTTATTCAAGAAT | 2194 |
| ***GLT1*** | Human | 12 | TTTGCCTGTCACCTTTCGTTG | TTAGAGTTGCTTTCCCTGTGGTTC | 504/369 |
| ***GLT1*** | Human | Intron 10 | GGCAACTGGGGATGTACA | ACGCTGGGGAGTTTATTCAAGAAT<br>CCAGAAGGCTCAGAAGT | -In10: 835<br>+In10: 345 |
| ***GLT1*** | Human | qRT-PCR | TAGCCGCCATCTTTATAGCCC | CGGCTGTCAGAATGAGGAGC | 150 |
| ***MAPT/ TAU*** | Human | 10 | CTGAAGCACCAGCCAGGAGG | TGGTCTGTCTTGGCTTTGGC | 367/274 |
| ***Mbnl1*** | Mouse | 7 | TGGTGGGAGAAATGCTGTATGC | GCTGCCCAATACCAGGTCAAC | 270/216 |
| ***MBNL1*** | Human | 7 | TGGTGGGAGAAATGCTGTATGC | GCTGCCCAATACCAGGTCAAC | 270/216 |
| ***Mbnl2*** | Mouse | 5 | CTTTGGTAAGGGATGAAGAGCAC | ACCGTAACCGTTTGTATGGATTAC | 255/201 |
| ***MBNL2*** | Human | 5 | CTTTGGTAAGGGATGAAGAGCAC | ACCGTAACCGTTTGTATGGATTAC | 255/201 |
| ***Sept4*** | Mouse | qRT-PCR | GGTGGCAGGAGAATCTGGTC | CCGATCCCGGTACAAGTCAG | 76 |
| ***ß-ACTIN*** | Human | N/A | CCGTCTTCCCCTCCATCG | CCTCGTCGCCCACATAGG | 87 |
| ***Tbp1*** | Mouse | N/A | GGTGTGCACAGGAGCCAAGAGTG | AGCTACTGAACTGCTGGTGGGTC | 192 |
| ***TBP1*** | Human | N/A | GGTGTGCACAGGAGCCAAGAGTG | AGCTACTGAACTGCTGGTGGGTC | 192 |

qRT-PCR, quantitative RT-PCR; -In10, intron 10 exclusion; +in10, intron 10 inclusion; -In11, intron 11 exclusion; +in11, intron 11 inclusion; N/A, not applicable.

**Table S6. Primary antibodies for western blot immunodetection (related to Figure 3, 4, 5 and 6).**

| Antigene | Supplier; vendor reference; RRID | PAGE (%) | Species origin | Blocking and incubation conditions | Ab dilution |
|---|---|---|---|---|---|
| **Actin** | BD Biosciences; 612656; AB_2289199 | 10-12 | mouse | 5% blotto, 1h, RT | 1/5,000 |
| **CALB1** | Swant; cb38; AB_10000340 | 12 | rabbit | 5% blotto, 1h, RT | 1/500,000 |
| **CALB2** | Abcam; ab1550; AB_90764 | 12 | rabbit | 5% blotto, 1h, RT | 1/5,000 |
| **CELF1** | Millipore; 05-621; AB_309851 | 10 | mouse | 5% blotto, 1h, RT | 1/1,000 |
| **CELF2** | Sigma; C9367; AB_1078584 | 10 | mouse | 5% blotto, 2h, RT | 1/1,000 |
| **GAPDH** | Genetex; GTX627408; AB_11174761 | 10-12 | mouse | 5% blotto, 1h, RT | 1/10,000 |
| **GLAST** | Abcam; ab416; AB_304334 | 10 | rabbit | 5% blotto, 1h, RT | 1/5,000 |
| **GLT1** | Alomone; AGC-022; AB_2039891 | 10 | rabbit | 5% blotto, 1h, RT | 1/1,000 |
| **GLUR2** | Abcam; ab206293; N/A | 10 | rabbit | 5% blotto, 1h, RT | 1/2000 |
| **NMDAR1** | ThermoFisher Scientific; 32-0500; AB_2533060 | 10 | mouse | 5% blotto, 1h, RT | 1/500 |
| **PSD95** | Abcam; ab2723; AB_303248 | 10 | mouse | 5% blotto, 1h, RT | 1/1000 |
| **PVALB** | Millipore; MAB1572; AB_2174013 | 12 | mouse | 2.5 BSA, 1h, RT | 1/500 |

N/A, not applicable; RT, room temperature.

**Table S7. Sequences of MBNL1 and MBNL2 shRNA (related to Figure 5).**

| Gene | Sequence | Complementary sequence |
|---|---|---|
| ***MBNL1*** | AACACGGAAUGUAAAUUUGCA TT | UGCAAAUUUACAUUCCGUGUUTT |
| ***MBNL2*** | CACCGUAACCGUUUGUAUTT | CAUACAAACGGUUACGGUTT |

## SUPPLEMENTAL FIGURES

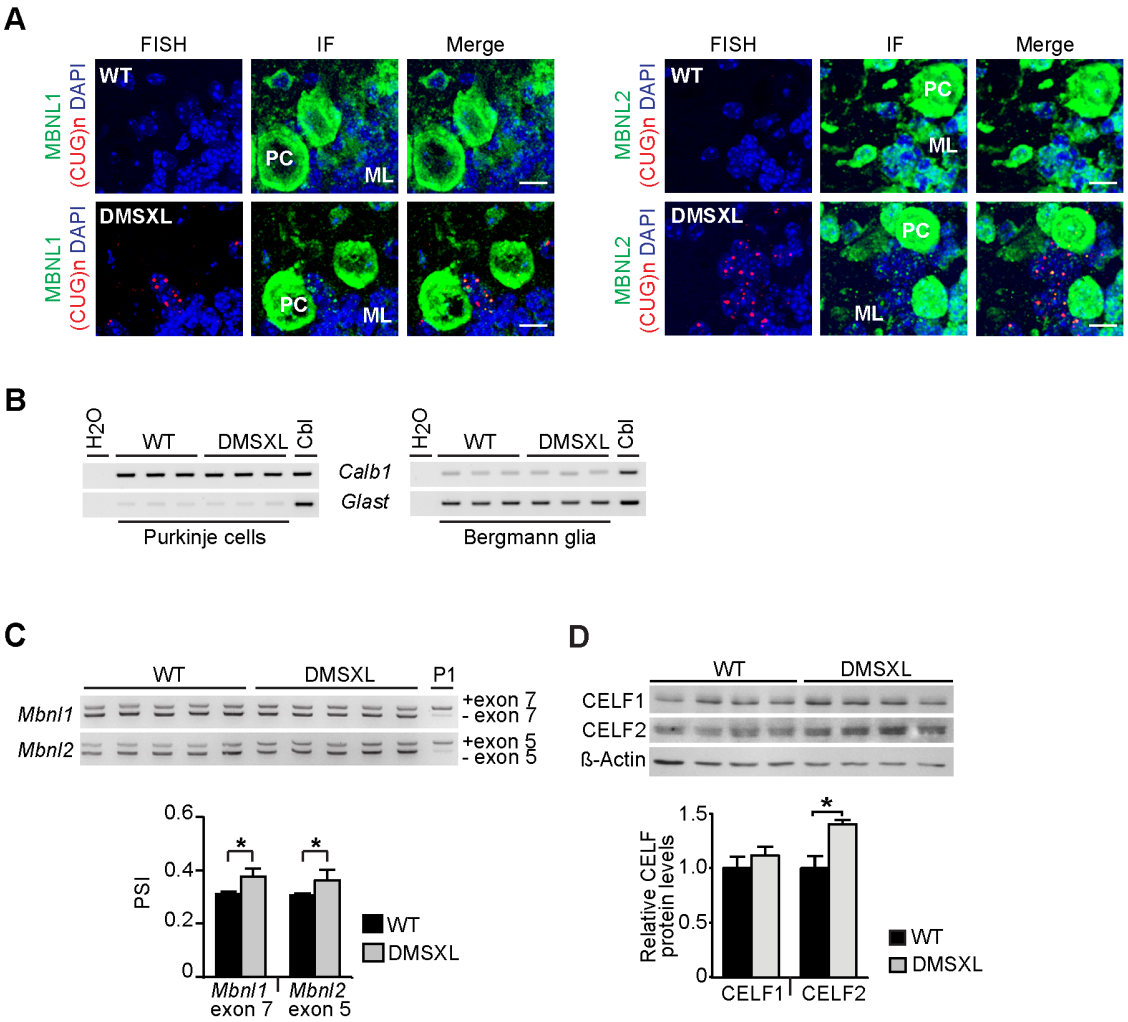


**Figure S1. RNA foci, splicing and CELF protein levels in DMSXL cerebellum (related to Figure 1). (A)** FISH detection of RNA foci (red) and immunofluorescence of MBNL1 and MBNL2 (green) in WT and DMSXL mouse cerebellum. The scale bar represents 10 µm. PC, Purkinje cells; ML, molecular layer. **(B)** RT-PCR expression analysis of RNA transcripts primarily expressed in Purkinje cells (calbindin 1, *Calb1*) and in Bergmann glia (*Glast*), to confirm the nature of the cells collected by laser cell microdissection from the cerebellum of WT and DMSXL mice (n=3 animals, each genotype). *Calb1* transcripts were found predominantly in collected Purkinje cells, while *Glast* showed higher expression in microdissected Bergmann astrocytes. $H_2O$, no DNA control; Cbl, mouse cerebellum tissue control. **(C)** RT-PCR analysis of splicing profiles of *Mbnl1* and *Mbnl2* mRNA transcripts in the cerebellum of 2-month-old DMSXL and WT mice (n=5, each genotype) and in WT newborn animals (P1, pool of 3 animals). The graphs represent the mean PSI (±SEM) of alternative exons. **(D)** To determine the contribution of CELF protein dysregulation to missplicing, we quantified CELF1 and CELF2 levels in whole cerebellum by western blot (n=4, each genotype). The graphs represent the mean (±SEM) relative to normalized WT controls. Only CELF2 was significantly upregulated in DMSXL mice. ß-Actin was used as internal control. **P*<0.05; Mann-Whitney U test.

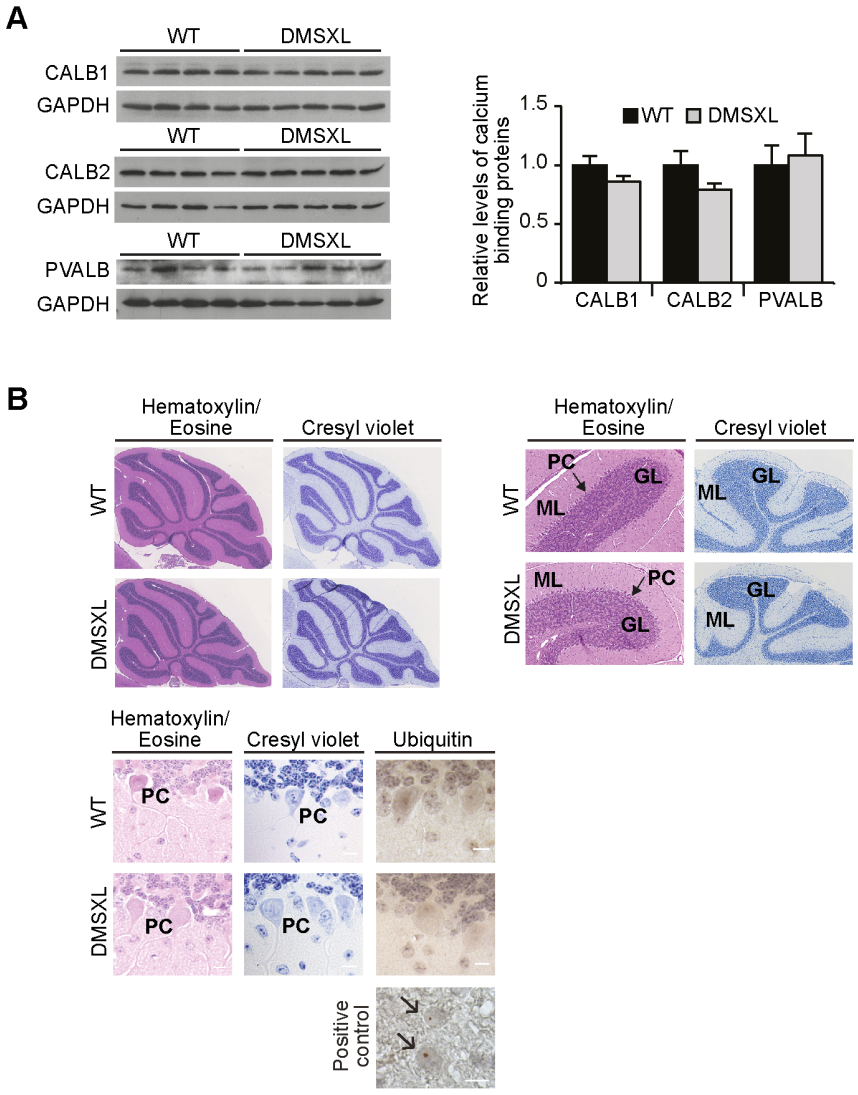


**Figure S2. Expression of calcium-binding proteins is not altered in DMSXL cerebellum (related to Figure 2). (A)** Western blot analysis of key calcium-buffering proteins (calbindin 1, CALB1; calbindin 2/calretinin, CALB2; and parvalbumin, PVALB) in the cerebellum of DMSXL mice (n=5), relative to WT controls (n=4). The graphs represent average protein levels (±SEM), relative to normalized WT controls. GAPDH was used as loading control. No significant difference was found in protein levels in DMSXL cerebellum. **(B)** Signs of neurodegeneration and histopathology in DMSXL cerebellum were investigated by standard hematoxylin-eosin and cresyl violet staining. Proteotoxicity was studied by the immunodetection of ubiquitin aggregates. Lower magnification pictures (top panels) do not show evidence of overall changes in cerebellum structure, morphology or cell density in DMSXL mice. Higher magnification pictures (bottom panels) do not reveal obvious changes in cell morphology, neurodegeneration or ongoing protein stress. FXTAS knock-in mouse brains were used as positive controls for the accumulation of ubiquitin-containing protein aggregates. PC, Purkinje cell; GL, granular layer; ML, molecular layer.

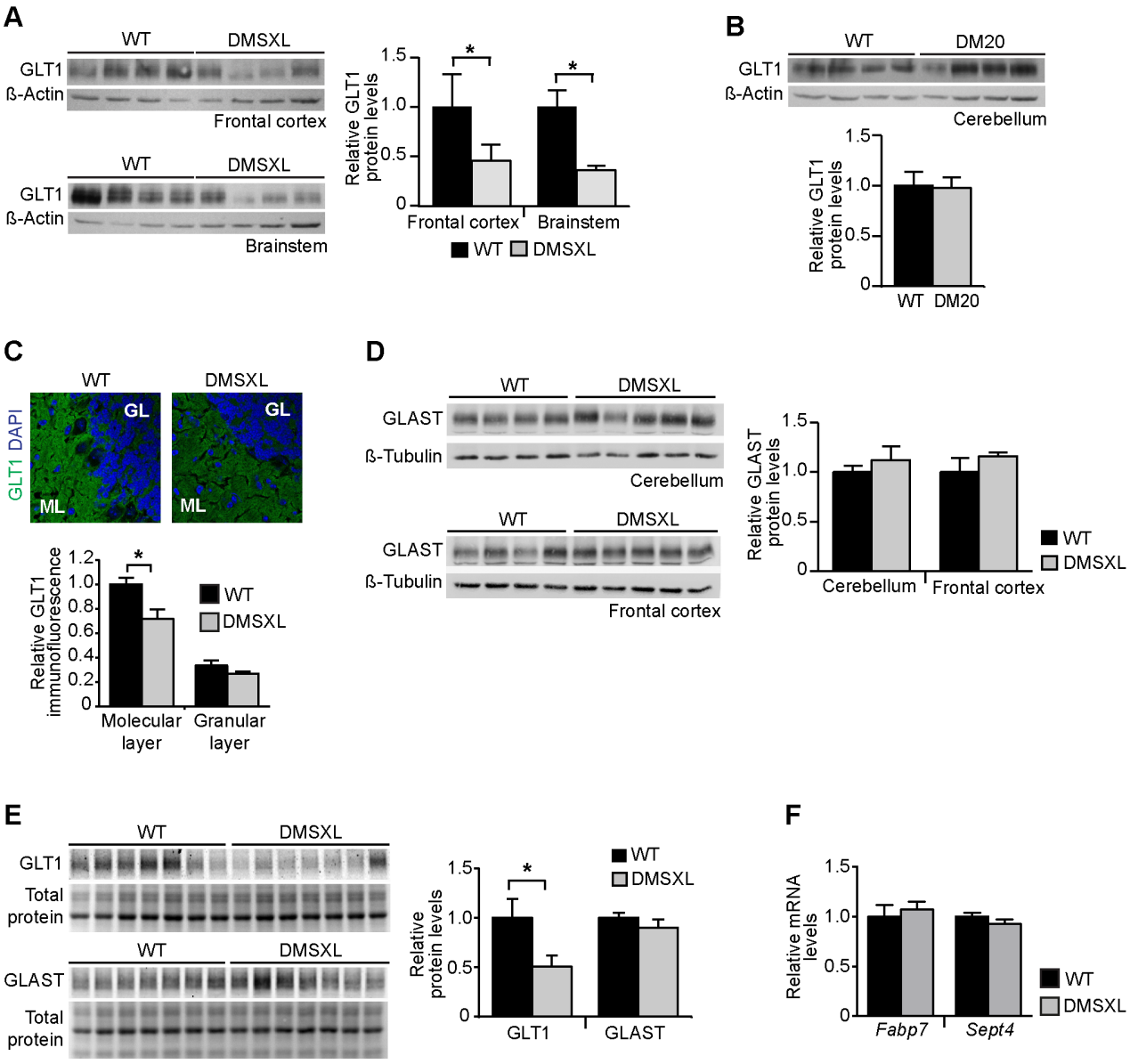


**Figure S3**. **GLT1 is downregulated in multiple brain regions of DMSXL mice (related to Figure 3). (A)** To assess the extent of GLT1 downregulation, we quantified GLT1 protein levels in additional brain regions from 2-month-old mice by western blot. GLT1 protein was significantly downregulated in the frontal cortex and brainstem of DMSXL mice, compared to WT controls (n=4, each genotype). ß-Actin was used as loading control. **(B)** Quantification of GLT1 protein levels in control DM20 transgenic mice, relative to WT littermates (n=4, each genotype). Overexpression of short *DMPK* transcripts is not sufficient to affect GLT1 steady-state levels. **(C)** Semi-quantitative analysis of GLT1 immunofluorescence (±SEM) in the molecular and granular layers in the cerebellum of two-month-old DMSXL and WT mice. Representative pictures of three independent analyses. The same camera acquisition settings were used for both images. **(D)** Western blot analysis of GLAST protein expression in the cerebellum and frontal cortex of DMSXL (n=5) and WT mice (n=4). ß-Tubulin was used as loading control. **(E)** Quantification of GLT1 and GLAST protein steady-state levels in DMSXL and WT primary astrocytes (n=7, each genotype). Representative western blot analysis of three technical replicates. Total protein was visualized by stain-free protocols and used as loading control. GLT1 show a significant 50% reduction in DMSXL primary astrocytes, while GLAST protein levels remain unchanged. **(F)** Quantification of Bergmann-specific *Fabp7* and *Sept4* transcripts in the cerebellum of DMSXL and WT mice (n=6, each group). Graphs represent the mean ± SEM. **P*<0.05, Mann-Whitney U test.

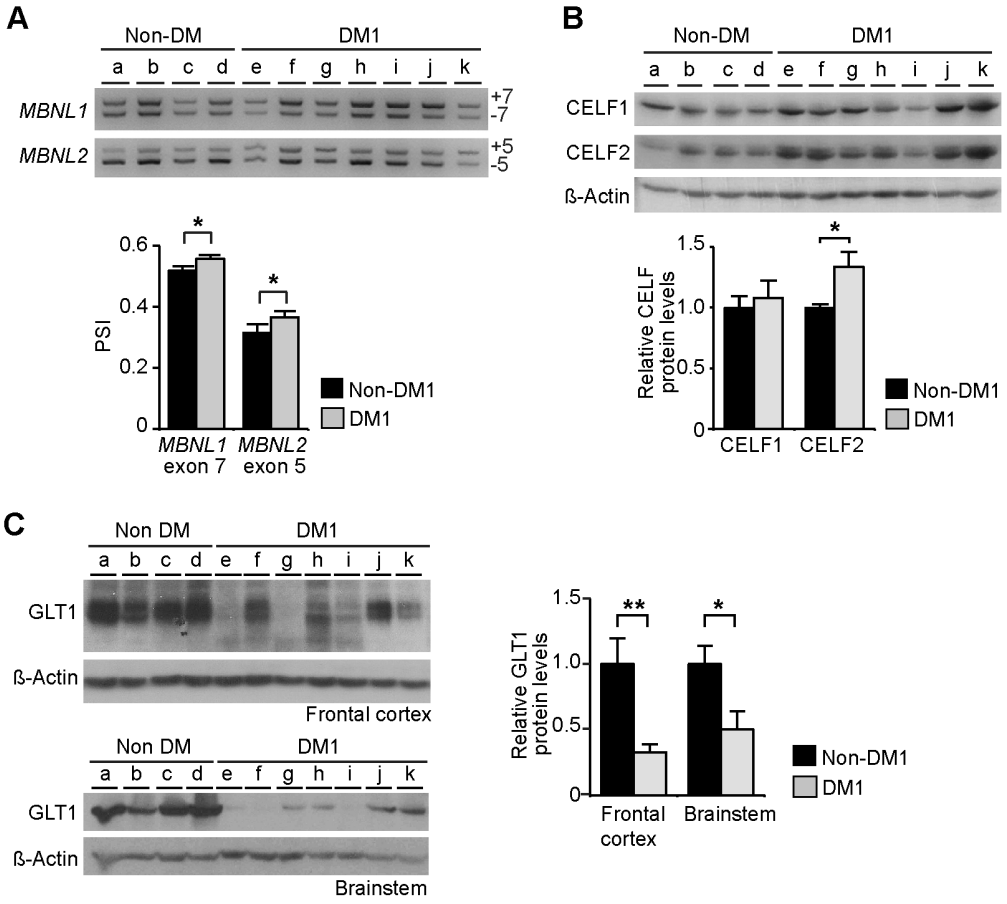


**Figure S4. RNA splicing and GLT1 protein levels in human DM1 brains (related to Figure 4). (A)** RT-PCR analysis of *MBNL1* exon 7 and *MBNL1* exon 5 in human cerebellum tissue samples in adult DM1 patients (n=7), relative to non-DM controls (n=4). The graphs represent the mean PSI (±SEM) of the alternative exons studied. **(B)** Quantification of CELF1 and CELF2 proteins by western blot in the cerebellum of DM1 patients (n=7), relative to non-DM controls (n=4), revealed significant upregulation of CELF2, to an extent similar to DMSXL mice. ß-Actin was used as loading control. **(C)** Western blot analysis of GLT1 steady-state levels in the frontal cortex and brainstem of adult DM1 patients and non-DM controls. GLT1 is significantly downregulated in DM1 frontal cortex and brainstem. ß-Actin was used as loading control **P*<0.05, ***P*<0.01; Mann-Whitney U test.

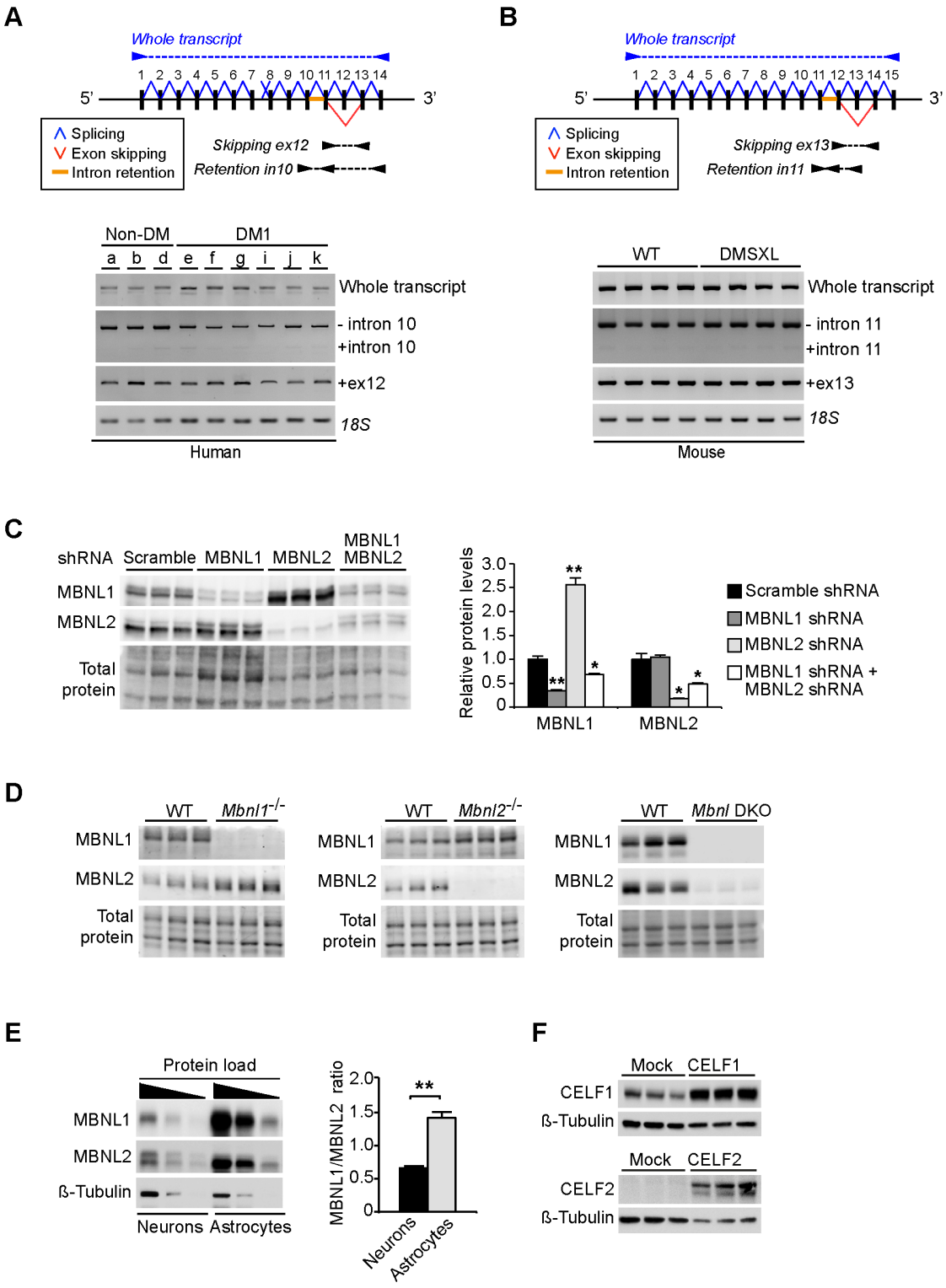
A
Whole transcript
1 2 3 4 5 6 7 8 9 10 11 12 13 14
5'
3'
Splicing
Exon skipping
Intron retention
Skipping ex12
Retention in10
Non-DM
DM1
a b d e f g i j k
Whole transcript
- intron 10
+intron 10
+ex12
18S
Human
B
Whole transcript
1 2 3 4 5 6 7 8 9 10 11 12 13 14 15
5'
3'
Splicing
Exon skipping
Intron retention
Skipping ex13
Retention in11
WT
DMSXL
Whole transcript
- intron 11
+intron 11
+ex13
18S
Mouse
C
shRNA
Scramble
MBNL1
MBNL2
MBNL1 MBNL2
MBNL1
MBNL2
Total protein
Relative protein levels
3.0
2.5
2.0
1.5
1.0
0.5
0
MBNL1
MBNL2
Scramble shRNA
MBNL1 shRNA
MBNL2 shRNA
MBNL1 shRNA + MBNL2 shRNA
D
WT
Mbnl1-/-
MBNL1
MBNL2
Total protein
WT
Mbnl2-/-
MBNL1
MBNL2
Total protein
WT
Mbnl DKO
MBNL1
MBNL2
Total protein
E
Protein load
MBNL1
MBNL2
ß-Tubulin
Neurons
Astrocytes
MBNL1/MBNL2 ratio
2.0
1.5
1.0
0.5
0
Neurons
Astrocytes
F
Mock
CELF1
CELF1
ß-Tubulin
Mock
CELF2
CELF2
ß-Tubulin

**Figure S5. GLT1 downregulation is not associated with splicing abnormalities and is mediated by MBNL1 inactivation (related to Figure 5). (A)** RT-PCR analysis of full-length *GLT1* mRNA, alternative exons and intron inclusion in human brains. The top illustration represents the human *GLT1* gene with 14 exons and shows the alternative splicing events studied. The arrowheads represent the location of the oligonucleotide primers used in the splicing analysis of whole transcript, skipping of exon 12 and inclusion intron 10. The results revealed no obvious differences between DM1 (n=6) and non-DM cerebella (n=3). **(B)** RT-PCR analysis of full-length *Glt1* mRNA, alternative exon 13 and intron 11 inclusion in the cerebellum of 2-month-old mice. The location of oligonucleotide primers (arrowheads) is indicated on the mouse gene. DMSXL cerebellum did not show obvious missplicing events, compared to WT controls (n=4, each genotype). **(C)** MBNL1 and MBNL2 detection by western blot following knocking down of these proteins by shRNA in T98G cells. Total protein was visualized by stain-free protocols and used as loading control. The graphs represent average protein levels (±SEM) relative to normalized scramble shRNA controls. MBNL1 was decreased down to 34% in cells transfected with MBNL1 shRNA. MBNL2 shRNA-treated cells showed MBNL2 protein levels down to 18% of scramble controls, but a 155% compensatory increase of MBNL1. MBNL1 and MBNL2 double knocking-down was more modest that individual strategies, resulting in protein levels that were 69% and 48% of those in scramble controls, respectively. **(D)** Western blot expression analysis of MBNL1 and MBNL2 proteins *Mbnl1*$^{-/-}$, *Mbnl2*$^{-/-}$ and *Mbnl* double knock out (DKO) mice, and in WT littermate controls (n=3, each genotype). Mice were aged 3-4 months. Total protein was visualized by stain-free protocols and used as loading control. **(E)** Western blot detection and quantification of MBNL1 and MBNL2 protein levels in primary neurons and astrocytes. Decreasing amounts of a protein pool of whole cell lysate from three WT cultures were electrophoresed and immunodetected. Both MBNL1 and MBNL2 proteins are more abundant in astrocytes. The graph represents the MBNL1/MBNL2 expression ratio in each cell type (mean ± SEM), and shows that MBNL1 relative expression is twofold higher in mouse primary astrocytes than in neurons. ß-Tubulin was used as loading control. **(F)** Western blot immunoblotting showing CELF1 and CELF2 upregulation in T98G cells transfected with expressing vectors. ß–Tubulin was used as loading control. **P*<0.05, ***P*<0.01; one-way ANOVA in (C) and Mann-Whitney U test in (E).

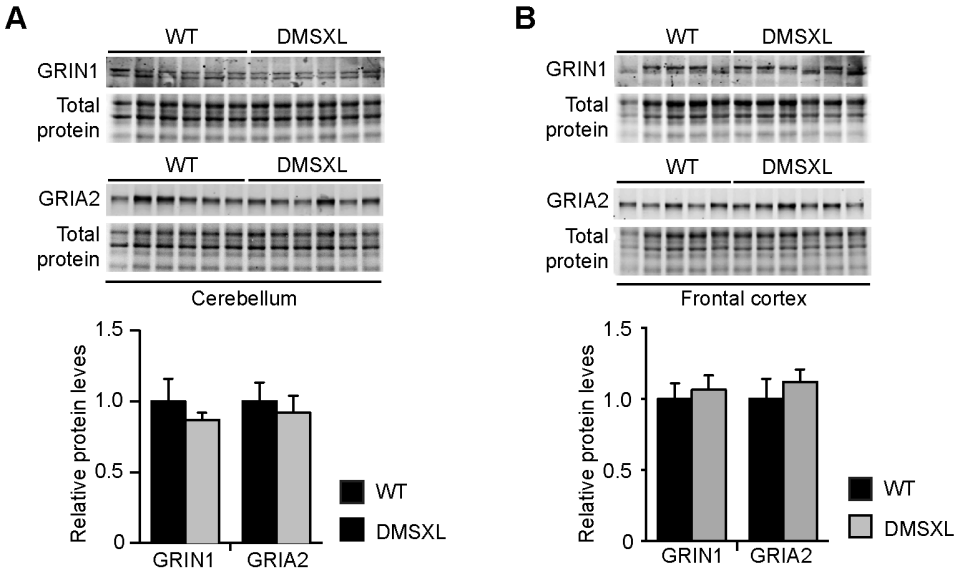


**Figure S6. Glutamate receptor expression in mouse brain tissue (related to Figure 6).** Quantification of GRIN1 and GRIA2 glutamate receptor subunits in the **(A)** cerebellum and **(B)** frontal cortex of 2-month-old DMSXL and WT controls (n=5-6, each genotype). Representative western blots of three technical replicates. Total protein was visualized by stain-free protocols and used as loading control. The graphs represent the mean (±SEM) relative protein levels, normalized to WT controls, and show no significant differences in the expression of glutamate receptors in DMSXL brain tissue.

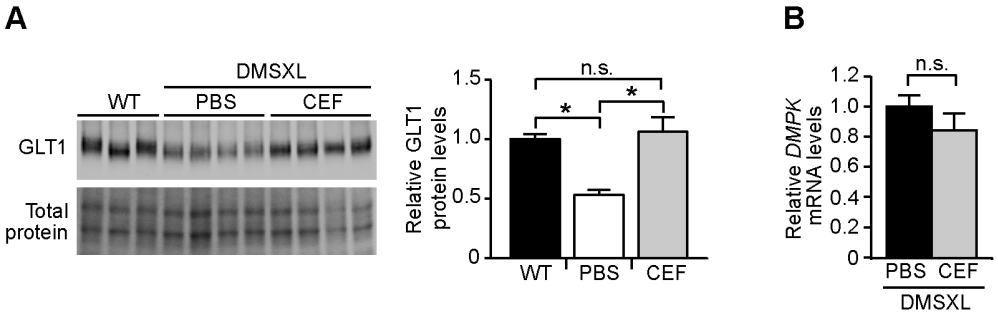


**Figure S7. Ceftriaxone upregulates GLT1 but does not change *DMPK* transcript levels in DMSXL mice (related to Figure 7). (A)** We confirmed that ceftriaxone increased GLT1 in DMSXL mice to levels undistinguishable from those detected in WT controls. Representative western blot analysis of GLT1 levels in the cerebellum of 2-month-old DMSXL mice following PBS or ceftriaxone treatment (200 mg/kg, daily i.p. injections, over 5 consecutive days) (n=4, each treatment group). WT controls are also shown (n=3). Total protein was visualized by stain-free protocols and used as loading control. The graph represents the mean levels of GLT1 protein (±SEM) in the cerebellum of DMSXL mice injected with ceftriaxone, PBS and in WT controls. **(B)** Real-time PCR quantification of expanded *DMPK* transcripts in the cerebellum of DMSXL mice treated with ceftriaxone (n=6) or PBS (n=6) showed no effect of the antibiotic on transgene expression. **P*<0.05, one-way ANOVA in (A); n.s. not statistically significant, Mann-Whitney U test in (B).

## SUPPLEMENTAL EXPERIMENTAL PROCEDURES AND METHODS

**Mouse genotyping.**
Mouse experiments were performed with wild-type controls of the same litter to reduce inter-individual variability. DMSXL transgenic mice were generated and genotyped as previously described (Gomes-Pereira et al., 2007; Hernandez-Hernandez et al., 2013). All DMSXL mice used for this work were adult (2-4 months) homozygotes, unless stated otherwise. The control DM20 line expresses non-pathogenic 20-CTG tracts (Seznec et al., 2001; Seznec et al., 2000). *Glt1* knock-out mice on C57BL/6 background (Tanaka et al., 1997) were provided by Prof. Niels Christian Danbolt (University of Oslo, Norway). The *Glt1* transgenic status was determined by multiplex PCR of tail DNA, using P1-GLT1 (5'-GGGTTGTAGATGTGTAGAGATGG-3'), P2-GLT1 (5'-CCTGACAGAGATCAGAGCACGT-3') and P3-GLT1 (5'-ATTCGCAGCGCATCGCCTTCTA-3') oligonucleotide primers. *Glt1* wild-type alleles generate a 469-bp product, while the disrupted allele generates a 210-bp allele.

**Fluorescent in situ hybridization (FISH).**
Ribonuclear inclusions were detected with a 5'-Cy3-labelled (CAG)5 PNA probe, as previously described (Huguet et al., 2012). Immunofluorescence (IF) combined with fluorescent *in situ* hybridization (FISH) was performed as previously described (Hernandez-Hernandez et al., 2013). Antibody references and working dilutions are listed in **Table S3**.

**Laser Capture Microdissection (LCM).**
Purkinje cells and surrounding cells were individually microdissected from one to two-month-old DMSXL and wild-type control mouse cerebellum, using a Palm Micro Beam (Carl Zeiss). RNA extraction, cDNA synthesis and RT-PCR analysis of candidate genes performed as previously described (Peixoto et al., 2004). Average of 100 Purkinje cells and 300 surrounding cells were separately collected in triplicate from three DMSXL mice and from three wild-type control mice. For each cDNA sample, three replicates of the RT-PCR reactions were performed. The sequences of the oligonucleotide primers used in the RT-PCR analysis of Purkinje and Bergmann cells laser microdissected from DMSXL cerebellum are listed in **Table S4**.

**RT-PCR analysis of alternative splicing.**
Total RNA was extracted from half mouse cerebellum collected 2-month-old mice, following tissue homogenization with stainless steel beads, and using a TRIZOL extraction protocol combined with a commercially available RNA Purification Kit, as previously described (Huguet et al., 2012). cDNA synthesis, semi-quantitative RT-PCR analysis of alternative splicing and qRT-PCR quantification of *DMPK* transcripts were performed as described elsewhere (Gomes-Pereira et al., 2007; Hernandez-Hernandez et al., 2013), using oligonucleotide primers listed in **Tables S5**. All samples were normalized to TATA-binding protein (Tbp) or ß-actin. The Percent of Spliced In (PSI) was used to quantify the splicing level of alternative exons: PSI = (intensity of inclusion isoform) / (intensity of inclusion isoform + intensity of exclusion isoform) x 100.

**Western blot analysis.**
Total protein was extracted from 20-30 mg brain tissue dissected from 2-month-old mice, using RIPA buffer (ThermoFisher Scientific; 89901), supplemented with 0.05% CHAPS (Sigma; C3023), 1x complete protease inhibitors (Roche; 04693124001), 1x Phospho STOP phosphatase inhibitors (Roche; 04693124001). Protein concentrations in the supernatants were determined using a Bio-Rad DCTM protein assay (Bio-Rad; 500-0114). Protein integrity was checked by Coomassie stain of a 10% SDS-polyacrylamide gel. Volumes corresponding to 30-60 µg of protein were mixed with Laemmli sample buffer and boiled for 5 min. Proteins were resolved in 10% or 12% SDS-polyacrylamide gels and transferred onto PVDF membranes. Following Ponceau red staining to verify the efficiency of protein transfer, membranes were blocked in 1X TBS-T (10 mM Tris-HCl, 0.15 M NaCl, 0.05% Tween 20) containing blotto (Santa Cruz Biotech; sc2325) and incubated overnight at 4°C with the corresponding primary antibody. After three washes with 1X TBS-T, membranes were incubated at room temperature during 1 h with the appropriated HRP-secondary antibody. Primary antibody references, working dilutions and blocking conditions are indicated in **Table S6**. After washing with 1X TBS-T, antibody binding was visualized by chemiluminiscence (PerkinElmer). Densitometric analysis with Quantity One® 1D Analysis Software (Bio-Rad) has been performed to quantify signal intensity. Quantitative western blot results are represented as means of steady-state levels (±SEM) in transgenic animals, relative to normalized controls. Total protein electrophoresed through thialo-containing polyacrylamide gels (Bio-Rad) was visualized under UV light.

**Electrophysiological and behavioral assessment.**
*In vivo electrophysiological study in alert mice.* Two-month old DMSXL and control mice were surgically prepared for chronic recording of neuronal activity in the cerebellum. The experimental session for extracellular recording of Purkinje cells (PCs) activity and local field potential (LFP) analysis in the cerebellar cortex was performed as previously described

(Cheron et al., 2004). The strength of the rhythmicity was quantified with a rhythm index (Cheron et al., 2004; Sugihara and Furukawa, 1995).
*The runway test.* Motor coordination was examined by the runway test as previously described (Servais and Cheron, 2005). In this test, 3-4 month old DMSXL (n=20) and control (n=21) mice, male and females included, ran along an elevated runway with low obstacles intended to impede progress. The runway was 100 cm long and 0.7 cm width. Obstacles being of 1 cm diameter wood rod and 0.7 cm width were placed every 10 cm along the runway. Mice were placed on one extremity of the runway and had to move along the runway to reach the other end. The number of slips of the right hind leg was counted. Each mouse underwent four consecutive trials per day during 5 consecutive days. The test was repeated following a test-free period of three weeks, over one day (four consecutive trials), to assess the learning capacity of mice.

**iTraq proteomics analysis.**
The analysis of mouse brain proteome by isobaric tagging for relative and absolute quantifications (iTRAQ) mass spectrometry was performed on individual DMSXL and wild-type male mice, aged 2 months (n=4 per genotype, for whole cell proteins extracts; n=2 for membrane bound protein fraction). Membrane-bound protein fractions were purified from mouse cerebellum, as previously described (Cox and Emili, 2006).
*iTraq labeling.* Protein iTRAQ labeling was performed according to the manufacturer's instructions (iTRAQ 4plex kit, ABSCIEX). Briefly, protein pellets (100 µg) were suspended in 20 µL of 500 mM triethylammonium bicarbonate (TEAB) and 1 µL of 2% SDS, they were then reduced with 2 µL of 50 mM tris-(2-carboxyethyl) phosphine (TCEP) for 1h at 60°C and finally alkylated with 1 µL of 200 mM methyl methanethiosulfonate (MMTS) for 10 min at room temperature. Proteins were digested with 2 µg of sequencing grade modified trypsin (Promega) for 16h at 37°C. The resulted peptides were labeled with iTRAQ reagents and quenched with Milli-Q water. The labeled samples were mixed in a 1:1:1:1 ratio and stored at -20°C.
*Sample clean-up by SCX & Sep-Pak.* An aliquot of the iTRAQ 4-plex-labeled peptide mixture (100 µg) was cleaned up with a cation-exchange cartridge SCX (from ICAT Reagent Kit, ABSCIEX), equilibrated with 10 mM potassium phosphate, pH 3, 25% acetonitrile. Peptides were eluted with 500 µL of 350 mM potassium chloride, 25% acetonitrile and concentrated in a centrifugal evaporator, under vacuum. The sample was reconstituted in 0.1% trifluoroacetic acid and loaded on a Sep-Pak cartridge (Waters) for desalting. After washing, the peptides were eluted in 1 mL of 70% acetonitrile- 0.1% trifluoroacetic acid and dried in a vacuum concentrator.
*MS/MS Analysis.* Nano-LC-MS/MS analysis was performed on an Ultimate 3,000 Rapid Separation Liquid Chromatography (RSLC) system (Dionex) coupled to LTQ-Orbitrap Velos mass spectrometer (Thermo Scientific). Dried peptides were resuspended in 0.1% (v/v) trifluoroacetic acid, 10% acetonitrile, and pre-concentrated on a 75 µm i.d. reversed-phase (RP) trapping column and separated with an aqueous-organic gradient (solution "A": 0.1% formic acid in 5% acetonitrile; solution "B": 0.085% formic acid in 80% (acetonitrile; flow rate 400 nl/min) on a 75 µm RP column (Acclaim PepMap RSLC 75 µm x 15 cm, 2 µm, 100Å, Dionex). Samples were eluted using a linear gradient from 5% to 40% solvent B in 190 min. One FTMS full scan was performed (resolution 60,000; positive polarity; centroid data; scan range 400 to 2,000 m/z) and the 10 most intense signals were subjected to MS/MS fragmentation both in the collision-induced dissociation (CID) cell and high-energy collision dissociation (HCD) cell for the same precursor ion. CID fragmentation was performed with a target value of 5000, collision energy of 35 V, Q value of 0.25 and activation time of 10 ms while HCD was done using a target value of 50,000, collision energy of 50 V and activation time of 0.1 ms. LC-MS/MS data were transferred to the Proteome Discoverer software v1.2 to create the .mgf file, which was searched against the *Mus musculus* subset (16547 sequences) of the UniprotKB/Swissprot database (release 2012_06; 536796 sequences) using the Mascot search engine (version 2.2.07; Matrix Science) for protein identification and protein quantification. Fixed modification (iTRAQ 4plex (K) and N-terminus) and variable modification (Methylthio (C), Oxidation (M)) were allowed as well as one missed cleavage. Monoisotopic peptide mass tolerance was ± 5 ppm (after linear recalibration), and fragment mass tolerance was ± 0.5 Da. Filters for protein quantification were set as follow: protein ratio type was "weighted", normalization was done with summed intensities and outliers were removed automatically. Only proteins quantified with at least 2 peptides and with the ion score higher than 25 were retained. False discovery rate was less than 2%. Differences between the DMSXL and WT proteomes were evaluated by a Mann-Whitney U test ($P$<0.05), as previously described (Jeanson et al., 2014). To determine the most deregulated proteins, the standard deviation of the protein ratios was calculated for each experiment, and the Gaussian distributions were normalized. An average threshold was calculated to determine the most upregulated proteins (last 20% on the right of the Gaussian) and the most downregulated proteins (first 20% on the left of the Gaussian).
*GO enrichment analysis.* Gene Ontology (GO) enrichment analysis of differently expressed proteins was performed using the functional annotation tool Database for Annotation, Visualization and Integrated Discovery (DAVID) v.6.7 (http://david.abcc.ncifcrf.go) (Huang da et al., 2009). GO enrichment analysis integrated the information of the cellular components and biological processes associated with the deregulated proteins, to provide a list biological terms organized into classes of related genes/proteins. Significant GO terms were identified at a FDR <0.05.

**Fluorescence quantification of GLT1**
Confocal images of WT and DMSXL slices of cerebellum stained on the same glass slide were acquired as z-stacks at the 40x magnification with a Leica TSC SP8 SMD Confocal microscope, using the same laser power and PMT values. Z projections were analyzed using Fiji software (Schindelin et al., 2012) by drawing the granular and molecular layer and measuring the integrated density of the regions of interest.

**Tissue fractioning for western blot analysis**
Cytosolic and membrane-bound protein were prepared by serial centrifugation of tissue homogenates collected from the cerebellum of 2-month-old mice, in isotonic sucrose solution, as previously described (Nishida et al., 2004). The enrichment for cytosolic and cell membrane proteins was confirmed by immunodetection of GAPDH and PSD95, respectively.

**Glutamate uptake**
Uptake of radioactive glutamate by cultured astrocytes was performed using published methods (Beaule et al., 2009) and expressed as fmol of radioactive glutamate per µg of total protein. Glutamate transporter inhibitors were added to the medium, to inhibit total glutamate transporter (50 µM TBOA; Bio-Techne, 10/1/2532), GLT1-mediated glutamate transport (200 nM WAY-213613; Santa Cruz Biotechnology, sc-203720) or GLAST-mediated glutamate transport (5 µM UCPH 101; Santa Cruz Biotechnology, sc-361391)

**Fluorescent assay of glutamate neurotoxicity in neuroglial co-cultures**
The co-cultures of neurons and astrocytes were established as previously described (Kaech and Banker, 2006). Briefly, the astrocytes were purified from the frontal cortex of P1 mouse embryos and cultured for two weeks in DMEM low glucose (31885-023Life Technologies, 31885-023), supplemented with 10% FBS and 0.05 mg/ml gentamycin (Life Technologies; 15710). E16.5 mouse neurons were dissociated from embryonic frontal cortex in a mixture of trypsin/DNase I and plated in Neurobasal-A medium (Life Technologies, 10888022), supplemented with 1X B27 supplement (Life Technologies, 17504044), 0.5 mM L-Glutamine (Life Technologies, 25030024), 1% antibiotic and antimycotic (Life Technologies, 15240-096) and 5% FBS. The primary neurons from the WT and DMSXL mice and were infected with NeuroLight$^{RM}$ red lentivirus (Essen BioScience, 4584), encoding the mKate2 fluorescent protein under the Synapsin-1 Promoter (MOI=3) four hours after plating in serum free neuronal medium. The next day neurons were washed with Neurobasal medium to remove the lentivirus and primary astrocytes, cultured two weeks, were plated on top of neurons. Neuronal fluorescence was monitored by live cell video-microscopy (IncuCyte Live Cell Analysis System, Essen BioScience), by acquiring phase contrast and red fluorescent images each hour, using the Neurotrack module of acquisition and measurement of neurite extension. On day 8 of the mixed cultures, 50 µM of glutamate were added to the medium and neurite collapse monitored for 12-24 hours. If used, glutamate receptor antagonists were also added on day 8, together with glutamate (10 µM CNQX, antagonist of AMPA receptors, Abcam, ab120017; 10 µM (+)-MK 801 maleate, antagonist of NMDA receptors, Abcam, ab144485). The rate of neurite collapse was expressed as mm of length change, per mm$^2$ of surface studied, per day. For the rescuing assays, GLT1 was upregulated 30 hours prior to the assessment of glutamate neurotoxicity, either by transfection of GLT1-GFP-expressing plasmids (provided by Dr. Nicolas Reyes, Institute Pasteur, Paris, France) or by treating co-cultures with 10 µM ceftriaxone.

**Plasmid and shRNA transfection.**
Cultured cells were transfected with 250 ng/mL to 1.25 µg/mL of plasmid DNA using JetPrime transfection reagent and protocol (PolyPlus, 114-75). shRNA was transfected at a final concentration of 200 nM using Lipofectamine RNAiMax reagent and protocol (Life Technologies; 13778150). shRNA sequences are shown in the **Table S7**.

**Ceftriaxone treatment.**
Mouse intraperitoneal injections of ceftriaxone (Sigma; C5793) in PBS (20 µg/µl) were performed through a 27G needle to a final dose of 200 mg/kg. Male and female mice were injected at 2 months of age, daily over a period of five days, prior to molecular, electrophysiological and behavioral assessment. Daily injections of ceftriaxone continued during motor assessment in the runway test. Treatment control mice were injected with PBS (n=5 per group, including male and females).

**Microscope and images processing.**
Images were taken with a fluorescent microscope Zeiss ApoTome 2 or with a Leica TSC SP8 SMD Confocal microscope. Images were treated with ImageJ software (Schneider et al., 2012).

**Statistical analysis.**
Statistical analyses were performed with Prism (GraphPad Software, Inc), SPSS (v14.0, SPSS Inc©), Statistica (v6.0, StaatSoft®) and/or Excel software. When two groups were compared, we first performed a normality test. Parametric data were compared using a two-tailed Student's t-test (with equal or unequal variance, as appropriate). Non-parametric data were compared using a two-tailed Mann-Whitney U test. For one-way ANOVA, if statistical significance was achieved, we performed post-test analysis to account for multiple comparisons. Statistical significance was set at $P<0.05$. The data are presented as mean ± standard error of the mean (±SEM).

## SUPPLEMENTAL REFERENCES


Beaule, C., Swanstrom, A., Leone, M.J., and Herzog, E.D. (2009). Circadian modulation of gene expression, but not glutamate uptake, in mouse and rat cortical astrocytes. PLoS One *4*, e7476.

Cheron, G., Gall, D., Servais, L., Dan, B., Maex, R., and Schiffmann, S.N. (2004). Inactivation of calcium-binding protein genes induces 160 Hz oscillations in the cerebellar cortex of alert mice. J Neurosci *24*, 434-441.

Cox, B., and Emili, A. (2006). Tissue subcellular fractionation and protein extraction for use in mass-spectrometry-based proteomics. Nat Protoc *1*, 1872-1878.

Gomes-Pereira, M., Foiry, L., Nicole, A., Huguet, A., Junien, C., Munnich, A., and Gourdon, G. (2007). CTG trinucleotide repeat "big jumps": large expansions, small mice. PLoS Genet *3*, e52.

Hernandez-Hernandez, O., Guiraud-Dogan, C., Sicot, G., Huguet, A., Luilier, S., Steidl, E., Saenger, S., Marciniak, E., Obriot, H., Chevarin, C.*, et al.* (2013). Myotonic dystrophy CTG expansion affects synaptic vesicle proteins, neurotransmission and mouse behaviour. Brain *136*, 957-970.

Huang da, W., Sherman, B.T., and Lempicki, R.A. (2009). Systematic and integrative analysis of large gene lists using DAVID bioinformatics resources. Nat Protoc *4*, 44-57.

Huguet, A., Medja, F., Nicole, A., Vignaud, A., Guiraud-Dogan, C., Ferry, A., Decostre, V., Hogrel, J.Y., Metzger, F., Hoeflich, A.*, et al.* (2012). Molecular, physiological, and motor performance defects in DMSXL mice carrying >1,000 CTG repeats from the human DM1 locus. PLoS Genet *8*, e1003043.

Jeanson, L., Guerrera, I.C., Papon, J.F., Chhuon, C., Zadigue, P., Pruliere-Escabasse, V., Amselem, S., Escudier, E., Coste, A., and Edelman, A. (2014). Proteomic analysis of nasal epithelial cells from cystic fibrosis patients. PLoS One *9*, e108671.

Kaech, S., and Banker, G. (2006). Culturing hippocampal neurons. Nat Protoc *1*, 2406-2415.

Nishida, A., Iwata, H., Kudo, Y., Kobayashi, T., Matsuoka, Y., Kanai, Y., and Endou, H. (2004). Nicergoline enhances glutamate uptake via glutamate transporters in rat cortical synaptosomes. Biol Pharm Bull *27*, 817-820.

Peixoto, A., Monteiro, M., Rocha, B., and Veiga-Fernandes, H. (2004). Quantification of multiple gene expression in individual cells. Genome research *14*, 1938-1947.

Schindelin, J., Arganda-Carreras, I., Frise, E., Kaynig, V., Longair, M., Pietzsch, T., Preibisch, S., Rueden, C., Saalfeld, S., Schmid, B.*, et al.* (2012). Fiji: an open-source platform for biological-image analysis. Nat Methods *9*, 676-682.

Schneider, C.A., Rasband, W.S., and Eliceiri, K.W. (2012). NIH Image to ImageJ: 25 years of image analysis. Nat Methods *9*, 671-675.

Servais, L., and Cheron, G. (2005). Purkinje cell rhythmicity and synchronicity during modulation of fast cerebellar oscillation. Neuroscience *134*, 1247-1259.

Seznec, H., Agbulut, O., Sergeant, N., Savouret, C., Ghestem, A., Tabti, N., Willer, J.C., Ourth, L., Duros, C., Brisson, E.*, et al.* (2001). Mice transgenic for the human myotonic dystrophy region with expanded CTG repeats display muscular and brain abnormalities. Hum Mol Genet *10*, 2717-2726.

Seznec, H., Lia-Baldini, A.S., Duros, C., Fouquet, C., Lacroix, C., Hofmann-Radvanyi, H., Junien, C., and Gourdon, G. (2000). Transgenic mice carrying large human genomic sequences with expanded CTG repeat mimic closely the DM CTG repeat intergenerational and somatic instability. Hum Mol Genet *9*, 1185-1194.

Sugihara, I., and Furukawa, T. (1995). Potassium currents underlying the oscillatory response in hair cells of the goldfish sacculus. J Physiol *489 ( Pt 2)*, 443-453.

Tanaka, K., Watase, K., Manabe, T., Yamada, K., Watanabe, M., Takahashi, K., Iwama, H., Nishikawa, T., Ichihara, N., Kikuchi, T.*, et al.* (1997). Epilepsy and exacerbation of brain injury in mice lacking the glutamate transporter GLT-1. Science *276*, 1699-1702.

# Chapter V. Pathophysiological consequences of the DM1 CTG repeat expansion on neurons and astrocytes

# V.A. Introduction

## V.A.I Different cell types in the CNS

The notion that the brain is composed of different discrete neurons was very controversial in the 19th century. Among the first discoveries that corroborated this theory was the description of the biggest neurons in the brain, the Purkinje neurons of the cerebellum, by Johannes Evangelista Purkinje in 1837. The extremely useful silver nitrate staining technique developed by Camillo Golgi allowed him to describe in detail neurons in hippocampal and cerebellar tissue, around 1873. However he believed that these neurons formed a continuous network or reticulum. The detailed description of neurons of different brain regions, and their structure and projections, by Santiago Ramon y Cajal around 1888 allowed scientists to understand that the nervous system is composed of "absolutely autonomous units" and the notion of "**neuron**", "axon", "dendrites" and "synapse" were subsequently developed during the last decade of the 19th century (Guillery 2005). The description of non-neuronal nervous tissue followed as the new great debate of the century, starting with the description of the neuroglia as "nevernkitt" or nerve glue in 1856. The cellular nature of the **glia** was recognized thanks to the description of Henrich Müller in 1851 and Karl Bergmann in 1858 of the non-neuronal cells in the retina and cerebellar cortex, respectively, and of Otto Deiters in 1865 of the stellate glial cells which could be the astrocytes. Golgi also described stellate neuroglial cells connecting the blood vessels to brain parenchyma, while Ramon y Cajal developed the first staining for astrocytes, which labeled the glial fibrillary acid protein (GFAP), described the origin of astrocytes from the radial glia and demonstrated that they can divide in the brain. The name "**astrocyte**" was also adopted at the end of the 19th century and it was not until the second decade of the 20th century that **oligodendrocytes** and **microglia** were described, by Pío del Río Hortega (Parpura & Verkhratsky 2012; Pérez-Cerdá et al. 2015). Recently a new type of glia has been defined as the forth non-neuronal cell type in the CNS: the polydendrocytes or **NG2 glia**. Although classically

considered as oligodendrocytes precursor cells, new contributions to many cellular and physiological processes are being described for these cells (Nishiyama et al. 2009; Hill & Nishiyama 2014).

While the neurons are the functional unit of the brain, in charge of receiving and transmitting synaptic impulses, glial cells ensure the proper connectivity and functioning of the neurons: the astrocytes control the brain homeostatic levels of ions and neurotransmitters and form the blood-brain barrier, the oligodendrocytes generate the myelin sheathing that insulates the axons allowing rapid conduction of nerve impulse, the polydendrocytes generate oligodendrocytes and protoplasmic astrocytes and receive neuronal synaptic inputs and the microglia are immunocompetent phagocytic cells that act as the brain immune system (**Fig. V.1**) (Jäkel & Dimou 2017).

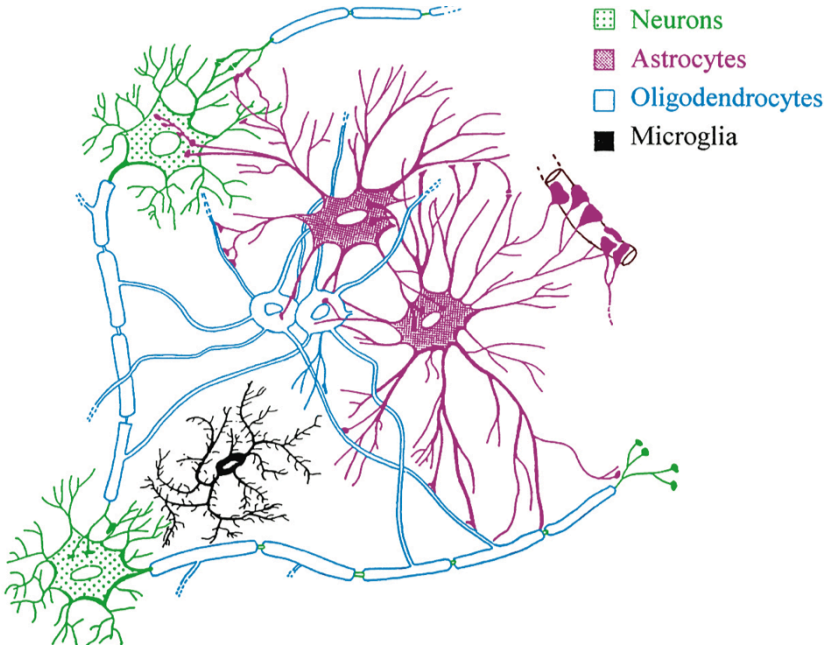


**Figure V.1. Representation of different brain cell types.** Schematic representation of different cell types of the brain and their interactions: neurons, astrocytes, oligodendrocytes and microglia (adapted from Baumann & Pham-Dinh 2001). Polydendrocytes are absent as their role and interaction with other brain cell is currently under investigation.

The bases of different brain cell types were thus settled at the beginnings of the 20$^{th}$ century and today we know that the human brain contains around 80 billion neuronal cells and around the same amount of glial cells, with an overall glial-to-neuron ratio of 1:1, which can be higher in the cerebral cortex (3.76:1) and much lower in the cerebellum (0,23:1) (Azevedo et al. 2009).

## V.A.II Neuronal cyto-architecture and brain diseases

Neurons are highly polarized cells showing different cellular domains: a dendritic arborization that collects neurotransmitters signals and integrates the synaptic input, the cell body where the nucleus is located and an elongated axon that will transmit action potentials to the synapse to activate neurotransmitter release. Proper connectivity of presynaptic axon terminals to postsynaptic dendritic spines is essential for the neuronal activity, and failure to establish this connectivity is linked to many neurological and neuropsychiatric disorders.

The shape and polarization of the neurons is controlled by the dynamics of the cytoskeleton, from the first steps of neuronal development until the fine regulation of dendrite spine morphology (Witte & Bradke 2008). The use of cultured neurons have permitted a better understanding of the main cytoskeletal changes that regulate neuronal polarization: neuritogenesis starts with the extension of actin-rich lamellipodial and filopodial protrusions, from a relatively round neuron, which will outgrow into thin minor neurites. Initially neurites show similar length and content in actin and microtubules until eventually one neurite acquires axonal specification and starts elongating following a guidance cue, while the remaining neurites acquire dendritic markers. The elongation of the axon, through the growth cone, is dependent of the polymerization, depolymerization and stability of actin filaments and microtubules, which are regulated by numerous cytoskeletal regulatory proteins. Finally, synaptic contacts are established between presynaptic axons and postsynaptic dendrites on another neuron to form the neuronal network (**Fig. V.2**) (Menon & Gupton 2016).

Many neurological disorders have been associated with defective neuronal arborization, dendritic spine formation and axonal growth. Among them, patients with autism spectrum disorder (ASD) show decreased dendritic branching but increased spine density; patients with schizophrenia show lower number and complexity of both dendrites and dendritic spines, as well as patients with Down syndrome or Alzheimer's disease (AD); while patients suffering of the

FXS show aberrant dendrite and spines morphology, with long, thin, immature dendritic spines (**Fig. V.3**) (Kulkarni & Firestein 2012).

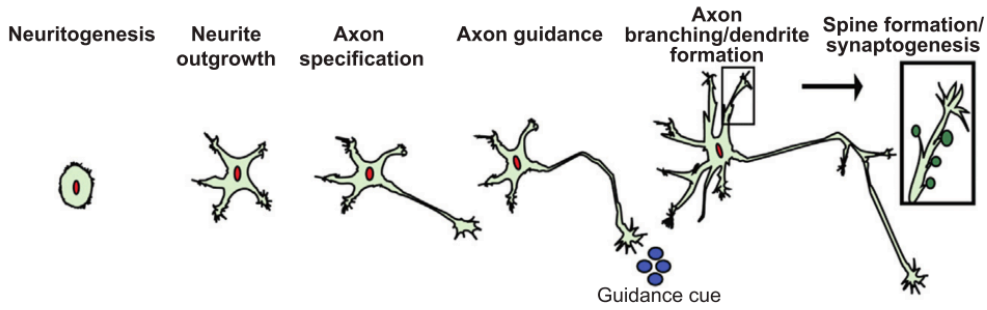


**Figure V.2. Developmental stages of a neuron.**
Schematic representations of the differentiation process of a neuron, form a round cell into a highly polarized cell, starting with neuritogenesis, neurite outgrowth, axon specification and elongation in response to guidance cues, dendrite formation and axon branching, and finishing with spine formation and synaptogenesis (Extracted from Menon & Gupton 2016).

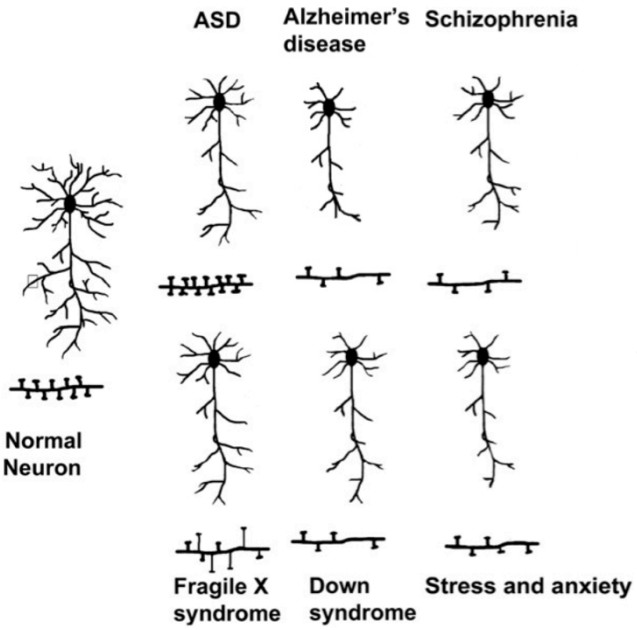


**Figure V.3. Cytoskeletal complexity of neurons in neurological diseases.**
Schematic representation of the overall cyto-architecture of neurons and dendritic spine morphology in normal brain compared to neurological disorders like autism spectrum disorder (ASD), Alzheimer's disease, schizophrenia, FXS, Down syndrome and stress and anxiety (Adapted from Kulkarni & Firestein 2012).

## V.A.III The esential role of the astrocytes

Astrocytes are highly heterogeneous in structure and function and they control almost all homeostatic tasks occurring during brain development and functioning. During brain development, radial glia differentiates into stellate astrocytes, as well as neurons and oligodendrocytes. In some brain regions, like the cortex, radial glia disappears after giving rise to stellate astrocytes, while in other brain regions, like the cerebellum, the radial glia remains as what we know as Bergmann glia. Two types of stellate astrocytes have been describes in rodent's brain: protoplasmic astrocytes, with a rich and complex morphology, located mostly in the gray matter in association with synapses and blood vessels, and fibrous astrocytes, bigger in size but less complex, located in the white matter in contact with blood vessels, neuronal axon fibers and myelin sheathings (**Fig. V.4**). In addition, two more varieties of astrocytes have been described in the human brain: the interlaminar astroglial, connecting several layers in the cortex; and varicose projection astroglia located in layers V-VI of the cortex, which extend long varicose processes to contact blood vessels. However the exact function of these two types of primate astrocytes is not fully known (Vasile et al. 2017).

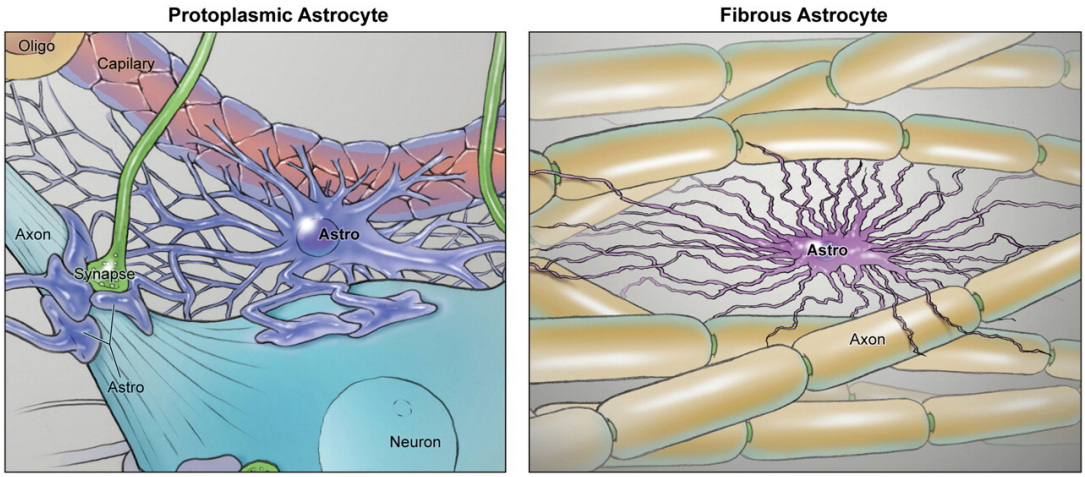


**Figure V.4. Cytoskeletal heterogeneity of astrocytes.**
Schematic representation of the two main types of astrocytes in mammals brain: protoplasmic astrocytes interacting with neuronal synapses and blood vessels, forming the neurovascular units; and fibrous astrocytes interacting with neurons' axon fibers and oligodendrocyte myelin sheathings (Extracted from Molofsk et al. 2012).

Astrocytes play an essential role in structural organization of the brain, by forming independent neurovascular units, and in synaptogenesis and synaptic maturation and function. Astrocytes control synaptic function by secreting tropic factors; uptaking excess neurotransmitters, such as glutamate, γ-aminobutyric acid (GABA), glycine and adenosine; and supplying neurons with glycine, a glutamate and GABA precursor. They are also involved in sensing brain hyperthermia, transporting water and scavenging reactive oxygen species (Verkhratsky et al. 2014).

Protoplasmic astrocytes take part in the tripartite synapse, by structurally enwrapping the dendritic spines and presynaptic terminals, and functionally interacting with them, by responding to neurotransmitters and releasing gliotransmitters that will modulate the synapse (Perez-Alvarez et al. 2014). This association is a fast, dynamic process, in which synapse activity regulates the plasticity of astrocytes processes around the synapse and the coverage and motility of the astrocytes processes will strengthen the synapse stability (Eroglu & Barres 2015; Lee & MacLean 2015). Moreover, one sole astrocyte can cover between 20,000 and 120,000 synapses in the rodent brain and up to 2 million synapses in human, thus modulating inter-neuronal communication and locally integrating information of an extremely large number of synapses (Vasile et al. 2017).

Astrocytes respond to trauma and infection by an heterogeneous process known as astrocyte reactivity or astrogliosis: they show an increase in the intermediate filament expression, particularly in the glial fibrillary acid protein (GFAP), a progressive cellular hypertrophy and increased proliferation. Following an insult that causes neuronal damage, astrocytes will surround and isolate the damaged area, thus having a short-term protective effect. However, long-term insults such as neurodegeneration can lead to prolonged astrogliosis that will limit functional recovery and increase damage in the affected area (Pekny et al. 2016).

Besides astrogliosis, many neurological diseases are associated with degeneration, loss of homeostatic function (asthenia) or pathological remodeling of the astrocytes. In epilepsy, various

astrocytic receptors, transporters and voltage channels are affected and synchronization of neuronal firing is lost. In HD astrogliosis was reported in association with abnormal expression of glutamate transporters and ion channels, resulting in neuronal degeneration (Pekny et al. 2016). In ALS astrocytes undergo degeneration and functional asthenia through downregulation of GLT1 glutamate transporter and atrophic changes are observed in Alzheimer's disease and in major depressive disorders (Verkhratsky & Parpura 2016). Thus, astrocytes represent an essential homeostatic and regulatory brain cell type and their dysfunction may contribute to virtually all neurological diseases and should be taken into account in the treatment of such diseases.

## V.A.IV Defective neuroglial communication in microsatellite-expansion diseases

The physical and functional interactions between brain cell types, especially at the tripartite synapse, is essential for proper CNS function, and perturbations in cell communication are associated with neurological conditions. Some microsatellite expansion disorders illustrate the importance of functional interactions between brain cell types.

Specific contribution of neuronal deregulation has been demonstrated in HD by the expression of an expanded CAG sequence in neurons, which led to neurodegeneration and induced astrogliosis and apoptosis in the mouse brain (Yu et al. 2003). On the other hand, specific expression of CAG repeats in the astrocytes led to reduced levels of GLT1, decreased glutamate uptake and increased susceptibility to seizures (Bradford et al. 2009), demonstrating the deleterious impact of astrocytes on neuronal electric activity.

In FXS mouse models, conditional loss of function of FMRP in hippocampal and cortical neurons led to altered dendritic complexity, reduced neuritogenesis and changes in synaptic markers (Amiri et al. 2014; Guo et al. 2011). Moreover, primary neurons derived from *Fmr1* KO mice show abnormal dendritic morphology and synaptic protein expression, which are

rescued when co-cultured with WT astrocytes. In contrast, while *Fmr1* KO astrocytes conditioned medium inhibited dendritic growth of WT neurons, suggesting abnormal neuro-glial communication in the FXS. GLT1 expression and glutamate uptake are also reduced in *Fmr1* KO mice, affecting neuronal excitability (Higashimori et al. 2013; Higashimori et al. 2016) further supporting abnormal neuroglial interaction in this disease.

As research advances in the microsatellite-expansion field it is becoming essential to tackle the contribution of neurons, astrocytes and astroglial interaction also to DM1 pathology, to better understand the mechanisms behind this devastating disease.

# V.B. Context of the study

## V.B.I Brain cell-specific abnormalities in DM1

Several histopathological and imaging studies have reported white matter abnormalities, discrete neuronal loss, intraneuronal neurofibrillary tangles and moderate gliosis in DM1 brain (Meola & Sansone 2007; Gourdon & Meola 2017). However, recent magnetic resonance spectroscopy studies found abnormalities in DM1 brain metabolites, suggestive of global neuronal impairment, but without gliosis (Takado et al. 2015). Thus, despite continuous advancement in the understanding of the DM1 neuropathogenesis, today we still do not know the specific contribution of each brain cell type to the neurological symptoms of DM1 patients.

Our laboratory has previously reported the accumulation of toxic RNA foci in both neurons and astrocytes in different brain regions of DMSXL mice and DM1 patients. In addition, DMSXL mice exhibit synaptic dysfunction and behavioral and electrophysiological defects, associated with abnormal expression and phosphorylation of neuron-specific proteins, like RAB3A and SYN1 (Hernandez-Hernandez et al. 2013); as well as and decreased expression of the astrocyte-specific glutamate transporter GLT1, associated with Purkinje cell hyperactivity in the cerebellum and high excitotoxicity in cell culture (Sicot et al. 2017). The abnormalities in neuronal and glial proteins have been confirmed in human DM1 brains, further supporting their

contribution to DM1 pathology. These results indicate that the CTG repeat expansion affects both neurons and astroglial cells and that DM1 neuropathogenesis involves both brain cell types.

Other laboratories have reported the toxic effects of the CTG expansion on neuronal differentiation. The differentiation of PC12 neuronal cell line is impaired by the expression of expanded CTG repeats, in association with abnormal expression of microtubule-associated proteins 1A, 2 and 6 (Quintero-Mora et al. 2002; Velázquez-Bernardino et al. 2012) thus suggesting abnormal neuronal development in DM1 brain.

# V.C. Research objectives

Despite reports of astrogliosis and white matter abnormalities in DM1 brains (Ono et al. 1998; Gourdon & Meola 2017) the role of the glia in DM1 neuropathogenesis has not been further explored. Today we do not know to which extent individual brain cell types contribute to DM1 brain pathology, and which are the molecular mechanisms specifically deregulated in each cell type.

I used DMSXL mice as a source of primary brain cells to investigate the functional consequences of the CTG repeat expansion on two individual brain cell types: neurons and astrocytes. I have studied the *in vitro* cellular phenotype of these brain cells, in homogeneous cultures, and the neuroglial interaction, in co-cultures of mixed genotypes. Moreover, to better understand molecular mechanisms deregulated in each brain cell type I performed a global proteomics analysis that revealed novel deregulated pathways that could contribute to DM1 neuropathogenesis.

# V.D. Results

The experimental results of this study will be submitted soon for publication to the *Journal of Neuroscience*, and they are presented as so in the following pages. A brief summary of the results is presented below:

## Diana Dincã, Géraldine Sicot, Aline Huguet-Lachon, Cerina Chuuon, Chiara Ida Guerrera, Geneviève Gourdon, Mário Gomes-Pereira. **GUG RNA toxicity is associated with adhesion and migration deficits in astrocytes and abnormal neuritogenesis in myotonic dystrophy**

To better understand which brain cell type is mostly affected by the CTG repeat expansion I used primary neurons and astrocytes derived from DMSXL mouse brain. I started by investigating the RNA toxicity signs in these two of the major brain cell types. I observed a higher content of CUG foci in primary DMSXL astrocytes compared to neurons, associated with increased expression of the *DMPK* transgene and more severe missplicing in astrocytes. MBNL proteins are sequestered by the toxic foci in both cell types while, surprisingly, CELF protein levels are not affected.

I next investigated the consequences of marked RNA toxicity on the phenotype of primary DMSXL astrocytes. My results suggest growth defects of the overall astroglial population, not associated with a proliferation defects or increased apoptosis. Instead, defective population growth was correlated with abnormal adhesion and spreading of the astrocyte cytoskeleton. In agreement with these results, DMSXL astrocytes show lower number of focal adhesions, defective reorientation of the cytoskeleton and aberrant migration, compared to WT cells.

On the other hand, even if the levels of toxic RNAs are lower, they do affect DMSXL neurons development. Primary DMSXL neurons show abnormal neuritogenesis at late time points during differentiation. Neuritogenesis defects are further increased by the presence of DMSXL astrocytes, suggesting the contribution of abnormal neuroglial interactions to neuronal dysfunction.

To determine which are the deregulated molecular mechanisms associated with the brain cell defects described, I performed a global proteomics analysis of WT and DMSXL neurons and astrocytes. Interestingly, DMSXL astrocytes show a higher number of deregulated proteins than the DMSXL neurons, in accordance with a higher impact of the disease. We next performed a

gene ontology (GO) enrichment analysis of the most common biological processes and cell compartments associated with the proteins deregulated. Among the top 10 deregulated clusters we found cell adhesion and actin cytoskeleton regulation clusters in the astrocytes; while DMSXL neurons displayed significant enrichment for clusters that regulate the development of neuron projections and dendritic spines.

Together these results indicate a strong involvement of the astrocytes and neuroglial communication impairment to DM1 brain pathology.

# V.E. Discussion

The pathological contribution of the glia to DM1 pathology has already been reported in the cerebellum of DMSXL mice, where the loss of the glial glutamate transporter GLT1 is associated with abnormal neuronal activity and impaired motor performance (Sicot 2017). Here I report a higher impact of the toxic CUG RNAs on astrocytes, compared to neurons, associated with adhesion and cytoskeletal organization abnormalities and functional consequences of the astrocytes deregulation on neuronal development. The results of the global proteomics analysis performed on homogeneous cultures of neurons and astrocytes, independently, pointed to deregulated clusters of proteins that are in agreement with the abnormal phenotypes I have described in primary cell cultures. Moreover GO analysis also indicated deregulated protein clusters that have been previously suggested by the study of other DM1 models. Such is the case for the deregulation of RNA localization within the cells, deregulated in *Mbnl1* KO brain, heart and muscle; and RNA splicing, deregulated to different extents in all CTG-expressing cells.

New perspectives arise after these interesting results, to tackle the contribution of the neuronal and astroglial abnormalities to DM1 CNS pathology. First, the late neuritogenesis defects of DMSXL neurons could result in abnormal synaptic connectivity. The assessment of the density and complexity of synapses, both *in vitro* and *in vivo*, would give a better insight of the cytoskeletal complexity of the neurons in DM1. Second, astrocyte defects of cytoskeletal

dynamics could further be investigated by assessing the polymerization and depolymerization rates of actin filament and tubulin microtubules. It is conceivable that the cytoskeletal dynamics defects of the astrocytes lead to functional abnormalities at the tripartite synapse, which may translate in abnormal synaptic activity in different regions of the DM1 brain. Thus synaptic activity should further be investigated in DMSXL brains, as well as the dynamics of astroglial processes around the synapse. Third, complementary models should also be analyzed to determine the reproducibility of the cellular abnormalities observed in DMSXL primary neurons and astrocytes. Particularly, CTG-expressing human neurons and astrocytes, either derived from induced pluripotent stem cells or from different cell lines, could give further insight on the impact of the expanded RNAs on human DM1 brain cells. We are currently waiting for the validation of our results in human cell models and/or human tissue samples, to submit our manuscript for publication.

Finally, it is important to understand the contribution of other brain cell types, like oligodendrocytes or microglia, to DM1 pathology. The analysis of the effect of the CTG expansion on oligodendrocytes physiology is currently being performed in the laboratory.

# CUG RNA toxicity is associated with adhesion and migration deficits in astrocytes and abnormal neuritogenesis in myotonic dystrophy.

Abbreviated title: **Astroglial adhesion and migration deficits and neuritogenesis impairment in DM1**

**DINCÃ Diana[1,2], SICOT Géraldine[1,2], HUGUET-LACHON Aline[1,2], CHUUON Cerina[3], GUERRERA Ida Chiara[3], GOURDON Geneviève[1,2] and GOMES-PEREIRA Mário[1,2]**

[1] Inserm UMR 1163, Laboratory of CTGDM, Paris, France.

[2] Paris Descartes – Sorbonne Paris Cité University, Imagine Institute, Paris, France.

[3] Proteomics Platform 3P5-Necker, Université Paris Descartes-Structure Fédérative de Recherche Necker, Inserm US24/CNRS UMS3633, Paris, France

**Corresponding author:** GOMES-PEREIRA Mário - mario.pereira@inserm.fr; GOURDON Genevieve – genevieve.gourdon@inserm.fr

Number of pages: 33

Number of figures: 8

Number of words for Abstract: 144

Number of words for Introduction: 649

Number of words for Discussion: 914

**Acknowledgements:** We are grateful to the personnel of CERFE (Centre d'Exploration et de Recherche Fonctionelle Expérimentale, Genopole, Evry, France) and LEAT (Laboratoire d'Experimentation Animale, Imagine Institute, Paris, France) for attentively caring for the mice. We thank the Imagine Cell Imaging platform for the useful help in microscopy acquisitions and analyses. This study was supported by grants from AFM-Téléthon (France, project grant 19920 to M.G.-P.), INSERM (France), Université Paris Descartes (France), as well as PhD fellowships from Ministère Français de la Recherche et Technologie (France, to D.M.D. and G.S.), AFM-Téléthon (France, to D.M.D. and G.S.)

# ABSTRACT

Expanded CTG repeats in myotonic dystrophy type 1 (DM1) brain lead to multiple neurological manifestations, but the contribution of each brain cell type to brain dysfunction is not fully understood. We have studied the functional consequences of expanded CUG RNAs in primary neurons and astrocytes derived from a mouse model of DM1. We identified higher RNA toxicity levels in astrocytes compared to neurons, illustrated by a more severe missplicing of candidate transcripts. CUG RNA toxicity in astrocytes was associated with defective adhesion, cytoskeletal dynamics and migration. Neurons, however, showed late neuritogenesis defects, further perturbed by co-culture with DM1 mouse astrocytes. In line with the cell phenotypes reported, a global proteomics revealed the deregulation of protein clusters that control cell adhesion and cytoskeletal dynamics in astrocytes; and proteins implicated in the development of membrane projections in neurons. Our results identified novel deregulated pathways and illustrate the role of different cell types in DM1 brain pathology

# INTRODUCTION

Myotonic dystrophy type 1 (DM1, OMIM160900) is a complex autosomal multisystemic disease, affecting many tissues including muscle, heart and brain, in both adults and children (Harper 2001). The impairment of central nervous system (CNS) has a devastating impact on the quality of life of DM1 patients and their families. CNS-related symptoms follow the general anticipation phenomenon of DM1, characterized by increased severity and decreased age of onset from one generation to the next (Harper et al. 1992). Adult DM1 patients show apathy, avoidant personality, executive dysfunction and visuoconstructive impairment, while childhood and juvenile patients show attention deficits, social anxiety, communication problems and learning difficulties. Congenital patients show the most severe CNS symptoms, including reduced intelligence quotient (IQ), learning disabilities, and delayed speech (Gourdon & Meola 2017). Brain imaging studies reveal venticulomegaly, cortical atrophy and decreased integrity of the white matter (Mutchnick et al. 2016; Yoo et al. 2017), as well as impaired brain connectivity (Serra et al. 2014; Serra, Mancini, et al. 2016) in regions related to motor and non-motor clinical features. In spite of reports of both white matter and grey matter abnormalities, we still do not know the contribution of different brain cell types to CNS dysfunction in DM1.

DM1 is caused by the abnormal expansion of a CTG trinucleotide in the 3' untranslated region (UTR) of the *DMPK* gene (Brook et al. 1992). Expansion length varies between 50-100 CTG repeats in the late onset form of the disease, up to >1000 CTG repeats in the congenital form: larger repeat sizes are associated with a more severe and earlier onset form of the disease (Harley et al. 1993). CUG-containing RNAs accumulate in the nucleus of the cells under the form of toxic RNA foci, which perturb the localization and function of RNA-binding mediators (Pettersson et al. 2015). Among the perturbed mediators, MBNL proteins are directly sequestered by the toxic foci, and CELF (CUG-BP and ETR-3-like factors) family members are upregulated, possibly through PKCα/βII hyperphosphorylation and stabilization (Sicot et al. 2011). In the CNS of DM1 patients both MBNL1 and 2 co-localize with CUG RNA foci (Jiang et al. 2004); while CELF1 and CELF2 proteins show heterogeneous levels of expression among individuals (Dhaenens et al. 2011), with a marked upregulation of CELF2 in the frontal cortex (Hernandez-Hernandez et al. 2013). The deregulation of these two families of mediators in DM1 perturbs several downstream cellular mechanisms, such as alternative splicing, gene transcription and translation, mRNA stability, alternative polyadenylation and localization within the cell, as well as miRNA metabolism

(Sicot et al. 2011; Chau & Kalsotra 2015; Gourdon & Meola 2017). However we do not know to which extent these mechanisms are deregulated in individual brain cell types. It is important to study DM1 brain pathogenesis with cell type resolution, to fully understand the contribution of different cell types to the overall brain dysfunction, and to help us design future means of therapeutic intervention in the CNS.

To investigate the molecular and cellular mechanisms perturbed by the CTG expansion in the CNS, in a cell-specific manner, we have used the DMSXL mice as a renewable source of neurons and astrocytes. The transgenic DMSXL mice carry more than 1500 CTG repeats in the human *DMPK* locus (Gomes-Pereira et al. 2007), associated with toxic RNA foci and missplicing, as well as myotonia, muscle weakness, and cardiac and respiratory abnormalities (Huguet et al. 2012; Panaite et al. 2013; Algalarrondo et al. 2015). The expression of toxic CUG expansions in the CNS leads to behavioral and electrophysiological abnormalities, associated with abnormal expression and phosphorylation of synaptic and glial proteins (Hernandez-Hernandez et al. 2013; Sicot et al. 2017). Toxic RNAs are observed in both neurons and astrocytes in DMSXL and DM1 brains, suggesting that different brain cell types are affected. However we do not know the impact of RNA toxicity in the cell physiology of neurons or astrocytes.

We combined molecular, cellular and global proteomics analyses and found higher CUG RNA toxicity in astrocytes than in neurons, associated with the deregulation of adhesion and cytoskeleton dynamics and with a negative impact of astrocytes on neuronal growth and physiology.

# MATERIALS AND METHODS

***Transgenic mice.***

DMSXL and DM20 and transgenic mice (>90% C57BL/6 background) carry 45 kb of human genomic DNA from a DM1 patient or a healthy control individual, respectively (Seznec et al. 2000; Gomes-Pereira et al. 2007). The DMSXL mice used in this study carry more than 1500 CTG repeats, while DM20 mice carry a short *DMPK* transgene with 20 CTG repeats. Transgenic DM20 status assessed as previously reported (Hernandez-Hernandez et al. 2013). DMSXL status was assessed by multiplex PCR using the oligonucleotide primers, which hybridize the *DMPK* transgene and the transgene integration site in the mouse *Fbxl7* gene: FBF (forward, TCCTCAGAAGCACTCATCCG), FBFBR (reverse, AACCCTGTATTTGACCCCAG) and FBWDR (reverse, ACCTCCATCCTTTCAGCACC). FBF and FBFBR primers hybridize the mouse *Fbxl7* gene, amplifying a sequence of 167 bp in WT mice. FBWDR primer hybridizes specifically the human *DMPK* sequence, generating a 236 bp PCR product. Sex of the mice was unknown. This project has been conducted according to the ARRIVE guidelines (Animal Research: Reporting *In Vivo* Experiments), with the authorization for animal experimentation n° 75 003 in the animal facility with the approval n°: B 91 228 107 both delivered by Prefecture de police and the French veterinary department.

***Human tissue samples.***

Human frontal cortex samples were collected from different laboratories: Dr. Yasuhiro Suzuki (Asahikawa Medical Center, Japan) and Dr. Tohru Matsuura (Okayama University, Japan). All experiments using human samples were approved by the Ethics Committees of the host institutions. Written informed consent specimen use for research was obtained from all patients. Information relative to patients was previously described (Hernandez-Hernandez et al., 2013a ; Sicot et al 2017).

***Primary astrocytes cell culture.***

Primary dissociated cell cultures of cortical astrocytes were prepared from postnatal day 1 WT and DMSXL mouse littermates. After carefully removing the meninges in Leibovitz´s L-15 Medium (11415049 – Life Technologies) supplemented with 30µM Glucose (49139 – Sigma-Aldrich), the cortices were mechanically dissociated and cultured for 2 weeks in

DMEM low glucose (31885-023Life Technologies, 31885-023), supplemented with 10% FBS and 0.05 mg/ml gentamycin (Life Technologies; 15710). All experiments were performed using 2 weeks-cultured primary astrocytes, unless stated otherwise.

***Primary neurons cell culture.***

Primary dissociated cell cultures of cortical neurons were prepared from embryonic 16.5 WT and DMSXL littermates. After carefully removing the meninges in Glucose-supplemented Leibovitz L-15 medium, the cortices were washed twice with Neuronal medium: Neurobasal-A (Life Technologies, 10888022), supplemented with 1X B27 supplement (Life Technologies, 17504044), 0.5 mM L-Glutamine (Life Technologies, 25030024), 1% antibiotic and antimycotic (Life Technologies, 15240-096). Cortices were then incubated 15 min in Neuronal medium containing Trypsin (Life Technologies, 25300096) and DNAseI (Sigma-Aldrich, 11284932001) and washed with Neuronal medium supplemented with 5% FBS. After mechanical dissociation, cells were washed twice and counted before plating in suitable dishes coated with Poly-D-lysine (Sigma-Aldrich, P6407) and Laminin (Sigma-Aldrich L2020) in Neuronal medium containing 5% FBS. Medium was changed 4 h after plating to Neuronal medium with 100μM AraC (Sigma-Aldrich, C6645-25MG) and without FBS to avoid astrocytes proliferation. Half of the medium was changed each 3-4 days.

***Fluorescent in situ hybridization (FISH) and Immunofluorescence.***

Primary cells were fixed at 2 weeks *in vitro* for 15 min in 4% PFA (VWR, J61899.AP) and ribonuclear inclusions were detected using a 5'-Cy3-labelled (CAG)5 PNA probe, as previously described (Huguet et al. 2012). Immunofluorescence (IF) combined with fluorescent in situ hybridization (FISH) was performed as previously described (Hernandez-Hernandez et al. 2013). Primary antibodies and dilutions used are the following: Tuj1/β-tubulinIII (Covance, PRB-435P), GFAP (Dako cytomation Z0334), MBNL1 and MBNL2 (Gift from G. Morris), Vinculin (Sigma-Aldrich V9131), GM130 (BD laboratories 610822) and Pericentrin (Covance, PRB432C).

***Microscope imaging and image analysis.***

Images were acquired with a Zeiss ApoTome 2 fluorescent microscope or a Leica SP8 SMD confocal microscope (x63 and x40 objectives). RNA foci were counted in 3D stacks using the

Spot Detector plugin of the ICY bioimageanalysis open source program (http://icy.bioimageanalysis.org). MBNL1 and MBNL2 nucleo-cytoplasmic ratio was quantified on confocal images using nuclear DAPI or MBNL signal to create a mask of the nucleus and cytoplasm respectively, and to measure the MBNL1 and MBNL2 intensity inside the mask. Focal adhesions formation was quantified as previously described (Bruyère et al 2015), by measuring the number of Vinculin-rich clusters at 3 h post plating on confocal z stack projections, after background subtraction using rolling ball method, gamma adjustment of 1.4 and analysis of particles between 0.1 and 40$\mu m^2$. IF and FISH images were treated with Fiji - ImageJ software (Schindelin et al. 2012) to create the figures.

***RNA isolation, cDNA synthesis and RT-PCR analysis***

RNA extraction was performed with the RNeasy Mini kit (QIAGEN, ref. 74104) following the manufacturer's protocol, with an additional DNAse digestion step (RNase-Free DNase Set, QIAGEN, ref. 79254) after the first wash with RW1 buffer. RNA concentration was assessed using the NanoDrop and RNA quality was verified by electrophoresis on an agarose gel. cDNA synthesis and semi-quantitative reverse-transcriptase PCR analysis of alternative splicing were performed as previously described (Hernandez-Hernandez et al. 2013; Sicot et al. 2017), using the following oligonucleotide primers. *Ank2* exon 17: GAACGTGGTTCTCCGATTGT, CGTCTCTGGGGGTATGTCAG; *Clasp1* exons 23-25: CGCTAAAGTGGTTTCACAGTCCC, TTCTGCTACATCCTCAGTCTGCCG; *Mbnl1* exon 5: TGGTGGGAGAAATGCTGTATGC, GCTGCCCAATACCAGGTCAAC; *Mbnl2* exon 5: CTTTGGTAAGGGATGAAGAGCAC, ACCGTAACCGTTTGTATGGATTAC; *Tanc2*: exon 23: GCCATGATTGAGCATGTTGACTACGT, CCTCTTCCATCAGCTTG CTCAACA; *Mapt* exons 2 and 3: CACTCTGCTCCAAGACCAAG, TGTCTCCGATGCC TGCTTC; *Mapt* exon 10: CTGAAGCACCAGCCAGGAGG, TGGTCTGTCTTGGCTTT GGC; Polr2a: GGCTGTGCGGAAGGCTCTG, TGTCCTGGCG GTTGACCC.

***Quantitative RT-PCR.***

Human *DMPK*, murine *Dmpk* and *18S* internal control transcripts were quantified in a 7300 Real Time PCR System (Applied Biosystems) using Power SybrGreen detection (Thermo Scientific, 4367659) using oligonucleotide primers and conditions previously described (Huguet et al. 2012).

***Western blots***

Proteins from primary cells and mouse and human brain tissues were extracted using RIPA buffer (Thermo Scientific, 89901) supplemented with 0,05% CHAPS (Sigma, C3023), 1x complete protease inhibitor (Sigma-Aldrich, 04693124001) and 1x PhosSTOP phosphatase inhibitor (Sigma 04906845001). Protein concentrations were determined using the Pierce BCA Protein Assay Kit (Thermo Scientific, 23227). Between 10 and 40ug proteins were mixed with 2X Laemmli Sample Buffer (Sigma, S3401), denatured for 5 minutes at 95˚C and resolved in 10% TGX Stain-Free polyacrylamide gels (Bio-Rad 1610183). After electrophoresis gels were activated for 2 minutes under UV light, proteins were transferred onto Nitrocellulose membranes using Trans-Blot® Transfer System (Bio-Rad) and total protein on the membrane was imaged using the ChemiDoc Imaging System (Bio-Rad). Membranes were then blocked in 2.5-5% Blotto non-fat dry milk (Santa Cruz Biotech; sc2325) in 1x TBS-T (10mM Tris-HCl, 0,15M NaCl, 0,05% Tween 20) during 1h at room temperature (RT) and incubated with the primary antibody over night at 4˚C. After three washes in TBS-T membranes were incubated with IRDye® 800CW donkey anti-rabbit (LI-COR Biosciences, P/N 926-32213) or 680RD donkey anti-mouse (LI-COR Biosciences, P/N 926-68072) for 1h at RT, washed three times and imaged using LI-COR Odyssey ® CLx Imaging System. Band intensity was quantified using Image Studio Lite.

Primary antibodies: CELF1 (Milipore, 05-621), CELF2 (Sigma-Aldrich, C9367).

***Impedance-based real-time monitoring of cell adhesion and growth***

Cell population adhesion and growth was monitored using the *xCELLigence* RTCA MP system (ACEA Biosciences Inc), which measures the electrical impedance of the cells in real time, translated into a cell index proportional to the number, surface or adhesion strength of the plated cells. Primary neurons (200,000 cells/well) were plated onto Poly-D-lysin and Laminin coated E-plates (Ozyme, 5232368001) while primary astrocytes (20,000 cells/well) were plated on uncoated E-plates. After a 30-min settling of the cells at RT, impedance was measured each 5 minutes during the first 8 h and each 15 min for the following 72 h, inside the incubator.

***FACS analysis of astrocytes cell cycle***

Primary astrocytes were arrested in $G_0$ by completely removing the serum from the culture medium for 24 h. After cell cycle release in medium containing 5% of FBS, cells were incubated with 10 μM Bromodeoxyuridine (BrdU) (Euromedex, NU-122S) for 1 h, trypsinized, fixed O/N in 70% ethanol at -20˚C, and stained with antiBrdU-FITC (BD Horizon, 347583) and 3 μM propidium iodide (PI) (Sigma, P4170), before FACS detection of BrdU-FITC and PI in 10,000 cells per embryo. Three different biological replicates were analyzed per genotype. Cell cycle phases were considered as follows: $G_1$-phase cells are BrdU negative with low PI staining (200 intensity units), S-phase cells are BrdU positive and show a range of low to high PI intensity (200 to 400 intensity units) and $G_2$/M cells are BrdU negative with high PI intensity (400 intensity units).

***FACS analysis of astrocytes death***

Cell death was analyzed in astrocytes at 3 days post plating after O/N incubation with DMSO (solvent control) or 0.5μM Staurosporine (Euromedex, LS9300-A). Cells were trypsinized, counted and $10^6$ cells were stained with a mix of 5% Annexin V-FITC (BD Horizon, 556547) to detect apoptotic cells, PI to detect necrotic cells and 2.5 % Cd11b-V450 (BD Horizon, 560456) to exclude possible microglia contamination. Staining was performed for 15 min, prior to FACS analysis of 10,000 cells per embryo. Six different biological replicates were analyzed per genotype. The percentage of AnnexinV-positive, PI-positive WT and DMSXL astrocytes (negative for Cd11b staining) was analyzed in DMSO and Staurosporin conditions.

***Videomicroscopy monitoring of cells dynamics***

Primary astrocyte adhesion and spreading was monitored using the IncuCyte Zoom video-microscope (Essen BioScience) after seeding 20,000 cells/well in 96-wells plates and taking phase-contrast pictures every 45 minutes. Cell confluence was determined using the IncuCyte ZOOM basic analysis method. Cell surface was measured by manual tracing. Cell number was counted manually using Image J. Experiments were performed in triplicate. Astrocytes migration was assessed using the Cell Migration Assay kit and migration module of the IncuCyte followed by manual tracking of the astrocytes using Fiji Manual Tracking plugin and quantitative analysis of speed and mean square displacement, using DiPer macro on Microsoft Office Excel, as previously described (Gorelik & Gautreau 2014). The neuritogenesis of primary neurons was monitored in 30,000 neurons/well, in 96-well plates,

using the Neurotrack module of the IncuCyte on phase-contrast images for homogeneous neuronal cultures and on red-fluorescent channel images for co-culture experiments with the unmarked astrocytes. Pictures were taken every 3 hours.

***Primary cells co-culture and imaging.***

Co-cultures of neurons and astrocytes were performed as previously described (Sicot et al 2017). Briefly, primary neurons were cultured using the above protocol, plated at 30,000 cells/well and infected 4 h after plating (MOI=3) with NeuroLight Red Lentivirus (Essen BioScience, 4584), encoding the mKate fluorescent protein under the Synapsin-1 promoter, in serum-free Neuronal medium. The following day neurons are washed with Neuronal medium. Mouse primary astrocytes, cultured 2 weeks prior to neurons, were plated on top at a density of 50,000 cells/plate. Fluorescent images of co-cultures were acquired every 3 h for a total of 7 days *in vitro* (*DIV*). NeuroTrack analysis module of the IncuCyte Zoom video-microscope was used to quantify neurite length and arborization.

***Label-free quantitative LC-MS proteomics analysis of homogeneous primary neurons and primary astrocytes cultures***

Global proteomics analysis of homogeneous cultures of primary neurons and astrocytes at 2 weeks in culture were performed as previously described (Andreev et al. 2012) using the high resolution high mass accuracy mass spectrometer LTQ Orbitrap. 3 WT and 3 DMSXL littermates were studies for each cell type and significance analysis was performed with the paired t-test. Significantly deregulated proteins of each cell type ($p<0.05$) were used to perform a Gene Onthology (GO) enrichment analysis using the functional annotation tool Database for Annotation, Visualization and Integrated Discovery (DAVID) v.6.7 (http://david.abcc.ncifcrf.go) (Huang et al. 2009) followed by over-representation clustering using GO-Elite software (Zambon et al. 2012) to report sets of GO sets of non-overlapping terms. Significant GO terms were identified at a FDR <0.05.

***Statistical analysis.***

Statistical analyses were performed with Prism (GraphPad Software, Inc) and data are presented as mean ± standard error of the mean (±SEM) or as Tukey box-and-wiskers plots. Chi-square test was used to compare categorical variables between two groups. After performing a normality test on the numeric variables, we used two-tailed Student's t-test for

parametric data and Mann-Whitney U test for non-parametric data, when two groups were compared. When 3 or more groups were compared we performed a one-way ANOVA or Repeated-measures ANOVA on parametric data, or Kruskal Wallis test on non-parametric data. If statistical significance was achieved, we performed post-test analysis to account for multiple comparisons.

# RESULTS

## DM1 RNA toxicity is more pronounced in astrocytes than in neurons

To assess the impact of the DM1 CTG expansion on different brain cell types, we derived primary neurons and astrocytes from the frontal cortex of DMSXL mice and assessed the accumulation of expanded *DMPK* transcripts in nuclear foci (**Fig. 1A**). Nuclear foci were present in a significantly higher percentage of DMSXL astrocytes (98.6 % cells) compared to the DMSXL neurons (72.8% cells)($p<0.0001$, $\chi^2_{(1, N=342)}=54.79$). Moreover, the mean number of foci per cell was 3-fold higher in astrocytes than in neurons ($p<0.0001$, Mann Whitney $U=3496$, $n_{Astro}=217$, $n_{Neur}=125$) (**Fig. 1B).** This higher abundance of toxic RNA foci was associated with a 4- to 12-fold higher expression of the human *DMPK* transgene in DMSXL astrocytes relative to DMSXL neurons ($p<0,0001$, 2-way ANOVA $F_{(1, 12)}=399.3$) at 6, 12 and 30 days *in vitro* (*DIV*). Interestingly, the *DMPK* transgene expression profile followed the endogenous *Dmpk* gene in both types of brain cells (**Fig. 1C**), with a peak of expression at 12 *DIV*.

To investigate the impact of toxic RNA accumulation in brain cells, we assessed the sequestration of MBNL proteins by the nuclear foci and studied the expression of CELF1 and CELF2 in both cell types. Both DMSXL neurons and astrocytes showed MBNL1 and MBNL2 co-localization with expanded CUG foci (**Fig. 2A, 2B**). Surprisingly, the expression of expanded *DMPK* transcripts was not associated with abnormal levels of CELF1 and CELF2, as revealed by western blot quantification of CELF1 and CELF2 protein levels. No significant difference was observed between DMSXL and WT neurons (CELF1 $p=0.219$; CELF2 $p>0.9999$, Wilcoxon matched-pairs signed rank test) or DMSXL and WT astrocytes (CELF1 $p=0.109$; CELF2 $p=0.844$, Wilcoxon matched-pairs signed rank test) (**Fig. 2C, 2D**).

We explored the molecular consequences of MBNL sequestration in individual brain cell types through the analysis of candidate alternative splicing exons in primary DMSXL neurons and astrocytes. RT-PCR analysis showed that splicing deregulation was more pronounced in DMSXL astrocytes than in DMSXL neurons, relative to WT control cells (**Fig. 2E**), including a marked inclusion of the exon 5 of *Mbnl1* and *Mbnl2*. Since this exon regulates the nuclear localization of the MBNL proteins (Tran et al. 2011), we studied the impact of the missplicing on the intracellular distribution of MBNL1 and MBNL2 between nucleus and cytoplasm in DMSXL astrocytes. In line with the exon 5 missplicing, we found a significant increase in the nuclear localization of MBNL2 in DMSXL astrocytes relative to WT controls (**Fig. 2F**)

(MBNL2 $p<0.0001$, Mann Whitney $U=169$, $n_{WT}=26$, $n_{DMSXL}=44$). MBNL1 distribution remained, however, unchanged between genotypes (MBNL1 $p=0.224$, Mann Whitney $U=571$, $n_{WT}=38$, $n_{DMSXL}=36$).

Together, these data indicate that DMSXL astrocytes express higher levels of expanded CUG-containing *DMPK* transcripts, show more pronounced accumulation of toxic RNA foci that co-localize with MBNL proteins, and exhibit more severe spliceopathy relative to DMSXL neurons.

## Primary DMSXL astrocytes show abnormal population dynamics.

To assess the consequences of RNA toxicity on cell physiology, we studied the global population dynamics of DMSXL neurons and astrocytes through the monitoring of growth using the xCELLigence Real-Time Cell Analysis technology. xCELLigence uses the electrical impedance of the cells to provide real-time, non-invasive, quantitative readouts of the adhesion, proliferation and attachment of the cells to the substrate (Atienza et al. 2005). While primary DMSXL neurons displayed the same population growth dynamics as WT controls over 72 hours in culture ($p=0.4858$, 2-way RM ANOVA $F_{(1, 10)}=0.524$), primary DMSXL astrocytes showed a significantly lower cell index compared to WT cells ($p<0.0001$, 2-way RM ANOVA $F_{(1, 10)}=113.8$) (**Fig. 3A**). The lower cell index revealed a growth defect of DMSXL astrocytes, which could be accounted for by proliferation problems, increased cell death, and/or abnormal adhesion and spreading. We investigated the contribution of each one of these factors to the global phenotype of DMSXL astrocytes.

To analyze the contribution of cell proliferation we synchronized primary astrocytes by serum deprivation over 24 h. Following the addition of 5% FBS and cell cycle re-entry, we performed a bromodeoxyuridine (BrdU) incorporation and detection assay, combined with propidium iodide (PI) counterstaining. Both DMSXL and WT astrocytes showed similar distributions in different phases of the cell cycle ($p=0.2428$, 2-way ANOVA $F_{(1, 12)}=1.51$), excluding the hypothesis of defective cell proliferation in DMSXL astrocyte cultures (**Fig. 3B**). We next tested the contribution of cell death by quantifying AnnexinV binding and PI incorporation, indicators of early apoptotic and late cell death, respectively. FACS analysis revealed no difference between the number of AnnexinV- and PI-positive cells between DMSXL and WT astrocytes, in both basal conditions and upon chemical induction of cell death by staurosporin (Genotype $p=0.747$, 2-way ANOVA $F_{(1, 5)}=0.116$; Treatment $p=0.0002$, 2-way ANOVA $F_{(1, 5)}=89.54$ ) (**Fig. 3C**).

In conclusion, the pronounced molecular features of RNA toxicity in DMSXL astrocytes are associated with an overall defect in growth dynamics, with no abnormal proliferation or increased cell death.

## Primary DMSXL astrocytes exhibit abnormal adhesion and spreading

Finally, we tested if the lower DMSXL astrocyte cell index is caused by adhesion and/or spreading defects. To this end we used live cell videomicroscopy to monitor the adhesion and growth of DMSXL astrocytes. Interestingly, even if the same number of cells were initially plated and counted 45 min after plating ($p=0.1924$, unpaired t test $t_{(29)}=1.335$, $n_{WT}=15$, $n_{DMSXL}=16$ images ), the DMSXL astrocytes covered a smaller surface of the culture dish, when compared to WT controls (**Fig. 4A**). This difference was detected from an early time point (45 min after plating)($p=0.0286$, Mann-Whitney $U=0$, $n_{WT}=n_{DMSXL}=4$ embryos) and persisted through the following hours ($p=0.0048$, 2-way RM ANOVA $F_{(1, 6)}=18.93$) (**Fig. 4B**), suggesting defective adhesion and spreading. To verify if the expression of a short *DMPK* transgene could contribute to the adhesion and spreading defects of DMSXL astrocytes we have also monitored astrocytes derived from non-affected DM20 control mice (Seznec et al. 2001). DM20 astrocytes showed no difference in adhesion and spreading compared to WT cells, neither at 45 minutes ($p=0.310$; unpaired t test $t_{(12)}=1.061$) nor at later time points ($p=0.847$, 2way RM ANOVA $F_{(1, 12)}=0.039$) (**Fig. 4C**).

Given that the same number of DMSXL astrocytes covered less surface than WT cells, we assessed if the difference is due to a defective spreading of astrocytes attached to the culture dish. To this end we focused on individual cells already attached 45 minutes after plating, and measured changes in the cell surface over time. The analysis revealed significantly smaller size and slower cytoplasm spreading of individual DMSXL astrocytes from 90 min up to 12 h of culture, compared to WT controls ($p<0.0001$, 2-way RM ANOVA, $F_{(1, 134)}=24.82$) (**Fig. 4D**).

Since cell spreading is the combined result of continuous focal adhesions (FAs) assembly and cytoskeleton reorganization (Khalili & Ahmad 2015), we have measured FA assembly by immunofluorescent staining of vinculin clusters, which serve as structural link between the astrocyte actin cytoskeleton and the extracellular matrix (ECM). Cell surface measurement based on the actin fluorescent signal confirmed reduced DMSXL astrocyte surface at 3 h of culture (**Fig. 4E**) ($p=0.0003$, Mann Whitney $U=143331$, $n_{WT}=538$, $n_{DMSXL}=608$). More interestingly, the quantification of vinculin clusters indicated a significantly lower number of

FAs per cell (p=0.014, unpaired t test $t_{(22)}$=2.656, $n_{WT}$=12, $n_{DMSXL}$=12 images), suggesting defective establishment of FAs.

Taken together these results indicate that the growth dynamics defect of DMSXL astrocytes is associated with defective adhesion and cell spreading, in response to the CTG repeat expansion.

## Cytoskeleton reorientation and cell migration are also affected in DMSXL astrocytes

Defects in the control of cytoskeleton dynamics and cell adhesion are usually associated with abnormal cell polarization and motility (Webb et al. 2002) in different cell types, including astrocytes (Etienne-Manneville 2006). We tested if decreased FAs in DMSXL astrocytes affected cell migration in a wound-healing assay, in which cells undergo polarization perpendicularly to the wound, through the reorientation of the Golgi apparatus and the centrosome. During this process the centrosome relocates between the nucleus and the edge of migration to act as a microtubule-organizing center (MTOC), before the cell engages in migration (Etienne-Manneville 2006). We monitored DMSXL astrocytes reorientation through immunofluorescence staining of the Golgi apparatus and centrosome, and found a mild but significant defect in DMSXL astrocytes polarization compared to WT cells, 8 h after the wound (**Fig. 5A**) (p=0.0004, $\chi^2_{(1, N=5118)}$=12.71). We examined the impact of the defective cell reorientation on the migration pattern by time-lapse videomicroscopy and tracking of the migration path of individual astrocytes. DMSXL astrocytes migrated at a higher speed over 54 h of wound closure (p=<0.0001, unpaired t test $t_{(76)}$=4.172, $n_{WT}$=39, $n_{DMSXL}$=39 cells) and showed a higher mean square displacement (p<0.0001, 2-way RM ANOVA, $F_{(1, 3876)}$=760.4), indicating that they explored more surface area over time to reach the same final point, relative to WT astrocytes (**Fig. 5B**).

In conclusion, the detailed analysis cell adhesion phenotype revealed abnormalities in the spreading, polarization and migration of DMSXL astrocytes, likely mediated by the impact of the CTG expansion on the formation of focal adhesions and the fine control of the cytoskeleton dynamics.

## Primary DMSXL neurons show mild neuritogenesis defects.

Global population analysis of primary neurons growth by xCELLigence technology did not show an overall difference between DMSXL and WT neurons over 72 h of culture (**Fig. 3A**).

However, xCELLigence impedance measurements do not allow monitoring the maturation of individual neurons, and the branching of fine neurites. To further investigate the influence of the toxic RNA expansion on neuronal physiology we monitored primary neuron growth and neuritogenesis by time-lapse videomicroscopy, over longer periods of time. Bright field tracking of the neurite growth through the first 7 *DIV* revealed that DMSXL neurites grew 18.8% slower than WT neurites (p=0.0063, unpaired t test $t_{(3.96)}$=5.281, $n_{WT}$=3, $n_{DMSXL}$=3 embryos) (**Fig. 6A**), which translated into significantly reduced neurite length from 4.5 *DIV* onwards (genotype p=0.122, 2-way ANOVA $F_{(1, 2)}$=6.756; Bonferroni's multiple comparison $p_{4DIV}$=0.185, $p_{4,5DIV}$=0.023, $p_{5DIV}$=0.003, $p_{5,5DIV}$=0.0002, $p_{6\text{-}7DIV}$< 0.001). The DMSXL defect in late neuritogenesis was confirmed by the analysis of fluorescently labeled primary neurons, expressing mKate2 fluorescent protein under the Synapsin promoter (**Fig. 6B**). Monitoring of fluorescent neurites revealed a significant 25.8% reduction in the growth rate of DMSXL neurons compared to the WT controls (p=0.0061, unpaired t test $t_{(3.68)}$=5.681, $n_{WT}$=3, $n_{DMSXL}$=3 embryos).

These results indicate that CUG RNA toxicity in primary DMSXL neurons has a negative impact on neurite arborization at late time points in culture.

## DMSXL astrocytes enhance the neuritogenesis defects of the primary neurons.

We then tested if DMSXL astrocytes perturbed neuronal development and physiology. To this end we monitored neuritogenesis of DMSXL and WT neurons co-cultured with astrocytes of either genotype (**Fig. 7A**). Fluorescent time-lapse videomicroscopy of neurite growth revealed a significant reduction of 30.3% in DMSXL/DMSXL co-cultures, relative to WT/WT controls (p<0,0001, $t_{(84)}$=4.589, Holm-Sidack's multiple comparisons test), confirming the defective neuritogenesis phenotype of DMSXL neurons in the presence of astrocytes of the same genotype (**Fig. 7B**). More importantly, we found a negative impact of DMSXL astrocytes on the the physiology of both DMSXL and WT neurons, which resulted in significant lower neurite growth rates (WT neurons p=0.0129 $t_{(84)}$=3.032; DMSXL neurons, p=0.0881 $t_{(84)}$=2.034; Holm-Sidack's multiple comparisons test). Interestingly, the difference in neuritogenesis between DMSXL and WT neurons was abolished in the presence of DMSXL astrocytes (WT astrocytes, p=0.0369 $t_{(84)}$=2.554; DMSXL astrocytes p=0.1234 $t_{(84)}$=1.556; Holm-Sidack's multiple comparisons test) (**Fig. 7B**), corroborating the dominant effect of DMSXL astrocytes on neurite projection development.

To conclude, CUG-expressing astrocytes affect the neuronal development and physiology, through defective neuroglial interplay.

## Proteomic changes suggest deregulation of cell adhesion and cytoskeleton dynamics in DMSXL astrocytes and cell polarity in DMSXL neurons.

To determine the molecular pathways deregulated in each brain cell type in response to the CTG trinucleotide expansion we performed a global proteomics analysis to identify protein expression changes in primary DMSXL neurons and astrocytes. Overall, the primary DMSXL astrocytes showed a higher number of significantly deregulated proteins (376 proteins) compared to the primary DMSXL neurons (199 proteins) (paired t-test, $p<0.05$). We used the Gene-Elite tool (reference) to perform a gene ontology (GO) enrichment analysis of over-represented "biological processes" and "cell compartments. The results indicated that proteins involved in cell adhesion mediated by integrins and in actin-filament based processes were among the top 10 non-redundant clusters of deregulated proteins in DMSXL astrocytes. Interestingly, deregulated proteins were predominantly associated with actin-based structures, like filopodia and microvilli, as well as cell-cell and cell-substrate junctions. These results were coherent with the adhesion, spreading, repolarization and migration phenotypes of DMSXL astrocytes (**Fig. 8A**). Primary DMSXL neurons showed enrichment for the deregulation of proteins involved in the regulation of cell polarity, neuron projection development and intracellular transport, which were predominantly located in compartments like the dendritic spines and shafts. Similarly, changes in DMSXL neuron proteome likely contribute to neuritogenesis defects (**Fig. 8B**).

Both astroglial and neuronal proteome are deregulated in response to the CTG expansion and global proteomics analysis revealed relevant clusters of proteins related to the cellular abnormalities observed in DMSXL neurons and astrocytes.

# DISCUSSION

In the present study we have investigated the effect of DM1 toxic RNAs on neuronal and astroglial cell physiology. Our results indicate that RNA toxicity is more pronounced in astrocytes than in neurons, as illustrated by the higher foci content and more severe splicing abnormalities. As a consequence DMSXL astrocytes show adhesion, spreading, reorientation and migration defects, while DMSXL neurons show late neuritogenesis defects further aggravated by the presence of DMSXL astrocytes. Global proteomics analysis indicated the abnormal expression of proteins involved in adhesion and cytoskeleton dynamics in DMSXL astrocytes, and in the regulation of neurite projection in DMSXL neurons. In both cases, protein expression changes are in line with the cellular phenotypes described.

Both DMSXL neurons and DMSXL astrocytes show nuclear CUG foci accumulation and sequestration of MBNL proteins, as previously reported in DMSXL mice (Hernandez-Hernandez et al. 2013; Sicot et al. 2017) and human DM1 brains (Jiang et al. 2004; Michel et al. 2015). Interestingly, the presence and density of the toxic RNA foci is higher in astrocytes compared to neurons, in association with a higher expression of the *DMPK* transgene. As a consequence, splicing abnormalities of candidate transcripts are more pronounced in DMSXL astrocytes than in DMSXL neurons. This is particularly true for MBNL-dependent alternative splicing events, such as *Clasp1*, *Tanc2* and *Mbnl1*. The marked splicing switch in the exon 5 of *Mbnl2* is associated with increased nuclear localization of MBNL2 in the nucleus of the astrocytes, consistent with the involvement of this exon in protein nuclear localization, and demonstrating the functional impact of the missplicing event. Interestingly, most of the studied transcripts show a different splicing profile between WT neurons and WT astrocytes, illustrating the differential regulation of mRNA isoforms in these two brain cell types. However the functional implication of this variation remains to be further investigated.

CTG repeat expansion toxicity leads to marked astrocytes phenotypes, including decreased adhesion, cytoskeletal spreading, reorientation and migration defects, without influencing proliferation or cell death. Importantly, adhesion defects are not present in astrocytes overexpressing short *DMPK* transcripts. These results demonstrate the causative role of the CUG RNA repeat expansion in the development of these cell abnormalities.

Cell adhesion *in vitro* starts with the sedimentation and electrostatic attachment of the round cell to the extracellular matrix, followed by a flattening and attachment of the cell to the ECM via the integrin receptors, which cluster and activate Rho GTPase family members

to induce the assembly of focal adhesions (FAs) and actin stress fibers, leading to stable adhesion and cell spreading (Khalili & Ahmad 2015). Correct establishment of FAs is thus essential to provide mechanical anchorage and intracellular signaling for proper cell connectivity and cell migration (Wickstrom et al. 2011; Tang & Gerlach 2017) and the low number of FAs in DMSXL astrocytes could contribute to the migration abnormalities. FAs formation depends on the correct clustering of integrins, and abnormal integrins expression and localization has been linked to neurological abnormalities such as anxiety, stress, spatial and working memory defects and autism spectrum disorder (Park & Goda 2016). Moreover, actin cytoskeleton motility drives fast remodeling of astrocyte processes at the tripartite synapse, controlling the synaptic plasticity, and thus learning and memory, through a dynamic neuroglial interplay (Haber et al. 2006; Perez-Alvarez et al. 2014). Abnormal cytoskeleton dynamics of the astrocytes can therefore impact the physiological functioning of the tripartite synapse.

Primary DMSXL neurons show late neuritogenesis defects associated with milder signs of RNA toxicity, in agreement with previous studies reporting defective neuronal differentiation induced by the CTG expansion (Quintero-Mora 2002). The establishment and maintenance of neuronal cell architecture is essential for the correct functioning of the CNS. Indeed, defects in dendritic complexity and synaptic changes have been linked to behavior and cognitive disorders (Marchisella et al. 2016; Kulkarni & Firestein 2012), and could therefore pay a role in the etiology of CNS dysfunction in DM1

Interestingly, DMSXL neuritogenesis is further perturbed by the presence of DMSXL astrocytes suggesting marked abnormalities in neuroglial interplay in DM1 brain cells. Previous studies have strongly suggested astroglial dysfunction in DM1 brains. We have previously described abundant RNA foci accumulation in the cortical astrocytes of human patients and DMSXL mice (Hernandez-Hernandez et al. 2013), as well as in the Bergmann glia of the cerebellum (Sicot et al. 2017). The expression of toxic CUG RNA is astrocytes results in downregulation of the glial GLT1 glutamate transporter, which affects neuronal activity *in vivo*, and results in increased glutamate neurotoxicity (Sicot et al. 2017). The impact of astrocytes on defective neuronal arborization is also observed in FXS (FXS), where *Fmr1* loss of function in astrocytes induces abnormal dendritic morphology of WT hippocampal neurons in co-cultures (Jacobs & Doering 2010; Yang et al. 2012). Compromised astrocyte function also impacts neuronal transmission in Huntigton's disease (HD) and amyotrophic lateral sclerosis and frontotemporal dementia (ALS/FTD), where decreased expression of the glial specific glutamate transporter GLT1 leads to abnormal

neuronal excitability and excitotoxicity (Jiang et al. 2016; Howland et al. 2002; Higashimori et al. 2016). In conclusion, abnormal neuroglial interplay in DM1 could exacerbate defective neuritogenesis of neurons, and contribute to the neurological symptoms of the disease.

An unbiased global proteomics approach revealed that the astrocyte defects in adhesion and cytoskeleton dynamics are accompanied by abnormal expression of integrin- and actin-related proteins, while primary neurons abnormal neuritogenesis is linked to defective expression of cell polarity and neurite projection proteins. Detailed investigation of the implication of these molecular events in specific brain cell types will shed light into the brain cell-specific deregulated pathways. The integrated comparison with results of other global approaches, such as RNAseq, will allow a better understanding of the mechanisms of DM1 CNS pathology and pave the way for the identification of pharmacological targets for future therapies.

# FIGURES and LEGENDS

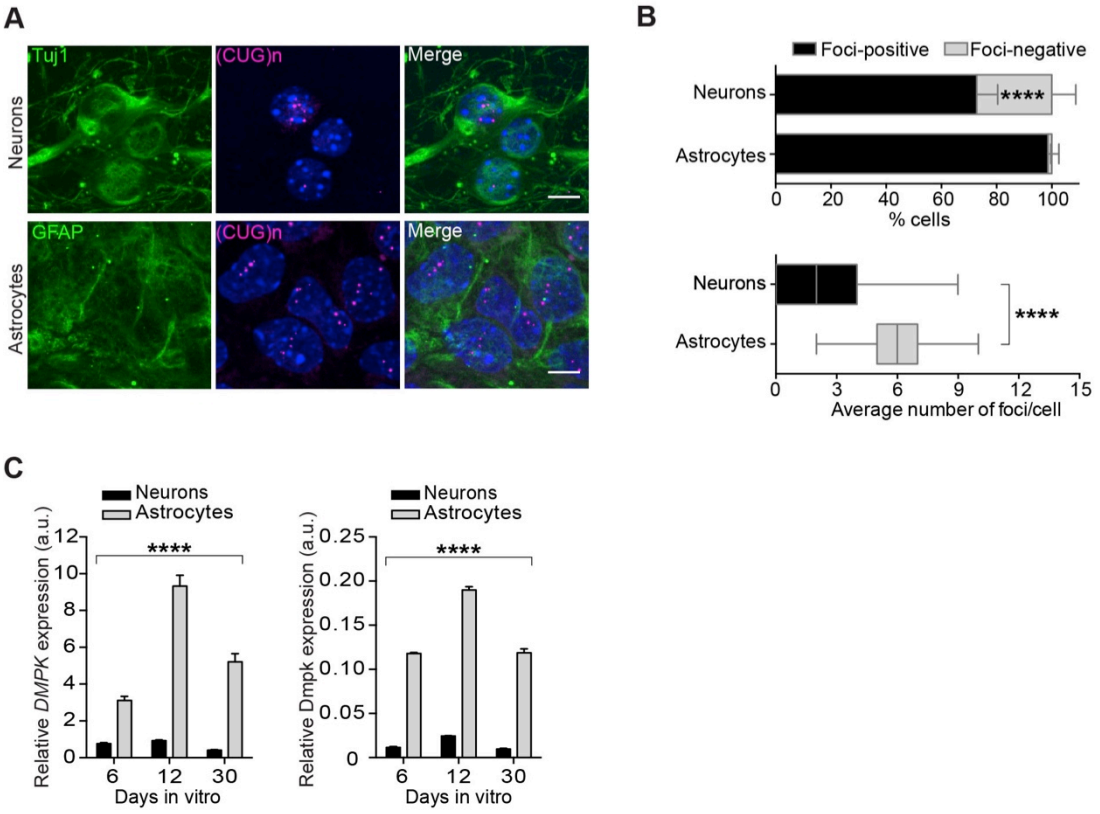


**Figure 1. DMSXL primary astrocytes show higher toxicity of expanded CUG transcripts compared to DMSXL neurons.**

**(A)** Representative FISH and immunofluorescence (IF) detection of expanded CUG RNAs (magenta) in Tuj1-expressing primary DMSXL neurons (green) and GFAP-expressing DMSXL astrocytes (green). The scale bar represents 10 μm. **(B)** Quantification of the percentage (± SEM) of primary DMSXL neurons and astrocytes exhibiting RNA foci in the nucleus and the average number of foci per nucleus in both cell types ($n_{Astro}$=217, $n_{Neur}$=125). **(C)** Expression of human *DMPK* transgene and mouse endogenous *Dmpk* relative to *18S* rRNA internal control in primary DMSXL neurons and astrocytes at 6, 12 and 30 days *in vitro*. Data represent means ± SEM, n=3 per group (**** p<0.0001).

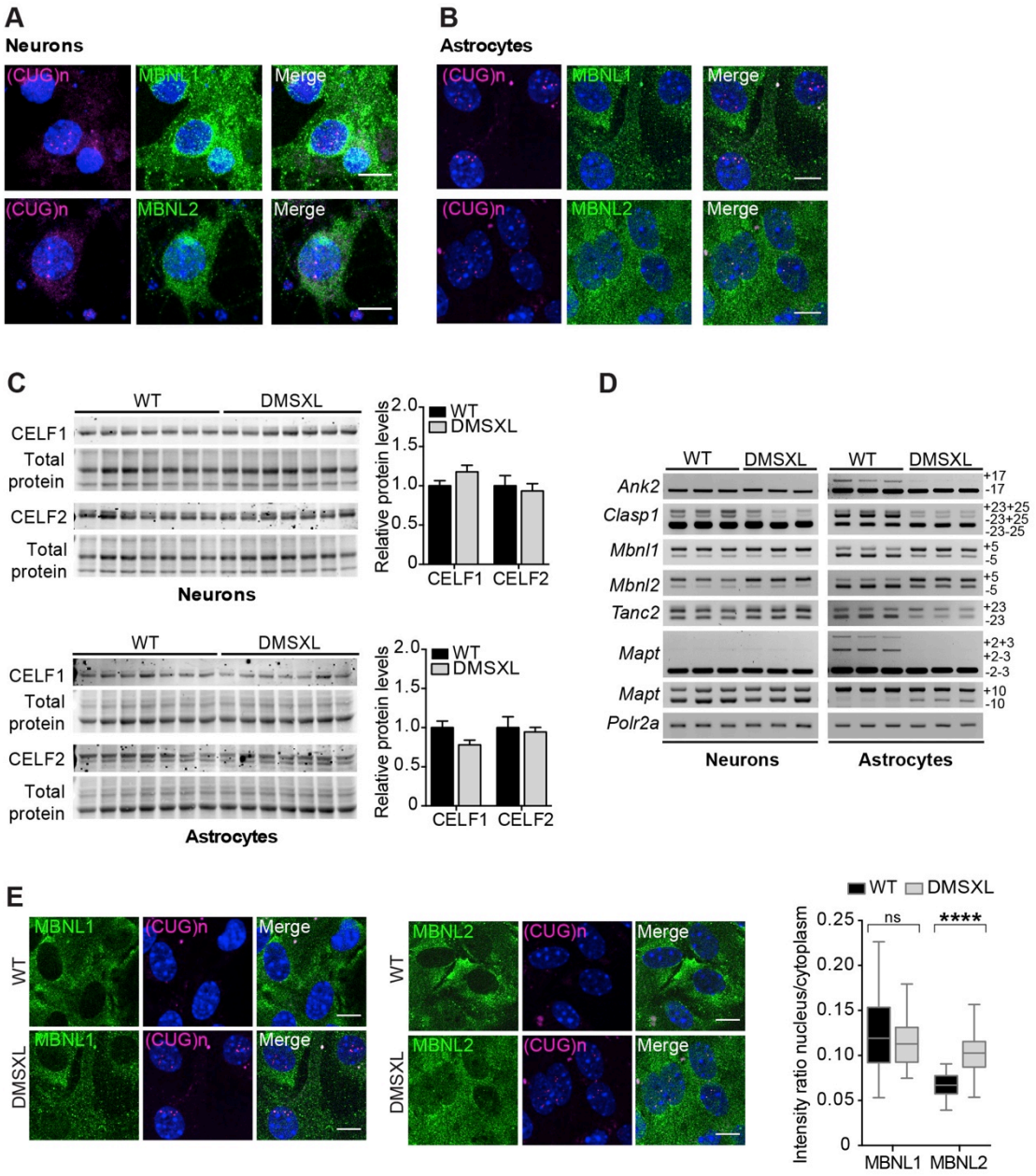


**Figure 2. Both DMSXL neurons and astrocytes show sequestration of MBNL proteins and no deregulation of CELF proteins, in association with splicing abnormalities.**

**(A)** FISH of RNA foci (magenta) combined with IF detection of MBNL1 and MBNL2 (green) in primary neurons and **(B)** primary astrocytes. **(C)** Western blot quantification of CELF 1 and CELF 2 levels in neurons and astrocytes (n=7 independent cultures per group). **(D)** Representative RT-PCR splicing analysis of *Ank2* exon 17, *Clasp1* exons 23 and 25, *Mbnl1* exon 5, *Mbnl2* exon 5, *Tanc2* exon23 and *Mapt* exon 2 and exon 10, in primary neurons and primary astrocytes at 2 weeks *in vitro* (n=3 independent cultures per group). **(E)** IF analysis of the nucleo-cytoplasmic localization of MBNL1 and MBNL2 in primary astrocytes (MBNL1 $n_{WT}$=38, $n_{DMSXL}$=36; MBNL2 $n_{WT}$=26, $n_{DMSXL}$=44). The scale bars represent 10 μm. Data represents means ± SEM (**** $p<0.0001$).

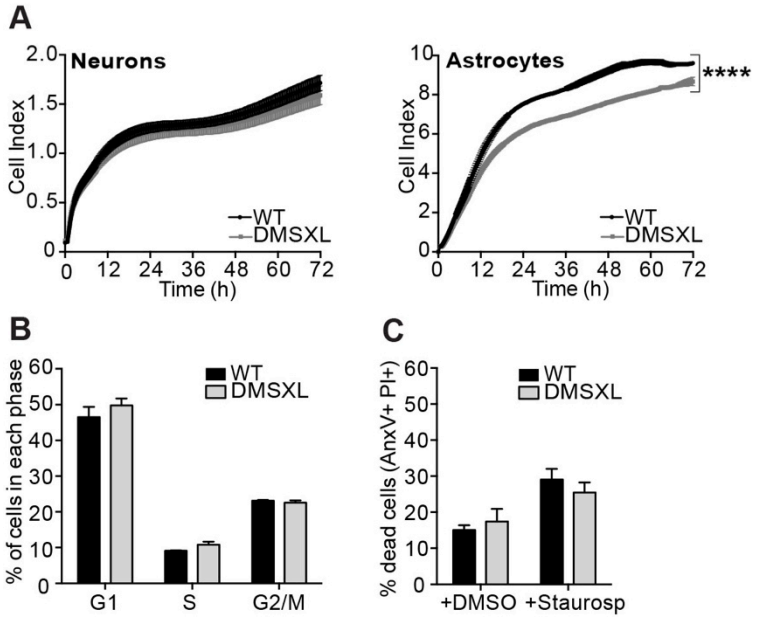


**Figure 3. DMSXL astrocytes show abnormal population dynamics, no associated with defective proliferation or death.**

**(A)** xCELLigence cell index measurement of adhesion and growth of primary neurons (200,000 cells/well, n=6 embryos per genotype) and primary astrocytes (100,000 cells/well, n=2 embryos per genotype, representative of 3 independent experiments). **(B)** Quantification of the percentage of DMSXL and WT astrocytes in $G_1$, S and $G_2$/M phases of the cell cycle by FACS analysis of DNA content (PI levels) and DNA synthesis (BrdU incorporation) (n=3 embryos per group). **(C)** FACS analysis of DMSXL and WT astrocyte cell death by the quantification of AnnxV+ (apoptotic) and PI+ (necrotic) cells in solvent control (DMSO) and in the presence of death-inducing Staurosporin (Saurosp) (n=6 embryos per group). Data are represented as mean ± SEM (**** $p<0.0001$).

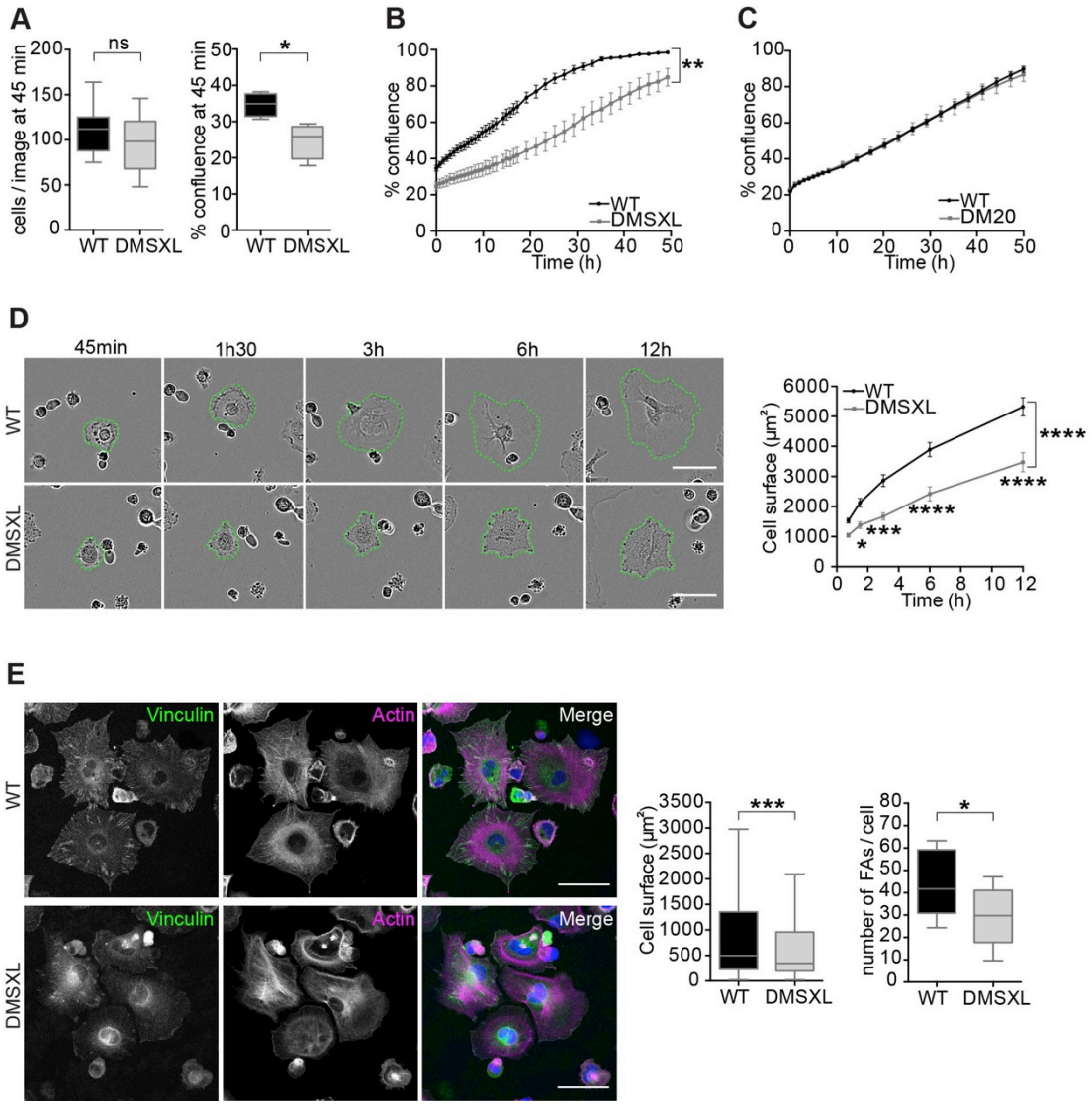


**Figure 4. Primary DMSXL astrocytes show adhesion and spreading defects associated with low number of FAs.**

**(A)** Videomicroscopy quantification of the number of living DMSXL and WT astrocytes attached 45 min after plating ($n_{WT}$=15, $n_{DMSXL}$=16 images) and **(B)** cell confluence from 45 min up to 50 h *in vitro* ($n_{WT}$=$n_{DMSXL}$=4 embryos). **(C)** Quantification of the confluence of DM20 and WT astrocytes from 45 min after plating up to 50 h in culture ($n_{WT}$=$n_{DMSXL}$=3 embryos). **(D)** Representative time-lapse bright field images and quantification of the surface of primary astrocytes attached from 45 min up to 12 h after plating ($n_{WT}$=72, $n_{DMSXL}$=64 cells) Scale bar corresponds to 50 µm. **(E)** Immunofluorescence images of vinculin-rich FAs and actin cytoskeleton of DMSXL and WT astrocytes following 3 h in culture. Quantification of the cell surface based on actin fluorescence ($n_{WT}$=538, $n_{DMSXL}$=608 cells). Quantification of FAs per cell, based on vinculin staining ($n_{WT}$=12, $n_{DMSXL}$=12 images). Scale bar corresponds to 50 µm (*p<0.05, ** p<0.01, *** p<0.001, **** p<0.0001).

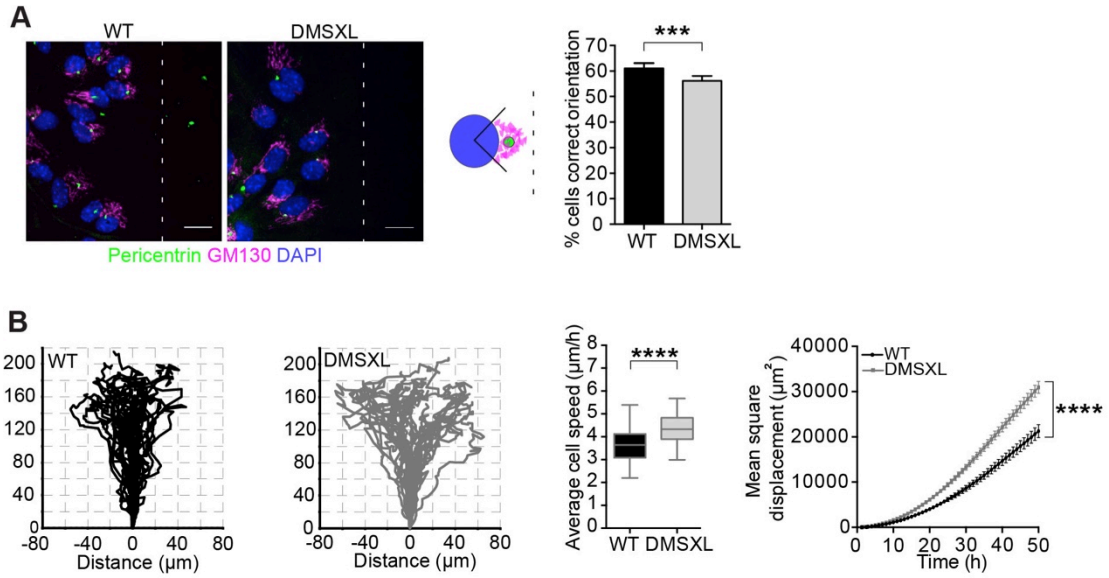


**Figure 5. Primary DMSXL astrocytes show abnormal cytoskeleton polarization and migration.**

**(A)** Analysis of MTOC and Golgi apparatus through the immunofluorescent labeling of pericentrin and GM130, respectively, 8 h after wound-induced migration. Percentage of cells with correct orientation (illustrated in the drawing) in DMSXL and WT astrocyte cultures ($n_{WT}$=2456, $n_{DMSXL}$=2662 cells). Scale bar represents 10 µm**. (D)** Time-lapse videomicroscopy migration tracking plots of individual DMSXL and WT astrocytes over 54 h, until complete wound closure. Quantification of average cell speed and mean square displacement of the astrocytes during migration ($n_{WT}$=39, $n_{DMSXL}$=39 cells). Data are represented as mean ± SEM (*** $p<0.001$, **** $p<0.0001$).

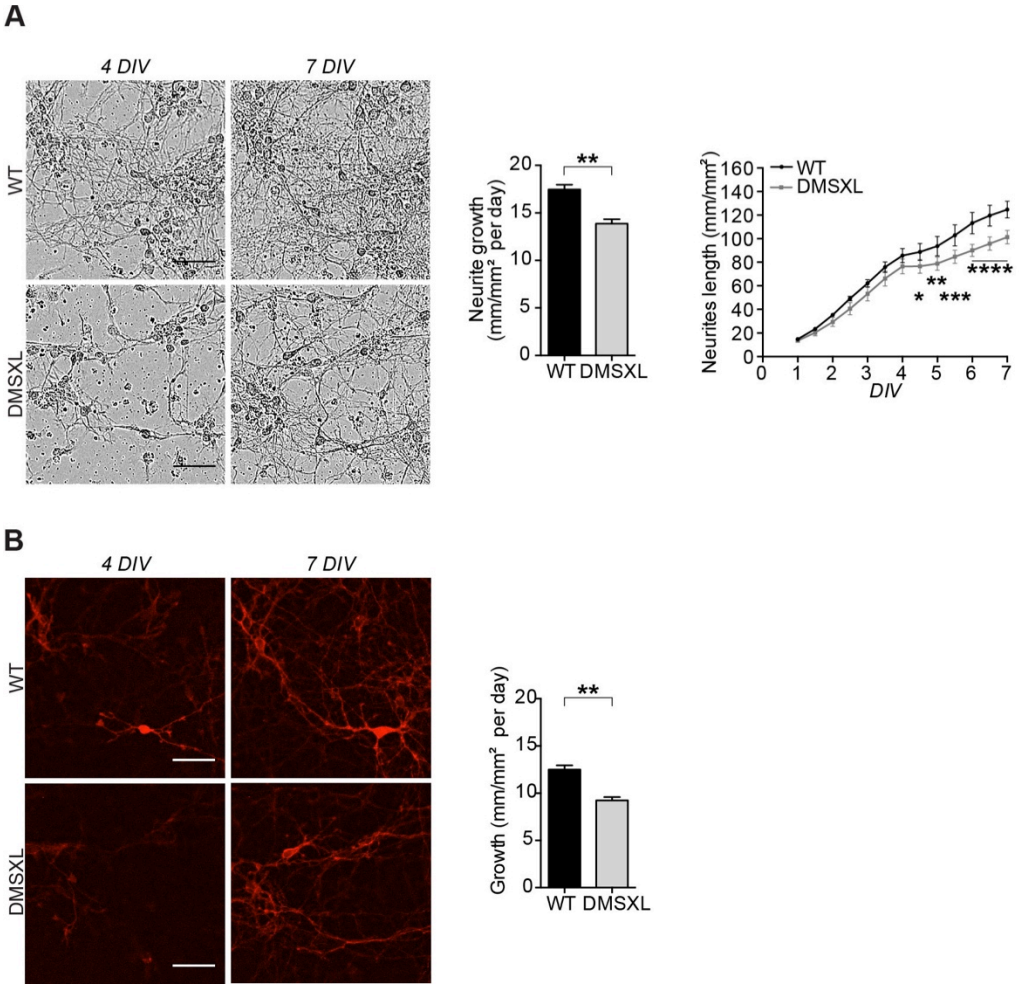


**Figure 6. Primary DMSXL neurons show late neuritogenesis defects.**

**(A)** Representative brightfield images of DMSXL and WT neurons at 4 and 7 *DIV,* showing neurite arborization in culture. Quantification of the speed of neurite growth and neurite length over 7 *DIV* ($n_{WT}$=3, $n_{DMSXL}$=3 embryos). **(B)** Representative images of red fluorescent neurons in the same DMSXL and WT cultures at 4 and 7*DIV*. Quantification of the speed of neurite growth by time-lapse videomicroscopy ($n_{WT}$=3, $n_{DMSXL}$=3 embryos). Scale bar represents 50 μm. Experiments were performed in triplicate (** $p<0.01$).

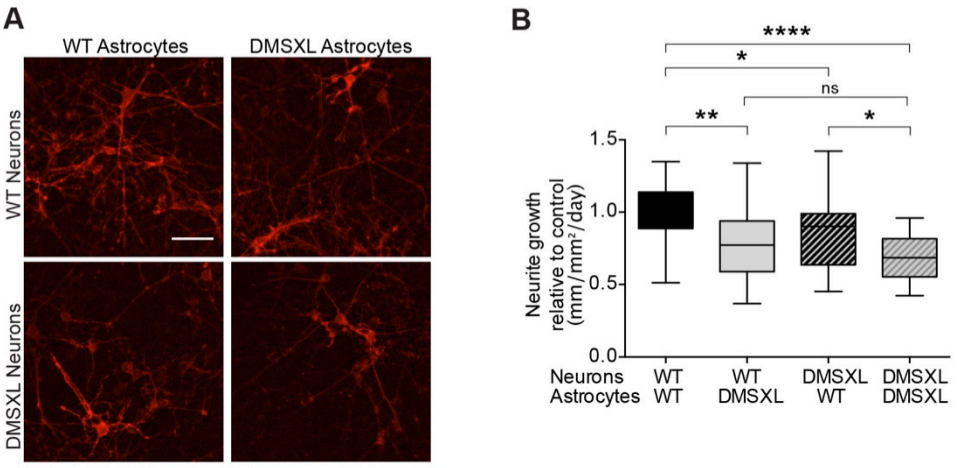


**Figure 7. DMSXL astrocytes have a negative impact on neuronal neuritogenesis.**

**(A)** Representative images of mKate2-expressing red fluorescent DMSXL and WT neurons co-cultured with unmarked DMSXL and WT astrocytes. **(B)** Quantification of the impact of astrocyte genotype on DMSXL and WT neurite growth in 4 independent co-culture experiments ($n_{WT}$=$n_{DMSXL}$=22 embryos). Scale bar represents 50 μm (*p<0.05, ** p<0.01, *** p<0.001, **** p<0.0001).

Figure 8

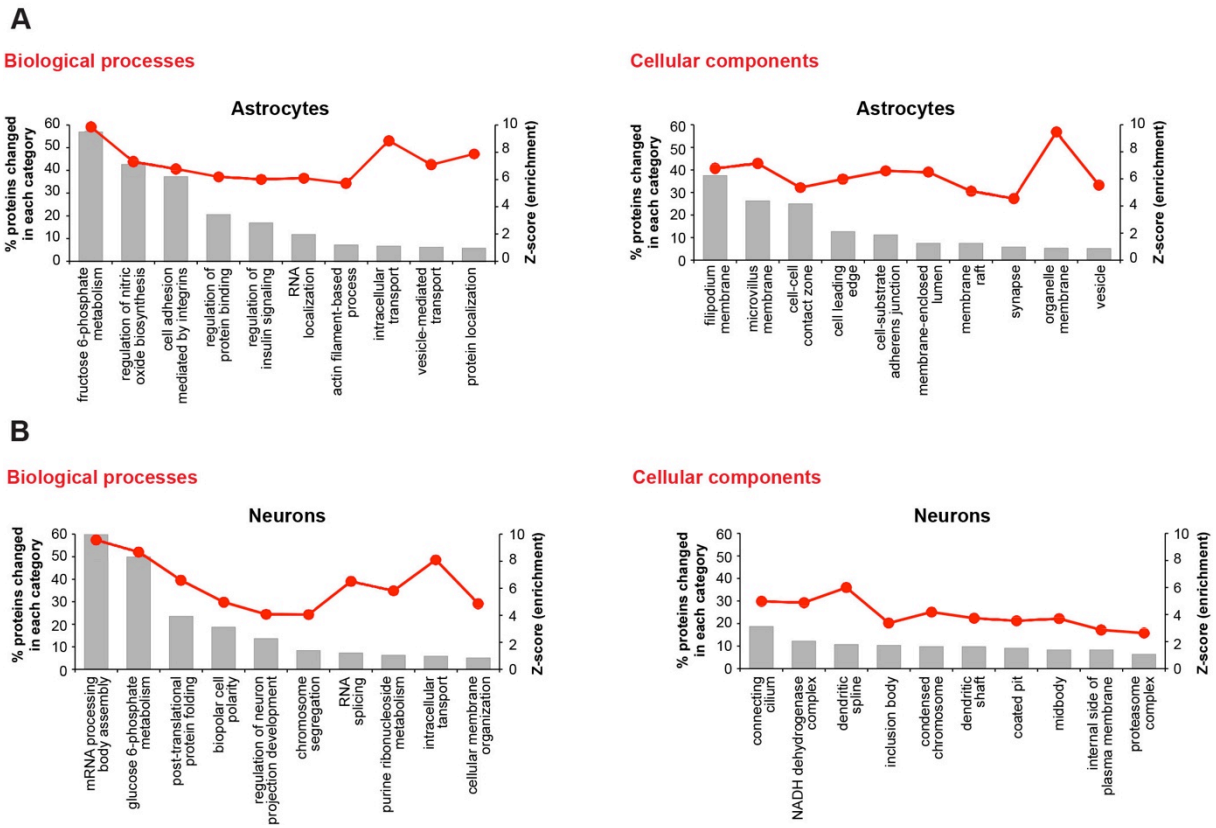


**Figure 8. DMSXL primary neurons and astrocytes show deregulation of clusters of proteins relevant for the cellular phenotypes observed.**

**(A)** GO enrichment analysis followed by GO-Elite over-representation of biological processes and cellular compartments associated with proteins deregulated in DMSXL astrocytes and **(B)** in DMSXL neurons. Representation of the 10 non-redundant terms showing the highest percentage of proteins deregulated. The enrichment score of each term (Z-score) is also presented.

## REFERENCES


Algalarrondo, V., Wahbi, K., Sebag, F., Gourdon, G., Beldjord, C., Azibi, K., … Hatem, S. N. (2015). Abnormal sodium current properties contribute to cardiac electrical and contractile dysfunction in a mouse model of myotonic dystrophy type 1. Neuromuscular Disorders, 25(4), 308–320. https://doi.org/10.1016/j.nmd.2014.11.018

Andreev, V. P., Petyuk, V. A., Brewer, H. M., Karpievitch, Y. V, Xie, F., Clarke, J., … Myers, A. J. (2012). Label-Free Quantitative LC − MS Proteomics of Alzheimer ' s Disease and Normally Aged Human Brains. Journal of Proteome Research, 11, 3053–3067.

Atienza, J. M., Zhu, J., Wang, X., Xu, X., & Abassi, Y. (2005). Dynamic Monitoring of Cell Adhesion and Spreading on Microelectronic Sensor Arrays. Journal of Biomolecular Screening, 10(8), 795–805. https://doi.org/10.1177/1087057105279635

Brook, J. D., McCurrach, M. E., Harley, H. G., Buckler, A. J., Church, D., Aburatani, H., … Housman, D. E. (1992). Molecular basis of myotonic dystrophy: Expansion of a trinucleotide (CTG) repeat at the 3' end of a transcript encoding a protein kinase family member. Cell, 68(4), 799–808. https://doi.org/10.1016/0092-8674(92)90154-5

Chau, A., & Kalsotra, A. (2015). Developmental insights into the pathology of and therapeutic strategies for DM1: Back to the basics. Developmental Dynamics, 244(3), 377–390. https://doi.org/10.1002/dvdy.24240

Dhaenens, C. M., Tran, H., Frandemiche, M. L., Carpentier, C., Schraen-Maschke, S., Sistiaga, A., … Sergeant, N. (2011). Mis-splicing of Tau exon 10 in myotonic dystrophy type 1 is reproduced by overexpression of CELF2 but not by MBNL1 silencing. Biochimica et Biophysica Acta - Molecular Basis of Disease, 1812(7), 732–742. https://doi.org/10.1016/j.bbadis.2011.03.010

Etienne-Manneville, S. (2006). In vitro assay of primary astrocyte migration as a tool to study Rho GTPase function in cell polarization. Methods in Enzymology, 406, 565–578. https://doi.org/10.1016/S0076-6879(06)06044-7

Gomes-Pereira, M., Foiry, L., Nicole, A., Huguet, A., Junien, C., Munnich, A., & Gourdon, G. (2007). CTG trinucleotide repeat "big jumps": Large expansions, small mice. PLoS Genetics, 3(4), 0488–0491. https://doi.org/10.1371/journal.pgen.0030052

Gorelik, R., & Gautreau, A. (2014). Quantitative and unbiased analysis of directional persistence in cell migration. Nature Protocols, 9(8), 1931–43. https://doi.org/10.1038/nprot.2014.131

Gourdon, G., & Meola, G. (2017). Myotonic Dystrophies: State of the Art of New Therapeutic Developments for the CNS. Frontiers in Cellular Neuroscience, 11(April), 1–14. https://doi.org/10.3389/fncel.2017.00101

Haber, M., Zhou, L., & Murai, K. K. (2006). Cooperative Astrocyte and Dendritic Spine Dynamics at Hippocampal Excitatory Synapses. Journal of Neuroscience, 26(35), 8881–8891. https://doi.org/10.1523/JNEUROSCI.1302-06.2006

Harley, H. G., Rundle, S. A., MacMillan, J. C., Myring, J., Brook, J. D., Crow, S., … Harper, P. S. (1993). Size of the unstable CTG repeat sequence in relation to phenotype and parental transmission in myotonic dystrophy. American Journal of Human Genetics, 52(6), 1164–74. Retrieved from

http://www.pubmedcentral.nih.gov/articlerender.fcgi?artid=1682262&tool=pmcentrez&rendertype=abstract

Harper, P. S. (2001). Myotonic Dystrophy 3rd ed. WB Saunders. Retrieved from https://books.google.com/books?id=kbVHVPhFCOYC&pgis=1

Harper, P. S., Harley, H. G., Reardon, W., & Shaw, D. J. (1992). Anticipation in myotonic dystrophy: new light on an old problem. American Journal of Human Genetics, 51(1), 10–6.

Hernandez-Hernandez, O., Guiraud-Dogan, C., Sicot, G., Huguet, A., Luilier, S., Steidl, E., … Gomes-Pereira, M. (2013). Myotonic dystrophy CTG expansion affects synaptic vesicle proteins, neurotransmission and mouse behaviour. Brain, 136(3), 957–970. https://doi.org/10.1093/brain/aws367

Higashimori, H., Schin, C. S., Chiang, M. S. R., Morel, L., Shoneye, T. A., Nelson, D. L., & Yang, Y. (2016). Selective Deletion of Astroglial FMRP Dysregulates Glutamate Transporter GLT1 and Contributes to FXS Phenotypes In Vivo. Journal of Neuroscience, 36(27), 7079–7094. https://doi.org/10.1523/JNEUROSCI.1069-16.2016

Howland, D. S., Liu, J., She, Y., Goad, B., Maragakis, N. J., Kim, B., … Rothstein, J. D. (2002). Focal loss of the glutamate transporter EAAT2 in a transgenic rat model of SOD1 mutant-mediated amyotrophic lateral sclerosis (ALS). Proceedings of the National Academy of Sciences of the United States of America, 99(3), 1604–1609. https://doi.org/10.1073/pnas.032539299

Huang, D. W., Lempicki, R. a, & Sherman, B. T. (2009). Systematic and integrative analysis of large gene lists using DAVID bioinformatics resources. Nature Protocols, 4(1), 44–57. https://doi.org/10.1038/nprot.2008.211

Huguet, A., Medja, F., Nicole, A., Vignaud, A., Guiraud-Dogan, C., Ferry, A., … Gourdon, G. (2012). Molecular, Physiological, and Motor Performance Defects in DMSXL Mice Carrying >1,000 CTG Repeats from the Human DM1 Locus. PLoS Genetics, 8(11), 1–19. https://doi.org/10.1371/journal.pgen.1003043

Jacobs, S., & Doering, L. C. (2010). Astrocytes Prevent Abnormal Neuronal Development in the Fragile X Mouse. Journal of Neuroscience, 30(12), 4508–4514. https://doi.org/10.1523/JNEUROSCI.5027-09.2010

Jiang, H., Mankodi, A., Swanson, M. S., Moxley, R. T., & Thornton, C. A. (2004). Myotonic dystrophy type 1 is associated with nuclear foci of mutant RNA, sequestration of muscleblind proteins and deregulated alternative splicing in neurons. Human Molecular Genetics, 13(24), 3079–3088. https://doi.org/10.1093/hmg/ddh327

Jiang, R., Diaz-Castro, B., Looger, L. L., & Khakh, B. S. (2016). Dysfunctional Calcium and Glutamate Signaling in Striatal Astrocytes from HD Model Mice. The Journal of Neuroscience, 36(12), 3453–3470. https://doi.org/10.1523/JNEUROSCI.3693-15.2016

Khalili, A. A., & Ahmad, M. R. (2015). A Review of cell adhesion studies for biomedical and biological applications. International Journal of Molecular Sciences, 16(8), 18149–18184. https://doi.org/10.3390/ijms160818149

Kulkarni, V. A., & Firestein, B. L. (2012). The dendritic tree and brain disorders. Molecular and Cellular Neuroscience, 50(1), 10–20. https://doi.org/10.1016/j.mcn.2012.03.005

Marchisella, F., Coffey, E. T., & Hollos, P. (2016). Microtubule and microtubule associated protein anomalies in psychiatric disease. Cytoskeleton, 73(10), 596–611. https://doi.org/10.1002/cm.21300

Michel, L., Huguet-Lachon, A., & Gourdon, G. (2015). Sense and antisense DMPK RNA foci accumulate in DM1 tissues during development. PLoS ONE, 10(9), 1–17. https://doi.org/10.1371/journal.pone.0137620

Mutchnick, I. S., Thatikunta, M. A., Gump, W. C., Stewart, D. L., & Moriarty, T. M. (2016). Congenital myotonic dystrophy: ventriculomegaly and shunt considerations for the pediatric neurosurgeon. Child's Nervous System, 32(4), 609–616. https://doi.org/10.1007/s00381-015-2993-y

Panaite, P. A., Kuntzer, T., Gourdon, G., & Barakat-Walter, I. (2013). Respiratory failure in a mouse model of myotonic dystrophy does not correlate with the CTG repeat length. Respiratory Physiology and Neurobiology, 189(1), 22–26. https://doi.org/10.1016/j.resp.2013.06.014

Park, Y. K., & Goda, Y. (2016). Integrins in synapse regulation. Nature Reviews Neuroscience, 17(12), 745–756. https://doi.org/10.1038/nrn.2016.138

Perez-Alvarez, A., Navarrete, M., Covelo, A., Martin, E. D., & Araque, A. (2014). Structural and functional plasticity of astrocyte processes and dendritic spine interactions. The Journal of Neuroscience : The Official Journal of the Society for Neuroscience, 34(38), 12738–44. https://doi.org/10.1523/JNEUROSCI.2401-14.2014

Pettersson, O. J., Aagaard, L., Jensen, T. G., & Damgaard, C. K. (2015). Molecular mechanisms in DM1 - A focus on foci. Nucleic Acids Research, 43(4), 2433–2441. https://doi.org/10.1093/nar/gkv029

Schindelin, J., Arganda-Carreras, I., Frise, E., Kaynig, V., Longair, M., Pietzsch, T., … Cardona, A. (2012). Fiji: an open-source platform for biological-image analysis. Nat Meth, 9(7), 676–682. Retrieved from http://dx.doi.org/10.1038/nmeth.2019

Serra, L., Mancini, M., Silvestri, G., Petrucci, A., Masciullo, M., Spanò, B., … Bozzali, M. (2016). Brain Connectomics ' Modification to Clarify Motor and Nonmotor Features of Myotonic Dystrophy Type 1, 2016. https://doi.org/10.1155/2016/2696085

Serra, L., Silvestri, G., Petrucci, A., Basile, B., Masciullo, M., Makovac, E., … Bozzali, M. (2014). Abnormal functional brain connectivity and personality traits in myotonic dystrophy type 1. JAMA Neurology, 71(5), 603–11. https://doi.org/10.1001/jamaneurol.2014.130

Seznec, H., Agbulut, O., Sergeant, N., Savouret, C., Ghestem, a, Tabti, N., … Gourdon, G. (2001). Mice transgenic for the human myotonic dystrophy region with expanded CTG repeats display muscular and brain abnormalities. Human Molecular Genetics, 10(23), 2717–2726. https://doi.org/10.1093/hmg/10.23.2717

Seznec, H., Lia-Baldini, S., Duros, C., Fouquet, C., Lacroix, C., Hofmann-Radvanyi, H., … Gourdon, G. (2000). Transgenic mice carrying large human genomic sequences with expanded CTG repeat mimic closely the DM CTG repeat intergenerational and somatic instability. Human Molecular Genetics, 9(8), 1185–1194. https://doi.org/10.1093/hmg/9.8.1185

Sicot, G., Gourdon, G., & Gomes-Pereira, M. (2011). Myotonic dystrophy, when simple repeats reveal complex pathogenic entities: New findings and future challenges. Human Molecular Genetics, 20(R2), 116–123. https://doi.org/10.1093/hmg/ddr343

Sicot, G., Servais, L., Dinca, D. M., Leroy, A., Prigogine, C., Medja, F., … Gomes-Pereira, M. (2017). Downregulation of the Glial GLT1 Glutamate Transporter and Purkinje Cell Dysfunction in a Mouse Model of Myotonic Dystrophy. Cell Reports, 19(13), 2718–2729. https://doi.org/10.1016/j.celrep.2017.06.006

Tang, D. D., & Gerlach, B. D. (2017). The roles and regulation of the actin cytoskeleton, intermediate filaments and microtubules in smooth muscle cell migration. Respiratory Research, 18(1), 54. https://doi.org/10.1186/s12931-017-0544-7

Tran, H., Gourrier, N., Lemercier-Neuillet, C., Dhaenens, C. M., Vautrin, A., Fernandez-Gomez, F. J., … Sergeant, N. (2011). Analysis of exonic regions involved in nuclear localization, splicing activity, and dimerization of muscleblind-like-1 isoforms. Journal of Biological Chemistry, 286(18), 16435–16446. https://doi.org/10.1074/jbc.M110.194928

Webb, D. J., Parsons, J. T., & Horwitz, A. F. (2002). Adhesion assembly, disassembly and turnover in migrating cells -- over and over and over again. Nature Cell Biology, 4(4), E97-100. https://doi.org/10.1038/ncb0402-e97

Wickstrom, S. A., Radovanac, K., & Fassler, R. (2011). Genetic Analyses of Integrin Signaling. Cold Spring Harbor Perspectives in Biology, 3(2), a005116–a005116. https://doi.org/10.1101/cshperspect.a005116

Yang, Q., Feng, B., Zhang, K., Guo, Y. yan, Liu, S. bing, Wu, Y. mei, … Zhao, M. gao. (2012). Excessive Astrocyte-Derived Neurotrophin-3 Contributes to the Abnormal Neuronal Dendritic Development in a Mouse Model of FXS. PLoS Genetics, 8(12). https://doi.org/10.1371/journal.pgen.1003172

Yoo, W.-K., Park, Y. G., Choi, Y. C., & Kim, S. M. (2017). Cortical Thickness and White Matter Integrity are Associated with CTG Expansion Size in Myotonic Dystrophy Type I. Yonsei Medical Journal, 58(4), 807. https://doi.org/10.3349/ymj.2017.58.4.807

Zambon, A. C., Gaj, S., Ho, I., Hanspers, K., Vranizan, K., Evelo, C. T., … Salomonis, N. (2012). GO-Elite: A flexible solution for pathway and ontology over-representation. Bioinformatics, 28(16), 2209–2210. https://doi.org/10.1093/bioinformatics/bts366

# Chapter VI. Changes in the phosphoproteome and the mechanisms of brain disease in DM1: a preliminary study

# VI.A. Introduction

## VI.A.I Role of the main kinases in brain function

As discussed in the previous chapters, proper brain development and function is achieved by finely regulating the availability and function of proteins involved in different signaling pathways. Together these pathways ensure the structural organization of neuronal networks and synaptic transmission. Many protein kinases are involved in this fine regulation, by activating or inhibiting the function of downstream targets through phosphorylation. Among them, glycogen synthase kinase 3 (GSK3) and cyclin-dependent kinase 5 (CDK5) play major roles in the regulation of neuronal development and migration, synaptic signaling, learning and memory (Salcedo-Tello et al. 2011; Kawauchi 2014).

## VI.A.II GSK3β regulation and involvement in brain pathology

GSK3 comprises two paralogs, GSK3α and GSK3β, which are highly similar in their catalytic domain. GSK3 is constitutively active within the cells and phosphorylated on Tyr279 in GSK3α and Tyr216 in GSK3β, through the activation of tyrosine kinase cell surface receptors (RTKs) signaling pathways or by autophosphorylation. Its activity can be inhibited by the phosphorylation of an N-terminal serine residue (Ser21 for GSK3α, and Ser9 for GSK3β) by AKT, PKC, PKA, p70S6K and p90RSK (Salcedo-Tello et al. 2011). An additional inhibitory site has been described for GSK3β on Ser389, directly phosphorylated by p38 MAPK (Thornton et al. 2008). GSK3 activity regulates neuronal proliferation and survival, differentiation, neuritogenesis and morphology, as well as neurotransmission (Cole 2012). Altered GSK3 activity has been linked to Alzheimer's disease (AD), in association with Tau hyperphosphorylation and increased production of amyloid-*β*; and schizophrenia, through interaction with DISC1, among other neurological diseases. Lithium has been used as a treatment for some of these diseases, given its inhibitory effect on GSK3 (Medina & Wandosell 2011).

## VI.A.III CDK5 regulation, function and disease involvement

CDK5 is a serine/threonine kinase highly active in neural tissue but less involved in proliferation and cell cycling, compared to other CDK family members. CDK5 becomes active upon association with the neuron-specific activators p35 and p39. Phosphorylation of the Tyr15 of CDK5 by Src-related tyrosine kinases further increases the activity of this kinase (Lopes & Agostinho 2011). Functional analysis revealed the implication of CDK5 in cytoskeletal organization, membrane trafficking, neuronal differentiation and cell cycle exit, neuronal migration and synaptic plasticity (Kawauchi 2014). CDK5 deregulation has also been linked to AD in association with Tau hyperphosphorylation and increased production of amyloid $\beta$; Parkinson's disease, through different mechanisms that include oxidative stress, mitochondrial abnormalities and deregulation of autophagy; as well as in HD, through a reduction in the protective phosphorylation of huntingtin (Cheung et al. 2006).

# VI.B. Context of the study

## VI.B.I Abnormal protein phosphorylation in DM1

Several proteins have shown phosphorylation abnormalities in DM1, in association with expression or activity defects. A deeper characterization of the DM1 phosphoproteome will provide a global view of phosphorylation defects in this condition, and will lead to a better understanding of the molecular pathways deregulated in response to the CTG expansion.

## VI.B.II CELF proteins

CELF1 (CUG-BP1) is upregulated in DM1 skeletal muscle (Savkur et al. 2001), heart (Timchenko et al. 2001), DM1 myoblasts (Dansithong et al. 2005) and DM1 brain (Hernandez-Hernandez et al. 2013). CELF1 upregulation is correlated with protein hyperphosphorylation in DM1 heart and myoblasts, in the nuclear fraction of COS cells expressing *DMPK* mRNA with

960 CTG repeats, in the heart of the EpA960/MCM mice expressing *DMPK-CUG*$^{960}$ mRNA, and in the frontal cortex and brainstem of DMSXL transgenic mice, expressing more than 1000 CTG repeats within the human *DMPK* locus (Kuyumcu-Martinez et al. 2007, Hernandez-Hernandez et al. 2013). The CUG expansion-induced hyperphosphorylation of CELF1 in the heart of DM1 patients and induced EpA960/MCM mice is likely mediated by the activation of PKCα/βII, which results in an increased half-life of the CELF1 protein (Kuyumcu-Martinez et al. 2007). Interestingly, the steady-state levels of CELF proteins decrease during normal heart and brain development (Hernandez-Hernandez et al. 2013; Kalsotra et al. 2008). The increased levels of these proteins induced by the CTG expansion contribute to the splicing and translation abnormalities observed in DM1 (Dasgupta & Ladd 2012; Ladd 2013; Chau & Kalsotra 2015)However we still do not know the causal molecular link between the CTG repeat expansion and PKC activation. Moreover, other kinases, including CyclinD3-cdk4/6 and AKT, can phosphorylate CELF proteins and alter their mRNA-binding and/or translational activity (Dasgupta & Ladd 2012). Little is known about the activity and levels of these kinases in DM1.

## VI.B.III Tau protein

Tau was also found to be abnormally hyperphosphorylated in DM1 brain samples. DM patients show neurofibrillary tangles (NFTs), which consist of intracellular aggregates of hyperphosphorylated tau. NFTs are mainly distributed among the hippocampus, enthorinal and temporal cortex, and they increase in number with the age of the patients (Kiuchi et al. 1991; Vermersch et al. 1996; Sergeant et al. 2001). The hyperphosphorylation of Tau in response to the DM1 repeat expansion was further confirmed in PC12 cells expressing 90 CTG repeats, in association with increased GSK3β activity (Hernandez-Hernandez et al. 2006). Given the fact that Tau is a direct target of GSK3β these results suggest that Tau hyperphosphorylation in DM1 brains can be caused by an increased activity of GSK3β, which may be specifically deregulated in DM1. In line with this hypothesis, increased expression and activity of GSK3β was also reported

in DM1 skeletal muscle (Jones et al. 2012) and in DM1 ES-derived neural stem cells (DM1-NSCs) (Denis et al. 2013). However, the levels and activity of GSK3β have not yet been directly investigated in the brain.

Prior to my arrival to the laboratory, our research group had already found Tau hyperphosphorylation in the frontal cortex, brainstem and hippocampus of DMSXL mice (**Fig. VI.1**) on Thr231 and Ser396. Both amino acids are direct targets of GSK3β and their hyperphosphorylation decreases Tau ability to bind and stabilize microtubules (Cho & Johnson 2004). However, defects in the levels and activity of GSK3β had not yet been directly assessed in the brain of DMSXL mice or DM1 patients to investigate a possible link between GSK3ß deregulation and abnormal Tau metabolism in the CNS.

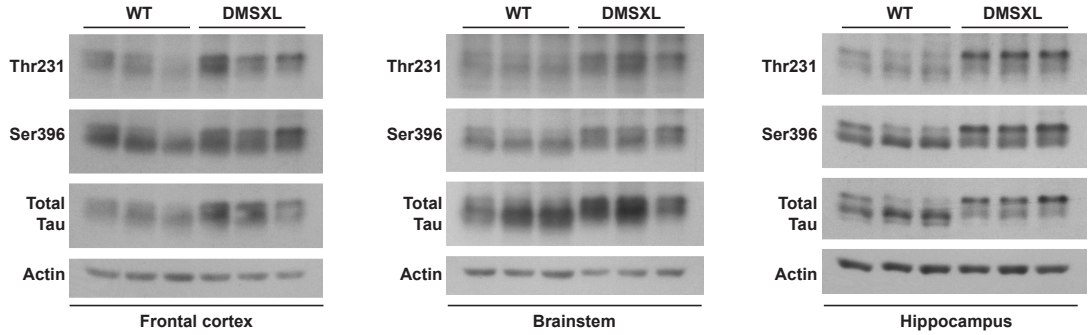


**Figure VI.1. Tau expression and phosphorylation in the CNS of DMSXL mice.**
Western blot analysis of Tau expression and phosphorylation on Thr231 and Ser396 in the frontal cortex, brainstem and hippocampus of DMSXL and WT mice aged 4 months (n=3 for each genotype). Actin and total Tau were used as protein loading controls.

## VI.B.IV SYN1 protein

Our laboratory has recently reported the hyperphosphorylation of SYN1 in DM1 brains: SYN1. Two amino acids, Ser9 and Ser553, are abnormally hyperphosphorylated in the frontal cortex of DM1 patients as well as in different regions of the DMSXL mouse brain. SYN1 hyperphosphorylation is induced by the CTG expansion, as well as by the upregulation of CELF1 and CELF2 alone, while the steady-state levels of SYN1 are not affected (Hernandez-

Hernandez et al. 2013). However we do not know the nature of the kinase that directly hyperphosphorylates SYN1 in DM1 brain. Ser9 is a direct target of PKA and CAMKI/IV while Ser553 is phosphorylated by MAPK and CDK5 (Cesca et al. 2010). Among these candidates, CDK5 plays a major role in brain development and function, phosphorylates Tau and contributes to the formation of NFTs (Duka et al. 2013; Noble et al. 2003)3

. Yet, CDK5 levels and activity in DM1 brains remain unexplored. Therefore, together with GSK3ß, CDK5 presents another interesting candidate kinase to study in DM1 CNS.

# VI.C. Research objectives

Given the phosphorylation defects observed in different DM1 tissues and cells I hypothesized that DM1 brain disease mechanisms may involve global deregulation of key kinases and significant changes in the phosphoproteome. I have started to test this hypothesis by the analysis of the expression and phosphorylation of two main candidate kinases of interest: GSK3β and CDK5. Then, I went one step further and performed a global and unbiased phosphoproteomics analysis. Importantly, since kinase levels and activity may vary between different brain cell types, global phosphoproteomics was carried out on homogeneous neuronal and astroglial cultures to allow for cell type resolution. This approach permitted a better characterization of changes in the proteome, associated with the CTG repeat expansion, in different brain cell types.

# VI.D. Results

## VI.D.I GSK3β expression and phosphorylation

The first I analyzed GSK3β, which is abnormally active in DM1 skeletal muscle and NSCs. I evaluated the expression and phosphorylation on the Ser9 (inactive form) and Tyr216 (active form) in the frontal cortex of DMSXL mice. The analysis was performed on young DMSXL mice at 1.5 months, and adult DMSXL mice at 6 months, in order to determine if the

phosphorylation status of GSK3 varies with age, since an increased activity of GSK3β at later stages in life could contribute to disease progression in humans. Quantitative western blot revealed no significant differences in the steady-state levels or in the phosphorylation of GSK3β, or GSK3α, in the frontal cortex of young and adult DMSXL mice, compared to WT controls (**Fig. VI.2A, B**).

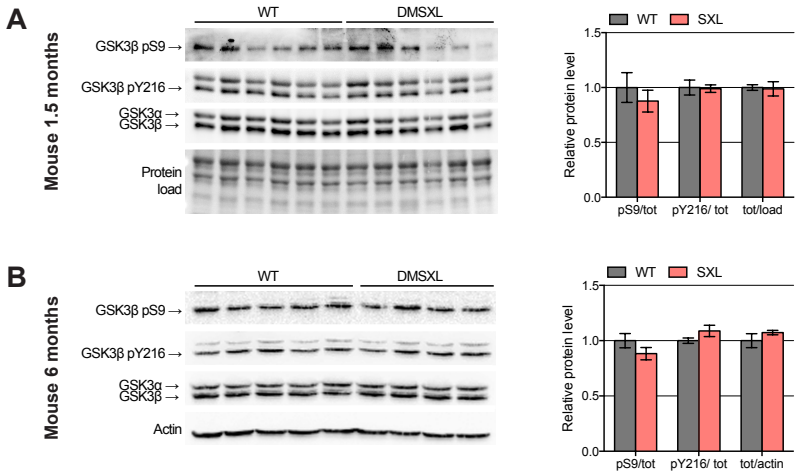


**Figure VI.2. GSK3β expression and phosphorylation in DMSXL frontal cortex.**
Western blot quantification of GSK3β expression and phosphorylation on Ser9 (pS9) and Tyr216 (pY216) residues in the frontal cortex of **(A)** 1.5-month-old DMSXL (n=6) and WT (n=6) mice and **(B)** 6-month-old DMSXL (n=4) and WT (n=5) mice. Phosphorylation levels were normalized to total GSK3β protein levels, while total steady-state levels (tot) were normalized to protein load (load) or actin loading control. Results are presented as average ± SEM. The membranes on the left are representative immunoblots of two to ten technical replicates.

These results suggest that the expression of transgenic *DMPK* transcripts containing CUG expansions is not sufficient to cause overt GSK3β abnormalities detectable in whole DMSXL brain tissue samples. However, since the brain contains different cell types, a cell type-specific defect could be masked by the brain heterogeneity of complex tissue samples. To further investigate if GSK3β is deregulated in a cell-specific manner I have analyzed the expression and phosphorylation of this kinase in primary neuron and astrocyte cultures derived from the frontal cortex of DMSXL mice. Neither primary neurons nor primary astrocytes showed a significant difference in GSK3β or GSK3α levels (**Fig. VI.3A, B**). However, the steady-state levels of

GSK3β showed a tendency to an increase of 17% in DMSXL astrocytes, compared to the WT (**Fig. VI.3B**), in contrast to DMSXL neurons that exhibited no such tendency.

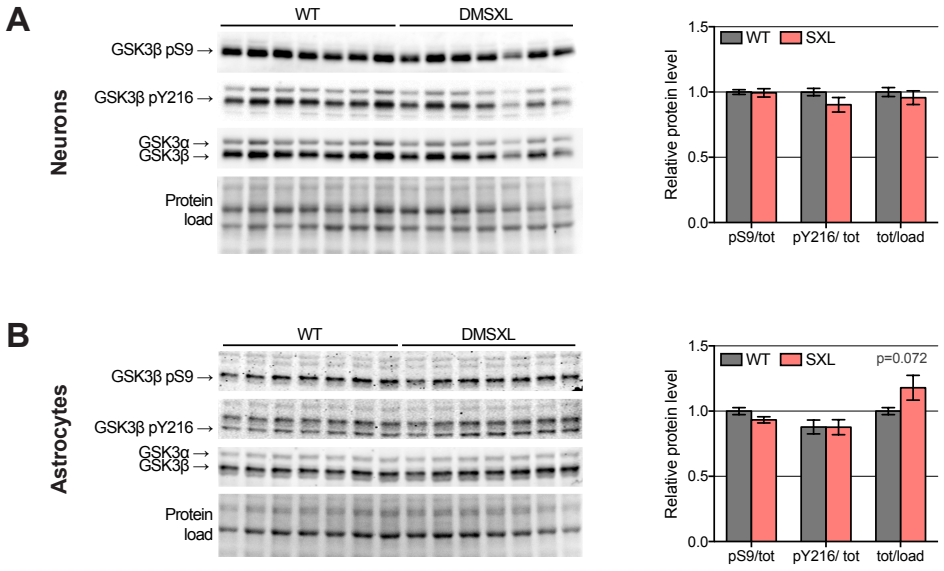


**Figure VI.3. GSK3β expression and phosphorylation in DMSXL primary neurons and astrocytes.** Western blot quantification of GSK3β expression and phosphorylation on Ser9 (pS9) and Tyr216 (pY216) residues in **(A)** primary DMSXL (n=7) and WT (n=7) neurons and **(B)** primary DMSXL (n=7) and WT (n=7) astrocytes. Phosphorylation levels are normalized to total GSK3β and steady-state levels (tot) are normalized to protein load (load). Results are presented as average ± SEM. Four technical replicates were performed for each cell type.

Following these results two hypotheses emerged: either GSK3β is not altered in the DM1 CNS or DMSXL mice do not recreate GSK3β defects induced by toxic CUG RNA repeats.

To distinguish between these two hypotheses, and specifically determine if the DMSXL mouse brain recapitulates DM1 GSK3β defects, I have then measured the levels of GSK3β directly in the frontal cortex of post-mortem DM1 samples. Like in the DMSXL brain, I have found no difference in phosphorylation or expression levels of GSK3β in DM1 frontal cortex, when compared to non-DM control samples (**Fig. VI.4**). Together with the mouse studies, these results corroborate the lack of overt changes in GSK3β levels and phosphorylation in DM1 brain.

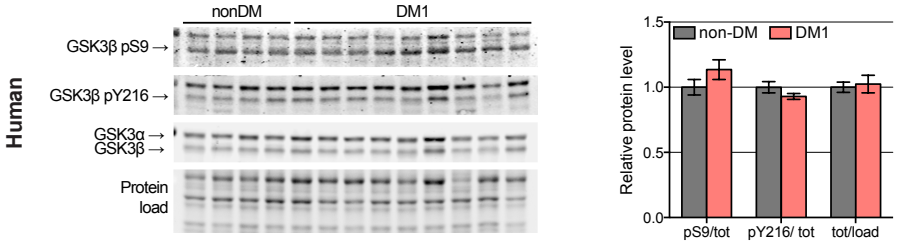


**Figure VI.4. GSK3β expression and phosphorylation in human DM1 frontal cortex**
Western blot quantification of GSK3β expression and phosphorylation on Ser9 (pS9) and Tyr216 (pY216) residues in DM1 patient frontal cortex (n=9) relative to non-DM control individuals (n=4). Phosphorylation levels are normalized to total GSK3β and steady-state levels (tot) are normalized to protein load (load). Results are presented as average ± SEM. Two technical replicates were performed.

## VI.D.II CDK5 expression and phosphorylation

Following the analysis of GSK3, I then focused on the second candidate kinase selected for this study: CDK5. Besides playing a pivotal role in neuronal development and function, CDK5 directly phosphorylates SYN1 at the Ser553 residue, as well as Tau at different Ser and Thr residues. To check whether CDK5 is deregulated in DM1 brain, I have analyzed steady-state levels and phosphorylation on Tyr15 residue (active form) in the frontal cortex of DMSXL mice at 4 months of age, the same age when SYN1 hyperphosporylation was detected. CDK5 levels and phosphorylation showed no significant differences between DMSXL and WT mice at this age. Nonetheless, the CDK5 phosphorylation showed a tendency to a decrease of nearly 25% in DMSXL frontal cortex (**Fig. VI.5A**).

Similarly, I have studied the parallel between the mouse findings and the human condition, through the analysis of the levels of expression and phosphorylation of CDK5 in the frontal cortex of DM1 and non-DM individuals. The great variability between samples and the poor quality of the immunodetection signal introduced additional difficulties in the quantification analysis. Nevertheless, I did not find any statistically significant difference between groups (**Fig. VI.5B**). Interestingly, the steady-state levels of CDK5 appeared to be increased in a few DM1

patients, resulting in an overall tendency to increased levels of total CDK5 relative to non-DM1 controls (**Fig. VI.5B**).

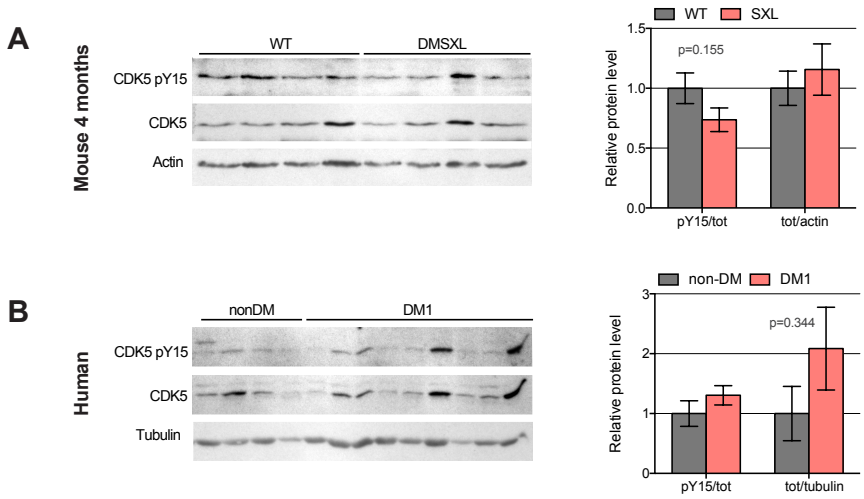


**Figure VI.5. CDK5 expression and phosphorylation in DMSXL and human DM1 frontal cortex.** Western blot quantification of CDK5 expression and phosphorylation on Tyr15 (pY15) residue in **(A)** 4 months DMSXL (n=4) and WT (n=4) frontal cortex and **(B)** DM1 patients frontal cortex (n=9) relative to non-DM control individuals (n=4). Phosphorylation levels were normalized to total CDK5 and steady state levels were normalized to loading control – actin or tubulin. Results are presented as average ± SEM. Two or three technical replicates were performed.

## VI.D.III Global phosphoproteomics analysis in neurons and astrocytes

The analysis of GSK3β and CDK5 candidate kinases did not reveal significant abnormalities in the brains of DMSXL mice or DM1 human patients. I then continued the investigation of DM1 phosphorylation abnormalities through a global phosphoproteomics approach. This high-resolution mass spectrometry study is more powerful, time-efficient and yields a broader view of the deregulated kinases and downstream pathways. To account for the possible differences between brain cell types, I have performed the analysis on homogeneous cultures of primary neurons and astrocytes, derived from the frontal cortex of DMSXL mice. Moreover, I have analyzed undifferentiated neurons, at 4 *days in vitro* (*DIV*), and differentiated

neurons, at 2 weeks *in vitro*, to understand the possible changes in the DM1 phosphoproteome during neuronal development.

Neuronal and astroglial proteins were trypsin-digested, enriched in phosphopeptides by titanium dioxide chromatography and the resulting peptides were quantified by LQT-Orbitrap label-free methods. This type of study allowed the detection of 3882 phosphopeptides in undifferentiated neurons, 4238 in differentiated neurons and 4566 in the astrocytes. In the first instance I focused on the most important differences in phosphorylation – differences that correspond to those cases when the phosphorylation signal is only detected in one of the two genotypes (ON/OFF phosphopeptides). In this way I hoped to reveal the most dramatic changes and get insight into the most severely affected pathways affected by DM1. *In silico* analysis revealed significantly hyper- or hypophosphorylated peptides in the DMSXL neurons and astrocytes compared to the WT. While at 4 *DIV* the primary DMSXL neurons showed a majority of hypo-phosphorylated peptides (63%), at 2 weeks *in vitro* a switch in the phosphorylation status was detected, with 57% of the peptides being abnormally hyperphosphorylated in the DMSXL neurons. The latter situation also applies to primary DMSXL astrocytes, with 56% of their peptides abnormally hyper-phosphorylated, compared to the WT astrocytes (**Table 1**). These phosphopeptides correspond to 894 deregulated proteins in the undifferentiated neurons, 1002 proteins in the differentiated neurons and 488 in the astrocytes.

**Table 1. Global summary of the phosphoproteomics analysis**

| | Neurons 4 days | Neurons 2weeks | Astrocytes |
|---|---|---|---|
| **Number of phosphopeptides** | 3882 | 4238 | 4566 |
| **ON/OFF phosphopeptides**<br>**% hyper (P) in DMSXL**<br>**% hypo(P) in DMSXL** | 1680<br>37%<br>63% | 1951<br>57%<br>43% | 644<br>56%<br>44% |
| **Number of proteins** | 894 | 1002 | 488 |
| **Number of kinases *** | 42 | 44 | 39 |

* Kinase substrate motifs present in more than 10 deregulated phosphopeptides

Importantly, the SYN1 and Tau phosphosites previously characterized appear as hyperphosphorylated in both undifferentiated and differentiated neurons, thereby validating our approach. In contrast, since the expression levels of these proteins are very low in astrocytes, they were not detected in primary DMSXL astroglial cultures. In addition, the global proteomics analysis did not reveal abnormal phosphorylation of GSK3β and CDK5 in DMSXL primary cultures, supporting the western blot results previously described

The *in silico* analysis allowed the identification of 39 to 44 different kinase-binding motifs, enriched in the deregulated phosphopeptides in each cell population studied (**Table VI.1**). One kinase in particular seems very interesting: casein kinase II binds 10% of the deregulated phosphopeptides in all three DMSXL primary cells. Other kinases that bind more than 7% of the deregulated phosphopeptides are PKA, PKC, GSK3 following ERK or CDK5 priming, G protein-coupled receptor kinase 1 (GRK1) and ERK1,2. The WW domain binding motif, a protein-protein interaction domain, also appears abnormally phosphorylated in 9% of the neuronal and 7% of the astroglial phosphopeptides pointing to a possible deregulation of the protein-protein interactions in DM1 (**Fig. VI.6**).

In order to identify the most pertinent clusters of deregulated genes or proteins, either involved in common biological processes or sharing the same cellular compartment or molecular function, I performed a Gene Ontology (GO) enrichment analysis. GO analysis identifies gene sets with high fold enrichment, indicative of a higher presence of a specific gene set in the analyzed collection of proteins compared to the proportion of that gene set in the total population of proteins in the studied organism (The Gene Onthology Consortium 2000; Huang 2008). The global analysis of the deregulated GO gene sets involved in common biological processes indicated that the majority of proteins belong to the regulation of nucleic acid metabolism cluster in the undifferentiated neurons, protein metabolism cluster in the differentiated neurons and signal transduction cluster in the astrocytes (**Fig. VI.7**).

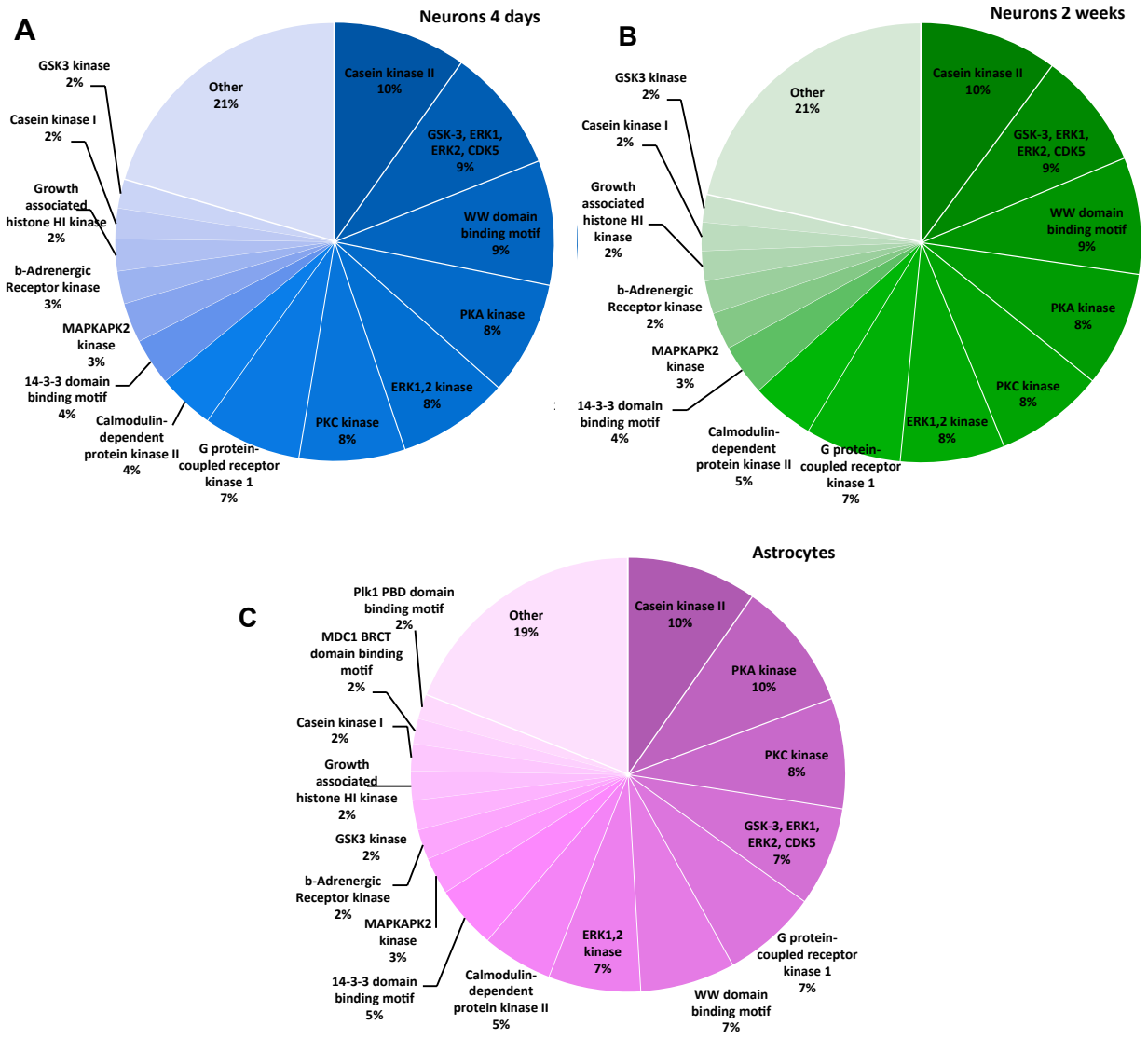


**Figure VI.6. Identification of the most abundant abnormally phosphorylated kinase-binding motifs.**

Pie chart representation of the most abundant kinase-binding motifs present in the deregulated phosphopeptides identified in **(A)** undifferentiated DMSXL primary neurons at 4 DIV, **(B)** differentiated DMSXL neurons at 2 weeks in vitro and **(C)** primary DMSXL astrocytes, when compared to WT cultures. Only the kinases binding more than 2% of the deregulated phosphopeptides are represented for each condition.

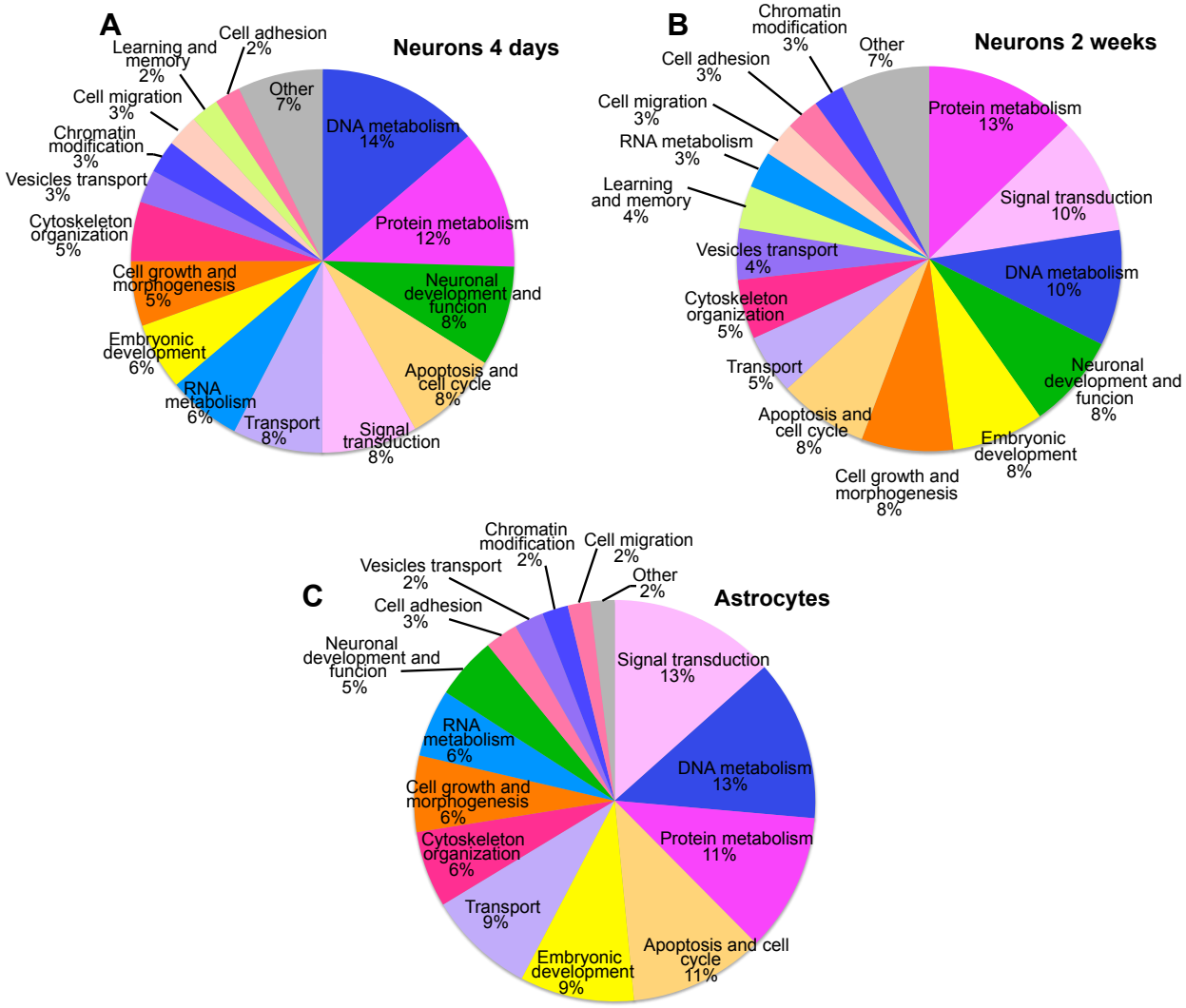


**Figure VI.7. Main deregulated clusters of gene sets following GO enrichment analysis of biological processes.**

Pie chart representation of the proportion of deregulated proteins contributing to a common biological process in **(A)** undifferentiated DMSXL primary neurons at 4 DIV, **(B)** differentiated DMSXL neurons at 2 weeks in vitro and **(C)** primary DMSXL astrocytes, compared to WT cultures. Only the clusters containing more than 2% of the deregulated proteins are represented.

However the individual gene sets showing the highest fold enrichment do not belong necessarily to the cluster with the highest number of proteins. The detailed representation of all the significantly enriched gene sets is presented in the supplementary figures S1-S3, at the end of this chapter. A simplified GO analysis of the over-enriched non-redundant clusters (GO-Elite, Zambon et al. 2012) has revealed the most significant and relevant pathways deregulated in the different cell types. Interestingly, proteins involved in cytoskeleton organization and in regulation of GTPase activity are among the 10 clusters showing the highest enrichment in all cell types pointing to possible common pathways deregulated by the CTG expansion that should be studied in priority. In addition, neurotransmitter transport and microtubule organization are also enriched in both undifferentiated and differentiated neurons, while actin filament-based processes and cellular morphogenesis appear enriched in astrocytes (**Fig. VI.8**). Together, these results suggest a global deregulation of the phosphorylation of proteins controlling the cytoskeleton dynamics in DM1.

# VI.E. Discussion

Phosphorylation abnormalities have been identified in CELF, Tau and SYN1 proteins in several DM1 tissues, mouse and cellular models. Kuyumcu-Martinez et. al. report PKC as the kinase responsible for the hyperphosphorylation and stabilization of CELF1 in DM1 heart. However, previous western blot analyses performed in the laboratory did not reveal obvious changes in PKC levels and phosphorylation in the brains of DMSXL mice and human patients. But a deeper and detailed quantitative immunodetection must be performed to resolve this question, especially because, although CELF1 is upregulated in DM1 brains, we still do not know if PKC is the responsible kinase.

In addition, we do not know the kinases responsible of Tau and SYN1 hyperphosphorylation in the CNS. Therefore, during my PhD project I have studied the expression and phosphorylation levels of two candidate kinases, GSK3β and CDK5, in the

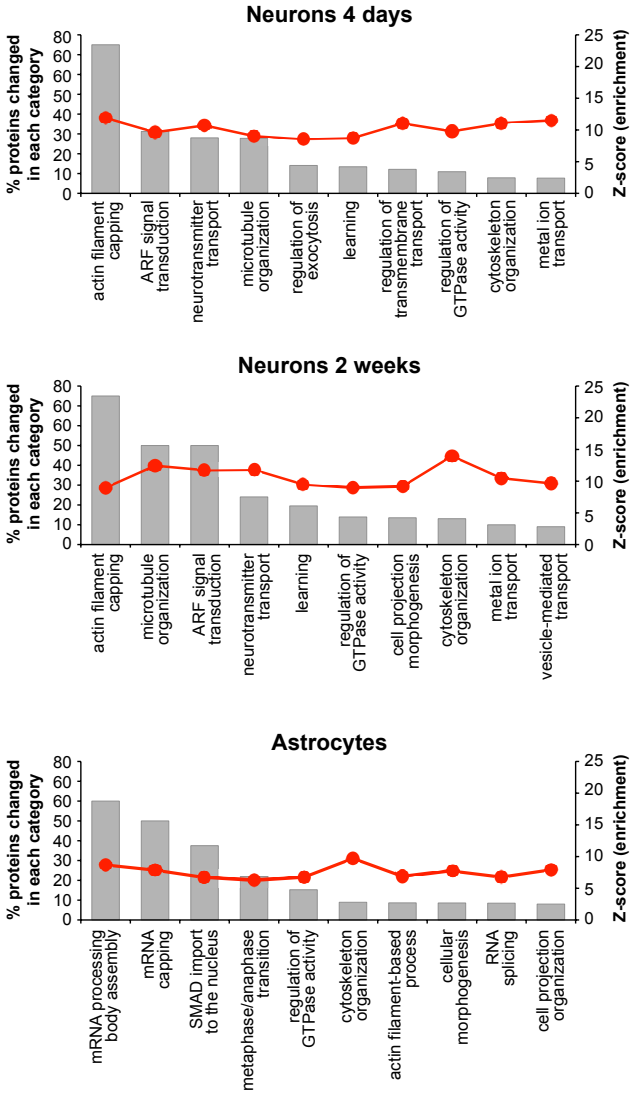


**Figure VI.8. Gene ontology enrichment and over-representation analysis (GO-Elite) of proteins deregulated in neurons and astrocytes.**
Bar chart representation of the 10 most deregulated gene sets in undifferentiated primary neurons at 4DIV (4 days), differentiated neurons at 2 weeks in vitro and differentiated astrocytes at 2 weeks in vitro. Horizontal bars indicate the number of proteins belonging to each gene set (left axis) and the red line indicates the fold enrichment of each gene set (right axis). Only the richest GO categories with at least 5 deregulated proteins, an adjusted enrichment P value lower than 0.05 and fold enrichment superior to 5 are included in the analysis at the 10 richest clusters are presented, ordered by number of proteins deregulated.

frontal cortex of the DMSXL mice and DM1 patients. My results show no significant difference between DMSXL and WT mice, or DM1 and non-DM samples, indicating that the hyperphosphorylation of Tau and SYN1 in DM1 brains cannot be explained by abnormalities in these two kinases.

Although GSK3β is upregulated in DM1 skeletal muscle (Jones et al. 2012) and its activity is increased in DM1-NSCs (Denis et al. 2013), the levels of this kinase remain unchanged in DM1 frontal cortex. Furthermore, neither active (phosphorylated Tyr216) nor inactive (phosphorylated Ser9) markers of GSK3β activity show abnormal expression, compared to non-DM controls. The reproducibility of the results in DMSXL mouse, primary cells and human

DM1 samples confirm and strengthen the lack of effect of the CTG repeat expansion on GSK3β metabolism in the CNS.

The analysis of GSK3β metabolism in the frontal cortex of DM1 patients and DMSXL mice did not provide compelling support for the mediating role of this kinase in the hyperphosphorylation of Tau, associated with DM1-tauopathy, as previously suggested in PC12 cells (Hernandez-Hernandez et al. 2006). It is conceivable that GSK3β deregulation is brain region-specific, and most pronounced in those areas of the brain that show most prominent Tau hyperphosphorylation and accumulation of NFTs, such as the hippocampus and enthorinal cortex (Kiuchi et al. 1991; Vermersch et al. 1996). On the other hand, Tau contains around 80 putative phosphorylation sites (Sergeant et al. 2005), from which around 45 are hyperphosphorylated in AD by different kinases, including p38MAPK, JNK, ERK and PKA, in association with the accumulation of NFTs (Duka et al. 2013). The expression and activity of these kinases should also be assessed in DM1 samples, to have a better understanding of the factors contributing to DM1 tauopathy and NFTs accumulation.

GSK3β has recently been suggested as a therapeutic target for DM1, and GSK3 inhibitors, such as TDZD-8 or lithium, have been proposed following their reported effect to increase grip strength and decrease myotonia in $HSA^{LR}$ mice (Wei et al. 2013). Although GSK3 inhibitors may prove beneficial in DM1 muscle, their use to tackle DM1 neurological dysfunction might be limited, given that we found no GSK3β abnormalities in DM1 brain.

Many different mechanisms regulate the expression and activity of GSK3β, including subcellular localization, target priming by another kinase, proteolytic cleavage and phosphorylation downstream of AKT, insulin receptor and PI3K, MAPK and MEK1/2, among others (Medina & Wandosell 2011). Tissue-specific deregulation of any of these regulatory events could contribute to the differences observed between DM1 muscle and brain.

SYN1 is hyperphosphorylated in DMSXL and DM1 brain at Ser9 and Ser553 residues. These residues are phosphorylation targets for PKA, CaMKI/IV, MAPK and CDK5 (Cesca et al. 2010). Among these kinases, CDK5 does not show significant abnormalities in DMSXL or DM1 frontal cortex, although human results should be interpreted carefully given the heterogeneity of the detection signal. Normal CDK5 expression and activity suggest that SYN1 hyperphosphorylation on Ser553 cannot be explained by CDK5 in DMSXL frontal cortex at 4 months of age.

In addition to phosphorylation, the availability of the CDK5 activators, p35 and p39, can also regulate the activity of this kinase. In some pathological conditions, calpain-mediated cleavage of p35 into a more stable activator (p25) leads to abnormal hyperphosphorylation of CDK5 targets (Kawauchi 2014). Thus the levels of CDK5 activators should also be assessed in to fully characterize the activity of this major kinase and its partners in DM1 brains. Moreover, the analysis of the levels and activity of the other kinases and phosphatases targeting SYN1 will give a better insight into the mechanisms responsible of SYN1 hyperphosphorylation in DM1 brain.

To extend our understanding of deregulated phosphorylation pathways in DM1 brain, in a cell-specific manner, I have performed a global phosphoproteomics analysis. The results revealed a high number of proteins showing significant phosphorylation abnormalities, in both DMSXL neurons and astrocytes, including Tau and SYN1. While in undifferentiated neurons most of the deregulated proteins are hypophosphorylated, in mature neurons and astrocytes the majority of proteins are hyperphosphorylated, indicating an overall increased kinase activity or decreased phosphatase activity in response to the CTG repeat expansion.

The phosphoproteomics pointed to new interesting candidate kinases, possibly deregulated in DM1. Among them, casein kinase 2 binds 10% of the peptides abnormally phosphorylated in each cell type. This pleiotropic kinase phosphorylates a wide variety of substrates including numerous transcription factors, synaptic vesicle proteins and structural proteins, including Tau (Venerando et al. 2014; Turner et al. 1999; Sergeant et al. 2005). Casein

kinase 2 is also involved in the control of the circadian rhythm (Tamaru et al. 2015)and thus the study of this kinase could shed light into possible the factors leading to hypersomnolence in DM1.

The GO-Elite analysis of the deregulated biological processes in DMSXL neurons and astrocytes also revealed interesting candidates and pathways that should be validated and functionally investigated. Among them, proteins controlling GTPase activity and cytoskeleton organization could have a major role in the defective neuritogenesis of DMSXL neurons and abnormal adhesion, spreading and migration of DMSXL described in chapter 3.

Validation of these phosphorylation abnormalities in adult DMSXL mouse and DM1 patients brains will provide a better understanding of the contribution of phosphorylation defects to DM1 CNS dysfunction. Furthermore, small chemical compounds capable of modulating the phosphorylation of candidate kinases and their downstream targets could provide promising paths for DM1 CNS drug development.

# SUPPLEMENTARY FIGURES:

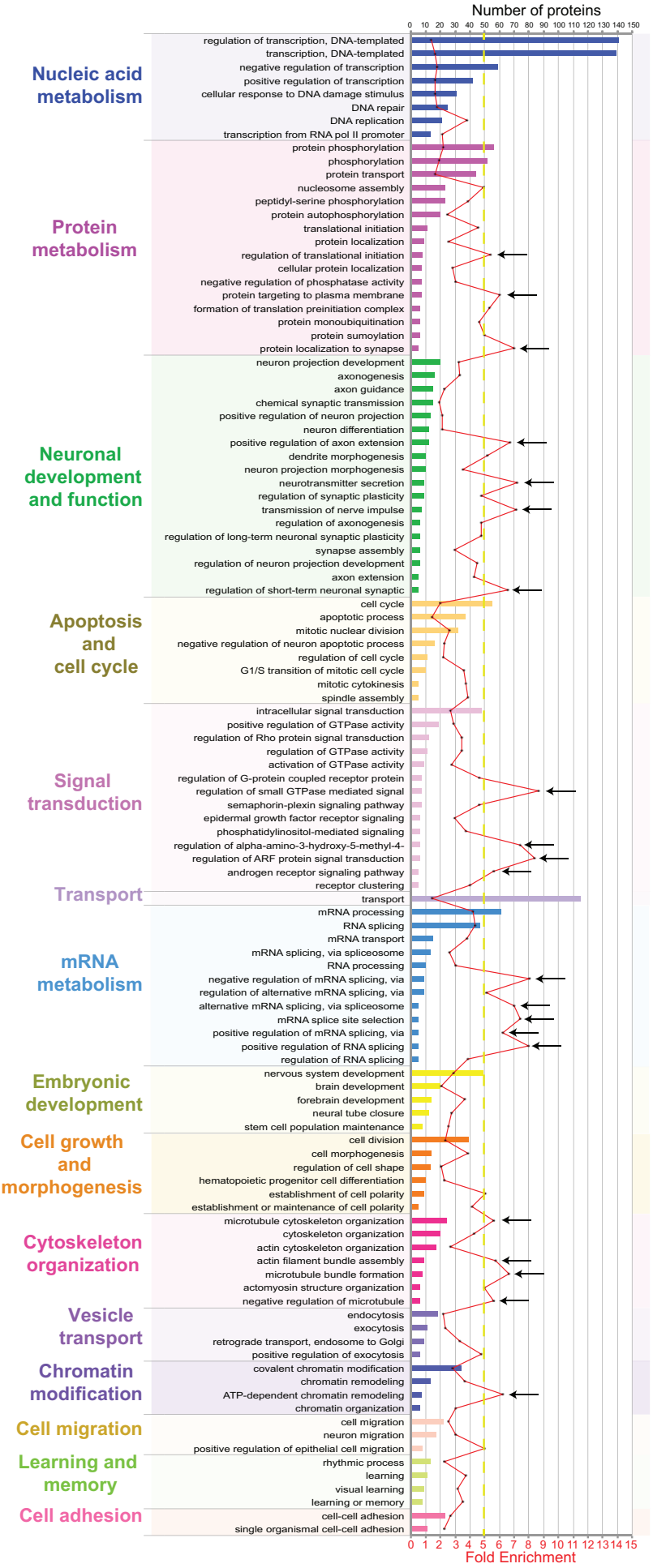


**Figure VI.S1. Gene ontology (GO) enrichment analysis of proteins deregulated in 4 *DIV* neurons.**
Bar chart representation of the major clusters and gene sets deregulated in undifferentiated primary neurons at 4DIV. Horizontal bars indicate the number of proteins belonging to each gene set (upper axis) and the red line indicates the fold enrichment of each gene set (lower axis). The gene sets showing fold enrichment superior to 5 (yellow line) are designated by arrows. Only the GO categories with an adjusted enrichment P value lower than 0.05 and a fold enrichment superior to 1.5 are included in the analysis and gene sets belonging to the same biological process cluster (same color) are ordered by number of proteins deregulated.

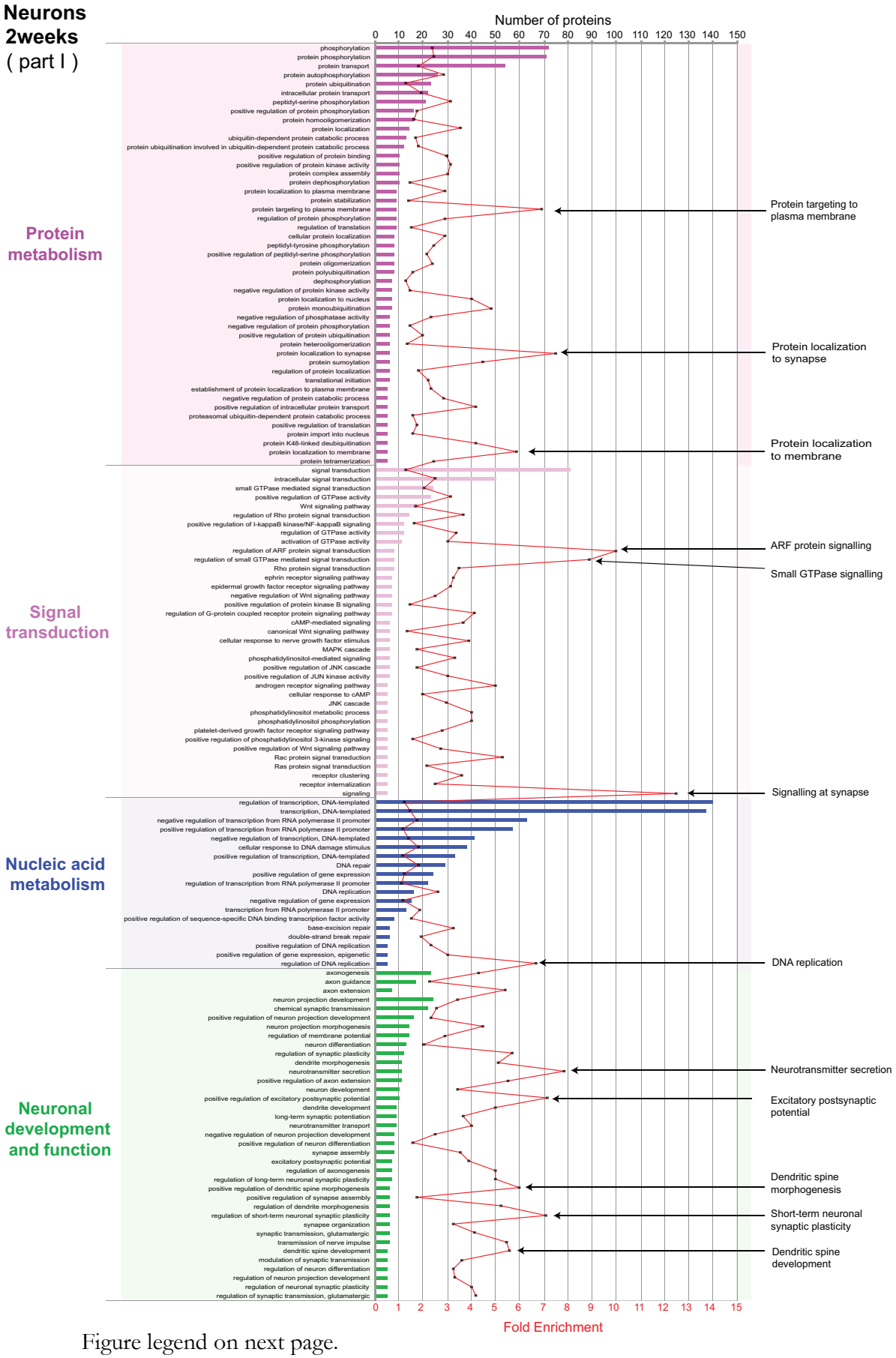


Figure legend on next page.

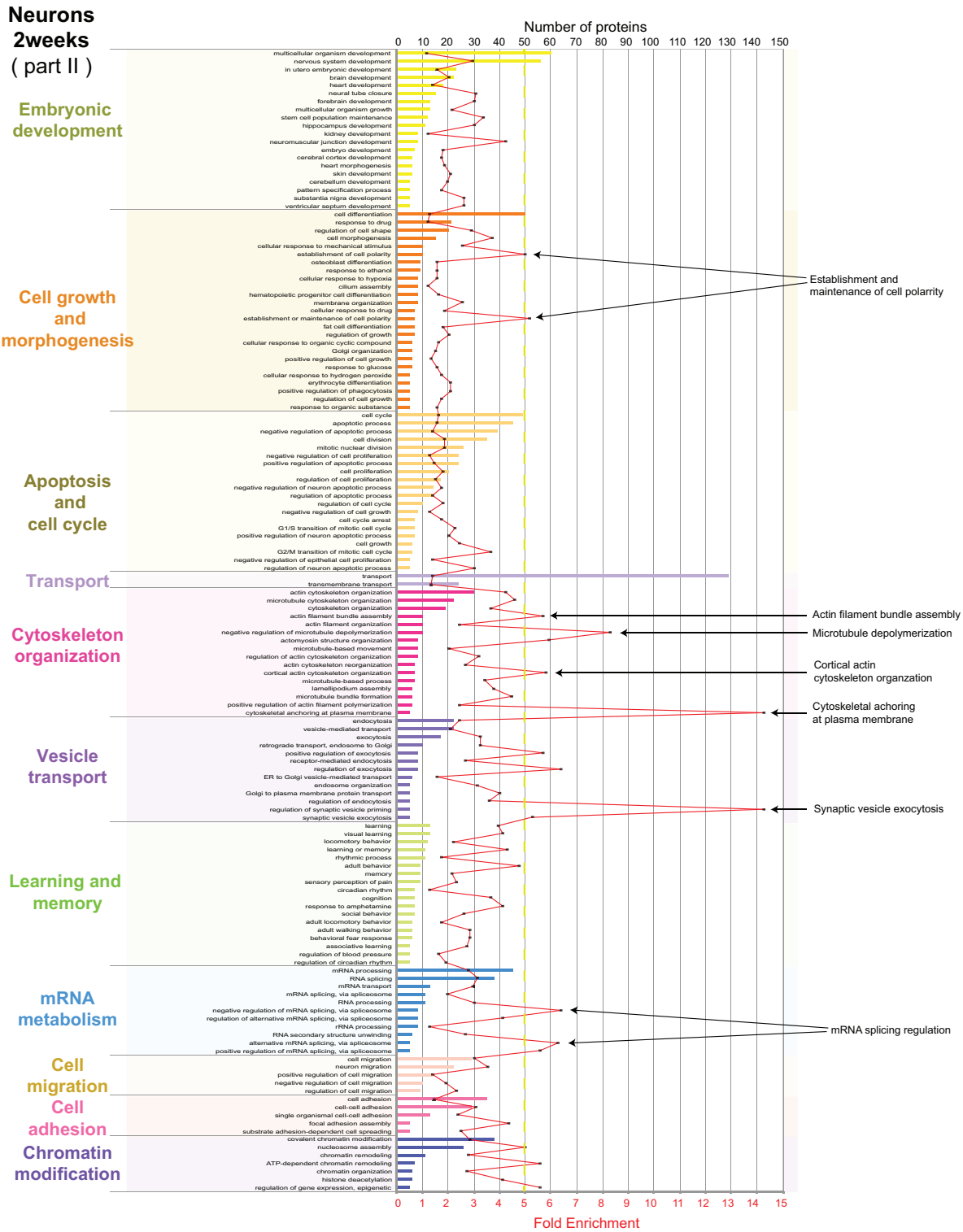


**Figure VI.S2. Gene ontology (GO) enrichment analysis of proteins deregulated in 2 weeks *in vitro* neurons.**

Bar chart representation of the deregulated major clusters and gene sets in differentiated primary neurons at 2 weeks in vitro. Horizontal bars indicate the number of proteins belonging to each gene set (upper axis) and the red line indicates the fold enrichment of each gene set (lower axis). The gene sets showing fold enrichment superior to 5 (yellow line) are designated by arrows. Only the GO categories with an adjusted enrichment P value lower than 0.05 and a fold enrichment superior to 1.5 are included in the analysis and gene sets belonging to the same biological process cluster (same color) are ordered by number of deregulated proteins.

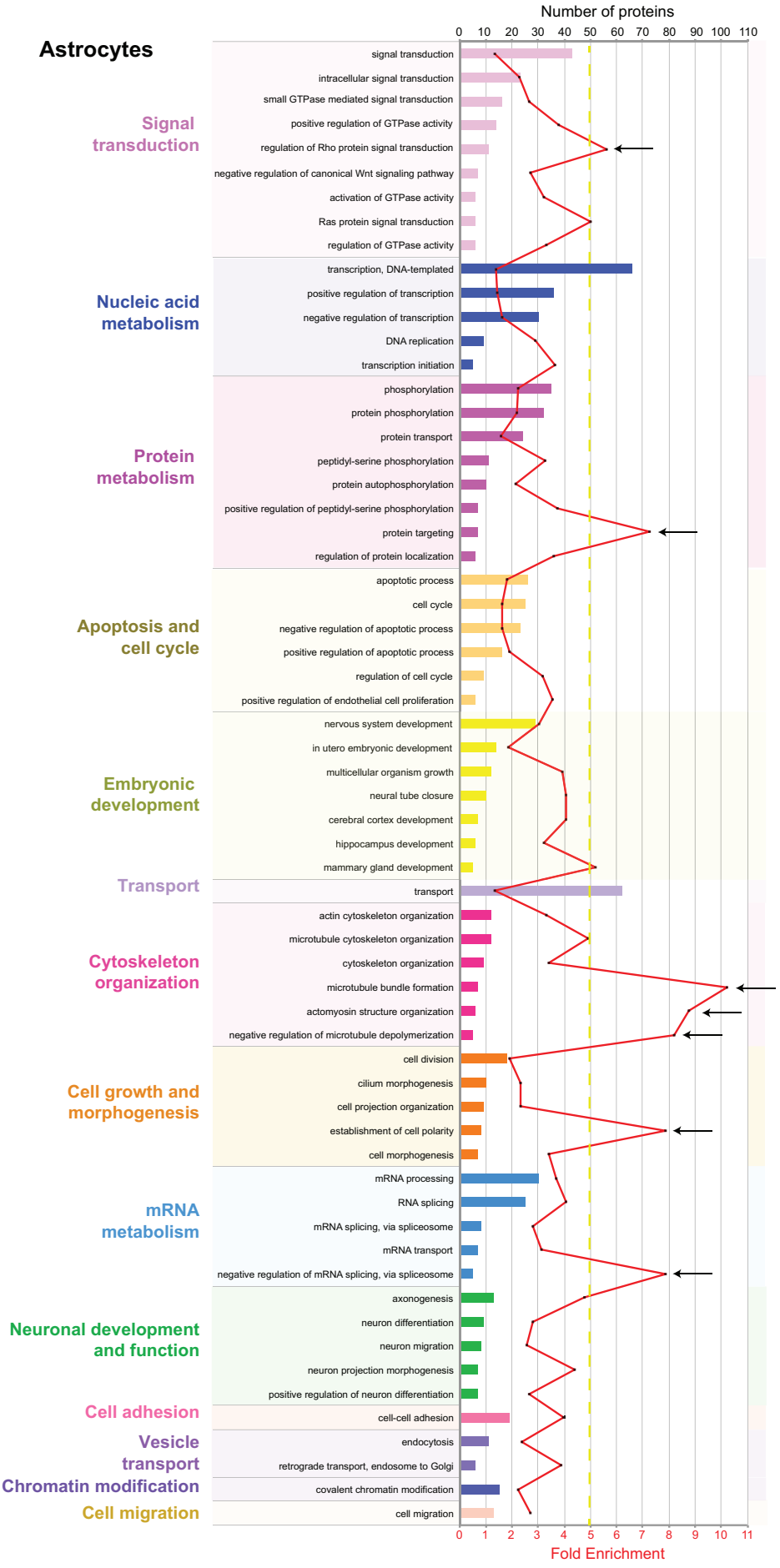


**Figure VI.S3. Gene ontology (GO) enrichment analysis of proteins deregulated in astrocytes.**
Bar chart representation of the deregulated major clusters and gene sets in primary astrocytes. Horizontal bars indicate the number of proteins belonging to each gene set (upper axis) and the red line indicates the fold enrichment of each gene set (lower axis). The gene sets showing fold enrichment superior to 5 (yellow line) are designated by arrows. Only the GO categories with an adjusted enrichment P value lower than 0.05 and a fold enrichment superior to 1.5 are included in the analysis and gene sets belonging to the same biological process cluster (same color) are ordered by number of deregulated proteins.

## SUPPLEMENTARY MATERIALS AND METHODS

### *Western blots*

Proteins from primary cells, mouse and human brain tissues were extracted using RIPA buffer (Thermo Scientific, 89901) supplemented with 0,05% CHAPS (Sigma, C3023), 1x complete protease inhibitor (Sigma-Aldrich, 04693124001) and 1x PhosSTOP phosphatase inhibitor (Sigma 04906845001). Protein concentrations were determined using the Pierce BCA Protein Assay Kit (Thermo Scientific, 23227). Between 10 and 40ug proteins were mixed with 2X Laemmli Sample Buffer (Sigma, S3401), denatured for 5 minutes at 95˚C and resolved in 10% TGX Stain-Free polyacrylamide gels (Bio-Rad 1610183). After electrophoresis gels were activated for 2 minutes under UV light, proteins were transferred onto Nitrocellulose membranes using Trans-Blot® Transfer System (Bio-Rad) and total protein on the membrane was imaged using the ChemiDoc Imaging System (Bio-Rad). Membranes were then blocked in 2.5-5% Blotto non-fat dry milk (Santa Cruz Biotech; sc2325) in 1x TBS-T (10mM Tris-HCl, 0,15M NaCl, 0,05% Tween 20) during 1h at room temperature (RT) and incubated with the primary antibody over night at 4˚C. After three washes in TBS-T membranes were incubated with IRDye® 800CW donkey anti-rabbit (LI-COR Biosciences, P/N 926-32213), 680RD donkey anti-mouse (LI-COR Biosciences, P/N 926-68072), goat anti-rabbit (Dako, P0448) or sheep anti-mouse (Jackson 515-035-062) for 1h at RT, washed three times and imaged using LI-COR Odyssey ® CLx Imaging System or ECL chemiluminiscence. Band intensity was quantified using Image Studio Lite.

Primary antibodies: GSK3 beta (SantaCruz, sc-71186), GSK3 beta Phospho (pY216) (SantaCruz, sc-135653), GSK3 beta Phospho (pS9) (SantaCruz, sc-11757), CDK5 (SantaCruz, sc-6247), CDK5 Phospho (pY15) (SantaCruz, sc-12918)

### *Label-free quantitative LC-MS phosphoproteomics analysis of homogeneous primary neurons and primary astrocytes cultures*

Global phosphoproteomics analysis of homogeneous cultures of primary neurons and astrocytes at 2 weeks in culture were performed as previously described (Andreev et al., 2012) using the high resolution high mass accuracy mass spectrometer LTQ Orbitrap. Samples were enriched in phosphopeptides using the High-Select TiO2 Phosphopeptide Enrichment Kit (Thermo Scientific, A32993). 3 WT and 3 DMSXL littermates were studies for each cell type and significance analysis was performed with the paired t-test. Significantly deregulated proteins of each cell type ($p<0.05$) were used to perform a Gene Onthology (GO) enrichment analysis using the functional annotation tool Database for Annotation, Visualization and Integrated Discovery (DAVID) v.6.7 (http://david.abcc.ncifcrf.go) (Huang, Lempicki, & Sherman, 2009) followed by over-representation clustering using GO-Elite software (Zambon et al., 2012) to report sets of GO sets of non-overlapping terms. Significant GO terms were identified at a FDR <0.05.

### *Statistical analysis.*

Statistical analyses were performed with Prism (GraphPad Software, Inc) and data are presented as mean ± standard error of the mean (±SEM) or as Tukey box-and-wiskers plots. Chi-square test was used to compare categorical variables between two groups. After performing a normality test on the numeric variables, we used two-tailed Student's t-test for parametric data and Mann-Whitney U test for non-parametric data, when two groups were compared. When 3 or more groups were compared we performed a one-way ANOVA or Repeated-measures ANOVA on parametric data, or Kruskal Wallis test on non-parametric data. If statistical significance was achieved, we performed post-test analysis to account for multiple comparisons.

# Chapter VII. – Conclusions and general discussion

My research results have contributed to better understand the molecular mechanisms behind DM1 brain dysfunction and the link between the expanded CTG repeats and the neurological symptoms. By taking advantage of the DMSXL transgenic mice, primary brain cells cultures and human DM1 samples, I have shown that both neurons and astrocytes are individually affected by the CTG repeat expansion. Interestingly, astrocytes show more pronounced molecular features of CUG RNA toxicity, in association with cell adhesion, migration and spreading defects, likely mediated by abnormalities in the expression and phosphorylation of proteins that regulate cytoskeleton dynamics. On the other hand, DM1 mouse neurons show neuritogenesis defects, in association with the deregulation of relevant proteins that control membrane projection and vesicle transport. Somehow some of the changes in protein expression and metabolism were not mediated by the canonical mechanism described in DM1, the deregulation of alternative splicing, thereby corroborating the idea that DM1 molecular mechanisms go beyond missplicing.

These findings are in line with cell autonomous disease mechanisms: molecular events taking place in astrocytes and neurons could directly explain the cellular phenotypes of each individual cell type. However, the situation appears to be more complex, involving also defective neuroglial interplay and non-cell autonomous disease mechanisms. In support of this view, I have shown that CUG RNA-expressing astrocytes have a negative impact on neuron development and maturation in culture. A contributing mechanism for abnormal neuroglia communication relies on the defective glutamate uptake by astrocytes, which in turn affects neuronal excitability and triggers neuronal dysfunction *in vivo* as well as glutamate excitotoxicity in culture systems.

The cell type-specific global proteomics approaches that I have developed will help identify disease intermediates and deregulated pathways with brain cell type

resolution, contributing to further dissect the contribution of cell autonomous and non-autonomous mechanisms to DM1 brain disease.

# VII.A. DMSXL mouse model and CNS dysfunction

In order to have a better view of the cerebral involvement in myotonic dystrophy I have used the DMSXL mouse model. This mouse model, created in our laboratory 20 years ago, contains a large fragment of 45 kb of the human DMPK locus with more than 1,000 CTG repeats (Gourdon et al. 1997; Seznec et al. 2000; Gomes-Pereira et al. 2007). They recreate important molecular hallmarks of DM1 including the instability of the CTG expansion, the nuclear accumulation of toxic expanded *DMPK* transcripts, the sequestration of MBNL and upregulation of CELF proteins and splicing defects in several tissues (Chapter I, Table I.4). The DMSXL mice represent the only mouse model that carries the CTG expansion within the full *DMPK* gene and its regulatory environment, thus expressing toxic RNAs in multiple tissues, including the CNS, and developing a multisystemic phenotype. Expanded CTG repeats are also expressed in the brain of the newly developed EpA960/CaMKII-Cre mice but their expression is driven by the CaMKIIα promoter and thus restricted to neurons of the forebrain (cortex, hippocampus, striatum, pallidum, thalamus and hypothalamus) (Wang et al. 2017). In addition the interruptions introduced in the CTG tract of these mice may have an impact in disease mechanisms and manifestations, as suggested by the analysis of DM1 families carrying interrupted expansions (Musova et al. 2009; Santoro et al. 2017). Therefore, the DMSXL mice are at this moment the closest model to mimic the human DM1 CNS and, providing a powerful tool to study the DM1 neuropathogenesis.

The expression of toxic CUG RNAs in different regions of DMSXL brain, including the frontal cortex, hippocampus and cerebellum, has been associated to different CNS-related phenotypes that resemble, to some extent, the neurological manifestations reported in DM1 patients. DMSXL mice show low exploratory activity, increased anxiety, anhedonia and spatial memory deficits (Hernandez-Hernandez et al. 2013). All these behavioral and cognitive abnormalities have already been described in DM1 patients (Gourdon & Meola 2017). These behavioral abnormalities are associated with synaptic proteins deregulation, short-term synaptic plasticity deficits and abnormal levels of dopamine and serotonin metabolites, which could contribute to anhedonia and depressive-like behaviors. Moreover, DMSXL mice show fine motor incoordination, in association with toxic RNA expression in the cerebellum, particularly in the Bergman glia, and hyperexcitability of the Purkinje neurons (Sicot et al. 2017). Together these results not only validate the DMSXL mice as suitable model to investigate brain disease mechanisms, but importantly they also point to future research directions. In particular, future studies of DM1 neuropathology should also take into account the cerebellum as a brain region affected by the CTG expansion, not only in other mouse models of DM1, but also in human patients.

However, a few considerations must be discussed and taken into account when using DMSXL mice. The integration site of the human transgene is within the mouse *Fbxl7* gene, disrupting its activity. FBXL7 constitutes a subunit of an E3 ubiquitin ligase and has a role in cell cycle arrest (Coon et al. 2012). Since we use DMSXL homozygotes in our studies, these mice likely exhibit full inactivation of the *Fbxl7* gene. Studies are currently underdoing to determine to which extent *Fbxl7* RNA and protein are detected in DMSXL mice. It is therefore conceivable that *Fbxl7* loss of function may contribute, directly or indirectly, to the molecular and physiological phenotypes found in DMSXL. To exclude this hypothesis we must validate our results in additional DM1 mouse models

and ideally in human tissue samples or cell models, whenever possible. Alternatively, our laboratory has recently obtained the *Fbxl7* KO mouse model, to use as a control for future experiments. It is noteworthy that *Fbxl7* KO mice animals have no reported phenotypes, notably in the CNS.

Our laboratory is also currently generating a second control mouse model, through TALEN-mediated excision of the CTG repeats from the transgene, in order to generate a control line that carries a no-repeat *DMPK* transgene integrated in the same locus of the mouse genome. These mice will represent the best control to our studies, since they will also recreate the overexpression of the human DMPK gene, found in DMSXL mice and recreated in the DM20 control lines.

Since these controls were not available for my projects, I have used WT or DM20 mice as control mice, and validated my results in human samples whenever possible.

## VII.B. Role of alternative splicing in brain pathology

The behavioral and electrophysiological abnormalities of DMSXL mice are associated with abnormalities in RAB3A and SYN1 synaptic proteins (Hernandez-Hernandez et al. 2013) and GLT1 glial glutamate transporter (Sicot et al. 2017). Both RAB3A upregulation and GLT1 downregulation are mediated by the sequestration and loss of function of MBNL1, while SYN1 hyperphosphorylation is dependent of the upregulation of CELF1 and CELF2. Despite the major role of MBNL and CELF proteins in mediating alternative splicing, none of these three genes show abnormal alternative splicing of their transcripts, in DMSXL or human DM1 brains (Chapter III - Hernández-Hernández et al. 2013, Chapter IV- Sicot et al. 2017). These results support the idea that DM1 disease mechanisms go beyond missplicing, and affect other

molecular mechanisms, such as APA (Batra et al. 2014), mRNA localization (Wang et al 2012), transcription (Osborne et al 2009), mRNA decay (Masuda et al 2011), miRNA biogenesis (Rau et al 2011) or translation (Timchenko et al 2004). Indeed, *Glt1* is found among the transcripts that show abnormal alternative polyadenilation in *Mbnl* double knock-out frontal cortex and in human DM1 brains (Batra et al 2014), but RT-PCR analysis of *GLT1* APA in our human DM1 brain samples did not provide conclusive results. Therefore, the direct link between MBNL and GLT1 protein abnormalities remains still to be determined. Interestingly our results demonstrate the critical role of *Mbnl1* inactivation in DM1 brain disease mechanisms. In contrast with the predominant role of *Mbnl2* sequestration previously proposed (Charazanis et al 2012), I have shown that *Mbnl1* controls the critical expression of GLT1 in the mouse brain, thereby affecting neuronal function. Another recent publication also claims a role for MBNL1 in neuronal dendrite maintenance (Wang et al 2017).

Other transcripts do show alternative splicing deregulation in DMSXL and DM1 brains, including *NMDAR1/Grin1*, *APP*, *MAPT/Tau* (Hernandez-Hernandez et al. 2013, Chapter V). In addition, DMSXL mice also show abnormal splicing of *Mbnl1* and *Mbnl2* exon 5, and 10, *Ldb3* exon 11, *Fxr1* exon 15 and 16, *Ank2* exon 17, *Clasp1* exon 23-25 and *Tanc2* exon 23 in different CNS regions and brain cells (Hernandez-Hernandez et al. 2013; Hernández-Hernández et al. 2013; Chapter V). These transcripts are direct targets of either MBNL or CELF proteins (Kalsotra et al. 2007, Suenaga et al. 2012, Caillet-Boudin et al. 2014) and their missplicing further supports deregulated function of MBNL and CELF mediators in DMSXL brain. Moreover, most of these transcripts show more severe splicing defects in cultured astrocytes than in neurons (Chapter V), suggesting a more severe spliceopathy in glial cells also *in vivo*. The difference in the severity of splicing deregulation between cell types could contribute to the variability in the degree of missplicing between brain regions. It is possible that the

milder splicing defects found in the cerebellum are accounted for, at least partly, by lower astrocyte content of this brain region, when compared to the frontal cortex, for instance.

The functional consequences of the missplicing events reported so far in the brain and their involvement in the onset of DM1 neurological symptoms remain still to be investigated. Interestingly, some of these transcripts, including *Ank2, Clasp1, Ldb3* and *Mapt/Tau* encode proteins that interact with microtubules or actin filaments and therefore, their missplicing could contribute to the abnormal regulation of cytoskeleton dynamics and neuritogenesis observed in the primary DMSXL astrocytes and neurons (Chapter V).

## VII.C. Neuronal and astroglial dysfunction and DM1 neuropathogenesis

Both DMSXL neurons and astrocytes show accumulation of CUG foci in their nucleus. However, the expression of toxic expanded transcripts is higher in astrocytes than in neurons and it is associated with more severe missplicing. In addition, while primary neurons show late neuritogenesis defects, primary DMSXL astrocytes show adhesion, spreading, cytoskeleton organization and cell migration defects. On one hand, many cognitive disorders, such as FXS, schizophrenia or autism spectrum disorder show defective neuritogenesis and dendritic complexity (Kulkarni & Firestein 2012), highlighting the importance of proper neuronal development and connectivity. On the other hand, astrocytes have an essential role in locally regulating the neuronal homeostasis and activity by forming closely connected neurovascular units and taking part in the tripartite synapse (Perez-Alvarez et al. 2014). Abnormalities in the cell-cell or cell-matrix contacts and dynamic remodeling of astrocytes lamellipodia around the synapse would lead to deregulation of synaptic activity and therefore abnormal CNS function. This hypothesis is supported by the enhanced neuritogenesis defects of

neurons co-cultured with DMSXL astrocytes (Chapter V) and by the increased glutamate-induced neuronal excitotoxicity in presence of DMSXL astrocytes, which show downregulation of GLT1 (Chapter IV). Abnormalities in structural and/or functional support of astrocytes for the neuronal activity likely lead to wider abnormal neuroglial interactions and CNS dysfunction in DM1 brains.

Other microsatellite expansion diseases, such as HD, ALS and FXS also show abnormal neuroglial interaction with a structural impact on neuronal arborization (Jacobs & Doering 2010; Yang et al. 2012) or a functional impact on neuronal excitability (Jiang et al. 2016; Howland et al. 2002; Higashimori et al. 2016). It is thus important to better understand the neuroglial interplay in DM1 brains to identify possible targets for therapeutic intervention. Some of the mouse models currently available will allow to further explore the contribution of individual brain cell types, and defective neuroglial interplay to DM1 brain disease. Among those, the EpA960 allow glial-specific expression of toxic RNA repeats, to complement the neuron specific lines recently published (Wang et al. 2017). Conditional *Mbnl1/Mbnl2* double KO can also be used to conditionally extinguish *Mbnl2* expression either in neurons or glial cells (Lee et al. 2013). Finally, the effects of CELF1 upregulation in individual brain cell lineages and their impact to CNS physiology can also be addressed in mouse conditional cell lines (Koshelev et al. 2010).

In the meantime, DMSXL primary cells that I have set up and characterized provide a great asset for future molecular and functional studies in culture, and they are currently being used in the laboratory to tackle multiple questions.

## VII.D. Altered proteome in DMSXL neurons and astrocytes

The individual analysis of neuronal and astroglial proteome and phosphoproteome revealed a large number of deregulated proteins in each brain cell

type. Among them we found already described protein deregulations such as hyperphosphorylation of SYN1 and Tau. However, other candidates such as CELF1 or CELF2, GSK3β and CDK5 did not show deregulated expression or phosphorylation in individual DMSXL neurons or astrocytes, confirming the results obtained by western blot analysis (Chapter V, VI).

CELF proteins are upregulated in skeletal muscle Savkur 2001), heart (Timchenko et al. 2001), DM1 myoblasts (Dasinthong et al. 2005) and DM1 brain (Hernandez-Hernandez et al. 2013) but their levels are not affected in primary neurons and astrocytes. The conflicting results obtained in individual brain cell types could suggest a differential regulation of these proteins by the complexity of tissue environment.

GSK3β is upregulated in DM1 skeletal muscle (Jones et al. 2012) and DM1-NSCs (Denis et al. 2013), however its expression in DMSXL and DM1 brains does not seem to be affected. This result should be taken into account in the interpretation of the results of the AMO pharma clinical trial that aims to inhibit GSK3β. It is possible that this strategy will not provide major benefits to the CNS.

The GO enrichment analysis of the global proteomics and phosphoproteomics results indicated promising molecular pathways that should be further investigated. Among them we found deregulation of proteins involved in the regulation of cytoskeleton organization, actin filament processes, neuron projection development and vesicle-mediated transport. These protein deregulations could explain the cellular abnormalities observed in DMSXL primary neurons and astrocytes (Chapter V). Further validation of these protein deregulations in mouse and human DM1 brains will shed light into their involvement in DM1 CNS pathology.

Importantly, the primary cell cultures established and studied during the course of my PhD will provide model system for functional validation. Rescue experiments

(through overexpression of downregulated proteins, knocking-down of upregulated candidates, or modulation of protein phosphorylation) will assess the implication of individual molecular events in the onset of cell phenotypes. In parallel, these cells will also offer the opportunity for the pre-clinical assessment and proof-of-principle experiments of pharmacological means to correction key molecular events and associated phenotypes.

DM1 serves as a good example of a logical approach of translational biomedical science. The path from the mapping of disease mutation to the setup of the first clinical trials has followed a rational route, through step-by-step dissection of the molecular events that link the CTG repeat expansion to the onset of disease symptoms. Research progress in the field has benefited tremendously from the generation of multiple and complementary mouse and cell models of the disease.

My work fits well in this framework. Through the use of mouse and cell models of DM1, my PhD project has contributed to the better understanding of disease mechanisms and provided new model systems for future studies, which I hope will feed the design of efficient therapies in the future.

# Chapter VIII. References


van Agtmaal, E.L. et al., 2017. CRISPR/Cas9-Induced (CTG/CAG)n Repeat Instability in the Myotonic Dystrophy Type 1 Locus: Implications for Therapeutic Genome Editing. *Molecular Therapy*, 25(1), pp.24–43.

Alam, A.H.M.K., Suzuki, H. & Tsukahara, T., 2009. Expression analysis of Fgf8a & Fgf8b in early stage of P19 cells during neural differentiation. *Cell Biology International*, 33(9), pp.1032–1037.

Algalarrondo, V. et al., 2015. Abnormal sodium current properties contribute to cardiac electrical and contractile dysfunction in a mouse model of myotonic dystrophy type 1. *Neuromuscular Disorders*, 25(4), pp.308–320.

Amiri, A. et al., 2014. Analysis of Fmr1 deletion in a subpopulation of post-mitotic neurons in mouse cortex and hippocampus. *Autism Research*, 7(1), pp.60–71.

Andreev, V.P. et al., 2012. Label-Free Quantitative LC − MS Proteomics of Alzheimer ' s Disease and Normally Aged Human Brains. *Journal of proteome research*, 11, pp.3053–3067.

Angeard, N. et al., 2011. A new window on neurocognitive dysfunction in the childhood form of myotonic dystrophy type 1 (DM1). *Neuromuscular Disorders*, 21(7), pp.468–476.

Angeard, N. et al., 2007. Cognitive profile in childhood myotonic dystrophy type 1: Is there a global impairment? *Neuromuscular Disorders*, 17(6), pp.451–458.

De Antonio, M. et al., 2016. Unravelling the myotonic dystrophy type 1 clinical spectrum: A systematic registry-based study with implications for disease classification. *Revue Neurologique*, 172(10), pp.572–580.

Ashizawa T, Dubel JR, H.Y., 1993. Somatic instability of CTG repeat in myotonic dystrophy. *Neurology*, 43(12), pp.2674–2678.

Aslanidis, C. et al., 1992. Cloning of the essential myotonic dystrophy region and mapping of the putative defect. *Nature*, 355(6360), pp.548–551.

Atienza, J.M. et al., 2005. Dynamic Monitoring of Cell Adhesion and Spreading on Microelectronic Sensor Arrays. *Journal of Biomolecular Screening*, 10(8), pp.795–805.

Azevedo, F.A.C. et al., 2009. Equal numbers of neuronal and nonneuronal cells make the human brain an isometrically scaled-up primate brain. *Journal of Comparative Neurology*, 513(5), pp.532–541.

Barceló, J.M. et al., 1993. Intergenerational stability of the myotonic dystrophy protomutation. *Human Molecular Genetics*, 2(6), pp.705–709.

Batra, R. et al., 2017. Elimination of Toxic Microsatellite Repeat Expansion RNA by RNA-Targeting Cas9. *Cell*, pp.1–14.

Batra, R. et al., 2014. Loss of MBNL leads to disruption of developmentally regulated alternative polyadenylation in RNA-mediated disease. *Molecular Cell*, 56(2), pp.311–322.

Baumann, N. & Pham-Dinh, D., 2001. Biology of oligodendrocyte and myelin in the mammalian central nervous system. *Physiological reviews*, 81(2), pp.871–927.

Bellion, A. & Métin, C., 2005. Early regionalisation of the neocortex and the medial ganglionic eminence. *Brain Research Bulletin*, 66(4–6), pp.402–409.

Bendotti, C. et al., 2001. Transgenic SOD1 G93A mice develop reduced GLT-1 in spinal cord without alterations in cerebrospinal fluid glutamate levels. *Journal of Neurochemistry*, 79(4), pp.737–746.

Benediktsson, A.M. et al., 2012. Neuronal activity regulates glutamate transporter dynamics in developing astrocytes. *Glia*, 60(2), pp.175–188.

Berul, C.I. et al., 1999. DMPK dosage alterations result in atrioventricular conduction abnormalities in a mouse myotonic dystrophy model. *Journal of Clinical Investigation*, 103(4), pp.1–7.

Bradford, J. et al., 2009. Expression of mutant huntingtin in mouse brain astrocytes causes age-dependent neurological symptoms. *Proceedings of the National Academy of Sciences of the United States of America*, 106,

pp.22480–22485.

Brockhoff, M. et al., 2017. Targeting deregulated AMPK / mTORC1 pathways improves muscle function in myotonic dystrophy type I. *The Journal of Clinical Investigation*, 127(2), pp.1–15.

van den Broek, W.J.A.A. et al., 2002. Somatic expansion behaviour of the (CTG)n repeat in myotonic dystrophy knock-in mice is differentially affected by Msh3 and Msh6 mismatch-repair proteins. *Human molecular genetics*, 11(2), pp.191–8.

Brook, J.D. et al., 1992. Molecular basis of myotonic dystrophy: Expansion of a trinucleotide (CTG) repeat at the 3' end of a transcript encoding a protein kinase family member. *Cell*, 68(4), pp.799–808.

Brunner, H.G. et al., 1993. Influence of sex of the transmitting parent as well as of parental allele size on the CTG expansion in myotonic dystrophy (DM). *American journal of human genetics*, 53(Dm), pp.1016–1023.

Caillet-Boudin, M.-L. et al., 2014. Brain pathology in myotonic dystrophy: when tauopathy meets spliceopathy and RNAopathy. *Frontiers in molecular neuroscience*, 6(January), p.57.

Campbell, C., 2012. Neurology & Neurophysiology Congenital Myotonic Dystrophy. , pp.1–8.

Cesca, F. et al., 2010. The synapsins: Key actors of synapse function and plasticity. *Progress in Neurobiology*, 91(4), pp.313–348.

Chamberlain, C.M. & Ranum, L.P.W., 2012. Mouse model of muscleblind-like 1 overexpression: Skeletal muscle effects and therapeutic promise. *Human Molecular Genetics*, 21(21), pp.4645–4654.

Chang, L. et al., 1998. Proton Spectroscopy in Myotonic Dystrophy. *Arch Neurol*, 55, pp.305–311.

Charizanis, K. et al., 2012. Muscleblind-like 2-Mediated Alternative Splicing in the Developing Brain and Dysregulation in Myotonic Dystrophy. *Neuron*, 75(3), pp.437–450.

Chau, A. & Kalsotra, A., 2015. Developmental insights into the pathology of and therapeutic strategies for DM1: Back to the basics. *Developmental Dynamics*, 244(3), pp.377–390.

Chen, G. et al., 2016. Phenylbutazone induces expression of MBNL1 and suppresses formation of MBNL1-CUG RNA foci in a mouse model of myotonic dystrophy. *Scientific reports*, 6(April), p.25317.

Cheung, Z.H., Fu, A.K.Y. & Ip, N.Y., 2006. Synaptic Roles of Cdk5: Implications in Higher Cognitive Functions and Neurodegenerative Diseases. *Neuron*, 50(1), pp.13–18.

Cho, D.H. et al., 2005. Antisense transcription and heterochromatin at the DM1 CTG repeats are constrained by CTCF. *Molecular Cell*, 20(3), pp.483–489.

Cho, D.H. & Tapscott, S.J., 2007. Myotonic dystrophy: Emerging mechanisms for DM1 and DM2. *Biochimica et Biophysica Acta - Molecular Basis of Disease*, 1772(2), pp.195–204.

Cho, J.-H. & Johnson, G.V.W., 2004. Primed phosphorylation of tau at Thr231 by glycogen synthase kinase 3beta (GSK3beta) plays a critical role in regulating tau's ability to bind and stabilize microtubules. *Journal of neurochemistry*, 88(2), pp.349–358.

Ciafaloni, E. et al., 2008. The hypocretin neurotransmission system in myotonic dystrophy type 1. *Neurology*, 70, pp.226–230.

Cinesi, C. et al., 2016. Contracting CAG/CTG repeats using the CRISPR-Cas9 nickase. *Nature Communications*, 7, p.13272.

Cleary, J.D. & Ranum, L.P.W., 2013. Repeat-associated non-ATG (RAN) translation in neurological disease. *Human Molecular Genetics*, 22(R1), pp.45–51.

Cole, A.R., 2012. GSK3 as a Sensor Determining Cell Fate in the Brain. *Frontiers in Molecular Neuroscience*, 5(February), pp.1–10.

Coon, T.A. et al., 2012. Novel E3 ligase component FBXL7 ubiquitinates and degrades Aurora A, causing mitotic arrest. *Cell Cycle*, 11(4), pp.721–729.

Cudkowicz, M.E. et al., 2014. Safety and efficacy of ceftriaxone for amyotrophic lateral sclerosis: A multi-stage, randomised, double-blind, placebo-controlled trial. *The Lancet Neurology*, 13(11), pp.1083–1091.

Danbolt, N.C., 2001. Glutamate uptake. *Progress in Neurobiology*, 65(1), pp.1–105.

Danbolt, N.C., Storm-Mathisen, J. & Kanner, B.I., 1992. An [Na+ + K+]coupled l-glutamate transporter purified from rat brain is located in glial cell processes. *Neuroscience*, 51(2), pp.295–310.

Dansithong, W. et al., 2005. MBNL1 is the primary determinant of focus formation and aberrant insulin receptor splicing in DM1. *The Journal of biological chemistry*, 280(Feb 18), pp.5773–5780.

Dansithong, W. et al., 2011. RNA steady-state defects in myotonic dystrophy are linked to nuclear exclusion of SHARP. *EMBO reports*, 12(7), pp.735–742.

Dasgupta, T. & Ladd, A.N., 2012. The importance of CELF control: molecular and biological roles of the

CUG-BP, Elav-like family of RNA binding proteins. *Wiley Interdiscip Rev RNA*, 3(1), pp.104–121.

Davis, B.M. et al., 1997. Expansion of a CUG trinucleotide repeat in the 3' untranslated region of myotonic dystrophy protein kinase transcripts results in nuclear retention of transcripts. *Genetics*, 94(July), pp.7388–7393.

Denis, J.A. et al., 2013. mTOR-dependent proliferation defect in human ES-derived neural stem cells affected by myotonic dystrophy type 1. *Journal of cell science*, 126(Pt 8), pp.1763–72.

Dhaenens, C.M. et al., 2011. Mis-splicing of Tau exon 10 in myotonic dystrophy type 1 is reproduced by overexpression of CELF2 but not by MBNL1 silencing. *Biochimica et Biophysica Acta - Molecular Basis of Disease*, 1812(7), pp.732–742.

Dingledine, R. et al., 1999. The glutamate receptor ion channels. *Pharmacological Reviews*, 51(1), pp.7–61.

Dogan, C. et al., 2016. Gender as a modifying factor influencing myotonic dystrophy type 1 phenotype severity and mortality: A nationwide multiple databases cross-sectional observational study. *PLoS ONE*, 11(2), pp.1–12.

Douniol, M. et al., 2009. Psychiatric and cognitive phenotype in children and adolescents with myotonic dystrophy. *European Child and Adolescent Psychiatry*, 18(12), pp.705–715.

Douniol, M. et al., 2012. Psychiatric and cognitive phenotype of childhood myotonic dystrophy type 1. *Developmental Medicine and Child Neurology*, 54(10), pp.905–911.

Duka, V. et al., 2013. Identification of the Sites of Tau Hyperphosphorylation and Activation of Tau Kinases in Synucleinopathies and Alzheimer's Diseases. *PLoS ONE*, 8(9), pp.1–11.

Ebralidze, A.A. et al., 2004. RNA Leaching of Transcription Factors Disrupts Transcription in Myotonic Dystrophy. , 303(5656), pp.383–387.

Echenne, B. & Bassez, G., 2013. *Congenital and infantile myotonic dystrophy* 1st ed., Elsevier B.V.

Ekström, A.B. et al., 2008. Autism spectrum conditons in myotonic dystrophy type 1: A study on 57 individuals with congenital and childhood forms. *American Journal of Medical Genetics, Part B: Neuropsychiatric Genetics*, 147(6), pp.918–926.

van Engelen, B., 2015. Cognitive behaviour therapy plus aerobic exercise training to increase activity in patients with myotonic dystrophy type 1 (DM1) compared to usual care (OPTIMISTIC): study protocol for randomised controlled trial. *Trials*, 16(1), p.224.

Eroglu, C. & Barres, B.A., 2015. Regulation of synaptic connectivity by glia. *Nature*, 468(7321), pp.223–231.

Etienne-Manneville, S., 2006. In vitro assay of primary astrocyte migration as a tool to study Rho GTPase function in cell polarization. *Methods in Enzymology*, 406, pp.565–578.

Fardaei, M. et al., 2002. Three proteins, MBNL, MBLL and MBXL, co-localize in vivo with nuclear foci of expanded-repeat transcripts in DM1 and DM2 cells. *Human molecular genetics*, 11(7), pp.805–14.

Flomen, R. & Makoff, A., 2011. Increased RNA editing in EAAT2 pre-mRNA from amyotrophic lateral sclerosis patients: Involvement of a cryptic polyadenylation site. *Neuroscience Letters*, 497(2), pp.139–143.

Foiry, L. et al., 2006. Msh3 is a limiting factor in the formation of intergenerational CTG expansions in DM1 transgenic mice. *Human Genetics*, 119(5), pp.520–526.

Foran, E. et al., 2014. Sumoylation of the astroglial glutamate transporter EAAT2 governs its intracellular compartmentalization. *Glia*, 62(8), pp.1241–1253.

Freyermuth, F. et al., 2016. Splicing misregulation of SCN5A contributes to cardiac-conduction delay and heart arrhythmia in myotonic dystrophy. *Nature Communications*, 7(11067), pp.1–7.

Fu, Y.H. et al., 1992. An unstable triplet repeat in a gene related to DM. *Science*, 255(5049), pp.1256–1258.

Fugier, C. et al., 2011. Misregulated alternative splicing of BIN1 is associated with T tubule alterations and muscle weakness in myotonic dystrophy. *Nature medicine*, 17(6), pp.720–725.

Furness, D.N. et al., 2008. A quantitative assessment of glutamate uptake into hippocampal synaptic terminals and astrocytes: New insights into a neuronal role for excitatory amino acid transporter 2 (EAAT2). *Neuroscience*, 157(1), pp.80–94.

Gallais, B. et al., 2017. Cognitive decline over time in adults with myotonic dystrophy type 1: A 9-year longitudinal study. *Neuromuscular Disorders*, 27(1), pp.61–72.

Gao, Y. et al., 2016. Genome Therapy of Myotonic Dystrophy Type 1 iPS Cells for Development of Autologous Stem Cell Therapy. *Molecular Therapy*, 24(8), pp.1378–1387.

Gao, Z. & Godbout, R., 2013. Reelin-Disabled-1 signaling in neuronal migration: Splicing takes the stage.

*Cell Mol Life Sci.*, 70(13), pp.2319–2329.

Garcia-Tandon, N. et al., 2012. Protein Kinase C (PKC)-promoted endocytosis of Glutamate transorter GLT1 requires ubiquitinatin ligase Nedd4-2-dependent ubiquitination but not phosphorylation. *J Biol Chem*, 287(23), pp.19177–19187.

Glickstein, M., Sultan, F. & Voogd, J., 2011. Functional localization in the cerebellum. *Cortex*, 47(1), pp.59–80.

Gomes-Pereira, M. et al., 2007. CTG trinucleotide repeat 'big jumps': Large expansions, small mice. *PLoS Genetics*, 3(4), pp.0488–0491.

Gomes-Pereira, M., Cooper, T.A. & Gourdon, G., 2011. Myotonic dystrophy mouse models: Towards rational therapy development. *Trends in Molecular Medicine*, 17(9), pp.506–517.

Gomes-Pereira, M. & Monckton, D.G., 2006. Chemical modifiers of unstable expanded simple sequence repeats: What goes up, could come down. *Mutation Research - Fundamental and Molecular Mechanisms of Mutagenesis*, 598(1–2), pp.15–34.

Gomes-Pereira, M. & Monckton, D.G., 2004. Chemically induced increases and decreases in the rate of expansion of a CAG·CTG triplet repeat. *Nucleic Acids Research*, 32(9), pp.2865–2872.

Goodrich, G.S. et al., 2013. Ceftriaxone Treatment after Traumatic Brain Injury Restores Expression of the Glutamate Transporter, GLT-1, Reduces Regional Gliosis, and Reduces Post-Traumatic Seizures in the Rat. *Journal of Neurotrauma*, 30(16), pp.1434–1441.

Goodwin, M. et al., 2015. MBNL Sequestration by Toxic RNAs and RNA Misprocessing in the Myotonic Dystrophy Brain. *Cell Reports*, 12(7), pp.1159–1168.

Gorelik, R. & Gautreau, A., 2014. Quantitative and unbiased analysis of directional persistence in cell migration. *Nature protocols*, 9(8), pp.1931–43.

Gourdon, G. et al., 1997. Moderate intergenerational and somatic instability of a 55-CTG repeat in transgenic mice. *Nature Genetics*, 15(2), pp.190–192.

Gourdon, G. & Meola, G., 2017. Myotonic Dystrophies: State of the Art of New Therapeutic Developments for the CNS. *Frontiers in Cellular Neuroscience*, 11(April), pp.1–14.

Grabowski, P., 2011. Alternative splicing takes shape during neuronal development. *Current Opinion in Genetics & Development*, 21(4), pp.388–394.

Grewer, C., Gameiro, A. & Rauen, T., 2014. *SLC1 glutamate transporters*,

Gudde, A.E.E.G. et al., 2017. Antisense transcription of the myotonic dystrophy locus yields low-abundant RNAs with and without (CAG)n repeat. *RNA Biology*, 0(0), pp.1–15.

Guillery, R.W., 2005. Observations of synaptic structures: origins of the neuron doctrine and its current status. *Philosophical transactions of the Royal Society of London. Series B, Biological sciences*, 360(1458), pp.1281–1307.

Guiraud-Dogan, C. et al., 2007. DM1 CTG expansions affect insulin receptor isoforms expression in various tissues of transgenic mice. *Biochimica et Biophysica Acta - Molecular Basis of Disease*, 1772(11–12), pp.1183–1191.

Guo, W. et al., 2011. Ablation of Fmrp in adult neural stem cells disrupts hippocampus-dependent learning. *Nature medicine*, 17(5), pp.559–565.

Haber, M., Zhou, L. & Murai, K.K., 2006. Cooperative Astrocyte and Dendritic Spine Dynamics at Hippocampal Excitatory Synapses. *Journal of Neuroscience*, 26(35), pp.8881–8891.

Harley, H.G. et al., 1993. Size of the unstable CTG repeat sequence in relation to phenotype and parental transmission in myotonic dystrophy. *American journal of human genetics*, 52(6), pp.1164–74.

Harper, P.S. et al., 1992. Anticipation in myotonic dystrophy: new light on an old problem. *American journal of human genetics*, 51(1), pp.10–6.

Harper, P.S., 2001. *Myotonic Dystrophy 3rd ed.*, WB Saunders.

Haugeto, O. et al., 1996. Brain glutamate transporter proteins form homomultimers. *Journal of Biological Chemistry*, 271(44), pp.27715–27722.

Hernandez-Hernandez, O. et al., 2013. Myotonic dystrophy CTG expansion affects synaptic vesicle proteins, neurotransmission and mouse behaviour. *Brain*, 136(3), pp.957–970.

Hernandez-Hernandez, O. et al., 2006. Myotonic Dystrophy Expanded CUG Repeats Disturb the Expression and Phosphorylation of Tau in PC12 Cells. *Journal of neuroscience research*, 84, pp.841–851.

Hernández-Hernández, O. et al., 2013. Synaptic protein dysregulation in myotonic dystrophy type 1. *Rare Diseases*, 1(1), p.e25553.

Higashimori, H. et al., 2013. Astroglial FMRP-dependent translational down-regulation of mglur5 underlies glutamate transporter GLT1 dysregulation in the fragile X mouse. *Human Molecular Genetics*, 22(10), pp.2041–2054.

Higashimori, H. et al., 2016. Selective Deletion of Astroglial FMRP Dysregulates Glutamate Transporter GLT1 and Contributes to Fragile X Syndrome Phenotypes In Vivo. *Journal of Neuroscience*, 36(27), pp.7079–7094.

Hill, R.A. & Nishiyama, A., 2014. NG2 cells (polydendrocytes): Listeners to the neural network with diverse properties. *Glia*, 62(8), pp.1195–1210.

Hilton-Jones, D. et al., 2012. Modafinil for excessive daytime sleepiness in myotonic dystrophy type 1 - The patients' perspective. *Neuromuscular Disorders*, 22(7), pp.597–603.

Howland, D.S. et al., 2002. Focal loss of the glutamate transporter EAAT2 in a transgenic rat model of SOD1 mutant-mediated amyotrophic lateral sclerosis (ALS). *Proceedings of the National Academy of Sciences of the United States of America*, 99(3), pp.1604–1609.

Hu, Y.Y. et al., 2015. Ceftriaxone modulates uptake activity of glial glutamate transporter-1 against global brain ischemia in rats. *Journal of Neurochemistry*, 132(2), pp.194–205.

Huang, D.W., Lempicki, R. a & Sherman, B.T., 2009. Systematic and integrative analysis of large gene lists using DAVID bioinformatics resources. *Nature Protocols*, 4(1), pp.44–57.

Huguet, A. et al., 2012. Molecular, Physiological, and Motor Performance Defects in DMSXL Mice Carrying >1,000 CTG Repeats from the Human DM1 Locus. *PLoS Genetics*, 8(11), pp.1–19.

Imbert, G. et al., 1993. Origin of the expansion mutation in myotonic dystrophy. *Nature Genetics*, 4, p.72–6.

Jacobs, S. & Doering, L.C., 2010. Astrocytes Prevent Abnormal Neuronal Development in the Fragile X Mouse. *Journal of Neuroscience*, 30(12), pp.4508–4514.

Jäkel, S. & Dimou, L., 2017. Glial Cells and Their Function in the Adult Brain: A Journey through the History of Their Ablation. *Frontiers in Cellular Neuroscience*, 11(February), pp.1–17.

Jansen, G. et al., 1996. Abnormal myotonic dystrophy protein kinase levels produce only mild myopathy in mice. *Nature genetics*, 13(3), pp.316–24.

Jauvin, D. et al., 2017. Targeting DMPK with Antisense Oligonucleotide Improves Muscle Strength in Myotonic Dystrophy Type 1 Mice. *Molecular Therapy - Nucleic Acids*, 7(June), pp.465–474.

Jean, S. et al., 2014. Comparisons of intellectual capacities between mild and classic adult-onset phenotypes of myotonic dystrophy type 1 (DM1). *Orphanet journal of rare diseases*, 9(1), p.186.

Jiang, H. et al., 2004. Myotonic dystrophy type 1 is associated with nuclear foci of mutant RNA, sequestration of muscleblind proteins and deregulated alternative splicing in neurons. *Human Molecular Genetics*, 13(24), pp.3079–3088.

Jiang, R. et al., 2016. Dysfunctional Calcium and Glutamate Signaling in Striatal Astrocytes from Huntington's Disease Model Mice. *The Journal of Neuroscience*, 36(12), pp.3453–3470.

Jones, K. et al., 2012. GSK3β mediates muscle pathology in myotonic dystrophy. *Journal of Clinical Investigation*, 122(12), pp.4461–4472.

Kalsotra, A. et al., 2008. A postnatal switch of CELF and MBNL proteins reprograms alternative splicing in the developing heart. *Proceedings of the National Academy of Sciences of the United States of America*, 105(51), pp.20333–20338.

Kanadia, R.N. et al., 2003. A Muscleblind Knockout Model for Myotonic Dystrophy. , 302(December), pp.1978–1981.

Katayama, S. et al., 2005. Antisense transcription in the mammalian transcriptome. *Science (New York, NY)*, 309(5740), pp.1564–1566.

Kawauchi, T., 2014. Cdk5 regulates multiple cellular events in neural development, function and disease. *Development Growth and Differentiation*, 56(5), pp.335–348.

Kew, J.N.C. & Kemp, J.A., 2005. Ionotropic and metabotropic glutamate receptor structure and pharmacology. *Psychopharmacology*, 179(1), pp.4–29.

Khalili, A.A. & Ahmad, M.R., 2015. A Review of cell adhesion studies for biomedical and biological applications. *International Journal of Molecular Sciences*, 16(8), pp.18149–18184.

Kim, J.-S., 2016. Genome editing comes of age. *Nat Protoc*, 11(9), pp.1573–1578.

Kim, T.-K. et al., 2010. Widespread transcription at neuronal activity-regulated enhancers. *Nature*, 465(7295), pp.182–187.

Kim, Y.K. et al., 2016. Disease phenotypes in a mouse model of RNA toxicity are independent of protein

kinase Cα and Protein Kinase Cβ. *PLoS ONE*, 11(9), pp.1–15.

Kiuchi, A. et al., 1991. Presenile appearance of abundant Alzheimer's neurofibrillary tangles without senile plaques in the brain in myotonic dystrophy. *Acta neuropathologica*, 82(1), pp.1–5.

Klesert, T.R. et al., 2000. Mice deficient in Six5 develop cataracts: implications for myotonic dystrophy. *Nat Genet*, 25(1), pp.105–109.

Kobayakawa, M., Tsuruya, N. & Kawamura, M., 2012. Theory of mind impairment in adult-onset myotonic dystrophy type 1. *Neuroscience Research*, 72(4), pp.341–346.

Kong, Q. et al., 2014. Small-molecule activator of glutamate transporter EAAT2 translation provides neuroprotection. *Journal of Clinical Investigation*, 124(3), pp.1255–1267.

Koshelev, M. et al., 2010. Heart-specific overexpression of CUGBP1 reproduces functional and molecular abnormalities of myotonic dystrophy type 1. *Human Molecular Genetics*, 19(6), pp.1066–1075.

Koutsoulidou, A. et al., 2015. Elevated muscle-specific miRNAs in serum of myotonic dystrophy patients relate to muscle disease progress. *PLoS ONE*, 10(4), pp.1–20.

Kulkarni, V.A. & Firestein, B.L., 2012. The dendritic tree and brain disorders. *Molecular and Cellular Neuroscience*, 50(1), pp.10–20.

Kuyumcu-Martinez, N.M., Wang, G.S. & Cooper, T.A., 2007. Increased Steady-State Levels of CUGBP1 in Myotonic Dystrophy 1 Are Due to PKC-Mediated Hyperphosphorylation. *Molecular Cell*, 28(1), pp.68–78.

Ladd, A.N., 2013. CUG-BP, Elav-like family (CELF)-mediated alternative splicing regulation in the brain during health and disease. *Mol Cell Neurosci.*, 0, pp.456–464.

Lander, E.S. et al., 2001. Initial sequencing and analysis of the human genome. *Nature*, 409(6822), pp.860–921.

Lee, C.J. & Irizarry, K., 2003. Alternative Splicing in the Nervous System : An Emerging Source of Diversity and Regulation.

Lee, J.A. et al., 2007. Depolarization and CaM kinase IV modulate NMDA receptor splicing through two essential RNA elements. *PLoS Biology*, 5(2), pp.0281–0294.

Lee, J.E., Bennett, C.F. & Cooper, T. a., 2012. RNase H-mediated degradation of toxic RNA in myotonic dystrophy type 1. *Proceedings of the National Academy of Sciences of the United States of America*, 109(11), pp.4221–6.

Lee, K.M. & MacLean, A.G., 2015. New advances on glial activation in health and disease. *World journal of virology*, 4(2), pp.42–55.

Lee, S.G. et al., 2008. Mechanism of ceftriaxone induction of excitatory amino acid transporter-2 expression and glutamate uptake in primary human astrocytes. *Journal of Biological Chemistry*, 283(19), pp.13116–13123.

Leroy, O. et al., 2006. ETR-3 Represses Tau Exons 2/3 Inclusion, a Splicing Event Abnormally Enhanced in Myotonic Dystrophy Type I. *Journal of neuroscience research*, 84, pp.852–859.

Li, Q., Lee, J.-A. & Black, D.L., 2007. Neuronal regulation of alternative pre-mRNA splicing. *Nature Reviews Neuroscience*, 8(11), pp.819–831.

Lin, X. et al., 2006. Failure of MBNL1-dependent post-natal splicing transitions in myotonic dystrophy. *Human Molecular Genetics*, 15(13), pp.2087–2097.

Liquori, C.L., 2001. Myotonic Dystrophy Type 2 Caused by a CCTG Expansion in Intron 1 of ZNF9. *Science*, 293(5531), pp.864–867.

Liu, F. & Gong, C.-X., 2008. Tau exon 10 alternative splicing and tauopathies. *Molecular neurodegeneration*, 3, p.8.

Lopes, J.P. & Agostinho, P., 2011. Cdk5: Multitasking between physiological and pathological conditions. *Progress in Neurobiology*, 94(1), pp.49–63.

Mahadevan, M. et al., 1992. Myotonic Dystrophy Mutation: An Unstable CTG Repeat in the 3′ Untranslated Region of the. *Science*, 255(5049), pp.1253–1255.

Mahadevan, M.S. et al., 2006. Reversible model of RNA toxicity and cardiac conduction defects in myotonic dystrophy. *Nature genetics*, 38(9), pp.1066–1070.

Mankodi, A. et al., 2000. Myotonic Dystrophy in Transgenic Mice Expressing an Expanded CUG Repeat. *Science*, 289(5485), pp.1769–1772.

Marchisella, F., Coffey, E.T. & Hollos, P., 2016. Microtubule and microtubule associated protein anomalies

in psychiatric disease. *Cytoskeleton*, 73(10), pp.596–611.

Martorell, L. et al., 1995. Comparison of CTG repeat length expansion and clinical progression of myotonic dystrophy over a five year period. *Journal of medical genetics*, 32(8), pp.593–6.

Martorell, L. et al., 2001. Frequency and stability of the myotonic dystrophy type 1 premutation. *Neurology*, 56(3), p.328–335.

Martorell, L. et al., 1998. Progression of somatic CTG repeat length heterogeneity in the blood cells of myotonic dystrophy patients. *Human Molecular Genetics*, 7(2), pp.307–312.

Masuda, A. et al., 2012. CUGBP1 and MBNL1 preferentially bind to 3' UTRs and facilitate mRNA decay. *Scientific reports*, 2, p.209.

Mattson, M.P., 2008. Glutamate and Neurotrophic Factors in Neuronal Plasticity and Disease. *Ann N Y Acad Sci*, 1144, pp.97–112.

McMurray, C.T., 2010. Mechanisms of trinucleotide repeat instability during human development. *Nature reviews. Genetics*, 11(11), pp.786–799.

Medina, M. & Wandosell, F., 2011. Deconstructing GSK-3: The Fine Regulation of Its Activity. *International journal of Alzheimer's disease*, 2011, p.479249.

Menon, S. & Gupton, S.L., 2016. *Building Blocks of Functioning Brain: Cytoskeletal Dynamics in Neuronal Development*, Elsevier Inc.

Meola, G. & Sansone, V., 2007. Cerebral involvement in myotonic dystrophies. *Muscle and Nerve*, 36(3), pp.294–306.

Michel, L., Huguet-Lachon, A. & Gourdon, G., 2015. Sense and antisense DMPK RNA foci accumulate in DM1 tissues during development. *PLoS ONE*, 10(9), pp.1–17.

Miller, B.R. et al., 2008. Up-regulation of GLT1 expression increases glutamate uptake and attenuates the Huntington's disease phenotype in the R6/2 mouse. *Neuroscience*, 153(1), pp.329–337.

Mines, M.A. & Jope, R.S., 2011. Glycogen synthase kinase-3: a promising therapeutic target for fragile x syndrome. *Frontiers in molecular neuroscience*, 4(November), p.35.

Mizukami, K. et al., 1999. An autopsy case of myotonic dystrophy with mental disorders and various neuropathologic features. *Psychiatry and Clinical Neurosciences*, 53(1), pp.51–55.

Molofsk, A. V. et al., 2012. Astrocytes and disease: A neurodevelopmental perspective. *Genes and Development*, 26(9), pp.891–907.

Monckton, D.G. et al., 1995. Somatic mosaicism, germline expansions, germline reversions and intergenerational reductions in myotonic dystrophy males: small pool PCR analyses. *Human Molecular Genetics*, 4(1), pp.1–8.

Morel, L. et al., 2013. Neuronal exosomal mirna-dependent translational regulation of astroglial glutamate transporter glt1. *Journal of Biological Chemistry*, 288(10), pp.7105–7116.

Mulders, S. a M. et al., 2009. Triplet-repeat oligonucleotide-mediated reversal of RNA toxicity in myotonic dystrophy. , 106(33), pp.13915–13920.

Münch, C. et al., 2000. Differential RNA cleavage and polyadenylation of the glutamate transporter EAAT2 in the human brain. *Molecular Brain Research*, 80(2), pp.244–251.

Murphy-Royal, C. et al., 2017. Astroglial glutamate transporters in the brain: Regulating neurotransmitter homeostasis and synaptic transmission. *Journal of Neuroscience Research*, 0(January).

Musova, Z. et al., 2009. Highly unstable sequence interruptions of the CTG repeat in the myotonic dystrophy gene. *American Journal of Medical Genetics, Part A*, 149(7), pp.1365–1369.

Mutchnick, I.S. et al., 2016. Congenital myotonic dystrophy: ventriculomegaly and shunt considerations for the pediatric neurosurgeon. *Child's Nervous System*, 32(4), pp.609–616.

Mykowska, A. et al., 2011. CAG repeats mimic CUG repeats in the misregulation of alternative splicing. *Nucleic Acids Research*, 39(20), pp.8938–8951.

Nakamori, M. et al., 2016. Oral administration of erythromycin decreases RNA toxicity in myotonic dystrophy. *Annals of Clinical and Translational Neurology*, 3(1), pp.42–54.

Nguyen, L. et al., 2015. Rationally Designed Small Molecules That Target Both the DNA and RNA Causing Myotonic Dystrophy Type 1. *Journal of the American Chemical Society*, 137(44), pp.14180–14189.

Nishiyama, A. et al., 2009. Polydendrocytes (NG2 cells): multifunctional cells with lineage plasticity. *Nature Reviews Neuroscience*, 10(1), pp.9–22.

Niswender, C.M. & Conn, P.J., 2010. Metabotropic Glutamate Receptors: Physiology, Pharmacology, and

Disease. *Annu Rev Pharmacol Toxicol*, 50, pp.295–322.

Noble, W. et al., 2003. Cdk5 is a key factor in tau aggregation and tangle formation in vivo. *Neuron*, 38(4), pp.555–565.

Okkersen, K. et al., 2017. Brain imaging in myotonic dystrophy type 1. *American Academy of Neurology*.

Ono, S. et al., 1998. Loss of serotonin-containing neurons in the raphe of patients with myotonic dystrophy: a quantitative immunohistochemical study and relation to hypersomnia. *Neurology*, 50(2), p.535–538.

Ono, S. et al., 1995. Myotonic dystrophy with alveolar hypoventilation a clinicopathological study and hypersomnia : *Journal of the Neurological Sciences*.

Orengo, J.P. et al., 2008. Expanded CTG repeats within the DMPK 3' UTR causes severe skeletal muscle wasting in an inducible mouse model for myotonic dystrophy. *Proc Natl Acad Sci U S A*, 105(7), pp.2646–2651.

Osborne, R.J. et al., 2009. Transcriptional and post-transcriptional impact of toxic RNA in myotonic dystrophy. *Human Molecular Genetics*, 18(8), pp.1471–1481.

Otten, A.D. & Tapscott, S.J., 1995. Triplet repeat expansion in myotonic dystrophy alters the adjacent chromatin structure. *Proceedings of the National Academy of Sciences of the United States of America*, 92(12), pp.5465–9.

Panaite, P.A. et al., 2013. Respiratory failure in a mouse model of myotonic dystrophy does not correlate with the CTG repeat length. *Respiratory Physiology and Neurobiology*, 189(1), pp.22–26.

Park, Y.K. & Goda, Y., 2016. Integrins in synapse regulation. *Nature Reviews Neuroscience*, 17(12), pp.745–756.

Parpura, V. & Verkhratsky, A., 2012. Astrocytes revisited: concise historic outlook on glutamate homeostasis and signaling. *Croatian medical journal*, 53(6), pp.518–28.

Pekny, M. et al., 2016. Astrocytes: a central element in neurological diseases. *Acta Neuropathologica*, 131(3), pp.323–345.

Perbellini, R. et al., 2011. Dysregulation and cellular mislocalization of specific miRNAs in myotonic dystrophy type 1. *Neuromuscular Disorders*, 21(2), pp.81–88.

Perez-Alvarez, A. et al., 2014. Structural and functional plasticity of astrocyte processes and dendritic spine interactions. *The Journal of neuroscience : the official journal of the Society for Neuroscience*, 34(38), pp.12738–44.

Pérez-Cerdá, Sánchez-Gómez & Matute, 2015. Pío del Río Hortega and the discovery of the oligodendrocytes. *Frontiers in neuroanatomy*, 9(July), p.92.

Perfetti, A. et al., 2016. Validation of plasma microRNAs as biomarkers for myotonic dystrophy type 1. *Scientific Reports*, 6(1), p.38174.

Perini, G.I. et al., 1999. Cognitive Impairment and ( CTG ) n Expansion in Myotonic Dystrophy Patients. *Biology Psychiatry*, 43(Dm), pp.425–431.

Petr, G.T. et al., 2015. Conditional Deletion of the Glutamate Transporter GLT-1 Reveals That Astrocytic GLT-1 Protects against Fatal Epilepsy While Neuronal GLT-1 Contributes Significantly to Glutamate Uptake into Synaptosomes. *Journal of Neuroscience*, 35(13), pp.5187–5201.

Pettersson, O.J. et al., 2015. Molecular mechanisms in DM1 - A focus on foci. *Nucleic Acids Research*, 43(4), pp.2433–2441.

Puelles, L. et al., 2000. Pallial and subpallial derivatives in the embryonic chick and mouse telencephalon, traced by the expression of the genes Dlx-2, Emx-1, Nkx-2.1, Pax-6, and Tbr-1. *Journal of Comparative Neurology*, 424(3), pp.409–438.

Quintero-Mora, M.L. et al., 2002. Expanded CTG repeats inhibit neuronal differentiation of the PC12 cell line. *Biochemical and Biophysical Research Communications*, 295(2), pp.289–294.

Rahul N. Kanadia, Carl R. Urbinati, Valerie J. Crusselle, Defang Luo, Young-Jae Lee, Jeffrey K. Harrison, S. Paul Oh, M.S.S., 2003. Developmental expression of mouse muscleblind genes Mbnl1, Mbnl2 and Mbnl3. , 3, pp.459–462.

Rajarajan, P. et al., 2016. Spatial genome organization and cognition. *Nature Reviews Neuroscience*, 17(11), pp.681–691.

Rakocevic-Stojanovic, V. et al., 2014. Significant impact of behavioral and cognitive impairment on quality of life in patients with myotonic dystrophy type 1. *Clinical Neurology and Neurosurgery*, 126, pp.76–81.

Rao, Y.S. & Pak, T.R., 2016. microRNAs and the adolescent brain: Filling the knowledge gap. *Neuroscience and Biobehavioral Reviews*, 70, pp.313–322.

Rau, F. et al., 2011. Misregulation of miR-1 processing is associated with heart defects in myotonic dystrophy. *Nature structural & molecular biology*, 18(7), pp.840–845.

Reddy, S. et al., 1996. Mice lacking the myotonic dystrophy protein kinase develop a late onset progressive myopathy. *Nature genetics*, 13(3), pp.325–35.

Romigi, A. et al., 2013. Sleep-Wake Cycle and Daytime Sleepiness in the Myotonic Dystrophies, Critical Care Medicine: Principles of Diagnosis and Management in the Adult. *Journal of Neurodegenerative Diseases Volume 2013 (2013)*, Volume 201, pp.483–487.

Rothstein, J.D. et al., 2005. Beta-lactam antibiotics offer neuroprotection by increasing glutamate transporter expression. *Nature*, 433(7021), pp.73–7.

Rothstein, J.D. et al., 1995. Selective loss of glial glutamate transporter GLT-1 in amyotrophic lateral sclerosis. *Annals of neurology*, 38(1), pp.73–84.

Salcedo-Tello, P., Ortiz-Matamoros, A. & Arias, C., 2011. GSK3 Function in the Brain during Development, Neuronal Plasticity, and Neurodegeneration. *International journal of Alzheimer's disease*, 2011, p.189728.

Santoro, M. et al., 2017. Myotonic dystrophy type 1: Role of CCG, CTC and CGG interruptions within DMPK alleles in the pathogenesis and molecular diagnosis. *Clinical Genetics*, pp.1–10.

Santra, A. & Kumar, R., 2014. Brain perfusion single photon emission computed tomography in major psychiatric disorders: From basics to clinical practice. *Indian Journal of Nuclear Medicine : IJNM : The Official Journal of the Society of Nuclear Medicine, India*, 29(4), pp.210–221.

Sarkar, P.S. et al., 2000. Heterozygous loss of Six5 in mice is sufficient to cause ocular cataracts. *Nature genetics*, 25(1), pp.110–4.

Sato, T., Joyner, A.L. & Nakamura, H., 2004. How does Fgf signaling from the isthmic organizer induce midbrain and cerebellum development? *Development Growth and Differentiation*, 46(6), pp.487–494.

Savkur, R.S., Philips, A. V & Cooper, T.A., 2001. Aberrant regulation of insulin receptor alternative splicing is associated with insulin resistance in myotonic dystrophy. *Nature genetics*, 29(1), pp.40–7.

Savouret, C. et al., 2003. CTG repeat instability and size variation timing in DNA repair-deficient mice. *EMBO Journal*, 22(9), pp.2264–2273.

Savouret, C. et al., 2004. MSH2-dependent germinal CTG repeat expansions are produced continuously in spermatogonia from DM1 transgenic mice. *Mol Cell Biol*, 24(2), pp.629–637.

Schara, U. & Schoser, B.G.H., 2006. Myotonic Dystrophies Type 1 and 2: A Summary on Current Aspects. *Seminars in Pediatric Neurology*, 13(2), pp.71–79.

Schindelin, J. et al., 2012. Fiji: an open-source platform for biological-image analysis. *Nat Meth*, 9(7), pp.676–682.

Schmahmann, J.D., 2004. Disorders of the cerebellum: ataxia, dysmetria of thought, and the cerebellar cognitive affective syndrome. *The Journal of neuropsychiatry and clinical neurosciences*, 16(3), pp.367–378.

Sergeant, N. et al., 2001. Dysregulation of human brain microtubule-associated tau mRNA maturation in myotonic dystrophy type 1. *Human molecular genetics*, 10(19), pp.2143–55.

Sergeant, N., Delacourte, A. & Buée, L., 2005. Tau protein as a differential biomarker of tauopathies. *Biochimica et Biophysica Acta - Molecular Basis of Disease*, 1739(2), pp.179–197.

Serra, L. et al., 2014. Abnormal functional brain connectivity and personality traits in myotonic dystrophy type 1. *JAMA neurology*, 71(5), pp.603–11.

Serra, L., Mancini, M., et al., 2016. Brain Connectomics ' Modification to Clarify Motor and Nonmotor Features of Myotonic Dystrophy Type 1. *Neural Plasticity*, 2016.

Serra, L., Cercignani, M., et al., 2016. 'I know that you know that I know': Neural substrates associated with social cognition deficits in DM1 patients. *PLoS ONE*, 11(6), pp.1–13.

Seznec, H. et al., 2001. Mice transgenic for the human myotonic dystrophy region with expanded CTG repeats display muscular and brain abnormalities. *Human molecular genetics*, 10(23), pp.2717–2726.

Seznec, H. et al., 2000. Transgenic mice carrying large human genomic sequences with expanded CTG repeat mimic closely the DM CTG repeat intergenerational and somatic instability. *Human molecular genetics*, 9(8), pp.1185–1194.

Siboni, R.B. et al., 2015. Actinomycin D Specifically Reduces Expanded CUG Repeat RNA in Myotonic Dystrophy Models. *Cell Reports*, 13(11), pp.2386–2394.

Sicot, G. et al., 2017. Downregulation of the Glial GLT1 Glutamate Transporter and Purkinje Cell Dysfunction in a Mouse Model of Myotonic Dystrophy. *Cell Reports*, 19(13), pp.2718–2729.

Sicot, G. & Gomes-Pereira, M., 2013. RNA toxicity in human disease and animal models: From the uncovering of a new mechanism to the development of promising therapies. *Biochimica et Biophysica Acta - Molecular Basis of Disease*, 1832(9), pp.1390–1409.

Sicot, G., Gourdon, G. & Gomes-Pereira, M., 2011. Myotonic dystrophy, when simple repeats reveal complex pathogenic entities: New findings and future challenges. *Human Molecular Genetics*, 20(R2), pp.116–123.

Sistiaga, A. et al., 2010. Cognitive/personality pattern and triplet expansion size in adult myotonic dystrophy type 1 (DM1): CTG repeats, cognition and personality in DM1. *Psychological medicine*, 40(3), pp.487–95.

Smith, C.A. & Gutmann, L., 2016. Myotonic Dystrophy Type 1 Management and Therapeutics. *Current Treatment Options in Neurology*, 18(12).

Subramanian, S., Mishra, R.K. & Singh, L., 2003. Genome-wide analysis of microsatellite repeats in humans: their abundance and density in specific genomic regions. *Genome biology*, 4(2), p.R13.

Suenaga, K. et al., 2012. Muscleblind-like 1 knockout mice reveal novel splicing defects in the myotonic dystrophy brain. *PLoS ONE*, 7(3).

Takado, Y. et al., 2015. Diffuse brain abnormalities in myotonic dystrophy type 1 detected by 3.0 t proton magnetic resonance spectroscopy. *European Neurology*, 73(3–4), pp.247–256.

Takahashi, K., Foster, J.B. & Lin, C.-L.G., 2015. Glutamate transporter EAAT2: regulation, function, and potential as a therapeutic target for neurological and psychiatric disease. *Cellular and Molecular Life Sciences*, 72(18), pp.3489–3506.

Takamori, S., 2006. VGLUTs: 'exciting' times for glutamatergic research? *Neuroscience research*, 55(4), pp.343–351.

Takarada, T. et al., 2015. Resveratrol enhances splicing of insulin receptor exon 11 in myotonic dystrophy type 1 fibroblasts. *Brain and Development*, 37(7), pp.661–668.

Tamaru, T. et al., 2015. CRY Drives Cyclic CK2-Mediated BMAL1 Phosphorylation to Control the Mammalian Circadian Clock. *PLoS Biology*, 13(11), pp.1–25.

Tanaka, K. et al., 1997. Epilepsy and Exacerbation of Brain Injury in Mice Lacking the Glutamate Transporter GLT-1. *Science*, 276(5319), pp.1699–1702.

Taneja, K.L. et al., 1995. Foci of trinucleotide repeat transcripts in nuclei of myotonic dystrophy cells and tissues. *Journal of Cell Biology*, 128(6), pp.995–1002.

Tang, D.D. & Gerlach, B.D., 2017. The roles and regulation of the actin cytoskeleton, intermediate filaments and microtubules in smooth muscle cell migration. *Respiratory Research*, 18(1), p.54.

Tang, Z.Z. et al., 2012. Muscle weakness in myotonic dystrophy associated with misregulated splicing and altered gating of Ca v1.1 calcium channel. *Human Molecular Genetics*, 21(6), pp.1312–1324.

Theadom, A. et al., 2014. Prevalence of muscular dystrophies: A systematic literature review. *Neuroepidemiology*, 43(3–4), pp.259–268.

Thornton, C.A., Johnson, K. & Moxley, R.T., 1994. Myotonic dystrophy patients have larger CTG expansions in skeletal muscle than in leukocytes. *Annals of Neurology*, 35(1), pp.104–107.

Thornton, T.M. et al., 2008. Phosphorylation by p38 MAPK as an Alternative Pathway for GSK3 Inactivation. *Science*, 320(5876), pp.667–670.

Timchenko, N.A. et al., 2004. Overexpression of CUG Triplet Repeat-binding Protein, CUGBP1, in Mice Inhibits Myogenesis. *Journal of Biological Chemistry*, 279(13), pp.13129–13139.

Timchenko, N.A. et al., 2001. RNA CUG Repeats Sequester CUGBP1 and Alter Protein Levels and Activity of CUGBP1. *Journal of Biological Chemistry*, 276(11), pp.7820–7826.

Tomé, S. et al., 2009. MSH2 ATPase domain mutation affects CTG•CAG repeat instability in transgenic mice. *PLoS Genetics*, 5(5).

Tran, H. et al., 2011. Analysis of exonic regions involved in nuclear localization, splicing activity, and dimerization of muscleblind-like-1 isoforms. *Journal of Biological Chemistry*, 286(18), pp.16435–16446.

Turner, K.M., Burgoyne, R.D. & Morgan, A., 1999. Protein phosphorylation and the regulation of synaptic membrane traffic. , pp.459–464.

Vasile, F., Dossi, E. & Rouach, N., 2017. Human astrocytes: structure and functions in the healthy brain. *Brain Structure and Function*, 222(5), pp.1–13.

Velázquez-Bernardino, P. et al., 2012. Myotonic dystrophy type 1-associated CTG repeats disturb the expression and subcellular distribution of microtubule-associated proteins MAP1A, MAP2, and MAP6/STOP in PC12 cells. *Molecular Biology Reports*, 39(1), pp.415–424.

Venerando, A., Ruzzene, M. & Pinna, L.A., 2014. Casein kinase: the triple meaning of a misnomer. *The Biochemical journal*, 460(2), pp.141–56.

Verkhratsky, A., Nedergaard, M. & Hertz, L., 2014. Why are Astrocytes Important? *Neurochemical Research*, 40(2), pp.389–401.

Verkhratsky, A. & Parpura, V., 2016. Astrogliopathology in neurological, neurodevelopmental and psychiatric disorders. *Neurobiology of Disease*, 85, pp.254–261.

Vermersch, P. et al., 1996. Specific tau variants in the brains of patients with myotonic dystrophy. *Neurology*, 47(3), pp.711–7.

Vielhaber, S. et al., 2006. Brain 1H magnetic resonance spectroscopic differences in myotonic dystrophy type 2 and type 1. *Muscle & nerve*, 34(2), pp.145–152.

Wang, E.T. et al., 2012. Transcriptome-wide regulation of pre-mRNA splicing and mRNA localization by muscleblind proteins. *Cell*, 150(4), pp.710–724.

Wang, G.S. et al., 2007. Elevation of RNA-binding protein CUGBP1 is an early event in an inducible heart-specific mouse model of myotonic dystrophy. *Journal of Clinical Investigation*, 117(10), pp.2802–2811.

Wang, G.S. et al., 2009. PKC inhibition ameliorates the cardiac phenotype in a mouse model of myotonic dystrophy type 1. *Journal of Clinical Investigation*, 119(12), pp.3797–3806.

Wang, P.-Y. et al., 2017. Reduced cytoplasmic MBNL1 is an early event in a brain-specific mouse model of myotonic dystrophy. *Human Molecular Genetics*, 26(12), pp.2247–2257.

Wang, Y.H. et al., 1994. Preferential nucleosome assembly at DNA triplet repeats from the myotonic dystrophy gene. *Science (New York, N.Y.)*, 265(5172), pp.669–71.

Ward, A.J. et al., 2010. CUGBP1 overexpression in mouse skeletal muscle reproduces features of myotonic dystrophy type 1. *Human Molecular Genetics*, 19(18), pp.3614–3622.

Wardlaw, J.M., Valdés Hernández, M.C. & Muñoz-Maniega, S., 2015. What are white matter hyperintensities made of? Relevance to vascular cognitive impairment. *Journal of the American Heart Association*, 4(6), p.1140.

Warf, M.B. et al., 2009. Pentamidine reverses the splicing defects associated with myotonic dystrophy. *Proceedings of the National Academy of Sciences of the United States of America*, 106(44), pp.18551–18556.

Watson, C., Paxinos, G. & Puelles, L. (Luis), 2012. *The mouse nervous system*, Elsevier Academic Press.

Webb, D.J., Parsons, J.T. & Horwitz, A.F., 2002. Adhesion assembly, disassembly and turnover in migrating cells -- over and over and over again. *Nature cell biology*, 4(4), pp.E97-100.

Wei, C. et al., 2013. GSK3β is a new therapeutic target for myotonic dystrophy type 1. *Rare diseases (Austin, Tex.)*, 1, p.e26555.

Wheeler, T.M. et al., 2007. Correction of ClC-1 splicing eliminates chloride channelopathy and myotonia in mouse models of myotonic dystrophy. *Journal of Clinical Investigation*, 117(12), pp.3952–3957.

Wheeler, T.M. et al., 2009. Reversal of RNA Dominance by Displacement of Protein Sequestered on Triplet Repeat RNA. *Science*, 325(5938), pp.336–339.

Wheeler, T.M. et al., 2012. Targeting nuclear RNA for in vivo correction of myotonic dystrophy. *Nature*, 488(7409), pp.111–5.

Wickstrom, S.A., Radovanac, K. & Fassler, R., 2011. Genetic Analyses of Integrin Signaling. *Cold Spring Harbor Perspectives in Biology*, 3(2), pp.a005116–a005116.

Wiles, C.M. et al., 2006. Falls and stumbles in myotonic dystrophy. *Journal of neurology, neurosurgery, and psychiatry*, 77(3), pp.393–6.

Winblad, S., Lindberg, C. & Hansen, S., 2006. Cognitive deficits and CTG repeat expansion size in classical myotonic dystrophy type 1 (DM1). *Behavioral and brain functions : BBF*, 2, p.16.

Witte, H. & Bradke, F., 2008. The role of the cytoskeleton during neuronal polarization. *Current Opinion in Neurobiology*, 18(5), pp.479–487.

Wojciechowska, M. & Krzyzosiak, W.J., 2011. Cellular toxicity of expanded RNA repeats: Focus on RNA foci. *Human Molecular Genetics*, 20(19), pp.3811–3821.

Xia, G. et al., 2015. Genome modification leads to phenotype reversal in human myotonic dystrophy type

1 induced pluripotent stem cell-derived neural stem cells. *Stem Cells*, 33(6), pp.1829–1838.

Xie, J. et al., 2005. A consensus CaMK IV-responsive RNA sequence mediates regulation of alternative exons in neurons. *RNA (New York, N.Y.)*, 11(12), pp.1825–34.

Yadava, R.S. et al., 2008. RNA toxicity in myotonic muscular dystrophy induces NKX2-5 expression. *Nature genetics*, 40(1), pp.61–8.

Yang, Q. et al., 2012. Excessive Astrocyte-Derived Neurotrophin-3 Contributes to the Abnormal Neuronal Dendritic Development in a Mouse Model of Fragile X Syndrome. *PLoS Genetics*, 8(12).

Yano, M. et al., 2010. Nova2 Regulates Neuronal Migration through an RNA Switch in Disabled-1 Signaling. *Neuron*, 66(6), pp.848–858.

Yoo, W.-K. et al., 2017. Cortical Thickness and White Matter Integrity are Associated with CTG Expansion Size in Myotonic Dystrophy Type I. *Yonsei Medical Journal*, 58(4), p.807.

Yoshimura, N. et al., 1990. Topography of Alzheimer's neurofibrillary change distribution in myotonic dystrophy. *Clinical Neurology and Neurosurgery*, 5, pp.234–239.

Yu, H. et al., 2011. Daytime sleepiness and REM sleep characteristics in myotonic dystrophy: a case-control study. *Sleep*, 34(1), pp.165–170.

Yu, Z.-X. et al., 2003. Mutant huntingtin causes context-dependent neurodegeneration in mice with Huntington's disease. *The Journal of neuroscience : the official journal of the Society for Neuroscience*, 23(6), pp.2193–2202.

Yuan, Y. et al., 2007. Muscleblind-like 1 interacts with RNA hairpins in splicing target and pathogenic RNAs. *Nucleic Acids Research*, 35(16), pp.5474–5486.

Zambon, A.C. et al., 2012. GO-Elite: A flexible solution for pathway and ontology over-representation. *Bioinformatics*, 28(16), pp.2209–2210.

Zatz, M. et al., 1995. Analysis of the CTG repeat in skeletal muscle of young and adult myotonic dystrophy patients: When does the expansion occur? *Human Molecular Genetics*, 4(3), pp.401–406.

Zhang, W. et al., 2002. Region-specific alternative splicing in the nervous system: implications for regulation by the RNA-binding protein NAPOR. *RNA (New York, N.Y.)*, 8(5), pp.671–685.

Zhuo, M., 2017. Ionotropic glutamate receptors contribute to pain transmission and chronic pain. *Neuropharmacology*, 112, pp.228–234.

Zschocke, J. et al., 2005. Differential promotion of glutamate transporter expression and function by glucocorticoids in astrocytes from various brain regions. *Journal of Biological Chemistry*, 280(41), pp.34924–34932.

Zu, T. et al., 2011. Non-ATG – initiated translation directed by microsatellite expansions. *PNAS*, 108(1), pp.260–265.

# CURRICULUM VITAE

## DIANA MIHAELA DINCĂ

22 Avenue Bourgain
92130, Issy-les-Moulineaux, FRANCE

Phone : 0033 695 880 889
Email : diana.m.dinca@gmail.com

## EDUCATION

**2013-2017** **PhD candidate in Neurobiology and Human Genetics –** Imagine Institute Inserm U1163, Paris-Descartes Univeristy. *Subject:* Mechanisms of brain dysfunction in myotonic dystrophy type 1

**2012-2013** **MSC in Genetics, Cellular and Developmental Biology and Evolution –** Paris-Sud University. *Graduated with highest honors (2nd/21)*

**2007-2012** **BSc in Biology –** University of Valencia – SPAIN. *Graduated with highest honors (7th/156)*
4th **year BSc degree: Erasmus exchange** in Paris-Sud Univeristy – FRANCE.

## PROFESSIONAL EXPERIENCE

### Research

**2013-2017** **CTG repeat instability and Myotonic dystrophy Laboratory –** INSERM U1163, Imagine Institute. FRANCE
*Head of laboratory:* Dr. Geneviève Gourdon, PhD, HDR; *Supervisor:* Dr. Mário Gomes-Pereira, PhD, HDR
*Subject:* Impact of the CTG expansion on neuronal and astroglial physiology
*Technical skills:* splicing analysis, quantitative PCR, western blotting, mouse brain microdissection, cell culture – primary neurons and astrocytes, in situ hybridization, immunofluorescence, high resolution microscopy

**2012-2013** **CTG repeat instability and Myotonic dystrophy Laboratory –** INSERM U781. FRANCE
*Head of laboratory:* Dr. Geneviève Gourdon, PhD, HDR; *Supervisor:* Dr. Mário Gomes-Pereira, PhD, HDR
*Subject:* Synaptic protein deregulation in myotonic dystrophy type 1: mechanisms and consequences
*Technical skills:* splicing analysis, quantitative PCR, western blotting, mouse brain microdissection.

**2011-2012** **Nutrient-mediated signaling Unit –** Biomedicine Institute of Valencia. SPAIN
*Head of laboratory:* Dr. Pascual Sanz; *Supervisor:* Dr. Teresa Rubio
*Subject:* Role of the sumoylation of AMPK protein in the glucose signaling and its pathological consequences
*Technical skills:* cell culture, protein measurements, western blotting

**2010-2011** **Cell signaling and morphogenesis Laboratory –** CGM-CNRS. FRANCE
*Head of laboratory:* Dr. Anne-Marie Pret; *Supervisor:* Dr. François Agnes
*Subject:* Cellular and genetic analysis of the role of cell polarity in the choice of life or death in *Drosophila melanogaster*
*Technical skills:* *Drosophila* microdissection, immunofluorescence, confocal microscopy, statistical analysis

**2009-2010** **Development and molecular genetics Laboratory –** University of Valencia. SPAIN
*Head of laboratory:* Dr. Ruben Artero; *Supervisor:* Dr. Amparo Garcia López
*Subject:* Genetic and chemical modifiers of a CUG toxicity model in *Drosophila melanogaster*
*Technical skills:* *Drosophila* breeding and stocks management, DNA and RNA extraction, scientific image analysis.

### Teaching:

**2014-2016** **Biology Teacher –** Frontiers in Life Science Paris-Descartes University-CRI (+120 hours)
Organize and teach theoretical lectures and tutorials for 1st and 2nd year Bachelor students
Propose final exam questions and participate in exam marking

**2013-2016** **Supervisor for ESTBA and MSc-Santé training students**
Teach technical, analytical and writing skills to summer project students and Master's candidates

### Administration:

**2016-2017** **National coordinator** – Réseau BIOTechno, **Secretary** – Forum BIOTechno Paris 2017
Coordinate the national team in organizing workshops for PhDs professional insertion in 4 cities in France

**2016-2017** **Inter-associative manager** – Young Researchers of Imagine Institute Association (YR2I)
Organize professional and social events in collaboration with different PhD associations in Paris

**2014-2016** **Treasurer and founding member** – Imagine Sport Association
Manage the annual budget, keep up-to-date records, provide regular financial reports to the board

## EXPERTISE AND CONSULTANCY

**2016-2017** **On-site Manager of the IncuCyte video-microscope** – Imagine Institute of Genetic Diseases
Led the trial and acquisition of two video-microscopes (+100.000€) by the institute for the scientific teams
Helped +35 users to establish experimental protocols, currently providing technical training and analytical expertise

**May 2016 &** **Scientific committee member** of the 2nd and 3rd Young Researchers of Imagine Institute Congress
**May 2017** Co-organizer and chairwoman of the Debating competition

## TRAINING AND CERTIFICATES

**Feb-Nov 2017** **Cycle Decouverte de la France Entrepreneuriale** – ISEFRE / ESCP Europe
**Mar 2016** **Certificate in Business and Administration: Project Manager** – CFDIP, University Sorbonne Paris Cité
**Feb 2015** **Career in consulting** – open new attractive career perspectives after your PhD – CFDIP, Paris Diderot University
**Sep 2014** Training and certification for animal experimentation, Level B: **Project developer** – Paris-Descartes University
**Apr 2014** Training for supervisors of laboratories of biosafety levels 2 and 3 – INSERM Regional delegation

## SCIENTIFIC ORAL PRESENTATIONS

**Sep 2017** **IDMC11, San Francisco** – CUG RNA toxicity in astrocytes is associated with adhesion and migration deficits and affects neuritogenesis
**Sep 2017** **SANOFI Incucyte user meeting, Paris** (*invited speaker*) – Investigating astroglial and neuronal phenotypes in a mouse model of DM1 by live cell monitoring
**May 2017** **Young Researchers in Life Sciences, Paris** – Brain cell specificity and abnormal neuroglia interaction in DM1
**Nov 2016** ***Imagine* Monday Seminars, Paris** – The unusual suspects: Astrocytes dysfunction in myotonic dystrophy
**Jul 2016** **10th Annual LMB Graduate Student Symposium, Cambridge** – Investigating astroglial and neuronal phenotypes in a mouse model of DM1
**Apr 2016** **Symposium xCELLigence OZYME, Marseille** *(invited speaker)* – Investigating astroglial and neuronal phenotypes in a mouse model of DM1

## HONORS AND AWARDS

**June 2017** **Best poster presentation** at the *Colloque des Jeunes Chercheurs AFM Téléthon* out of 96 young scientists
**May 2017** **Best oral presentation – public's choice** at the *Young Researchers in Life Sciences Congress* out of 32 selected presentations
**June 2015** **Best poster presentation** at the 10th *International Myotonic Dystrophy Consortium* out of +120 international scientists

## SCIENTIFIC PUBLICATIONS

**2017** Géraldine Sicot *, Laurent Servais *, **Diana M. Dincã** *, Axelle Leroy, Cynthia Prigogine, Fadia Medja, Sandra O. Braz, Aline Huguet-Lachon, Cerina Chhuon, Annie Nicole, Noëmy Gueriba, Ruan Oliveira, Bernard Dan, Denis Furling, Maurice S. Swanson, Ida Chiara Guerrera, Guy Cheron, Geneviève Gourdon and Mário Gomes-Pereira Downregulation of the Glial GLT1 Glutamate Transporter and Purkinje Cell Dysfunction in a Mouse Model of Myotonic Dystrophy – Cell Reports (2017) 19, 2718-2729 [*co-first author]

**2013** Oscar Hernández-Hernández, Géraldine Sicot**, Diana M. Dincã**, Aline Huguet, Annie Nicole, Luc Buée, Arnold Munnich, Nicolas Sergeant, Geneviève Gourdon and Mário Gomes-Pereira. Synaptic protein dysregulation in myotonic dystrophy type 1 – Rare diseases (2013) 1: e25553

## PERSONAL SKILLS AND COMPETENCES

**Languages:** Fluent speaking and writing in **English, French, Spanish** and **Catalan.** Mother tongue: **Romanian**

**Volunteer activities:** Vice-president and fitness coach at the Imagine Sports Association, promoting sports among scientists
Portrait for the Café des Roumains Association for the sociocultural project "Je suis Roumain (aussi)"